DNA 4734Z

AN INTERIM REPORT ON COLLATERAL DAMAGE

Science Applications, Inc.
P.O. Box 2351
La Jolla, California 92038

October 1978

Interim Report for Period 11 August 1976—13 December 1977

CONTRACT No. DNA 001-77-C-0081

APPROVED FOR PUBLIC RELEASE;
DISTRIBUTION UNLIMITED.

THIS WORK SPONSORED BY THE DEFENSE NUCLEAR AGENCY
UNDER RDT&E RMSS CODE B364076464 V99QAXNL12203 H2590D.

Prepared for
Director
DEFENSE NUCLEAR AGENCY
Washington, D. C. 20305

Destroy this report when it is no longer needed. Do not return to sender.

PLEASE NOTIFY THE DEFENSE NUCLEAR AGENCY, ATTN: TISI, WASHINGTON, D.C. 20305, IF YOUR ADDRESS IS INCORRECT, IF YOU WISH TO BE DELETED FROM THE DISTRIBUTION LIST, OR IF THE ADDRESSEE IS NO LONGER EMPLOYED BY YOUR ORGANIZATION.

UNCLASSIFIED

SECURITY CLASSIFICATION OF THIS PAGE (When Data Entered)

REPORT DOCUMENTATION PAGE		READ INSTRUCTIONS BEFORE COMPLETING FORM
1. REPORT NUMBER DNA 4734Z	2. GOVT ACCESSION NO.	3. RECIPIENT'S CATALOG NUMBER
4. TITLE (and Subtitle) AN INTERIM REPORT ON COLLATERAL DAMAGE		5. TYPE OF REPORT & PERIOD COVERED Interim Report for Period 11 Aug 76—13 Dec 77
		6. PERFORMING ORG. REPORT NUMBER SAI-76-822-LJ
7. AUTHOR(s) M. K. Drake D. C. Kaul W. A. Woolson M. P. Fricke C. J. Rindfleisch, Jr. D. E. Groce J. B. Swenson		8. CONTRACT OR GRANT NUMBER(s) DNA 001-77-C-0081
9. PERFORMING ORGANIZATION NAME AND ADDRESS Science Applications, Inc. P.O. Box 2351 La Jolla, California 92038		10. PROGRAM ELEMENT, PROJECT, TASK AREA & WORK UNIT NUMBERS NWED Subtask V99QAXNL122-03
11. CONTROLLING OFFICE NAME AND ADDRESS Director Defense Nuclear Agency Washington, D.C. 20305		12. REPORT DATE October 1978 13. NUMBER OF PAGES 496
14. MONITORING AGENCY NAME & ADDRESS(if different from Controlling Office)		15. SECURITY CLASS (of this report) UNCLASSIFIED 15a. DECLASSIFICATION DOWNGRADING SCHEDULE

16. DISTRIBUTION STATEMENT (of this Report)

Approved for public release; distribution unlimited.

17. DISTRIBUTION STATEMENT (of the abstract entered in Block 20, if different from Report)

18. SUPPLEMENTARY NOTES

This work sponsored by the Defense Nuclear Agency under RDT&E RMSS Code B364076464 V99QAXNL12203 H2590D.

19. KEY WORDS (Continue on reverse side if necessary and identify by block number)

Collateral Damage	Fire Effects	Airblast
Weapon Effects	Airblast Effects	Civilian Casualties
Personnel Response	Burns	
Casualty Criteria	Nuclear Radiation	
Damage Functions	Thermal Radiation	

20. ABSTRACT (Continue on reverse side if necessary and identify by block number)

This is an interim report on collateral damage produced by nuclear weapons. It contains the results of a comprehensive analysis of the uncertainties related to the effects of nuclear weapons on personnel. The results indicate which of the uncertainties and/or normal variations are the most important with respect to the ability to accurately predict collateral damage.

DD FORM 1 JAN 73 1473 EDITION OF 1 NOV 65 IS OBSOLETE

UNCLASSIFIED

SECURITY CLASSIFICATION OF THIS PAGE (When Data Entered)

20. ABSTRACT (Continued)

This report is not intended to be a weapon employment planner's manual. Rather, it serves as a consistent data base for selection of casualty criteria and uncertainty information to be incorporated into such a manual.

A summary is provided of the important weapon environment uncertainties, as well as uncertainties in personnel shelters and biomedical response to weapon environments. Fatality and injury damage functions are provided for weapon yields from 0.1 to 100 KT at three heights-of-burst and for three sheltering conditions.

PREFACE

The authors wish to express their appreciation to the numerous individuals, companies, laboratories, and agencies that have assisted in the collection of data, provided guidance on interpreting the data, and reviews during the course of this effort, as well as this document. Special appreciation is extended to Mr. Peter Haas (DNA) for his foresight and encouragement, to Dr. Cyrus (Skip) Knowles (DNA) for his in-depth technical review and helpful criticisms provided during the entire project, to the Defense Nuclear Agency Staff who supervised the effort including COL Dirk Lueders, MAJ William Brown, CAPT John Zawila, and Mr. Morton Rubenstein.

For their technical contributions, the authors thank Dr. Harold Brode (PSRC) on nuclear weapon effects, COL Edwin Still (DNA) on personnel response to nuclear radiation, Dr. Donald Richmond (Lovelace Foundation) on personnel response to air blast, and Mr. Williard Derksen (NRL) on personnel response to thermal radiation.

Our appreciation is extended to the many people who prepared the data for this report including Ruth Simons and Betty McGehee and to Marilyn Milan and Drusilla Ezell for helping to prepare the report. Special thanks are given to Marilyn Readel for typing and putting it all together.

TABLE OF CONTENTS

TABLE OF CONTENTS (continued)

LIST OF FIGURES

LIST OF FIGURES (Continued)

LIST OF FIGURES (Continued)

LIST OF FIGURES (Continued)

LIST OF FIGURES (Continued)

LIST OF FIGURES (Continued)

LIST OF FIGURES (Continued)

LIST OF FIGURES (Continued)

LIST OF FIGURES (Continued)

LIST OF FIGURES (Continued)

LIST OF FIGURES (Continued)

LIST OF FIGURES (Continued)

LIST OF FIGURES (Continued)

LIST OF TABLES

LIST OF TABLES (Continued)

LIST OF TABLES (Continued)

LIST OF TABLES (Continued)

1. INTRODUCTION

Nuclear weapons may produce significant levels of undesired damage collateral to achieving the desired effects on the enemy. This collateral damage, which will be defined later in more detail, is broadly taken to mean any form of undesired damage including civilian casualties and damage to the civilian infrastructure. The type and degree of collateral damage produced by nuclear weapons depends on many factors including the proximity of civilian populations to target areas, the population sheltering available, the amount of warning, civil defense actions, the type and yield of weapons, the weapon height-of-burst, etc.

This is an interim report on collateral damage. The emphasis of this report is on civilian casualties produced by prompt weapon effects, and it summarizes the results obtained under Defense Nuclear Agency contracts DNA001-76-C-0039 and DNA001-77-C-0081.

1.1 PURPOSE OF REPORT

The objective of this report is to be a resource on phenomena related to collateral damage produced by nuclear weapons. It is complementary to a report prepared by Science Applications, Inc., on collateral damage produced by conventional weapons (Ref. 1.1) which was compiled under a separate effort for the Defense Nuclear Agency, contracts DNA001-76-C-0085, Subtask 4 and DNA001-76-C-0039, Amendment P00001.

This report is not intended to be a weapon employment planner's manual. Rather, one of its prime purposes it to serve as a consistent data base for selection of casualty criteria and uncertainty information to be incorporated into such manuals and to assist in establishing collateral damage guidelines

related to the employment of nuclear weapons. The Defense Nuclear Agency sponsored an effort to develop recommendations for such guidelines, i.e., the Nuclear Effects Damage Assessment Guidelines Working Group (NEDAG) (Ref. 1.2)

This report contains the results of a comprehensive analysis of the uncertainties related to the effects of nuclear weapons on personnel. The results indicate which of the uncertainties and/or normal variations are the most important with respect to the ability to accurately predict collateral damage. Certain of these important uncertainties can be reduced by additional experimental and/or analytical effort. This report identifies those areas where additional efforts would have a significant impact on reducing uncertainties.

1.2 TYPES OF COLLATERAL DAMAGE

As is well known, nuclear weapons produce a variety of effects. These can create various forms of direct and indirect damage to civilians and civilian structures. Considering the damage produced by the prompt effects of nuclear weapons, some forms of damage are obvious and immediate (civilians killed outright, structures damaged, etc.) while other forms are not so obvious and may become apparent weeks after the attack (damage to the infrastructure, e.g , degraded health-care systems which may increase the fatality rate for those seriously injured). Still other forms of damage may occur years after the attack (e.g., life-shortening effects such as increased incidence of cancer).

A convenient way to classify collateral damage is to divide it into two categories. health effects and property damage. Health effects are direct effects on the untargeted population including fatalities, injuries and long-term effects produced by nuclear weapons. Property damage would include structural damage such as residences (houses, apartments,

hotels, etc.), public buildings (schools, churches, libraries, museums, etc.), historic structures, commercial industrial and government buildings. Property damage would also include damage to health-care facilities (hospitals, clinics, etc.), utility facilities (electric power, gas, water, sanitation, etc.), transportation facilities and structures (roads, bridges, terminals, etc.), as well as damage to croplands and wildlands that directly or indirectly impact upon the health and well-being of the affected population. The list of items for potential property damage is very extensive.

Another way to examine collateral damage is to determine how nuclear weapons affect the "infrastructure" The infrastructure may be thought of as being a complicated network of interrelated socio-economic systems such as the health-care system, law-enforcement system, etc. Such systems are made up of organized groups of people (frequently trained personnel), facilities, and material Damage to these systems can be assessed in terms of property damage, financial impact, as well as the direct impact on the population such as aggravating health effects. Examples of such systems are given below.

- Health care systems (hospitals, clinics, personnel, supplies)
- Sanitation systems (sewers, treatment plants, trash and garbage removal).
- Water supply systems (wells, reservoirs, water lines, treatment plants).
- Electric power systems (power plants, transmission grids, transformer stations).
- Natural gas systems (plants, booster stations, gas lines).

- Communication systems (radio/TV stations, telephone lines and distribution facilities).
- Food supply systems (crops in-the-field, unprocessed commodities, processed foods in storage).
- Fire-fighting systems (facilities, equipment, personnel, supplies).
- Law enforcement systems (facilities, equipment, personnel, supplies).
- Emergency control systems (Civil Defense, communications, etc.).
- Transportation systems (rail systems, road systems, public transportation systems, air travel systems).
- Financial systems (banks, money supplies, etc.).
- Consumer goods supply systems (warehouses, stores, manufacturing facilities).

1.3 EMPHASIS OF COMPLETED ANALYSIS

The analysis performed during the initial phase of this effort was devoted to early-time casualties (fatalities, injuries, and threshold effects) which manifest themselves within 60 days and result from the prompt environment of nuclear weapons. The primary casualty producing effects include radiation sickness (from the ionizing radiation of prompt gamma rays, prompt neutrons, air-secondary gamma rays and fission-product gamma rays), airblast injury (produced by the direct effects on body organs, the secondary effects of debris and missile impact on the body and the tertiary effects of whole body translation and impact), and thermal burns (from direct thermal radiation and fires).

A detailed analysis was made of the uncertainties related to weapon-produced environment on the exposed personnel. This analysis included uncertainties and normal variations of weapon output characteristics, the free-field environments (initial nuclear radiation, airblast, and thermal radiation),

and modifications to these environments due to atmospheric effects (e.g., weather), terrain effects and structural effects. Also, uncertainties and variations in personnel response to the individual weapon environments were compiled.

A methodology was developed for assessing the impact of the uncertainties and to generate damage functions for personnel in various sheltering conditions. This methodology also provides estimates of the confidence levels for the damage functions. Monte Carlo techniques were used to obtain both the damage functions as well as their confidence levels.

1.4 APPROACH

The approach to this program is summarized in Figure 1.1. A survey was made of previous research and analysis on the effects of nuclear weapons on personnel. This included research sponsored by many government agencies including significant programs sponsored by the Defense Nuclear Agency and the Defense Civil Preparedness Agency. The results of this survey and a compilation of biomedical effects of nuclear weapons are given below in Section 5

One of the objectives was to identify low probability phenomena which may be important at large distances from the burst point, i.e., phenomena which may have been ignored in previous personnel criteria analysis but none-the-less could be an important contributor to casualty production at large ranges. If such effects are responsible for one- to ten-percent casualty probabilities, at large ranges, it could be significant from a collateral damage viewpoint.

During the early stages of the current effort, one such phenomena was identified which warrented a separate task conducted during the current research period. i.e., fires produced

COMPILE, REVIEW AND ANALYZE DATA RELEVANT TO CASUALTY PREDICTIONS

- CONSIDER ALL PROMPT EFFECTS (INITIAL NUCLEAR RADIATION, THERMAL RADIATION AND AIRBLAST EFFECTS)
- SCOPE THE IMPACT OF FIRES ON CASUALTY PRODUCTION
- IDENTIFY LOW PROBABILITY PHENOMENA, WHICH MAY BE IMPORTANT AT LARGE RANGES

QUANTIFY UNCERTAINTIES IN WEAPON EFFECTS DATA

- WEAPON ENVIRONMENTS (AIRBLAST, ETC.)
- PERSONNEL RESPONSE (CASUALTY CRITERIA, ETC.)
- SHELTERING CHARACTERISTICS (NUCLEAR RADIATION PROTECTION FACTORS, ETC.)

DEVELOP DAMAGE FUNCTIONS FOR CASUALTY PREDICTIONS

- FATALITIES, INJURIES AND THRESHOLD EFFECTS
- SELECTED SHELTERING CATEGORIES
- LOW-YIELD (0.1 TO 10 KT) AIRBURST FISSION AND ER WEAPONS

Figure 1.1. Program Approach.

by nuclear weapons and the casualties resulting from people being burned or overcome by smoke and toxic combustion gases. A small analysis effort was performed on the impact of fires on casualty production. The results of this effort are given in Section 4.3 of this report.

An assessment was made of the inherent uncertainties and the normal variations which are present in the nuclear weapon effects data and the casualty response data. Basically, these data were obtained from the survey of biomedical responses and DNA summaries of weapon test results. However, the most valuable information on these uncertainties was obtained from the experts in the field. The uncertainties related to weapon output and environments are given in Section 3 and those related to sheltering characteristics are given in Section 4 and in Section 5 for personnel response.

The set of damage functions is the basic part of any methodology for predicting the probability of damage produced by nuclear weapons. Figure 1.2 shows a typical representation of a damage function for casualty predictions. These functions are generally very specific, e.g., the probability as a function of range that a stated level of damage will be produced by a warhead of a given type and yield when detonated at a given height-of-burst.

The damage function can be represented in a closed analytic form (e.g., the complement of the cumulative lognormal function) or a generalized form (e.g., pointwise in range). It may be explicit (e.g., AP-550 methodology) or implicit (e.g., FM101-31 methodology).

Confidence limits, as shown in Figure 1.2, are not now incorporated into any of the standard damage methodologies. The current methodologies use safe-sided criteria, if required, to achieve the degree of assurance required in weapon employment planning.

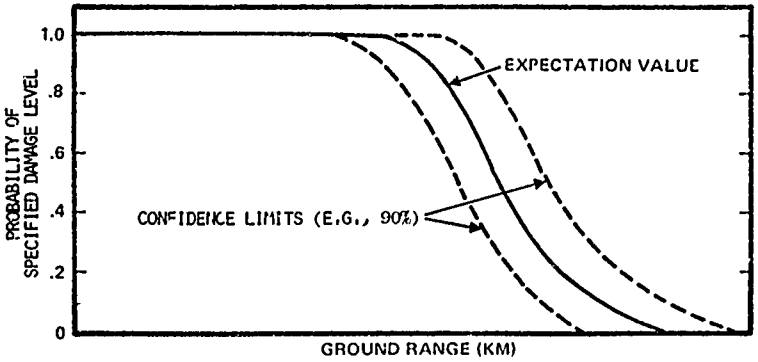

DAMAGE FUNCTION

WEAPON DATA

- TYPE
- YIELD
- HOB

SHELTERING TYPE

DAMAGE LEVEL

$$\left[\begin{array}{c}\text{DAMAGE}\\ \text{FUNCTION}\end{array}\right]\cdot\left[\begin{array}{c}\text{POPULATION}\\ \text{DISTRIBUTION}\end{array}\right]\cdot\left[\begin{array}{c}\text{WEAPON}\\ \text{CEP}\end{array}\right]\cdot\left[\begin{array}{c}\text{PROBABILITY}\\ \text{OF ARRIVAL}\end{array}\right]\cdot\left[\begin{array}{c}\text{WEAPON}\\ \text{RELIABILITY}\end{array}\right]=\left[\begin{array}{c}\text{DAMAGE}\\ \text{EXPECTANCY}\end{array}\right]$$

Figure 1.2. Damage function for predicting casualties.

The approach used in this analysis was to assess the uncertainties and variations in the weapon effects data. This is shown schematically in Figure 1.3 where the uncertainty analysis starts with the source and continues with the uncertainties in free-field weapon environments and the additional uncertainties caused by environment modifications, the uncertainties in sheltering characteristics, and finally the uncertainties in personnel response to the weapon environments.

The parameters which represent the various uncertainties are numerous, complex, and interdependent. A Monte Carlo procedure was developed for performing error propagation analysis. This is shown schematically in Figure 1.4. Details of the procedure are given in Section 6 of this report.

The results of the analysis procedure are 1) the damage function for a specific set of conditions (the weapon environments are folded with the response function) and 2) the confidence estimates for the damage function. An example of the various individual contributions to the damage function is shown in Figure 1.5, and the combined (final) damage function is shown in Figure 1.6 along with the 90-percent confidence limits. This figure also shown a comparison between the results of our current work and damage functions obtained from AP-550 data (two versions).

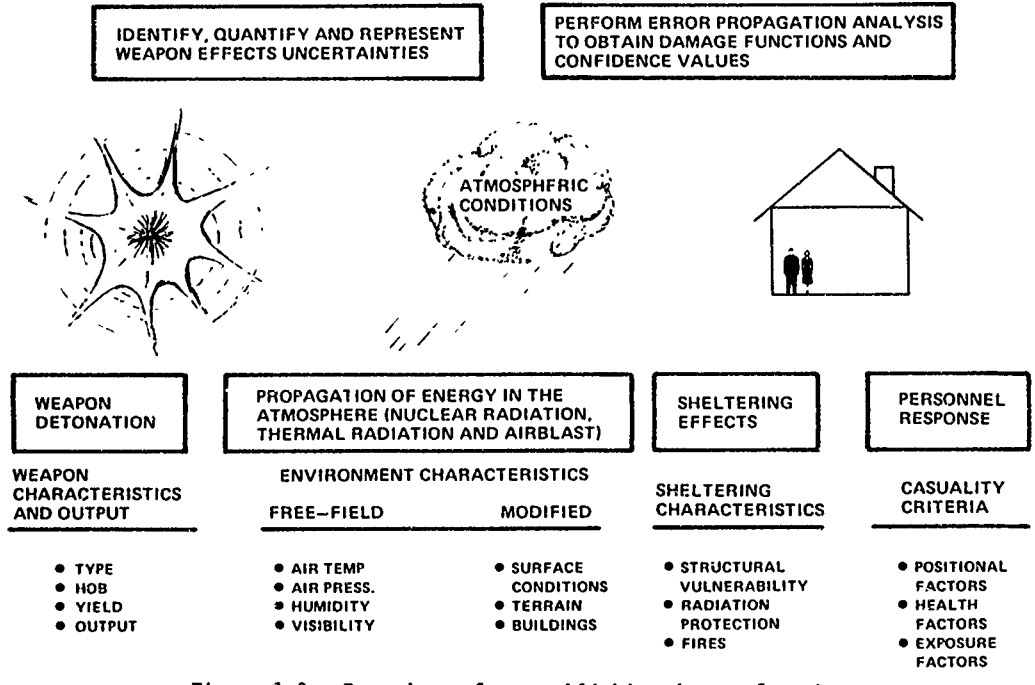

Figure 1.3. Procedures for establishing damage functions and their uncertainties.

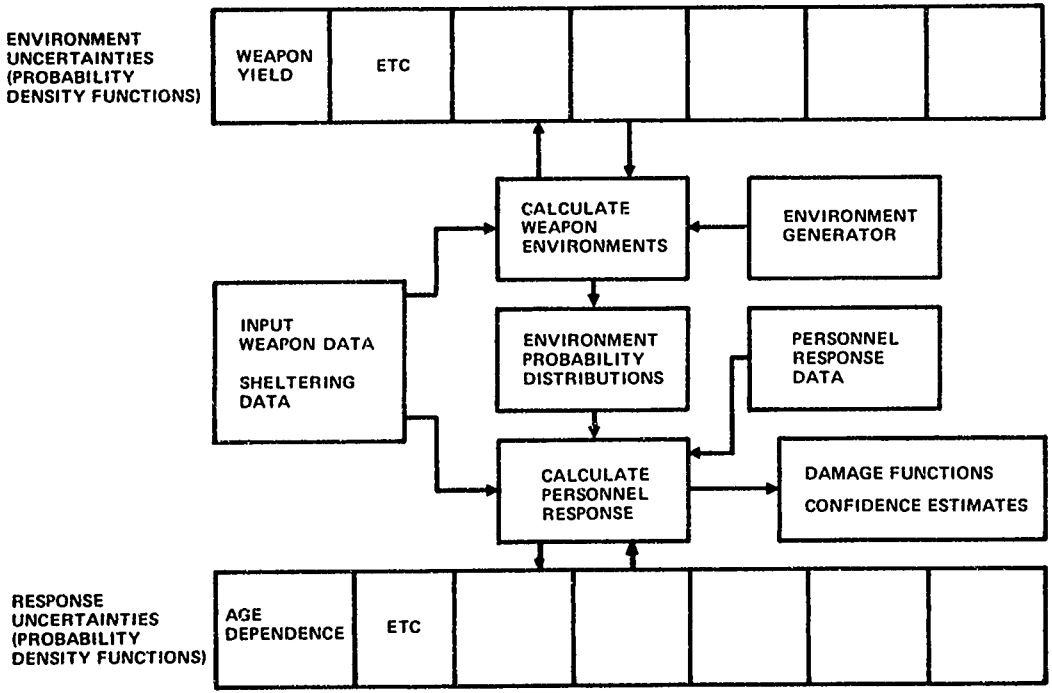

Figure 1.4. Schematic of numerical procedures for uncertainty propagation (Monte Carlo Code).

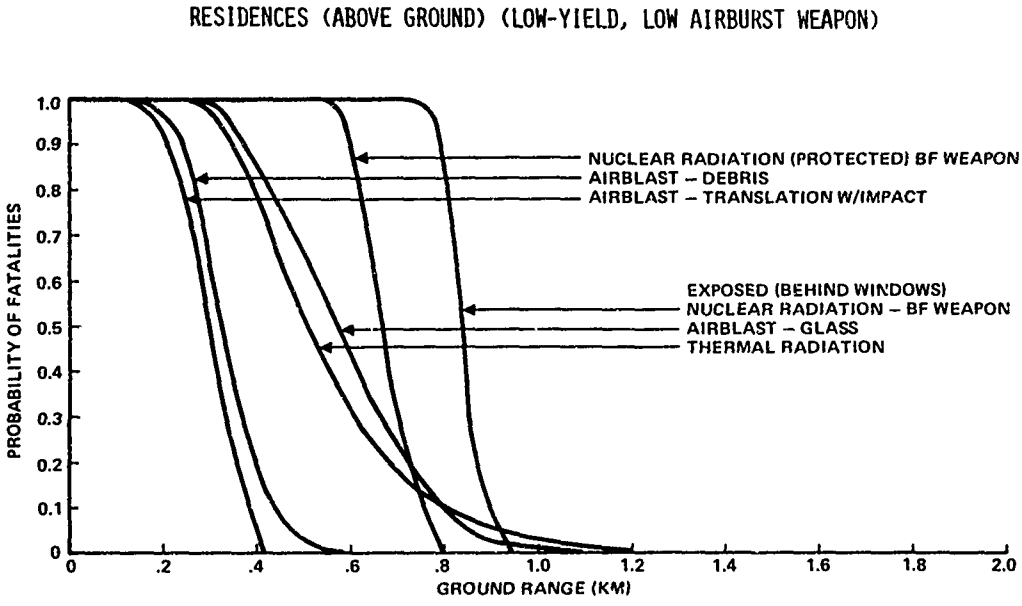

Figure 1.5. Contributions to fatality damage function.

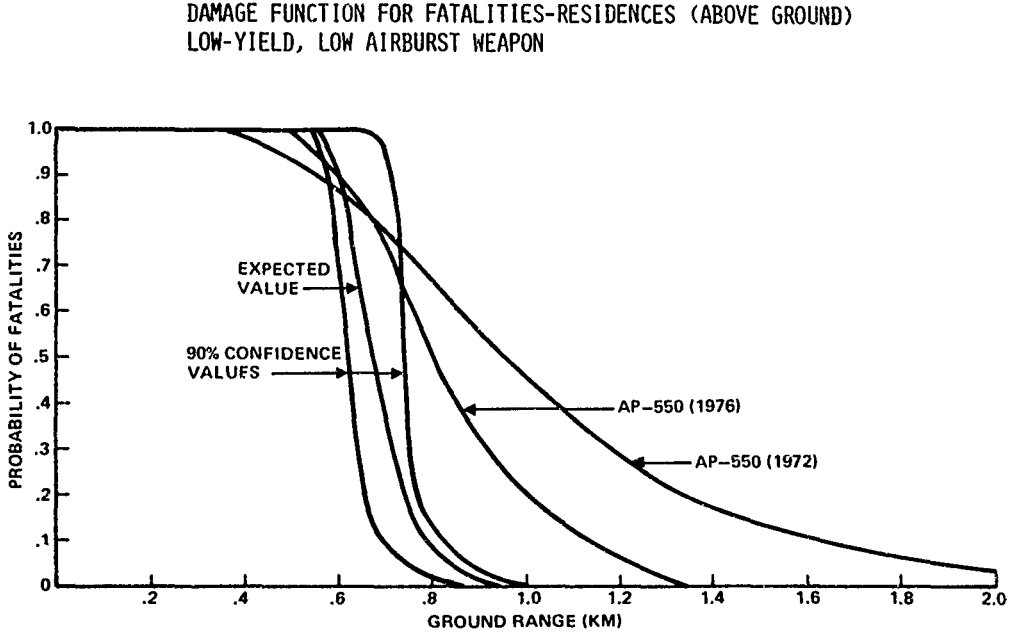

Figure 1.6. Comparison of current methodology and "VN System".

1.5 REFERENCES

1.1 Yengst, W.C., J.B. Swenson and K.H. Mueller, "Evaluations of Collateral Damage," DNA4264F, 15 November 1976.

1.2 Hudson, C.I., Jr., "Guidelines for Nuclear Weapon Employment Constraints," SAI-78-212-LJ, 15 February 1978 (unpublished).

1.3 FM101-31-1 (FMFM 11-4A), Staff Officers' Field Manual - Nuclear Weapons Employment Effects Data, March 1977.

1.4 AP-550-1-2-60-INT, "Physical Vulnerability Handbook - Nuclear Weapons," Change 3, 1 June 1976.

2. POTENTIAL SOURCES OF PERSONNEL CASUALTIES

The varied phenomena produced by nuclear weapons manifest themselves by producing different forms of damage. Table 2.1 summarizes some of the important types of damage produced by nuclear weapons and the energy component which is the primary cause of the damage.

The relative importance of these various energy components changes with weapon yield. Initial nuclear radiation is usually the dominant personnel casualty-producing mechanism for low-yield weapons ($\leq$1 KT), while airblast and thermal radiation effects are usually the dominant causes of personnel casualties for higher-yield weapons ($\geq$ 30 KT). Figure 2.1 shows the ranges of selected weapon environment levels of interest for collateral damage produced by low-yield weapons detonated at a 200-ft/KT$^{1/3}$ scaled height-of-burst. For example, this figure shows that, for people in the open (no protection from any weapon effects), the range to 150 rads is larger than the range to 2 cal/cm^2 for all weapon yields below about 1 KT.

It is important to recognize that when weapon effects vulnerability levels are stated, they are, in reality, indexed to a single aspect of the weapon phenomena, e.g., damage levels for airblast-sensitive objects are indexed to either the peak overpressure or the peak dynamic pressure. Vulnerability values (e.g., 10 psi to produce a given damage level) frequently change as a function of weapon yield. Peak overpressure levels for specific airblast effects tend to decrease with increasing yield (due to the increased impulse resulting from increased pulse lengths), and radiance levels (cal/cm^2) for specific thermal radiation effects tend to increase with yield (again due to the increased thermal pulse length which results in decreased temperature rises due to thermal conduction).

Table 2.1. Types of damage.

Energy Component	Type of Damage
Airblast	Personnel fatalities and injuries (direct and indirect airblast effects)
	Structural and equipment damage
Nuclear Radiation	Personnel fatalities and injuries
	Creation of contaminated areas
Thermal Radiation	Personnel fatalities and injuries
	Fires (structures, croplands and wildlands)
EMP	Damage to Command, Control and Communication Systems
Ground Shock	Underground shelters
	Underground services (waterlines, gaslines, etc.)

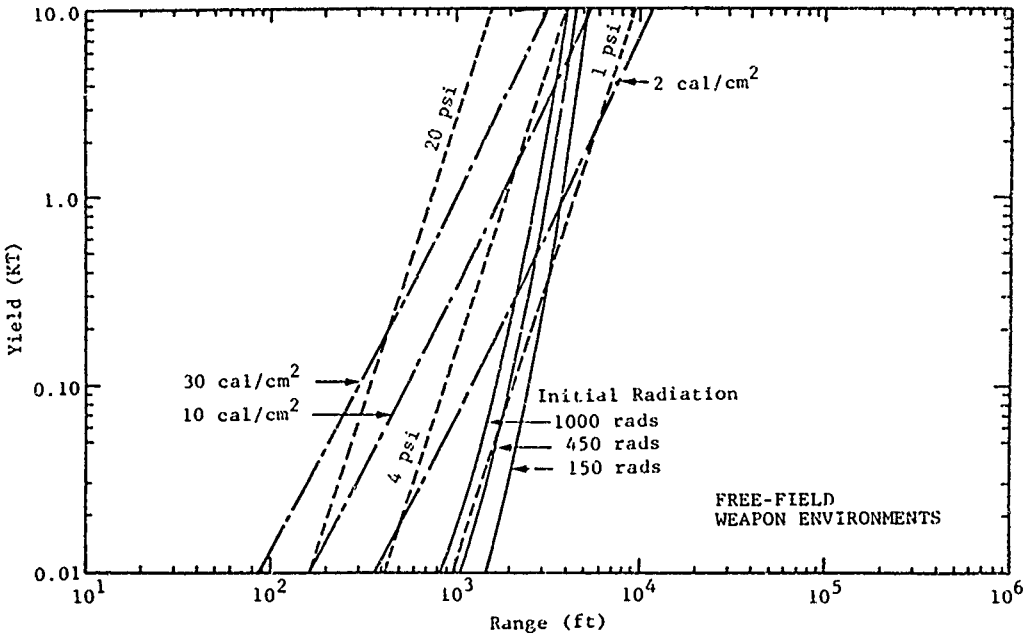

Figure 2.1. Yield as a function of range for producing selected nuclear environment levels primarily of interest for collateral damage, air burst - 200 ft/KT$^{1/3}$.

Essentially all of the nuclear radiation produced by airburst weapons is emitted within one minute (the defined time limits of "initial" nuclear radiation) independent of weapon yield. The human body is not sensitive to variations in time-of-exposures for time periods less than one minute. However, it can recover to some extent from radiation exposures if the exposure is received over a much longer time period (days) or is given in pulses separated in time. Therefore, all radiation exposures experienced by an individual within a time period of about one day need to be added before any prediction of the consequences can be made.

In this section, the personnel casualty mechanisms considered thus far are described briefly. A detailed discussion and numerical values for casualty criteria are presented in Section 5.

2.1 NUCLEAR RADIATION EFFECTS

As was stated earlier and shown in Figure 2.1, nuclear radiation is the dominant cause of casualties for low-yield nuclear weapons. This is basically true regardless of the type of radiation protection provided by most shelters.

Radiation effects on man may be categorized in a number of different ways. Some have proposed dividing the effects into "somatic" and "genetic" effects, where somatic effects appear in the individual irradiated and genetic only in subsequent progeny. Somatic effects can be subdivided into early ($\leq$ 60 days) and late effects and each effect further categorized as shown in Table 2.2.

Only three of these effects will be considered in our present assessment of collateral damage: prodromal response, hemotological depression and early lethality. These are to be

Table 2.2. Somatic effects.

Early Effects

- Skin - erythema and moist desquamation
- Prodromal response (radiation sickness)
  - gastrointestinal (anorexia, nausea, vomiting, diarrhea, intestinal cramps, salivation, dehydration and weight loss)
  - neuromuscular (easy fatigability, apathy or listlessness, sweating, fever, headache, and hypotension followed by hypotensive shock)
- Hematological depression
- Early lethality
- Decreased fertility and increased sterility

Late Effects

- Permanent or delayed skin changes
- Increased incidence of cataract
- Increased incidence of leukemia and other neoplastic disease

considered within the following injury hierarchy:

- Non-apparent or latent injuries usually long-term or genetic (not considered here as noted above),
- apparent (symptom) injuries not serious enough to require intervention by another individual,
- burdening injuries which require aid from another individual, especially the health-care system, and
- lethal injuries.

Both apparent and lethal injuries have definitive symptoms and end-points, whereas a burdening level is quite difficult to define but is of immense importance because of the implications it makes on the quantity of health care necessary to support the individuals irradiated.

There are large errors associated with prediction of casualties due to radiation. Ninety percent confidence limits for predictions of the free-field dose are about $\pm$35% at one kilometer, and are about $\pm$ 50% for the doses associated with particular radiation responses of man. However, the large uncertainties (order of factor of three) in radiation protection factors dominate those given above for typical structures. Additional analysis of radiation protection factors appropriate for specific areas of interest would reduce these uncertainties. However, since nuclear radiation decreases approximately a factor of two for each additional 100 meters of range, large uncertainties in exposure response and protection do not result in large range uncertainties.

2.2 THERMAL RADIATION EFFECTS

Thermal radiation effects can be an important factor in casualty production for those individuals directly exposed to the fireball. Simple avoidance procedures and protection can significantly reduce the consequences of thermal radiation effects.

Our present study is limited to acute effects over a relatively short time ($\lesssim$ 60 days). Long-term disabilities and treatment (skin grafts, etc.) extending over years may be equally important in considering the entire extent of the collateral damage picture. Moreover, we shall only consider here the effects produced by direct exposure to thermal radiation, viz. flash burns and flame, or contact, burns through clothing; casualties caused by fires ignited by nuclear weapons are discussed in Section 4.3.

The extent and severity of flash burns depends directly on the total amount of the thermal radiation actually received or transmitted to the skin, its duration and, to some extent, its frequency spectrum. Individuals burned will receive a mixture of burn degrees, thus complicating the degree of seriousness of the burns.

There are numerous other factors involved in developing casualty criteria for thermal radiation, such as.

- Burn area (percent of body area)
- Mixture of different burn degrees
- Age dependence
- Part of body burned
- Clothing type (varies with time of year)
- Skin condition (color and temperature).

Very modest sheltering provides adequate protection from thermal radiation, therefore, the probability of exposure is the important factor for those individuals in built-up areas and in houses. There is a finite chance of exposure through windows and other openings for people in aboveground portions of residences and other structures. The probability of exposure for these conditions is very uncertain, but an operational assumption of 5 to 10% probability of being exposed may be appropriate.

The 90% confidence limits for free-field thermal radiation exposure uncertainties are about ± 35%. However, this is small compared to the combined uncertainties for personnel exposure and response, about a factor of three (at 90% confidence). Therefore, the probability of exposure and personnel response dominate the overall uncertainty.

2.3 DIRECT AND INDIRECT AIRBLAST EFFECTS

Although airblast effects produced by nuclear weapons are similar to those produced by conventional explosives, these effects are somewhat more difficult to analyze; and the casualty criteria generally have larger uncertainties than do those for nuclear radiation or thermal radiation. Table 2.3 summarizes the basic damage mechanisms produced by airblast.

Table 2.3. Airblast damage mechanisms.

Category	Mechanism
Primary	Direct effect on body organs (lungs, eardrums, etc.)
Secondary	Impact of energized debris and missiles (pieces of structures, stones, glass)
Tertiary	Whole-body translation (with and without impact of body with rigid object).

Primary Airblast Effects. As the blast wave engulfs the body, movement of different tissue masses causes shear waves to be generated which accelerate parts of the same organ to different velocities. As a result, tears or ruptures occur. Gas-filled organs are especially susceptible to this damage, with lungs being of greatest concern. As the lung tissue

is disorganized, fat and air emboli can enter pulmonary veins. These emboli, in turn, can lead to further damage or death to an organism via coronary or cerebral damage.

Although most of the body organs are susceptible to direct airblast effects, damage to the lungs tends to dominate fatalities and burdening injuries. The vulnerability of lungs to airblast effects is strongly dependent on orientational and positional factors (parallel or perpendicular to the blast wave and proximity to a blast-wave reflecting surface) as well as the pulse rise time and is weakly dependent on weapon yield (pulse length).

Secondary Airblast Effects. These effects include injuries and fatalities caused by the impact of energized debris (building and other structural fragments and missiles) lofted by the blast waves. They also include casualties resulting from structural failure of shelters (houses, basements, etc.). Secondary airblast effects are often the dominant airblast-related effects for people in or near unhardened structures.

Glass fragments created by the blast wave are one of the most serious missile hazards for low-yield nuclear weapons. However, glass fragments are highly directional, and thus only a small portion of rooms will be subject to these hazards (even though glass fragments may be found on any part of the floor after the explosion, the fragments which have a significant probability of causing serious wounds are very directional). Glass fragments are rapidly accelerated, and the casualty criteria for this hazard are thus relatively insensitive to the blast-wave duration (or weapon yield).

The criteria for hazards from other types of blast-energized missiles are highly variable, depending on missile size, shape, velocity, and region of body struck. For example, missiles of the same mass but different shape may vary in potential casualty production by a factor of three or more in their impact velocities.

Tertiary Airblast Effects. Whole-body translation of the human body due to blast-wind loading is termed a tertiary effect. This can result in the body being translated and then coming to rest by means of either a sudden impact or decelerative tumbling. If blast winds are sufficiently strong, the subject can be completely airborne for a brief period of time. The rate at which the subject loses kinetic energy is directly related to the probability of casualty. For this reason, decelerative tumbling or impact with a yielding surface presents the subject with the greatest probability of survival. The orientation of the body prior to arrival of the drag forces greatly affects the body motion produced.

Uncertainties. Uncertainties in personnel response to airblast effects are highly dependent on the type of shelter. For people in the open, direct effects (lung damage and eardrum rupture) and translation effects will dominate airblast injuries. As indicated, both translation effects and direct effects are very sensitive to body orientational and positional factors. For translation and impact with a flat, rigid object within about 10 feet of body travel, the uncertainty in a specific personnel response is about $\pm$ 50% in peak overpressure for a 90% confidence. For an individual located close to a reflecting surface, the uncertainty in personnel response to direct effects is about $\pm$ 40% for a 90% confidence.

For people located in aboveground portions of structures or in residential basements, the dominant damage mechanism results from structural failure and accompanying debris. This effect is very sensitive to the type of structure and the modes of failure. Therefore, the uncertainty in this effect is primarily due to the variation in types of structures and their dynamic breakup behavior more so than the understanding of basic

biomedical effects. Until additional analysis has been performed on the different types of structures which may be located in target areas, subjected to a loading characteristic of the airblast from low-yield weapons, the uncertainties in the casualty criteria for this effect must be taken to be fairly large. Present estimates of these uncertainties for 90% confidence are about a factor of two or three in peak overpressure for injuries and fatalities.

2.4 COMBINED INJURIES

Casualty probabilities P_i from different effects (airblast, thermal radiation, and the total ionizing radiation) are customarily combined as independent phenomena, viz. the total casualty probability is $P_{ind} = 1 - \pi_i(1-P_i)$. Any different combination of casualty probabilities is termed a "combined injury effect". These include both "synergistic" effects, $P > P_{ind}$, and "antagonistic" effects, $P < P_{ind}$, where one trauma either lowers or increases resistance to another trauma. A very brief review of animal experiments was made in an attempt to estimate the possible consequences of synergistic effects on fatality predictions for effects separated by short time intervals ($\lesssim$ 1 day).

The biomedical data examined were not satisfyingly consistent, and two trial algorithms, believed to bracket most of the data, were adopted for synergistically combining fatality probabilities from different effects: a "pessimistic" (high fatality) combination and an "optimistic" (low fatality) combination. These two algorithms were then used to calculate the fatality probability vs. ground range for one burst and shelter situation of interest; and the results were compared to those obtained

with the usual, independent combination algorithm. For the particular burst/shelter condition examined, the "pessimistic" synergistic combination results in significantly higher fatality probabilities at the larger ground ranges than the upper 90% confidence limit of the independent combination. Additional research is required on combined effects to determine whether or not they should be considered in casualty assessments.

3. WEAPON ENVIRONMENTS AND RELATED UNCERTAINTIES

This section contains a summary of the weapon environments and their uncertainties that are related to casualty effects. The weapon environments considered in the current analysis includes those produced by low-air bursts, i.e., at an altitude that precludes early-time fallout and significant levels of delayed radiation from activated surface materials. This altitude was considered to be at least a scaled height-of-burst of 180 feet/$KT^{1/3}$ (Ref. 3.1).

The weapon environments considered in this analysis included initial nuclear radiation (that radiation emitted within the first minute after the burst), airblast (with primary emphasis on peak overpressure) and thermal radiation. Nuclear radiation included prompt neutrons and gamma rays as well as secondary gamma rays (induced in the air, ground and structures).

Results from weapon environment physics computer codes in conjunction with experiemntal data are used to generate state-of-the-art prediction of weapon environments. Often these state-of-the-art results are modeled and incorporated into a fast-running, easy-to-use systems code for analysis of weapon effects. This modeling introduces an additional level of uncertainty in calculated environments which must be distinguished from the uncertainties associated with methods used for state-of-the-art physics predictions. For example, the uncertainties result from the Monte Carlo code, MORSE (Ref. 3.2) for nuclear radiation transport problem are different than the uncertainties associated with the use of the analyst model code, ATR (Ref. 3.3).

The uncertainty analysis discussed here is based on state-of-the-art predictions of weapon environments when possible or practical. Estimates will be presented, in certain instances, of the additional uncertainty in going from state-of-the-art to system models.

The output produced by nuclear weapons can vary from one warhead type to another. One could, with considerable difficulty, obtain uncertainties in weapon environments for all of the weapons in stockpile. We have not done this; we have assessed the uncertainties in environments for warhead classes, i.e., the main classes as described in EM-1 (Ref. 3.1). We have attempted to identify cases where the uncertainties for particular weapons are considerably different.

The weapon yield uncertainty (total energy output) is common to all of the weapon environments. There are a number of factors which influence the yield uncertainties including random errors related to material tolerances and impurities and to variations in the assembly. There may be non-random variations due to design characteristics. Bias errors or additional random errors may result from limited testing of the device type or weaponized system.

The uncertainty in weapon yield, for those warheads that are within a given class, is not generally a significant factor in casualty prediction. This uncertainty is typically less than than 15% (2σ - two standard deviations).

3.1 INITIAL NUCLEAR RADIATION

The most important aspects of initial nuclear radiation for collateral damage assessment are those properties which produce free-field radiation exposures in the range from a few to

about 10,000 rads (free-in-air tissue kerma or bone marrow dose). For a one-kiloton weapon, the ground range of interest is from about 0.5 to 2.0 km. This means that the most important aspects are the initial characteristics of the nuclear radiation output, the generation of secondary gamma rays by the interaction of neutrons with oxygen, nitrogen and hydrogen in air and the radiation transport of neutrons and gamma rays through significant distances in the atmosphere. The effects of the air/ground interface, structures and other shielding materials on both the radiation transport and secondary gamma-ray generation are also significant.

3.1.1 Uncertainty Parameters Considered

Estimates of nuclear radiation-related phenomena, such as dose, are primarily based on theoretical calculations. The calculational techniques and nuclear physics data required for these estimates have been calibrated and verified by a large number of physics measurements and benchmark analysis. Since the estimates are based on theoretical techniques, the uncertainty analysis involves a large number of parameters. The uncertainty analysis for nuclear radiation are divided into three parts, (1) those related to the source, (2) those related to radiation transport in the atmosphere, and (3) those related to transport through structures. These categories of uncertainties can be further partitioned into uncertainties associated with the problem configuration due either to random variation or lack of knowledge and uncertainties associated with physics used to predict the radiation environments for a specified configuration. The uncertainties studied in this analysis are provided in Table 3.1

Table 3.1 Uncertainty parameters for nuclear radiation environments.

	Source	Transport in Atmosphere	Transport in Structures
Configuration Uncertainties	Weapon Yield	Weapon detonation and target altitudes Air temperature and pressure Humidity/rain/snow Ground composition terrain Ground cover	Structure design Structure material Location/orientation of people
Paysics Uncertainties	Total neutron and gamma-ray output Neutron and gamma-ray energy distribution Neutron and gamma-ray angular distribution	Fireball rise and hydrodynamic enhancement models	Geometry modeling Nuclear data a) Neutron cross section b) Secondary gamma-ray production cross sections c) Gamma-ray cross sections

3.1.2 Source-Related Uncertainties

In addition to the yield uncertainty, there are uncertainties in the intensity of the prompt neutrons and gamma-rays as well as in their energy and angular distributions. The analysis for source-related uncertainties was performed for warhead classes since there are generally similarities in the nuclear radiation output for various warheads with each class.

It is important to realize that uncertainties in the total nuclear radiation source, in its energy variation and in its angular distribution are not necessarily independent. Prediction of weapon source terms commence with "burn calculations" which provide, in part, the generation of the neutrons and gamma rays during the initial phase of detonation. "Output calculations" are then performed to describe the transport of neutrons, and gamma rays and production of neutron induced secondary gamma rays during device disassembly. The output calculations may only model the bare device or may include effects of weaponization and the weapon carrier. The resulting source terms from output calculations depend on the level of geometrical detail (primarily affects the angular distribution and gamma-ray output) and the length of time past detonation that the calculation considers (primarily affects total intensity and energy distribution). For example, source terms from output calculations carried out to longer times will show more neutrons output and a softer energy spectrum due to longer interactions times in the debris. Thus the uncertainty in total neutron output is not independent of the uncertainty in the spectrum.

We assume for this analysis, that the output calculations provide all the significant radiation sources. Then given this fact, we ask the questions what are the calculational uncertainties

in the total output, the energy distribution and the angular distribution. On this basis, they become relatively independent parameters for uncertainty analysis.

Total Neutron and Gamma-Ray Output

The number of neutrons emitted per KT of yield (and associated uncertainties) is frequently reported separately from the total yield discussed above. For some cases these two effects are not separate, but the variation in neutron yield is for all practical purposes proportional to the variation in the total yield. The neutron yield, expressed in moles/KT, is also one parameter that is used in deciding to which warhead class a given device should be assigned. Thus, there is some natural variation associated with the classification schemes.

As discussed above one component of the uncertainty in neutron leakage per KT of yield is associated with the calculational method used in determining the neutron output. Calculations for many systems are performed for one-dimensional models of a bare device and, therefore, do not include the effects of weaponization of the device, warhead design, and warhead carrier. When one-dimensional models are used for calculation efficiency, the geometric model must be chosen with care. Typically two-dimensional calculations may indicate a 10-20% increase in total neutron leakage and the neutron spectrum will have a softer (lower energy) tail.

The uncertainty in the neutron output* (moles/KT) is about $\pm$20% for weapons within a warhead class when two-dimensional calculations have been performed for a weaponized system. The uncertainty is about $\pm$25% when one-dimensional calculations have been made. The uncertainties in total neutron output will have a direct effect on the neutron dose uncertainty as well as on

*Depends on the specific weapon.

the dose from air-secondary gamma rays. These uncertainties are in addition to the direct influence of total energy yield uncertainty.

The gamma-ray output, expressed in gamma-ray efficiency or MeV per KT of yield, is strongly dependent on the weapon class and the calculational model used. Estimates based on one-dimensional model of bare devices generally underestimate the intensity and the hardness of the gamma-ray energy spectrum. In general, if the prompt gamma-ray intensity is significant from a personnel dose exposure point of view, the gamma-ray output is dominated by neutron capture and inelastic scattering reactions in the warhead materials and in the weapon carrier. The intensity of the gamma rays is therefore sensitive to the gamma-ray production cross sections utilized in the calculations and is dependent to some extent on the number of neutrons remaining in the debris at the end of the calculation. Typically the inclusion of two-dimensional effects or the inclusion of a carrier model will increase the number of gamma rays predicted.

Comparisons of calculated and measured gamma-ray output indicates that, in some cases, the number of gamma rays/KT can be calculated for a given weapon test to within 20%. Experimental errors may be ±30% so that conclusions about uncertainties are questionable. If the base case is considered to be a weaponized system with carrier, an uncertainty of ±30% is reasonable. If the base case is a one-dimensional calculation of a bare device with a large fraction of neutrons remaining in the debris, then the uncertainty may be $^{+30}_{-70}$%. For most fission devices, the uncertainties would be of the order of ±30%.

Neutron/Gamma-Ray Energy Spectrum

The neutron spectrum uncertainties appear to be mostly associated with those neutron energies less than 0.1 MeV and above 10 MeV. The spectrum variation at low energies depends

on the amount of neutrons left in the debris at the end of the calculation and the weaponization treatment used in the calculation. Variations of a factor of ten or higher in the number of neutrons per unit energy below 0.1 MeV can result. The high energy (>10 MeV) component is sensitive to whether the weapon is a thermonuclear device. The uncertainties in energy spectra must be folded with the effects of transport in the atmosphere before they are meaningful.

Gamma-ray energy spectra may vary due to the calculational models, the cross sections and the treatment of movement of the materials during the calculation. The precision of experimental measurements to verify gamma-ray spectra limits the ability to place uncertainty estimates on weapon output. Uncertainties in spectra can be categorized by variations over 2-3 MeV wide energy intervals. An uncertainty of $\pm$40% over a 2 MeV interval is reasonable. The uncertainties in neutron and gamma-ray energy distributions, described above, must be translated into uncertainties in radiation exposure doses. To determine the effect on dose of various source energies, adjoint calculations were performed in an air-over-ground geometry using the DOT discrete ordinates code. Three importantance functions were generated which indicated the contribution to the dose as a function of some particle energy.

The importance functions are shown in Figure 3.1 for prompt neutrons and gamma rays at 1000 meters from a source located 120 meters above the air-ground interface. Also shown in the figure is the importance functions for secondary gamma rays (those created by neutron interactions) as a function of the neutron energy (which created the gamma rays).

The neutron dose importance is approximately constant above 2 MeV and decreases rapidly below 2 MeV. The secondary gamma-ray importance function has two distinct energy intervals. Above 7 MeV neutron energies, the gamma rays from inelastic

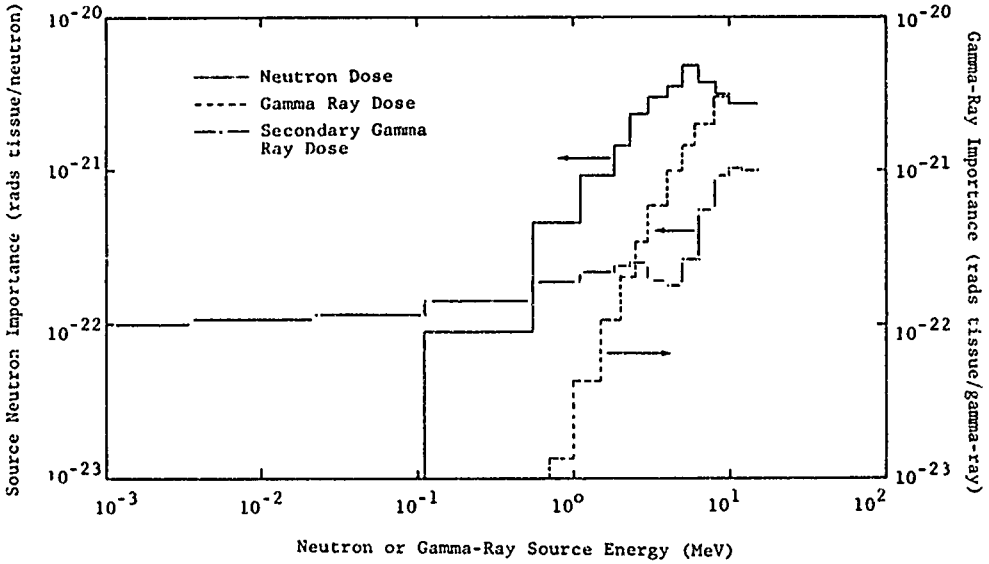

Figure 3.1. Source particle importance in contribution to tissue dose at a ground range of 1000 m for a source at 120 m.

scattering in ground materials and charged particle reactions in air make the significant contributions to the gamma-ray dose. Source neutrons with energies less than 0.1 MeV produce gamma rays by radiative neutron capture reactions in air as well as ground materials. Since secondary gamma-ray energies as well as total energy is fairly independent of the neutron's energy, this part of the response function is constant with energy (0.001 to 0.1 MeV).

The energy importance of prompt gamma rays decreases very rapidly as the gamma-ray energy decreases. Since the importance falls almost proportional to energy, i.e., decreases a factor of 20 for a gamma ray energy change from 10 to 1 MeV, the dose is almost proportional to total gamma-ray energy above 1 MeV with only a small change due to shape.

To determine the impact on dose of changes in neutron source spectral shapes, changes for three broad energy intervals were considered. These energy intervals were <0.1 MeV, 0.1 to 8 MeV and >8 MeV. Changes in dose were determined for positive and negative changes of $\mp$45%, $\pm$15%, $\pm$30%, respectively, in the number of neutrons for the energy bands. That is, if neutrons were removed from one interval, they were added to another. For prompt gamma rays the number of gamma rays in a 2 MeV-wide interval was changed by 40%. Again, when gamma-rays were removed from one interval they were added to another. Table 3.2 shows the effect on tissue dose of the uncertainties in source spectral shape. Changes in tissue dose vary from 12% for secondary gamma rays to 16% for neutrons to 30% for prompt gamma rays.

The importance of source energy spectrum for fission product gamma rays was determined for a 10-KT burst at 130 meters above the ground. A simple time-averaged energy spectrum was

Table 3.2. Uncertainty in tissue dose due to uncertainties in source energy spectra.

Dose Component	Dose Uncertainty (%) * (2σ)
Prompt Neutrons	± 16
Prompt Gamma Rays	± 30
Secondary Gamma Rays	± 12

*at one kilometer.

used, curve labeled IDEA(75) in Figure 3.2, and a time-energy distribution for uranium and plutonium was also considered. A change in this component of dose of about 50% can result. Results from ATR-4 are also given.

Uncertainties in the Neutron and Gamma-Ray Angular Distributions

The angular distributions of the neutron output from weapons is generally treated as being isotropic. It is therefore appropriate to treat any variations in the angular distribution as being an uncertainty.

The variations in angular distributions are due to the effects of asymmetric warhead and/or weapon design factors. These effects were analyzed for several weapon systems. In the most extreme case, there was a factor of five reduction in the number of neutrons emitted in the forward angles as compared to those emitted at 90^{o} (to the side). For other cases, more typical of tactical nuclear weapons, there were variations of about ±25%. These variations, now considered to be uncertainties, must be folded into the radiation transport analysis to determine the uncertainty in dose.

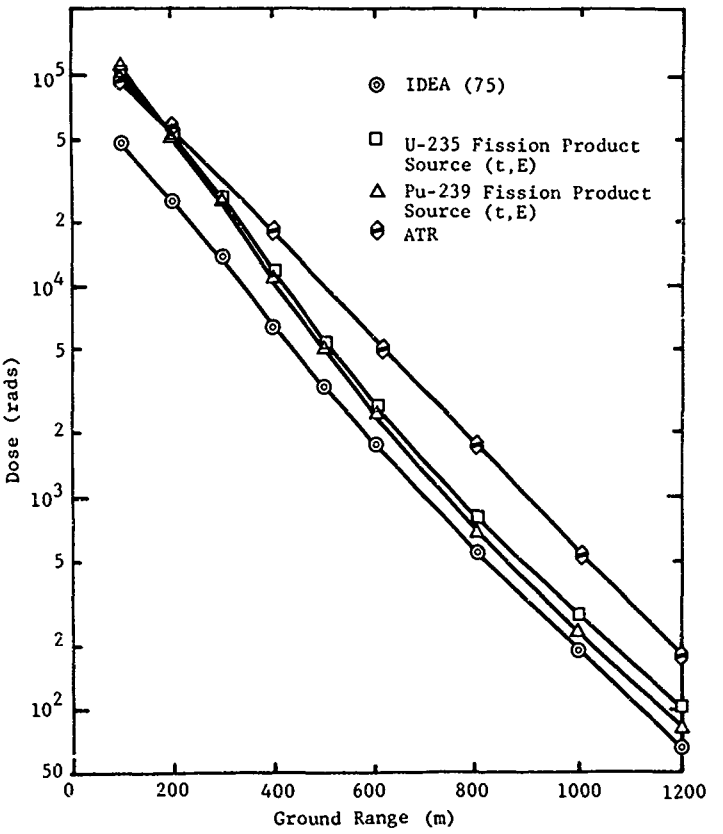

Figure 3.2. Calculated tissue dose from three fission product gamma-ray source models in IDEA. Results from ATR are also given for the 10 KT burst 130 meters above ground.

The angular variations of output gamma-rays are generally less than for neutrons for the same weapon. Again the variations in gamma-ray angular distributions must be treated as uncertainties and they result from asymmetries in the warhead and packaging configuration. In the most extreme case analyzed, there was a 30% reduction in gamma-rays emitted in the forward direction compared to the number emitted at 90^{o}.

An analysis was made of the impact that angular variations of neutrons and gamma-rays on the exposure dose. Calculations were made to obtain the energy-angular dependent importance function in infinite air. Although the air-ground interface has an effect on the importance function, it was considered to be secondary in this analysis. The analysis was made for three source spectra (appropriate for output neutron and gamma-ray energy spectra for different warhead types). Figure 3.3 shows the angular importance at 600 and 900 meters for a boosted fission source. The results from the other sources were similar to that from the boosted fission source.

The asymmetry in the neutron importance indicates that a neutron emitted toward the detector is about 20 times more important than one emitted in the opposite direction. Thus a reduction in the source emitted toward the detector will have a significant reduction in the dose whereas a shadowing of the source in the backward direction is not as important.

The angular importance of neutrons emitted in various directions also affects the secondary gamma rays with a resulting variation in dose of a factor of 5. A far larger variation results for prompt gamma rays in which the importance varies by a factor of about 4000 between the forward and backward directions. Because of numerical problems in calculating gradients of a few thousand or more, there is some uncertainty in the actual values in the backward direction.

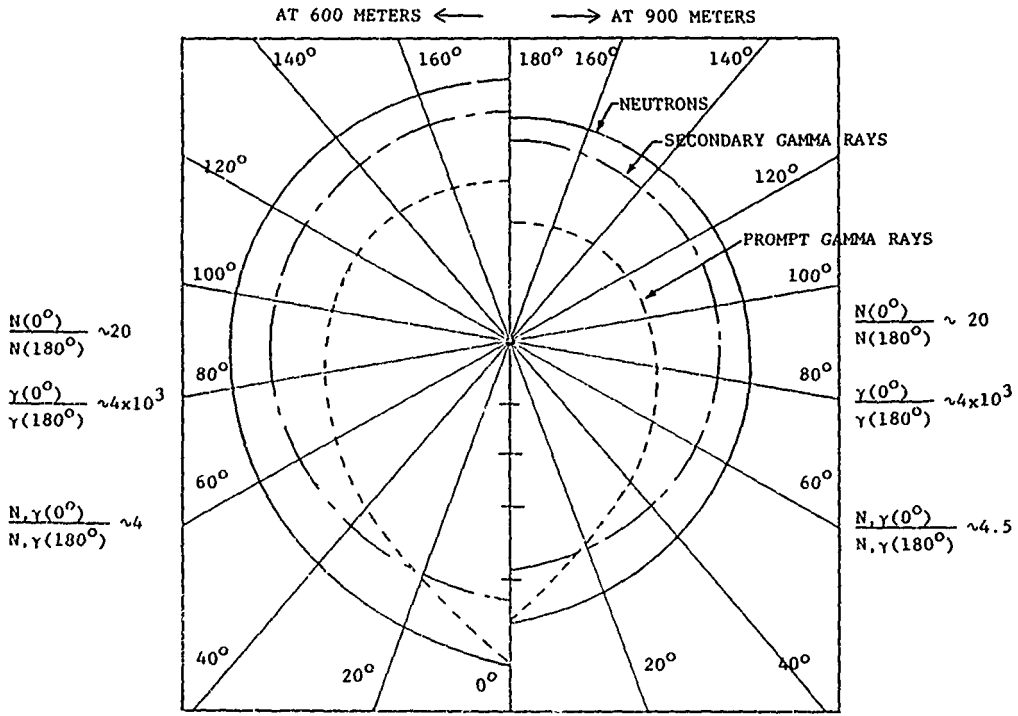

Figure 3.3. Source particle angular importance for a boosted fission weapon.

Since the importance calculations are one-dimensional, the angles are measured from the source-detector axis. In practice, a weapon may be oriented at almost any angle with respect to this axis. For purposes of this analysis, the ratio of the dose in the forward, backward and side direction relative to an isotropic source was determined for a "typical" source. Table 3.3 gives the results.

Table 3.3. Effect of source asymmetry on tissue dose at 900 meters.

	Ratio of Dose to Isotropic Source		
	Forward	Backward	Side
Neutrons	0.93	0.83	1.20
Secondary Gamma Rays	0.99	0.95	1.03
Prompt Gamma Rays			
(Source 1)	0.80	0.46	1.38
(Source 2)	0.94	0.72	1.20

An analysis was made of the impact of uncertainties related to neutron energy and angular distribution on the neutron dose for a low yield boosted fission weapon. The combined effects are shown in Figure 3.4. This figure shows that uncertainties due to energy and angular distributions made on independent contributions of about 20 percent (2σ) uncertainty in the neutron base at 1 km from the burst point. This uncertainty will approximately double with each additional km from the burst point.

3.1.3 Radiation Transport in the Atmosphere

There are several important uncertainties related to transport in the atmosphere. These uncertainties include configuration and physics uncertainties involved in the prediction of the propagation of nuclear radiation from the source through the atmosphere

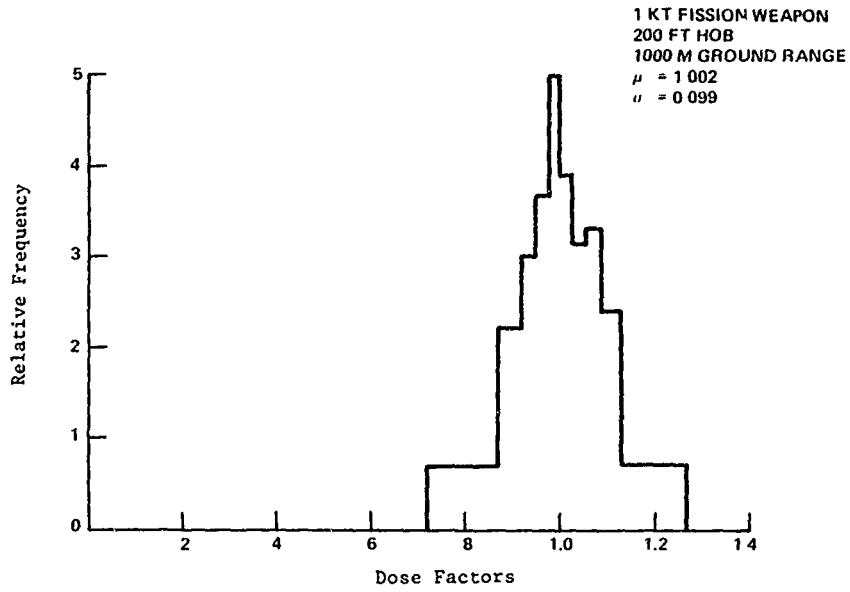

Figure 3 4. Impact of neutron energy and angular distribution uncertainties of dose uncertainty

(and ground) to the vicinity of the target. The effects of the transport in the vicinity of target (such as transport through a structure) is discussed later. The radiation environment which does not include the target-specific details is often called the "free field" environment. Thus, here we discuss the uncertainties associated with the estimation of the free field environment.

Atmospheric Density

It is possible to predict the radiation environment for a given air density if it is known; however, the effect of variations in atmospheric density due to changes in altitude, temperature and barametric pressure are treated in air at sea level are scaled to other densities using the mass thickness of air between the source and detector for the two densities. By picking the actual density from a frequency distribution based on meterological data, an estimate of the "uncertainty" can be calculated.

The technique for scaling radiation transport to different atmospheric densities is commonly referred to as "Rho-r" scaling. It is mathematically rigorous for a time independent problem for a point source in a uniform, homogeneous spherical system. The prescription for Rho-r scaling is given by three equations:

$$\text{if} \qquad \rho_1 = K\rho_2$$

$$\text{and if} \qquad R_1\rho_1 = R_2\rho_2$$

$$\text{then} \qquad \phi_1(R_1) = K^2\phi_2(R_2)$$

where K is the density scale factor and ρ_i, R_i, $\phi_i(R_i)$ are the density, slant range, and flux in system i. Thus, if one has a data base of fluxes computed with a density ρ_2 he can find the flux in a system with density ρ_1. Application of Rho-r scaling would be strictly true in air over ground geometry if we permit the

ground density to change by the same ratio as the air density. Of course, the HOB and ground range also change by the same ratio. The effect on the dose from scaling the slant range, however, dominates effects from altering the HOB or ground density. To compensate for air density variations we will apply Rho-r scaling to the dose as a function of slant range and ignore scaling for the HOB or ground density. The ratio of the dose as a function of the density ratio is presented in Figure 3.5 for the neutron, secondary gamma-ray and prompt gamma-ray components. The ratios are slighly different for each component because the variation with slant range is different. Note that a 10% reduction in density (approximately equivalent to going from sea level to 1000 m altitude) results in a 40-60% increase in the dose.

Air-Ground Correction

The ground has a significant effect on the transport of radiation due to the closeness to the source and detector of a high density (relative to air) material medium. The effects are greatest on the thermalization of neutrons and the production of secondary gamma rays. Most analyses in the past have been based on infinite air results with correction factors applied to account for the air-ground interface. Detailed air-ground calculations have been made (Refs. 3.4, 3.5 and 3.6) for a variety of conditions as noted in Table 3.3. The results of Pace, et al. (Ref. 3.5) were used to determine the ground correction factors for the ATR-4 code (Ref. 3.3).

The effects of ground composition on radiation transport was investigated by Gritzner, et al (Ref. 3.6) using one-dimensional sensitivity calculations. The calculation model for the study was slab geometry consisting of 50 cm of ground, a detector plane at 50 cm above the ground, a source plane at 100 m, and an air albedo surface at 700 m. A low yield thermonuclear source

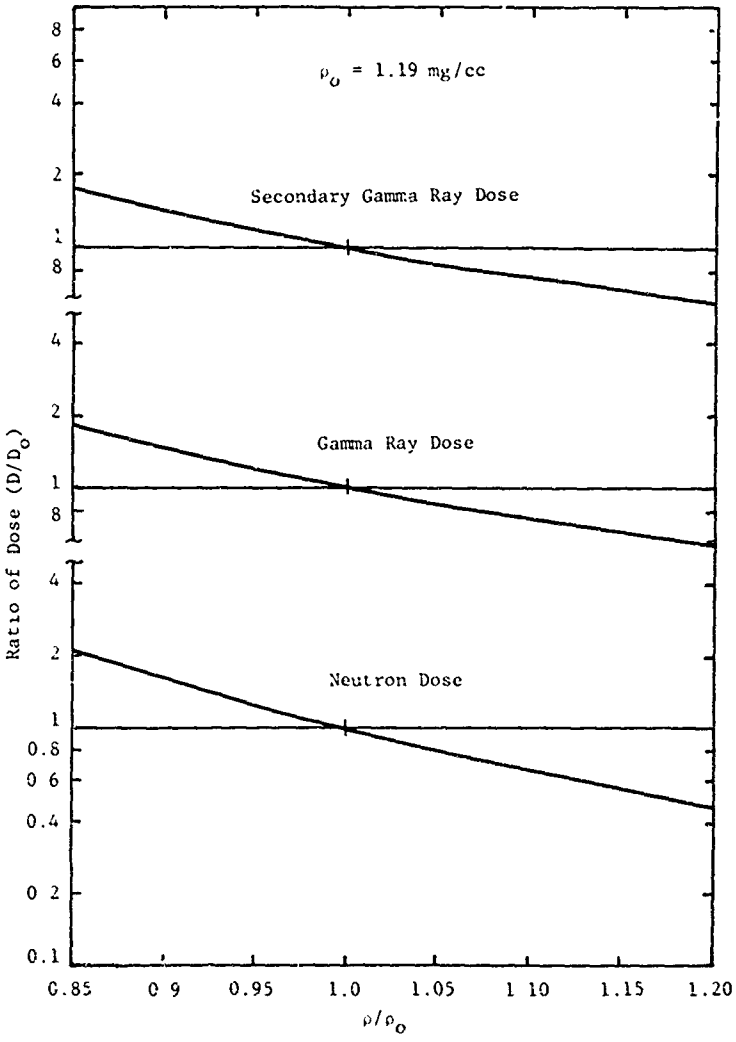

Figure 3.5 Variation of dose at 1000 meter ground range as a function of air density (130 meter HOB).

THIS
PAGE
IS
MISSING
IN
ORIGINAL
DOCUMENT

Table 3.4. Ground element sensitivities.

Element	Sensitivity*
H	-33.0
C	0.595
Ø	1.34
Na	0.462
Mg	1.93
Al	2.25
Si	1.33
K	5.24
Ca	0.0149
Ti	26.6
Cr	0.798
Mn	18.0
Fe	8.63
Mo	13.5

*Fractional change in dose due to a 1.0 atom/barn cm addition of the element.

Table 3.5. Composition of U.S. and Western European soils.

Atomic Concentration (atoms/barn·cm)[a]

Soil Type / Element	mean earth's crust	Central German Soils														United States Soils		
		sand	loess	clay	marl loam	shale	sand-stone	marl	lime-stone	granite	basalt	gneiss	slate	tuff	area wtd. average	sand (Florida)	clay (Hawaii)	Nevada desert
H	6.57(-4)	3.34(4)	9.70(-4)	5.35(-3)	3.09(-3)	3.34(3)	1.14(-3)	3.31(3)	2.68(-4)	4.01(-4)	1.20(-3)	8.98(-3)	2.18(-3)		1.10(-3)	8.00(-8)	5.02(-3)	4.18(-3)
C	1.60(-5)		8.02(-6)	4.52(-6)	1.12(3)	7.61(4)	1.37(5)	1.30(-3)	5.56(3)			4.63(-5)	1.07(3)	1.65(-4)	1.02(-3)		4.89(-3)	
O	1.76(3)	1.99(3)	1.56(-2)	1.90(-3)	1.65(2)	1.87(-3)	1.90(2)	1.97(-3)	1.61(2)	1.83(-2)	1.88(-2)	2.01(-2)	1.87(-3)		1.90(-2)	2.01(-2)	1.63(-1)	1.91(-2)
Na	7.33(-4)		2.35(-4)	1.15(4)	1.75(4)	1.53(4)	3.99(-5)	1.17(-4)	3.88(-5)	8.84(-4)	6.13(-4)	9.12(-4)	2.90(4)		9.81(-5)	2.00(7)	4.20(-5)	3.41(-4)
Mg	2.10(-4)	1.46(3)	2.24(-4)	9.23(4)	2.07(-4)	2.63(-4)	1.05(4)	3.81(-4)	1.20(-4)	2.06(-5)	8.58(-4)	6.93(-5)	3.84(-4)		1.61(-4)		9.40(-5)	9.90(6)
Al	1.53(-3)	1.54(-4)	9.23(-4)	1.78(-3)	1.23(-3)	1.83(3)	1.08(-3)	1.52(-3)	1.43(-4)	1.46(-3)	1.97(-3)	3.08(-3)	1.56(-3)		7.74(-4)	1.30(-6)	4.19(-3)	1.54(-3)
Si	5.04(3)	8.70(3)	6.02(-3)	9.46(-3)	5.83(-3)	9.83(3)	7.97(3)	4.42(3)	4.11(4)	1.34(-3)	4.96(-3)	9.53(-3)	5.51(-3)		6.63(-3)	1.00(-3)	2.10(-3)	6.84(-3)
K	3.09(-3)	1.43(-4)	2.84(-4)	8.14(-4)	3.84(-4)	4.14(4)	5.78(-4)	4.80(-4)	7.07(5)	8.27(-4)	2.09(-4)	1.79(-3)	3.84(-4)		2.90(-4)		1.34(-4)	6.18(-4)
Ca	5.46(-4)	1.07(-4)	7.41(-4)	3.65(-4)	9.68(-4)	3.34(-4)	1.07(3)	1.18(-3)	8.55(-3)	5.27(-5)	9.56(-4)	1.72(-3)	8.33(-4)		9.56(4)		6.80(5)	3.61(-4)
Ti	3.56(-3)				2.04(-3)	4.80(3)		8.66(-3)		1.31(3)	2.00(-4)	7.78(-3)	4.30(-3)		4.83(-3)	3.00(-7)	1.58(-3)	3.40(-3)
Cr														1.27(-4)			8.00(-6)	
Mn	1.10(-3)				4.24(4)			7.64(5)		9.48(-5)	2.35(-3)	3.35(-3)		6.84(5)	1.15(-3)		3.22(-4)	4.60(-4)
Fe	3.39(-4)	1.31(3)	1.88(-4)	3.32(-4)	2.15(-4)	9.08(-4)	3.80(4)	3.93(-4)	5.28(-3)	2.52(-4)	9.35(-4)	6.93(-4)	4.34(-4)	1.05(-2)	1.75(-4)	5.00(-7)	1.15(-3)	3.54(-3)
Mo														1.87(-3)				

a. Atomic concentrations are given for a ground density of 1 gm/cm^3.

Table 3.6. Sensitivity of total dose to soil type.

Soil Type	Correction Factor, C*
Mean Earth's Crust	1.0
Central German	
sand	1.03
loess	0.99
clay	0.71
marl/loam	0.92
shale	0.84
sandstone	0.98
marl	0.84
limestone	1.01
granite	1.03
basalt	0.99
gneiss	0.61
slate	0.92
topsoil	1.15
United States	
beach sand	1.05
lava clay	0.72
Nevada desert	0.82

*The correction factor is the ratio of the dose expected for the particular soil to the dose obtained for the baseline case.

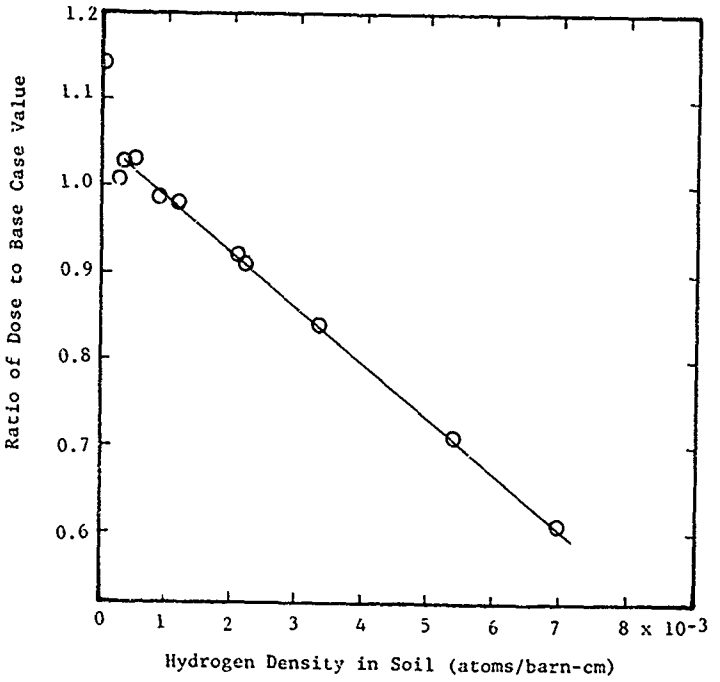

Figure 3.6. Correlation of total tissue dose with hydrogen content of soil.

Gritzner's, et al, sensitivity data has two limitations for direct use in the uncertainty analysis of damage functions. In the first place, the relative contribution to total dose from neutrons, secondary gamma rays, and prompt gamma rays changes as a function of ground range. In the one-dimensional calculations of Gritzner there was no ground range dependence, and thus the sensitivity results are appropriate only for the ranges for which dose contributions are nearly equal to Gritzner's. For the model used, 90% of the dose from neutrons and secondary gamma rays came from neutrons. A typical value at 1-km ground range is about 75%. Secondly, the analysis was performed for relatively low concentrations of hydrogen. At higher concentrations, the addition of more hydrogen probably has less relative effect than at lower initial concentrations.

The air-over-ground calculations of Gritzner (Ref. 3.6) and Pace (Ref. 3.5) and the air-over-seawater calculations of Pace (Ref. 3.5) can be used to investigate the effect of hydrogen content in the soil on transport. The Gritzner calculations used a hydrogen content of 1.753×10^{-3} atoms/barn-cm in a soil of density 1.6 gm/cc. Pace used a hydrogen concentration of 9.7×10^{-3} atoms/barn-cm in soil of density 1.7 gm/cc. A comparison of dose ratio from these two calculations for three source spectra and two burst heights is shown in Table 3.7. It is clear that the variation is significant (as much as a factor of 16); and it is a strong function of source spectra and height-of-burst. Comparisons of the neutron dose in air-over-ground and air-over-seawater are shown in Table 3.8 from the Pace data. The hydrogen content of seawater was taken to be 6.64×10^{-2} atoms/barn-cm.

The variation of hydrogen content in the soil results in a major uncertainty in the tissue dose. Further work is needed to accomplish the following tasks:

Table 3.7. Ratio of dose calculated for dry soil to dose calculated for wet soil.

Ground Range(m)	Surface Burst								
	S_1 *			S_2			S_3		
	N	γ	(N,γ)	N	γ	(N,γ)	N	γ	(N,γ)
205	1.35	0.76	0.76	1.71	0.82	1.32	1.21	0.82	1.08
410	1.28	0.69	0.93	1.53	0.78	1.42	1.20	0.78	1.10
615	1.22	0.62	1.01	1.37	0.70	1.40	1.12	0.74	1.08
820	1.28	0.59	1.16	1.28	0.68	1.39	1.11	0.72	1.16
1025	1.40	0.58	1.23	1.32	0.64	1.40	1.19	0.70	1.23
	61 Meter Height of Burst								
	S_1			S_2			S_3		
207	1.42	1.01	0.77	1.9	1.09	1.22	1.38	1.11	1.03
411	1.41	0.96	0.84	1.69	1.02	1.19	1.35	1.07	1.02
615	1.54	0.92	0.91	1.60	1.01	1.22	1.31	1.01	0.96
820	1.51	0.89	1.04	1.51	0.99	1.20	1.33	1.05	1.02
1026	1.68	0.84	1.15	1.53	0.96	1.24	1.42	1.04	1.14

* Sources:

S1 Boosted fission

S2 Enhanced radiation

S3 Suppressed radiation

1. Quantification of the dose variation as a function hydrogen content over the range of interest as function of source spectra, height-of-burst and ground range

2. Determining the range of hydrogen congent in soils.

3. Effects of rain water and water retention by plants on radiation transport.

Table 3.8. Summary of neutron tissue dose calculations for air-over-ground and air-over-seawater.

Ground Range (m)	Neutron Dose in Rads/Source Neutron					
	Fission Source			14 MeV Source		
	A/G	A/SW	Ratio	A/G	A/SW	Ratio
515	1.73-20	1.14-20	1.52	5.35-20	4.27-20	1.25
995	3.50-22	2.29-22	1.53	1.98-21	1.48-21	1.34

Terrain Effects

Detailed radiation environments computed for tactical nuclear weapon detonations almost always use a flat air/ground interface, i.e., level terrain. The treatment of the air/ground interface as a plane results in a less complex problem computationally, provides a good model to compare with test data in most instances; and has a more universal application than models incorporating realistic terrain. The distances of interest for the study of military and collateral damage from low to intermediate yield are in the range of several kilometers. Thus, terrain features which might effect the radiation environment involving geographic areas of a couple of square kilometers introduce an uncertainty in the damage estimates using flat earth radiation environment calculations.

A study of terrain effects on radiation environments from tactical nuclear weapons was performed by Albert, et al. (Ref. 3.7). This research, although not definitive, provides the most detailed data base available from which to ascertain uncertainty in damage due to terrain effects on radiation transport. Albert's work is summarized here. Albert investigated the effect of dense forest cover, topography, and small bodies of water on the tissue dose from prompt neutrons, prompt gamma rays, and secondary gamma rays.

The study of the effect of dense forest covers showed that for ground ranges greater than 300 meters the ratio of dose in the forest to the dose in open is relatively constant. The dose ratio varied 10% to 15% with different source spectra. The maximum attenuation of about 0.35 was found for surface bursts which increased to about 0.6 for a 160 m burst height. The attenuation was found to be dominated by the character of the forest near the detector and thus interpolation for less dense forest conditions should be based on the distribution around the detector.

Analysis of radiation environments produced in valleys indicated that the dose could be predicted by geometric scaling of the flat earth data. That is, the dose corresponding to true ground ranges, shown in Figure 3.7, as distinguished from the map ground range, agreed with the flat earth, conventional transport calculation.

Calculations of the terrain effects from hills showed that no significant effect could be attributed to the presence of the hill when a line of sight existed between the source and detector. In shadowed regions, terrain attenuation of up to factors of five for common terrain were found.

An analysis by Albert for situations in which terrain obscured the line of sight between the source and detector showed a reasonable pattern of consistency when the attentuation factors were plotted as functions of the angle the intervening terrain

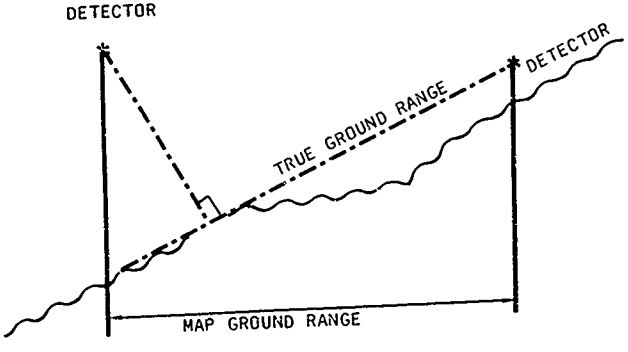

Figure 3.7. Depiction of true and map ground ranges from a nuclear burst in a valley.

subtends with the source and detector. These angles α_s and α_D are illustrated in Figure 3.8.

The terrain attenuation factor defined as the ratio of the tissue dose at a given horizontal range for flat earth to the corresponding value with terrain is plotted as contours in Figure 3.9 for α_s and α_D values. The solid lines are estimates of the iso-attentuation factor contour and the symbols show calculated data points. The agreement is reasonable.

Calculations including small bodies of water found no significant effects on the dose from tactical nuclear weapons. Thus we have neglected the possible uncertainties arising from the presence of lakes and rivers

Cross Sections

There are two components of the possible uncertainties due to cross sections. One is due to the lack of knowledge of the detailed cross sections and the other is due to the processing and use of the data in computer codes For the effect of uncertainties in the basic data, the DNA evaluation of oxygen and nitrogen contain error files which give the uncertainty for each cross section. These data have been processed by ORNL staff with the resulting uncertainty of total dose in air from a thermonuclear source determined. In addition, the specific cross sections that are most important to the calculation of dose were determined.

The sensitivities calculated for the several partial cross sections involved in the problem are a measure of the influence or importance of the particular cross sections for the problem result. Table 3.9 shows the sensitivies calculated by Bartine (Ref. 3.8). The tissue dose can be seen to be primarily sensitive to the nitrogen neutron cross sections.

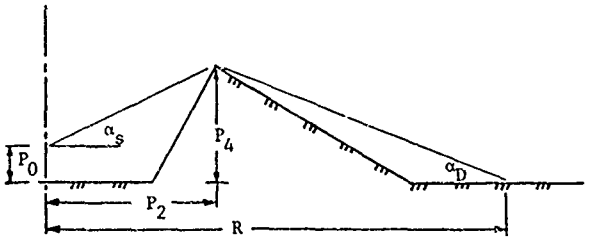

$$\alpha_s = \arctan\left(\frac{P_4 - P_0}{P_2}\right)$$

$$\alpha_D = \arctan\left(\frac{P_4}{R - P_2}\right)$$

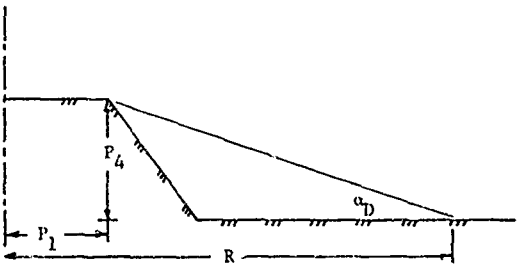

$$\alpha_D = \arctan\left(\frac{P_4}{R - P_1}\right)$$

Figure 3.8. Illustration of subtended angles for obscuring terrain.

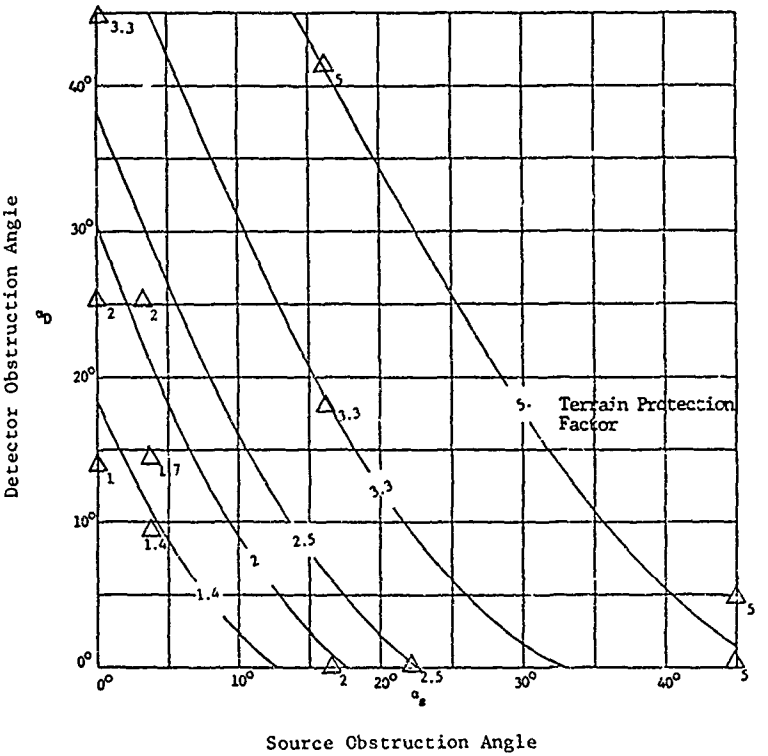

Figure 3.9. A Simple parameterization of the idealized hill calculations (triangles indicate calculated results for specific geometries).

Table 3.9. Sensitivity of the total tissue dose to the indicated nitrogen and oxygen cross sections.

Reaction	Sensitivity (Relative Importance)* N_2	O_2	Air (Total)
$\Sigma_{COLL\ (N+\gamma)}$	-6.08	-1.42	-7.50
$\Sigma_{COLL\ (N)}$	-5.25	-1.16	-6.41
$\Sigma_{COLL\ (\gamma)}$	-0.83	-0.26	-1.09
Σ_{EL}	-3.17	-0.94	-4.11
Σ_{INEL}	-0.55	0.09	-0.64
Σ_{ABS}	-1.53	-0.13	-1.66
$\Sigma_{(N,\gamma)}$	+0.12	0.00	+0.12
$\Sigma_{(N,P)}$	-0.45	-0.01	-0.46
$\Sigma_{(N,D)}$	-0.10	0.00	-0.10
$\Sigma_{(N,T)}$	-0.08		-0.08
$\Sigma_{(N,P)} + \Sigma_{(N,D)} + \Sigma_{(N,T)}$	-0.63	-0.01	-0.64
$\Sigma_{(N,\alpha)}$	-1.00	-0.12	
$\Sigma_{(n,2\alpha)}$	-0.02		-0.02
$\Sigma_{(N,N')}$	0.00		0.00

*Values in table represent the percent change in dose resulting from a 1 percent increase in all energies in that specific cross section.

Error estimates of the various cross sections can be combined with the sensitivity calculations to yield estimates of the resulting uncertainties in tissue dose. Table 3.10 shows the estimated uncertainties in the evaluated nitrogen neutron cross sections. Bartine's analysis was based on a rather coarse indication of the cross section energy dependent uncertainty correlations. The results of the tissue dose uncertainties due to neutron cross section uncertainties are shown in Table 3 11. The nitrogen (n,α) cross section was identified as the primary contributor to the uncertainty. The uncertainty in the tissue dose due to uncertainties in the nitrogen neutron cross section are quoted to be 29%. Tables similar to Tables 3.9 and 3.10 are included in Ref. 3.8 for the oxygen neutron cross sections and the nitrogen and oxygen gamma ray cross sections. The uncertainties resulting from these cross sections are negligibly small compared to the nitrogen neutron cross section.

A reiteration of Bartine's analysis was performed by Weisbin (Ref. 3.9) with the only change being improved uncertainty and uncertainty correlation estimates. The results of the sensitivity analysis were substantially lower (more than a fractor of two). The total tissue dose uncertainty was estimated to be 14.5%. The difference is attributable to the use of the more detailed covariance files available to the latter investigator. The sensitivity analyses performed were based on a very precise mathematical formalism, unfortunately, the results of the analysis are based on data (errors and covariance matrices) which are not so exact.

Analysis (Ref. 3.8) was also performed to determine uncertainties in results due to processing of cross sections into multigroup form (for use in discrete ordinates codes). Although, the analysis is not directly applicable to the problem of interest since the group structure is not that used in any of the recent calculations, it is believed that the estimate of 7%

Table 3.10. Estimated percent uncertainty in the evaluated nitrogen neutron cross sections (From Ref. 3.8)

Cross Section	Thermal	Midpoint of Energy Range (MeV) 1	1	2	5	8	11	14
Total	3	3	1	1	1	1	1	1
Elastic	3	3	1	1	10	10	15	10
Inelastic					30	20	20	20
(n α)	10	400	400	400	200	200	200	200
(n,d)+(n,p)+(n,t)	5	30	30	30	30	40	40	30
(n,α)				40	30	30	30	30
(n,2α)								50
(n,2n')								20

Table 3.11. Estimated percent uncertainty in total tissue dose due to estimated uncertainty in nitrogen neutron cross sections.

Cross Section	Midpoint of Energy Range (MeV)								Sum Over All Energy Ranges
	Thermal	0.1	1	2	5	8	11	14	
Total	0.0006	0.700	0.599	1.09	0.501	0.424	0.896	0.542	4.75 Corr[1]
Elastic	0.603[2]	2.47[2]	1.91[2]	8.98[2]	10.59[2]	4.73[2]	6.71	2.62	9.33 Corr > 10 MeV
Inelastic				0.017	1.15	2.04	6.92[2]	2.84[2]	3.21 Corr < 10 MeV
(n,γ)	0.53	0.63	0.02	0.024	0.006	0.004	0.00	0.00	1.21 Corr
(n,d)+(n,p) +(n,t)	0.287	2.28	1.79	2.33	1.92	2.35	1.13	0.703	12.79 Corr
(n,α)			0.284	8.60	10.34	3.54	0.86	0.54	24.16 Corr
(n,2α)							0.045	0.345	0.39 Corr
(n,2n)							0.002	0.017	0.02 Corr
									29.48

[1] Estimated overall calculational uncertainty due to uncertainties in neutron cross sections (Table 3.10).

[2] Uncorrelated summation of the uncertainties due to all measured cross sections for the designated energy range. Other summations assume total correlation.

uncertainty in the dose is reasonable. It is noted, however, that it would be possible to observe much larger effects of too few groups were used or if the group boundaries were not chosen with care.

Since data does not exist for ranges other than 2000 meters, the range dependence of the uncertainty factors has been "estimated". Table 3.12 gives the recommended values. It is realized that the values in Table 3.12 do not agree with the conclusions of Ref. 3.10. Staff at the Ballistics Research Laboratory conclude that based on their analysis using Monte Carlo techniques that:

> "Results show that the requirements for predicting radiation transport in air to ± 25% cannot be met with the accuracies currently available in the neutron cross sections for elastic scattering in nitrogen "

Further analysis is required to resolve the conflicting conclusions of the independent studies. However, such studies are beyond the scope of the current work.

Table 3.12. Dose uncertainties due to cross sections.

	Range (ρ = 1.19 mg/cc)	
	1000 m	2000 m
	Percent	
Neutron	15.	30.
Secondary gamma ray dose	15.	30.
Prompt gamma ray dose	5.	10.
Fission product dose	5.	10.

3.2 AIRBLAST

Airblast is the dominant cause of injuries and fatalities for people in structures for weapon yields greater than about 10 KT. As was briefly outlined in Section 2, there are three categories of blast related casualty mechanisms (direct effects on body organs, secondary effects of the impact of debris and glass on the body and tertiary effects of whole body translation). Direct effects are sensitive to the diffraction loading on the body and are dependent on the peak overpressure as well as the overpressure impulse. Secondary effects are dependent on the peak overpressure as well as the dynamic pressure. Tertiary effects are primarily dependent on the dynamic pressure.

The predictions of airblast properties (peak overpressure, dynamic pressure and impulse) are primarily based on experimental data. The current best estimate of airblast properties are given in Ref. 3.11 for the close-in properties and Ref. 3.1 for the lower level ($\lesssim$50 psi) airblast properties.

The uncertainties in airblast properties is dependent on a number of factors. These are summarized in Table 3.13. The major uncertainty areas are discussed below.

Table 3.13. Sources of Airblast Uncertainties

Source Related
Yield
Height of Burst
Propagation Related
Airblast Representation
Target Altitude
Weather (snow/rain)
Terrain
Temperature
Air Pressure
Around Structures

3.2.1 Height of Burst

Height of burst uncertainties for airburst weapons depend on the type of fuzes used and this is very weapon specific. For a given weapon system the height of burst uncertainty may depend on the range and on the height of burst setting. The uncertainties range from about five percent (two standard deviations) to about sixty percent. Most systems have height of burst uncertainties in the range from 20 to 30 percent.

Figure 3.10 shows the dependence of the peak overpressure on the height of burst for overpressures in the region of interest to collateral damage effects (~2 to 10 psi). At 10 psi, a 30 percent error in height of burst would result in an uncertainty of about seven percent in peak overpressure and less than five percent uncertainty in ground range. At 2 psi, a 30 percent uncertainty would result in an uncertainty of about two percent in peak overpressure and about five percent in ground range.

3.2.2 Yield Uncertainty

The uncertainty in weapon yield will depend on the specific weapon. With a few exceptions, these uncertainties are less than 15 percent (2 standard deviations). This uncertainty results in a range uncertainty of about 5 percent and an uncertainty of less than 10 percent in peak overpressure.

3.2.3 Airblast Representation

The data used in this analysis for airblast representatives was taken from Brode (Ref. 3.11) and EM-1 (Ref. 3.1). These data were, in turn, based on a theoretical and analytical interpretation of a series of experimental tests (Ref. 3.12). One measure of the uncertainties in airblast parameters (peak overpressure, dynamic pressure and overpressure impulses) can be determined by analyzing how well the experimental data could be fit. Cockoyne and Lofgren (Ref. 3.13) performed such an

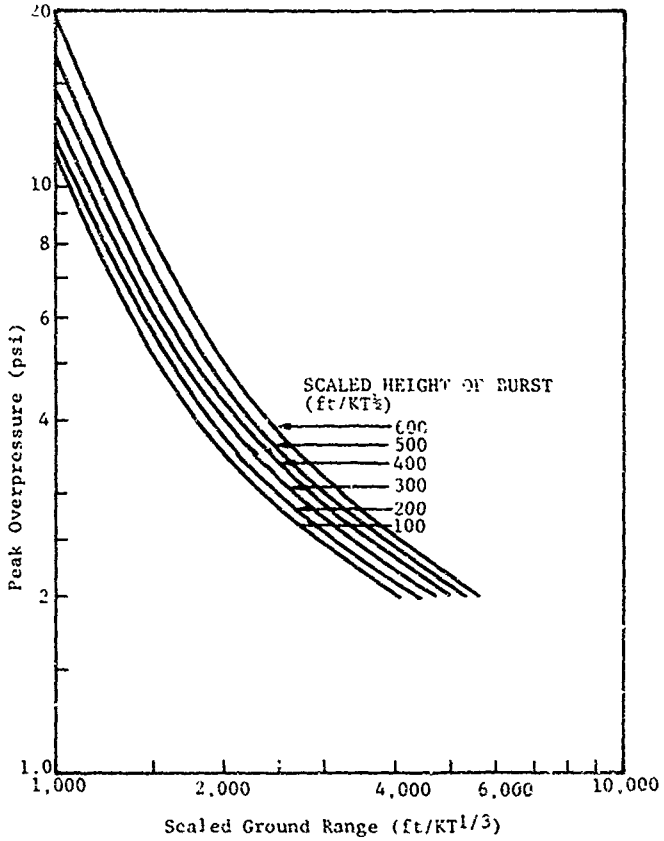

Figure 3.10 Peak Overpressure HOB Dependance.

analysis. The results of this analysis are shown in Tables 3.14 through 3.16 for peak overpressure, dynamic pressure and overpressure impulse, respectively. This analysis indicated that the uncertainties in ground range (for the same level of an airblast parameter) was approximately 20 to 30 percent. This is approximately 50 percent in peak overpressure at 10 psi and approximately 15 percent uncertainty in peak overpressure at 4 psi.

Cockoyne and Lofgren (Ref. 3.13) used all of the experimental data points in their analysis. Another way of assessing the uncertainty is to compare the best fit curves (for each set of experiment data) to the representations given in Ref. 3.1 and 3.12. The results of this analysis are shown in Figure 3.11 for near-surface burst tests and Figure 3.12 for low-air scaled heights of burst. Each point shown in the figure represents a point taken from the "best" curves drawn through the experimental points for a particular test. For near surface tests, 90 percent of the points fall within $\pm$15 percent (in ground range) of the values given in Ref. 3.1 and 3.11.

3.2.4 Rain or Fog

Although the effects of rain or fog on the blast wave are not well known (Ref. 3.1), there is qualitative agreement between theoretical predictions and the available experimental data. The vaporization of water absorbs a small amount of the energy that would otherwise to available for blast wave propagation. This effect is to reduce the intensity of the blast wave. Figure 3.13 shows the reduction in effective yield for light and heavy rain.

For a heavy rain condition, the yield reduction factor of a one kiloton weapon would be about 0.83 for the 5 psi peak overpressure region. This results in a reduction, in range, of approximately six percent or a reduction of about twelve percent in peak overpressure

Table 3.14. Uncertainties in Peak Overpressure Data

Uncertainty in Scaled Ground Range (%)[a]				
SHOB ($ft/KT^{1/3}$) / Scaled Range ($ft/KT^{1/3}$)	0-3.1	182-205	212-252	323-375
237	11	10	-[b]	
287	14	5	-	
348	10	10	-	
422	11	14	12	
511	13	16	22	6
620	07	22	22	-
750	11	28	25	25
909	9	23	14	14
1101	17	17	15	18
1334	09	14	13	13
1616	07	07	-	12
1957	11	15	-	13
2371	15	-	-	4
2873	04	-	-	16
Average	11	17	18	14

[a] Standard deviation

[b] No experimental data

Table 3.15. Uncertainties in peak dynamic pressure.

Uncertainty in Scaled Ground Range (%)			
SHOB ($ft/KT^{1/3}$) / Scaled Range ($ft/KT^{1/3}$)	0-3.1	182-204	2.2-252
316	.14	-	.32
681	11	.27	.14
1467	.14	.19	-
Average	.12	.23	.23

Table 3.16. Uncertainties in Overpressure Impulse Data

Uncertainty in Scaled Ground Range (%)[a]				
SHOB ($ft/KT^{1/3}$) / Scaled Range ($ft/KT^{1/3}$)	0-3.1	182-205	212-252	323-375
237	65	52	-[b]	-
287	57	35	-	-
348	49	20	-	-
422	15	32	23	-
511	71	43	14	18
620	17	20	30	-
750	69	23	25	42
909	26	21	12	58
1101	41	38	15	15
1334	17	16	11	15
1616	16	2	-	24
1957	18	27	-	11
2371	30	-	-	21
2873	22	-	-	28
Average	47	31	20	25

[a] Standard deviation

[b] No experimental data

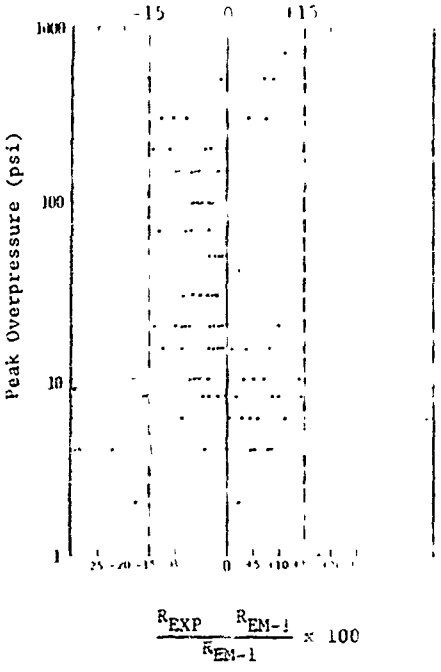

Figure 3.11. Comparison of Experimental and EM-1 Peak Overpressure Data for Near Surface Bursts

*Fairly broad uncertainties should be associated with each point in this plot since each represents a selected value on a curve through a scatter of data. This comment also applies to Figure 3.12. An independent analysis for HOB's 200 ft (scaled) indicated uncertainties of +20 and -55% at 10 psi, +25 and -40% at 15 psi, and +40 and -55% at 5 psi (95% of the data points).

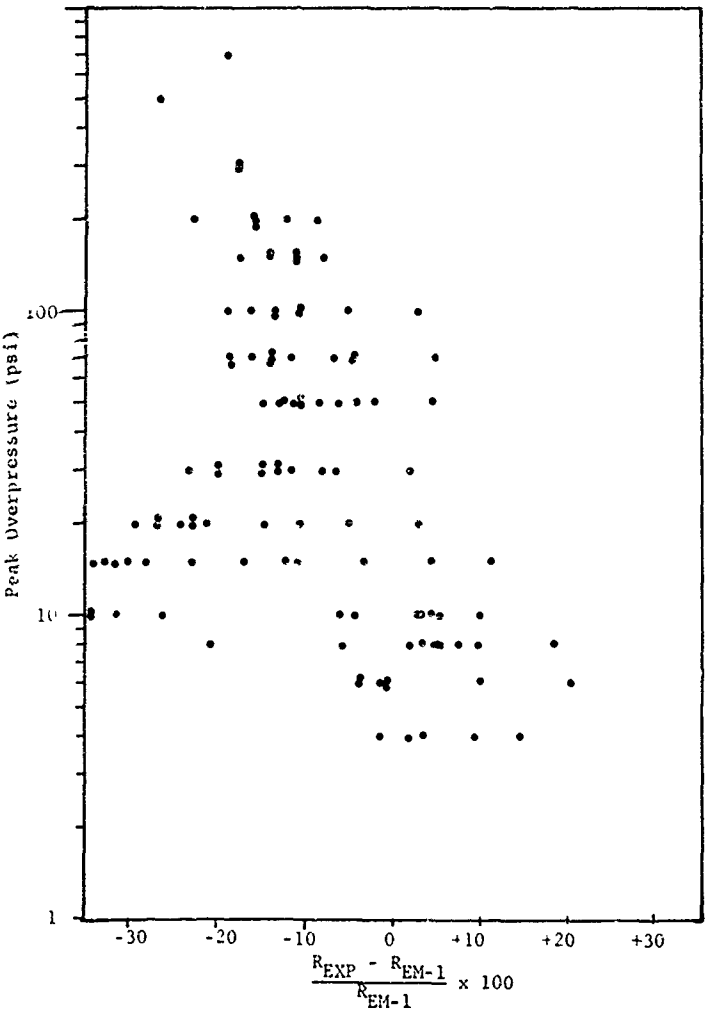

Figure 3.12. Comparison of Experimental and EM-1 Peak Overpressure Data for SHOB's in the Range from 180-220 ft/KT$^{1/3}$.

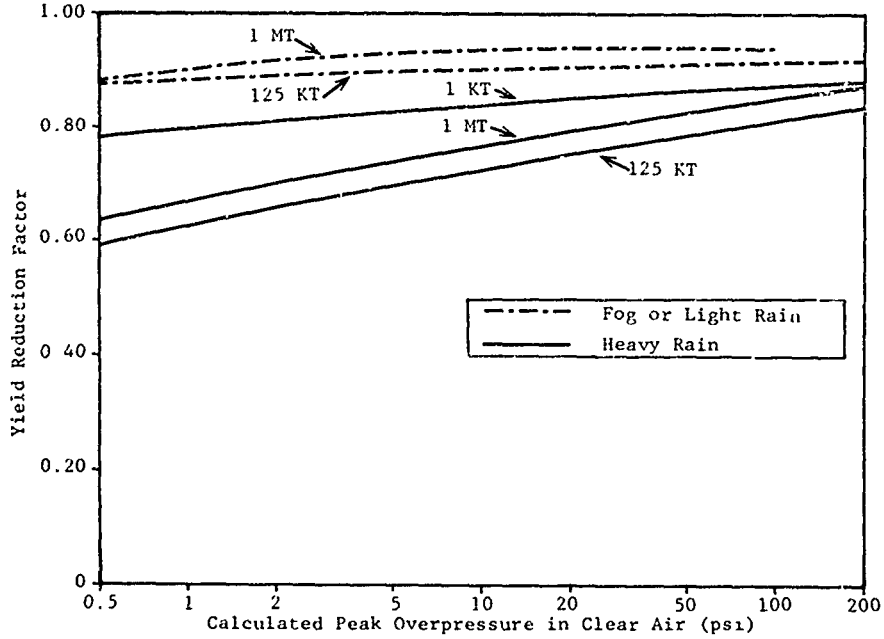

Figure 3.13. Reduction of Peak Overpressure at the Surface by Rain or Fog.

Since the affect of rain or fog will be to reduce the range of collateral damage effects (or reduce the blast wave intensity at a given range), it has not been used in generating the casualty damage functions given in Section 7 of this report.

3.2.5 Snow

Snow on the ground surface may have an effect on the reflected blast wave intensity (Ref. 3.1). When a shock front enters a layer of snow it is attenuated.* Drag forces on the snow crystals dissipate energy contained in the wind behind the shock front.

Current estimates indicate a thick layer of snow may reduce the range to a given overpressure as much as ten percent. Since the effect is to reduce the blast wave intensity, it was not used in generating the casualty damage functions.

3.2.6 Target Altitude

The target altitude will affect the intensity of the blast wave. Calculations of damage are typically based on sea-level airblast parameters. At higher altitudes the blast wave will be somewhat less (Ref. 3.1). Most target areas are located at altitudes of less than 3,000 feet above sea level. At 3,000 feet the peak overpressure is reduced approximately eleven percent (or about a six percent reduction in range to 10 psi). Since the affect of altitude on collateral damage effects is to always minimize them, it has not been considered in the casualty damage function generations.

3.2.7 Ambient Atmospheric Pressure

Variations in the atmospheric pressure will cause variations in the airblast parameters. However, the normal range in atmospheric pressure is ± 5 percent. This causes variations in ground ranges of less than 3 percent.

*Hard packed snow can make an ideal surface out of a non-ideal surface.

3.2.8 Terrain

Terrain features such as rising or falling slopes, ridges, valleys, etc., will affect the blast wave. If a shock wave that is travelling along the ground surface encounters a change in slope, the characteristics of the shock wave will change. If the terrain is characterized by large changes of slope, the changes in the blast wave can be significant. They can result in an overpressure increase by more than a factor of two or a decrease by more than a factor of three (Ref. 3.1).

Table 3.17 shows a comparison between the peak overpressure for a flat surface and the overpressure for rising or falling slopes. The slopes chosen for these comparisons are typical of those that might be expected around target areas. Also shown are the increase or decrease in ground range (from that expected for a given overpressure on a flat surface).

3.2.9 Summary of Airblast Uncertainties

The major areas of uncertainties in the airblast environments were discussed above. A summary of those uncertainties used for the generation of the damage function are summarized in Table 3.18. A Gaussian distribution was assumed for each of the uncertainties. The distributions were truncated at the high and low values shown in the table.

The uncertainties were used to estimate the probability distributions for peak overpressure at a series of range points. Figures 3.14 and 3.15 show example probability distributions at 500 and 1000 meters from ground zero for a one kiloton weapon detonated at a 200 foot height of burst. The error bars on the frequency distribution indicate the statistical accuracy of the calculation, i.e., any structure in the distribution smaller than the error bars has no significance. The area under the frequency distribution curve integrates to unity.

Table 3.17. Effect of Slopes on Peak Overpressure

RISING SLOPES			FALLING SLOPES		
8 psi Incident Peak Overpressure (Flat Surface)					
Slope (Degrees)	Peak Overpressure (psi)	Increase in Ground Range* (%)	Slope (Degrees)	Peak Overpressure (psi)	Decrease in Ground Range* (%)
+ 5	9	7	- 5	7	7
+ 10	11	24	- 10	6	15
+ 20	14	65	- 20	3.5	30
+ 30	17	100	- 30	2.3	40

*Increase (or decrease) to range at which the peak overpressure will be 8 psi.

Table 3.18. Summary of Airblast Uncertainties*

Parameter	Mean Value	Standard Deviation	Truncation Value	
			Low	High
Yield	1.0 KT	0.075 KT	0.0	1.5
HOB	200 ft	50 ft	0.0	400
Air Pressure	1015 mb	10 mb	900	1115
Slope	0^{o}	10^{o}	-30	+30
Range Factor**	1.0	0.15	0.0	2.0

*There was no explicit account of non-ideal surface effects, precursors or mechanical effects (build-up, vegetation, roughness, trees, etc.).

**Range uncertainty in the basic airblast representation.

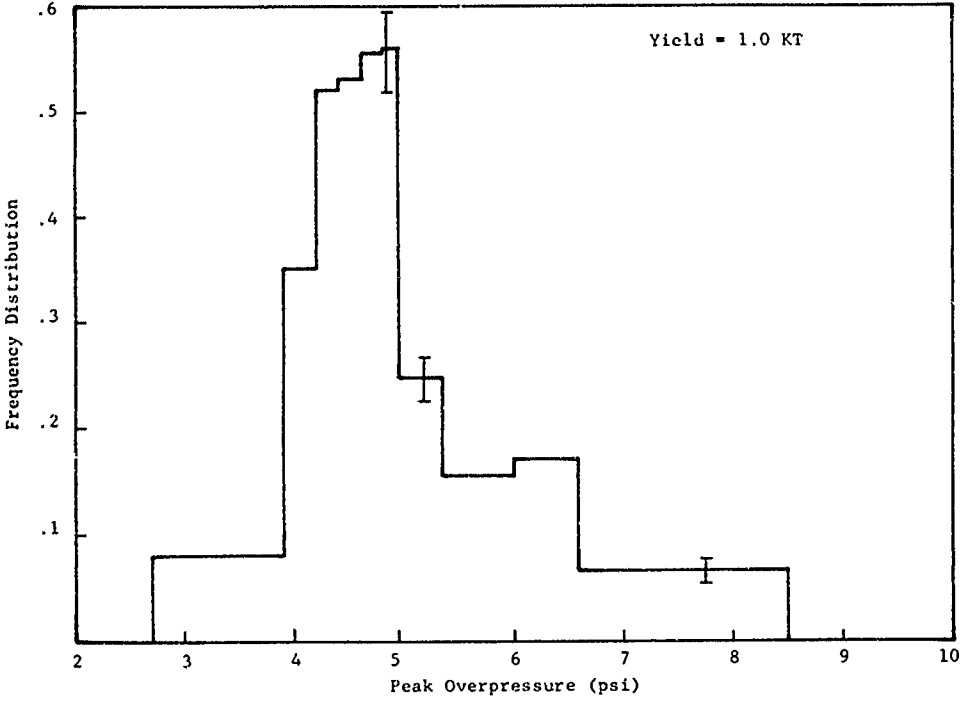

Figure 3.14. Probability Distribution of Peak Overpressure at 500 Meters.

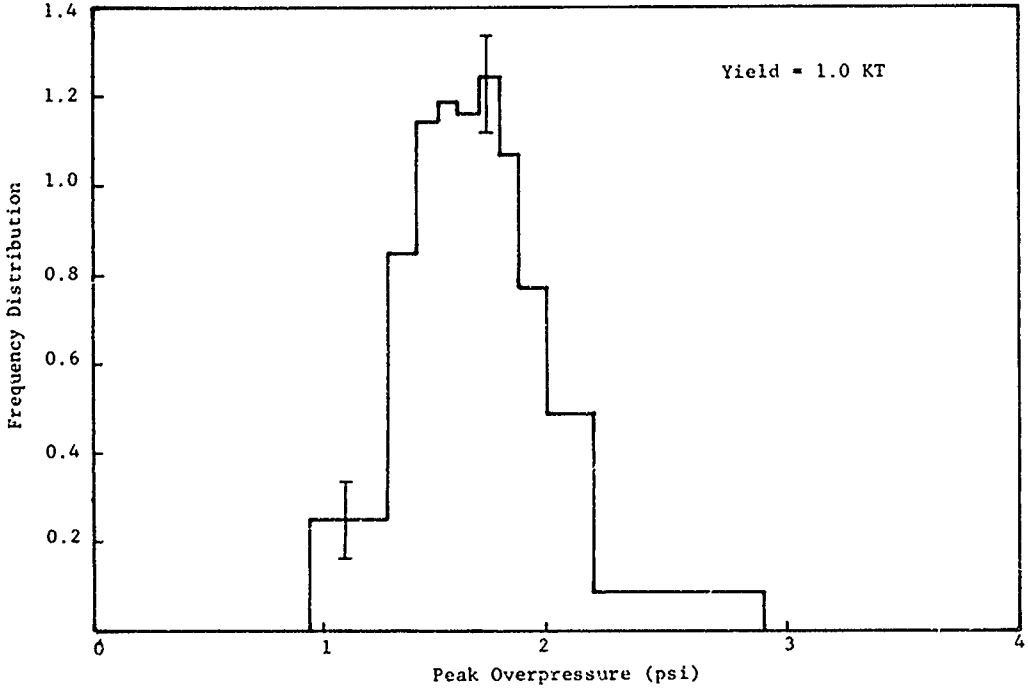

Figure 3.15. Probability Distribution of Peak Overpressure at 1000 meters.

3.3 THERMAL RADIATION

Thermal radiation emitted by a nuclear weapon detonation can cause fatalities and serious injuries to people directly exposed to the fireball. Thermal effects (for people in the open) extend to larger distances than do nuclear radiation or airblast effects for weapon yields greater than about 3 KT. Thermal effects are also the primary cause of fires resulting from nuclear weapons.

If there is little atmospheric attenuation of the thermal radiation, the total thermal radiation energy can be regarded as being spread uniformly over the surface of a sphere and the simple procedures given in EM-1 (Ref. 3.1) or Classtone and Dolan (Ref. 3.14) can be used to assess radiant exposure levels. However, if there conditions of clouds, heavy smoke or haze, precipitation, snow cover, etc., more sophisticated procedures are required. Several calculational models have been developed to handle these effects, including the THERMX code developed by SAI which was used in this analysis (Ref. 3.15).

There are a number of factors involved in determining the uncertainties in predicted radiant exposure levels. Most of these factors result from normal variations in atmospheric conditions and ground cover. The uncertainty parameters considered in this analysis are given in Table 3.19.

Table 3.19. Thermal Radiation Uncertainties

Weapon Yield
Thermal Partition
Air Pressure
Relative Humidity
Cloud Cover
Altitude
Ground Albedo
Height of Burst
Temperature
Meteorological Range
Cloud Ceiling
Range Uncertainty Factor*

*Uncertainty in basic thermal radiation predictions.

3.3.1 Thermal Partition

The results of analysis performed by Kaman Sciences was used to assess the uncertainties in the thermal partition (the fraction of the total explosion energy emitted as thermal radiation) for air burst weapons. This analyses indicated that from 58 independent experiments, the mean value of the thermal partition was 0.35 and the uncertainty was 13 percent (standard deviation). The distribution of the experimental values is shown in Figure 3.16. Here the fraction of the experimental points is shown as a function of the ratio of the experimentally observed value to the mean value.

3.3.2 Radiant Exposure Predictions

An analysis was made of the experimentally measured radiant exposures. Comparisons were made between the experimental values and those obtained from by using the THERMX code. The

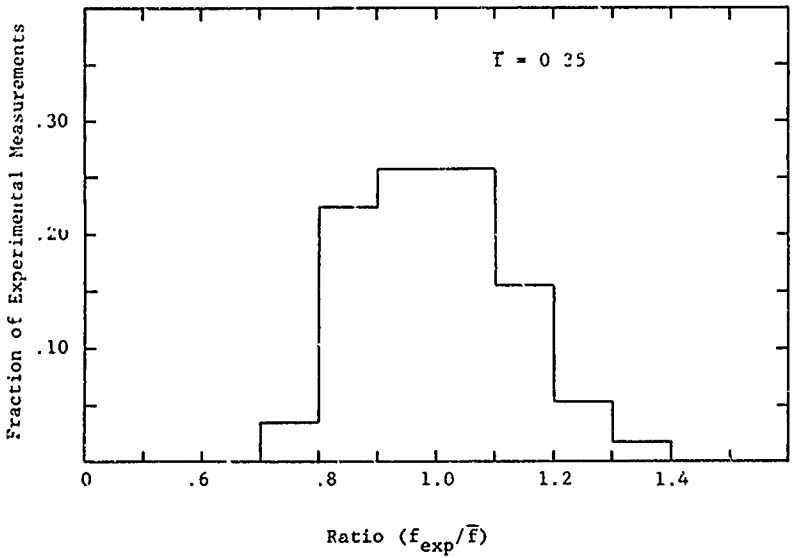

Figure 3.16. Frequency Distribution of Experimentally Determined Thermal Partitions.

experimental data were taken from a series of nuclear weapon test results. These were a series of tests which have been used to establish thermal radiation scaling laws, i.e., atmospheric conditions were good.

For purposes of comparison of measured values of radiant exposure Q, it was decided to present plots of the quantity QR^2/W (i.e., normalizing to unit yield and removing the inverse-distance-squared factor). The variation of this quantity from a constant value then displays all effects of atmospheric absorption and scattering as well as effects of ground and cloud albedos.

The 23 shots selected were those listed in Table I of "New Thermal Scaling Laws for Low-Altitude Nuclear Burst" in Vol. 1 of "Nuclear Weapons Thermal Radiation Phenomena" (1974). Shots 1 through 10 were above a ground surface (shown in Table 3.20) and 11 were above water. These shots were selected on the basis of adequate thermal data for a low-altitude burst. The data points for each shot are plotted together with the comparable quantity predicted by the program THERMX.

The data points have been corrected for filter transmission and misalignment (when this was stated not to have been done in the data tabulation). Data points have been excluded if a footnote indicated reasonable concern for accuracy, or if one measurement of a set was clearly in conflict with several other apparently valid and consistent points. No points were excluded simply because they did not "look" good.

An analysis of the spread in the experimental data indicated that the standard deviation of the experimental data was about 30 percent for slant ranges between one and two kilometers, 20 percent for two to four kilometers and 20 percent for four to ten kilometers. There was observed a slight trend of underpredicting the radiant exposures by the THERMX code at ranges beyond about three kilometers.

Table 3.20. Summary of Weapon Tests (over ground surfaces) for Thermal Radiation*

Number	Surface	Height of Burst (ft)	Yield (kt)	Shot	Operation
1	Desert	1,132	14.0	Charlie	(Buster-Jangle)
2	"	1,417	21.0	Dog	(Buster-Jangle)
3	"	1,314	31.0	Easy	(Buster-Jangle)
4	"	3,447	31.0	Charlie	(Tumbler-Snapper)
5	"	1,040	19.0	Dog	(Tumbler-Snapper)
6	"	6,022	11.0	Dixie	(Upshot-Knothole)
7	"	2,423	27.0	Encore	(Upshot-Knothole)
8	"	524	15.0	Grable	(Upshot-Knothole)
9	"	1,334	61.0	Climax	(Upshot-Knothole)
10	"	739	3.0	Wasp Prime	(Teapot)

*The atmospheric conditions were exceptionally clear for these tests. It would have been useful to have examined near surface tests and data for tests conducted under less favorable atmospheric conditions.

Foil data and aircraft data have been excluded from the final graphs of Q^{exp}/Q^{th}. The accuracy of the foil data was stated to be poorer than that of calorimeter data. Aircraft data (depending on the aircraft altitude) may be significantly too high for proper comparison with ground data.

The ratio of observed radiant exposure Q to the predicted value is also plotted versus slant range in Figure 3.17.

3.3 3 Atmospheric Conditions

The air pressure, relative humidity, target altitude and air temperature affect the attenuation and the scatter of thermal radiation. These effects will not be described here, however, the values used in the analysis will be summarized below.

The ground albedo can affect radiant exposure levels, particularly when there is a cloud layer and the thermal radiation is reflected off a light colored ground cover (such as snow) and again reflected off the bottom of a cloud layer. There is considerable variation in the reflective properties of ground surfaces, e.g., almost zero for a newly plowed field to almost unity for a snow cover). A uniform distribution for ground albedo was assumed for this analysis (equal probability from zero to unity).

The meteorological range has an important affect on the attenuation of thermal radiation. Analysis was performed on the annual atmospheric conditions for northern Europe. Figure 3.18 shows the cumulative probability distribution of the visual range using annual weather statistics. The analysis showed a strong correlation between visual range and cloud ceiling (another important factor in predictions of radiant exposure levels). A joint probability distribution was used in the analysis for visual range and cloud ceilings.

3.3.4 Summary of Thermal Radiation Uncertainties

A summary of the uncertainties in thermal radiation environments is given in Table 3.21. These values were used in generating the damage functions shown in Section 7 of this report.

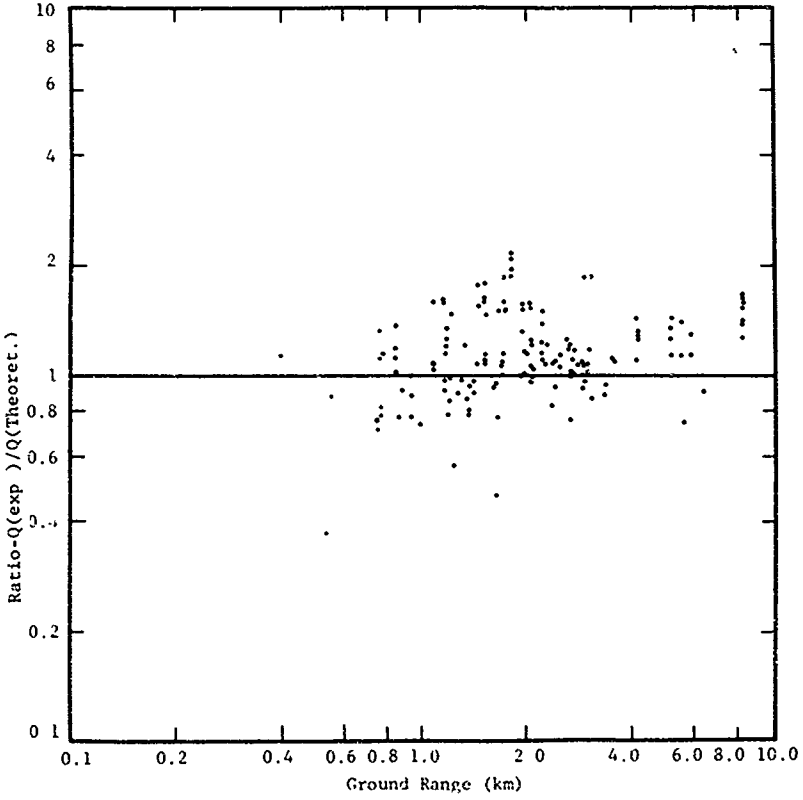

Figure 3.17. Comparison of Theoretical and Experimental Values of Thermal Fluence.

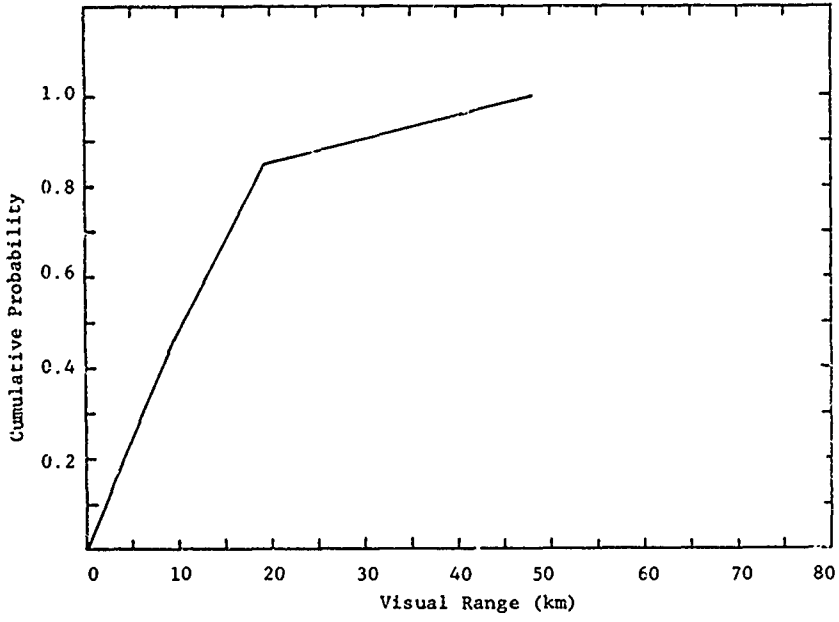

Figure 3.18. Cumulative Probability Distribution of Visual Range for Northern Europe (Annual Statistics).

Table 3.21. Thermal Radiation Uncertainties

Parameter	Mean Value	Standard Deviation	Distribution Type	Truncation Values Low	High
Energy Yield	1 0 KT	0.075 KT	Normal	0.0	1 5
Thermal Partition	0.35	0.04	Normal	0.0	0.5
Air Pressure	1015 MB	10 MB	Normal	900	1115
Relative Humidity	79%	10%	Normal	0	100
% Cloudy Days	53%	15%	Normal	0	100
Elevation	76 meters	8 meters	Normal	0	140
Ground Albedo	----	----	Uniform	0	1.0
Height of Burst	200 ft	50 ft	Normal	0	400
Temperature	8.3°C	11 0°C	Johnson SB	-25	37
Meteorological Range	10.5 KM	5 KM	Joint-Tabular	0	10
Cloud Ceiling	2.1 KM	1.3 KM			
Range Uncertainty Factor	1 0	0.2	Normal	0.0	2.0

3.4 REFERENCES

3.1 Dolan, P.J., Ed., "Capabilities of Nuclear Weapons," Defense Nuclear Agency Report DNA EM-1 (July 1972).

3.2 Engle, W.E., Jr. "A User's Manual for ANISN, A One-Dimensional Discrete Ordinates Transport Code with Anisotropic Scattering," K-1693 (1967).

3.3 Huszar, L., E.A. Straker and W A. Woolson, "Version 4 of ATR (Air Transport Radiation," SAI-76-561-LJ (1976)

3.4 Straker, E.A., "Time-Dependent Neutron and Secondary Gamma-Ray Transport in an Air-over-Ground Geometry, Vol. II, Tabulated Data," ORNL (1968).

3.5 Pace, J.V . III, D.E. Barine and F.R. Mynatt, "Neutron and Secondary Gamma-Ray Transport Calculations for 14 MeV and Fission Neutron Sources in an Air-over-Ground and Air-over-Seawater Geometries," ORNL-TM-4841 (1975).

3.6 Gritzner, M.L., et al., "Radiation Environment from Tactical Nuclear Weapons," SAI-76-534-HU (1975).

3.7 Albert, T.E., et al , "Terrain Effects on Tactical Nuclear Radiation Environments," SAI-76-577-HU (1975).

3.8 Bartine, D.E., E.M. Oblow and F.R. Mynatt, "Radiation Transport Cross Section Sensitivity Analysis - A General Approach Illustrated for a Thermonuclear Source in Air," Nuc. Sci. and Engr. 55, 147 (1974).

3.9 Weisbin, C.R., et al., "Cross Section and Method Uncertainties: The Application of Sensitivity Analysis to Study Their Relationship in Radiation Transport Benchmark Problem," ORNL-TM-4847, (Aug. 1975).

3.10 Beverly, W.B., et al., "The Effects of the Evaluation Assigned Nitrogen Nuclear Cross Section Uncertainties Upon the Transport of Neutrons in Air," BRL-R-1830 (1975).

3.11 Brode, H.L., "Height of Burst Effects at Height Overpressures," Rand Corp. Report DASA 2506 (July 1970).

3.12 Kingery, C.H., et al., "Nuclear Weapons Blast Phenomena, Volume V, Data Compendium," DASA 1200-V, Revised, October 1971.

3.13 Cockayne, J.E., and E.V. Lofgren, "Tactical Implictions of Air Blast Variations from Nuclear Weapon Tests," SAI Report SAI-76-677-WA (30 Nov. 1976)

3.14 Glasstone, S., and P.J. Dolan, The Effects of Nuclear Weapons, Third Edition, USDOD and USDOE (1977).

3.15 Drake, M.J., C.J. Rindfleisch, Jr. and D.C. Shreve, Collateral Damage Methodology and Vulnerability Representation, Monthly Progress Report, SAI-76-507-LJ (Jan. 1976).

4. SHELTERING CONDITIONS AND RELATED UNCERTAINTIES

4.1 NUCLEAR RADIATION PROTECTION FACTORS

Any mass of material between a nuclear radiation source, such as a nuclear weapon detonation, and personnel will reduce the dose to the personnel compared to the free-field dose at the same location. Personnel located behind buildings or in buildings will receive less dose than that which they would receive in an exposed free-field position.

The uncertainties in the predicted dose for people inside structures are relatively small (uncertainties in range) if state-of-the-art calculational techniques are used and if the following conditions are well known.

- The free-field dose contributions are known (neutron and gamma rays)
- The structure is isolated from any other structures
- The building materials and geometries
- The locations of people are known

The conditions listed above are almost never known. Even if they were known, such calculations are impractical for the purposes of estimating collateral damage. The usual practice is to define several classes of structures and to specify nuclear radiation protection factors that are appropriate for the class of structures. Table 4.1 lists the protection factors given in EM-1 (Ref. 4.1) and AP-550 (Ref. 4.2) for civilian structures.

The categories of structures listed in Table 4.1 have to include structures of the particular type throughout the world. For example, frame houses include all single-story residences (wood frame buildings, wall-bearing buildings and adobe buildings).

Table 4.1. Nuclear radiation protection factors.

Structure Type	Neutrons		Secondary Gamma Rays		Residual Gamma Rays	
	EM-1	AP-550	EM-1	AP-550	EM-1	AP-550
Frame house	1.25-3.3	1.8	1.0-1.25	1.1	1.7-3.3	2.2
Basements	1.25-10	2.2	1.7-10	2.9	10 0-20	13
Multistory Buildings						
Upper	1.0-1.1	1.05	1.1-1.25		100	10
Lower	1.0-1.1		1.7-3.3		10	

AP-550 lists a single value for each building type. EM-1 lists a range of protection factors but provides no guidance on the appropriate value to use for a given construction type.

Two investigations were made, recently, on protection factors appropriate for West German houses (Refs. 4.3 and 4.4). The conclusions from this research was that most German residences provide larger effective protection factors than would be obtained from the data in Table 4.1. There were two reasons for this: (1) the type of material used and the construction techniques provide higher protection factors, (2) the effects of multiple building protection. Based on the above research, a distribution of protection factors was developed. These are summarized in Table 4.2.

4.2 VULNERABILITY OF STRUCTURES TO AIRBLAST

Airblast effects from weapons of yield greater than about 10 KT produce important casualty damage mechanisms. For people in the open, the most important effects are direct effects on body organs and the effects of whole-body translation. However, for people located inside buildings or outside of buildings in a built-up area, the debris generated by light-to-moderate damage to the buildings or collapse of the buildings produce the most important damage mechanisms.

The uncertainties in airblast-related casualties are large. These uncertainties can be divided into three general areas. The first are the uncertainties in biomedical effects. These uncertainties will be discussed in Section 5 of this report. The second area is related to the basic understanding of how structures fail, the type of debris generated, and how this debris is blown about by the blast wave. The third area is related to the variations in structure types and the uncertainties in structure vulnerability. The last two areas are the most important ones

Table 4.2. Nuclear radiation protection factors for West German residences.*

	Aboveground Portions of Residences		Basements	
Percent of Buildings	Prompt Neutrons and Secondary Gamma Rays	Prompt and Fission Product Gamma Rays	Prompt Neutrons and Secondary Gamma Rays	Prompt and Fission Product Gamma Rays
	(Protection Factors)			
20	2	2	4	4
20	3	6	7	12
20	4	10	10	20
20	6	15	15	30
20	8	20	20	40

*These protection factor estimates must be considered preliminary. Definitive values would have to be based on actual structural survey results.

with respect to the uncertainties in predictions of airblast casualties for people in or near buildings.

An investigation was completed recently on a re-examination of the structural vulnerability (Ref. 4.5) which included structures of a type that are of interest to collateral damage estimates. A comparison was made of the structural vulnerabilities given in EM-1 (Ref. 4.1) and AP-550 (Ref. 4.2) and those derived from re-examining the Japanese experience as well as results from experiments conducted at the Nevada Test Site (NTS). The results of this research indicated that the vulnerability values given in EM-1 and AP-550 may be too large, i.e., about a factor of 1.5 for overpressure-sensitive structures and a factor of 5 for dynamic pressure-sensitive structures. Table 4.3 summarizes some of the results.

Table 4.3. Comparison of structural vulnerability.

Structure Type	Vulnerability (psi)*		
	AP-550	EM-1	Japanese and NTS Data
Load-bearing masonry buildings	$\Delta P = 5.8$	$\Delta P = 5.1$	$\Delta P = 3.2$
Wood-frame buildings	$\Delta p = 3.3$	$\Delta P = 3.5$	$\Delta P = 2.5$
Light steel-frame buildings	$q = 3.3$	$q = 2.5$	$q = 0.6$

* Vulnerability for 50% probability of severe damage.

Although debris-related casualty criteria are not directly proportional to structure failure criteria, they are correlated. The results of the structural analysis (Ref. 4.5) shown above indicate that the uncertainties in structural vulnerabilities are larger than indicated in either EM-1 (Ref. 4.1) or AP-550 (Ref. 4.2), and these uncertainties must be considered in assessing uncertainties in casualty criteria.

A program was initiated in 1976 to investigate the structural vulnerability of typical West German residences (Refs. 4.6 and 4.7). The analytical and experimental program was performed by Stanford Research Institute. During the first phase of the program, considerable information on the details of building construction in West Germany was collected and two major classes of buildings were identified as typical of small villages (masonry load-bearing wall buildings and half-timber Fachwerk buildings).

Based on the German building data gathered in the first phase of the program and in consultations with a West German-trained architect, SRI designed three identical structures which were tested during the DICE THROW event in White Sands, New Mexico in October 1976. The three structures (one half was of Fachwerk design and the other half was masonry design) were positioned such that the free-field peak overpressure were 7.0, 3.5 and 2.0 psi. The pre-shot predictions are shown in Table 4.4.

The test results were very similar to the pre-test predictions. The degree of damage was slightly less than the predictions. The DICE THROW test did tend to confirm that the current vulnerabilities given in EM-1 and AP-550 for load-bearing masonry buildings may be slightly high, but the test data indicated that the 3.2 psi value obtained in Ref. 4.5 is low.

Table 4.4. Predictions of wall collapse.

Overpressure (psi)	Fachwerk		Masonry Cavity	
	(Probability of Collapse, %)			
	Front Wall	Side Wall	Front Wall	Side Wall
7.0*	∿100	85	∿100	∿100
3.5	80	10	98	50
2.0**	15	∿0	∿1	0

* Actual values were 0.5 to 1.0 psi less.

** Actual values were slightly less.

4.3 FIRES

A preliminary examination was made of the impact on collateral damage of fires produced by tactical nuclear weapons and the resulting casualties. The effort included primary fires (those started by the thermal pulse), secondary fires (those started by secondary effects such as airblast, debris, etc.) and spread fires.

This section summarizes the results of this effort, which was primarily conducted at the Stanford Research Institute by Martin, et al. (Ref. 4.8). It should be recognized that this was a preliminary examination and, therefore, the results are still tentative. Recommendations for further work on selected research areas are provided.

4.3.1 Introduction

BACKGROUND

Fire is usually ignored in assessing damage from the conservative standpoint. But when assessing collateral damage the uncertainty of fire can not be ignored. This study was intended to provide some initial guidance about the importance of this mechanism, relative to other casualty-producing effects (e.g., airblast and initial radiation). This would be done using the methodology described in Section 6 to treat the effects of uncertainties in non-scenario-specific variables, i.e., those for which it is presently either impossible or impractical to treat other than as distributed variables but where enough is known about the probable range of the variables to estimate a distribution function.

Among damage assessment problems, fire effects are exceedingly complex, requiring the treatment of a remarkably large variety of weapon-burst, environment, and target parameters. This complexity, which has often caused the problem of fires following nuclear attack to be either ignored or treated in an inadequate, over-simplistic fashion, can now be handled in a more satisfactory way as a result of research efforts funded by DCPA (and its predecessor agency, OCD). It is still necessary, however, to attempt to generalize the analysis, substituting class-average statistics and stochastic variables for details and determinism, and to invent plausible algorithms where data do not exist.

The general approach being used here is to scale fire initiation data from the DCPA "Five-Cities Study" (for example, see Ref. 4.9), which were for weapon yields in the megaton range, to weapon yields in the range 0.1-10 0 KT and heights of burst from 200 to 600 ft/$KT^{1/3}$. These data are then used to compute probabilities of fire initiation and spread and subsequent casualty production caused by people caught in the burned-out region, e.g., because they are non-ambulatory due to injuries from other weapon effects, blocked by debris, overcome by smoke and toxic combustion gases, and so forth.

STUDY OBJECTIVES

This initial study has the principal objective of ascertaining the overall degree of improvement in predictions of casualties (produced by all weapon effects) that could be achieved from more detailed, yet practical (in both attainment and application), knowledge in the following areas.

1. Basic physical phenomena such as the several poorly understood blast-fire interactions that may extinguish or delay the development of primary fires, secondary (blast/shock induced) fire initiations, fire development and spread mechanisms, spread of wildland fires into populated areas, and the effects of weather conditions.

2. Target description such as different types of European structures and their spacings, contents, and wildland surroundings.

3. Operational factors such as the amelioratory effects of civil preparedness (e.g., covered windows) and fire-fighting efforts.

4. More detailed treatments of the casualty-producing mechanisms associated with fires, in particular the sequence of events that may impact movement and rescue, including their dynamic features in relation to the changing fire threat.

The remainder of this report contains a discussion of the approach now being used to model the physical aspects (initiation, development and spread) of fires. Example calculations are then given for two low-yield airbursts near a residential area, and the extent of the burned-out region is compared with that of other potential casualty-producing effects.

4.3.2 Primary and Secondary Fires

FIRE PREDICTIONS FOR LOW-YIELD WEAPONS

Fires in structures following a nuclear detonation are postulated to be the result of fires produced by three separate mechanisms:

1. Primary fires - those initiated by the thermal pulse of the bomb.

2. Secondary fires - those initiated by the blast effects of the bomb.

3. Spread fires - those resulting from subsequent propagation of both primary and secondary fires.

The primary fire threat to an urban target arises mainly from the initially small, incipient fires that result from the exposure of building contents by that portion of the direct thermal radiation from the nuclear fireball that is transmitted into rooms through windows and open doors. In many circumstances, exterior ignitions would play only a minor role. Normally, the exceptions would be the relatively infrequent cases where large accumulations of combustible litter or wildland fuels are in close proximity to structures having wooden exteriors It must be recognized, however, that structural damage resulting from any previous weapon effects (either nuclear or conventional) and the associated debris they may create will generally enhance the importance of exterior ignitions and increase the incendiary vulnerability of the urban target. In conducting this preliminary study, we have neglected the contribution of exterior ignitions since it was not possible to model these effects. The results may therefore tend to underestimate the fire problem. However, other assumptions may compensate for this neglect, and the unavoidably large uncertainties in the total analysis may mask it.

Secondary fires - those caused by blast effects rather than by the thermal radiation - require the coexistence (at the time of blast wave arrival) of fuels and energy sources in suitable combinations that mechanical damage or displacement can bring about contact between the two that is favorable for ignition of the fuels. This requirement represents an inherently low, but not insignificant, likelihood for secondary

fire starts in most urban occupancies experiencing blast overpressures capable of causing the requisite damage or displacement.

Whether a fire starts from primary or secondary causes, it has the propensity to grow and to spread to other structures that escaped initial fire starts. In time, this spreading of fire from structure to structure can cause much more damage than that represented by the initial fires alone. Because they take time to develop and since their outcome is subject to alteration by subsequent events, these spread fires impact survival and the conduct of emergency operations in several importantly different ways than initial fires do, and it is important to know their distributions in time (their dynamics) and in space. In this study, however, we neglect spread dynamics, and evaluate only the additional (ultimate) contribution made by spread fires.

To estimate the distribution of primary fire starts, this study makes use of a methodology that was originally proposed by John and Passel (Ref. 4.10) and subsequently developed into an analytical procedure at URS (Ref. 4.11) to estimate the frequency-spatial distribution of initial structural fires in a given urban use (or occupancy) class.

Basic Assumptions

The analytical methodology is built upon a foundation of the following postulates and assumptions:*

1. The primary fire threat arises from ignition of room contents. We have already noted that under "normal" circumstances exterior fires will contribute relatively little to the total urban fire problem. An additional justification for the neglect of exterior fires is to be found in the large thermal radiation exposures needed

*New fire research sponsored by DNA and DCPA may indicate that these assumptions are not valid.

to ignite (to sustained burning) sound wood of thicknesses typically used for wall sheathing, roof covering, external trim, and other exterior structural purposes. (A description of ignition thresholds is discussed later.)

2. Inside buildings, ignition of lightweight kindlings is not a sufficient condition for a sustained, building-threatening fire. Either a major fuel item - one that by itself is capable of flashing over the room in which it is located - must be ignited directly, requiring a higher exposure, typically, than that required to ignite kindlings, or one or more of the ignited kindlings must provide an indirect (or independent) route to the same endpoint.

3. The contributory roles of kindlings and major furnishings may be mathematically combined as a set of conditional probabilities for each of the separate fuel classes. These classes are then chosen in such a way as to minimize the number of quantifying properties that will require evaluation; e.g., class-average ignition thresholds and probabilities of (a) exposure, (b) ignition-given-exposure and (c) flashover-production-given-ignition.

4. The room contents are randomly distributed, at a uniform height above the floor, over the plan area of the room.

5. The frequency distributions of fuels (room contents) in each class, in each occupancy, etc., are well approximated by the Poisson statistic.

Model Description

In its simplest form, the methodology may be represented by the equation:

$$P_r = 1 - \exp[- \sum_i (\mu p_e p_f)_i] .$$

This equation predicts the probability, P_r, that a room (on a given floor, in a building of specified occupancy) whose windows are exposed to the thermal radiation from the fireball will suffer a fire that, if left unattended, will ultimately cause the room to become engulfed in fire (e.g., to "flashover"). The symbol i designates the separate classes of fuels into which the room contents have been classified. For convenience of analysis these classes will usually be chosen to discriminate between (1) those contents which each individually have the capability, once ignited, to flashover the room containing them ($i = +1$); (2) those lesser contents that, singly, lack the capability but may, if ignited, contribute to the development of a flashover situation ($i = -1$); and, to include as a separate and exclusive category, (3) those contents which are used to cover windows for privacy and the control of light ($i = 0$). The three essential fuel-class properties are n, the mean number of ignitable items in the class per room; P_e, the probability of thermal exposure; and p_f, the probability that ignition will lead to flashover. These properties are separately expressible as functions of the radiant exposure variable, Q.*

The analytical convenience afforded by the foregoing classification of room contents is readily seen in the following development. For the class $i = +1$, p_f, by definition, equals one. Similarly, by definition, p_e is practically close to unity for the class $i = 0$. Thus, the basic equation may be satisfactorily approximated by:

---

*In fact, however, neither P_e nor p_f are explicitly given as functions of Q. John and Passel (Ref. 4.10) proposed a correlation between p_f and Q that we might consider using. We do use the basic form of their empirical $P_e(\theta)$, and θ correlates with Q.

$$P_r \simeq 1 - \exp - [(\mu p_e)_{+1} + (\mu p_e p_f)_{-1} + (\mu p_f)_0] \ .$$

Now, the probability of exposure of any randomly selected point in the exposure plane (the horizontal plane within the room over which the contents, aside from window coverings, are assumed to be randomly distributed) may be related to the elevation angle θ (measured in radians) of the fireball line of sight by means of the following empirical expression:

$$p_e = k\, \theta^{1.7}\, e^{-4.7\theta}$$

Intuitively, one expects this probability to increase in proportion to the fraction of the exposed wall area that is represented by unobstructed window area, and, consistent with results of the Five-City Study, the foregoing equation may be modified accordingly:

$$p_e = 3 \frac{A_{window}}{A_{wall}}\, \theta^{1.7}\, e^{-4.7\theta}$$

We have chosen to equate p_e with the class $i = -1$ type fuels since most of its items will be of small cross section approximating points in the exposure plane. By extension, then, the probability of exposure of the $i = +1$ class contents will be proportionately larger in relation to their generally much larger cross section. Thus,

$$p_{e,+1} = (A_{+1}/A_{-1})\, p_{e,-1} \ .$$

In evaluating these exposure probabilities, we have chosen the distribution of (A_{window}/A_{wall}) values developed by IITRI from Five-City Study survey data (see Figure 4.1) and developed an approximate frequency distribution for (A_{+1}/A_{-1}) values from representative cross section data reported in Ref. 4.12.

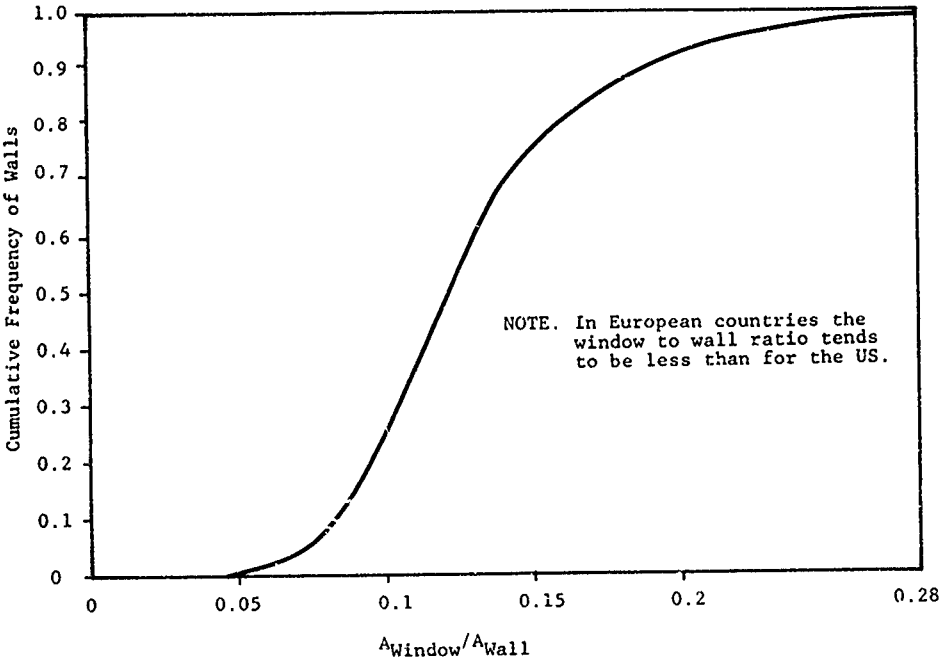

Figure 4.1. Frequency distribution for window areas. This is an average of survey data from San Jose, Detroit and Albuquerque.

In evaluating the fuel-class properties, the major uncertainties are the probabilities of producing room flashover given ignition of the minor-contents items, $p_{f,-1}$ and $p_{f,0}$. We have chosen to represent these by an identical log-normal distribution with its mean located at 0.01, to indicate the relatively much smaller capability such contents have or producing a flashover situation, and their 95% confidence limits set at 0.0002 and 0.5 to reflect our almost total ignorance of this factor.

In view of the foregoing, the basic equation may be simplified as follows:

$$P_r = 1 - \exp-\left[\frac{\mu_{+1}A_{+1}}{A_{-1}} + p_f(\mu_{-1} + \mu_0)\right] p_{e,-1}$$

Only the mean number distribution of ignitable fuels in each class remain to be evaluated.

These mean-number distributions may be expressed generally as the following nondimensional functions of the radiant exposure Q:

$$\frac{\mu_i(Q)}{M_i} = \left[1 + \frac{B + 1}{B - 1}\left(\frac{Q}{Q_{infl,i}}\right)^{-B}\right]^{-1}$$

where M_i represents the total count (mean number per room) of items in the ith class, and, therefore, its value depends only on the class and the occupancy (that is, it is completely independent of the weapon yield, burst height, etc.). The quantity Q_{infl} is the value of radiant exposure corresponding to the inflection point in the mean-number function. Although it will vary systematically with fuel class and occupancy, it is also a function of the conditions of burst and is the parameter used to extrapolate from one weapon burst situation to another. The

quantity B is a measure of the spread in ignition threshold values for the items comprising the class. The slope of the distribution function at the inflection point is equal to $(B^2 - 1)/4B$.

The mean-number coefficients used in the present analysis are derived by an extrapolative procedure from survey data acquired during the Five-City Study. The Five-City Study dealt with megaton-yield explosions; therefore, the reference Q_{infl} values must be scaled down over some three orders of magnitude in energy yield from the megaton range to yields of interest in the kiloton range. Scaled heights of burst were of comparable magnitude except that the Five-City Study included some surface bursts.

For the scaling of Q_{infl} we have used these equations:

$$Q_o = 2250 \frac{\rho c L}{a} \tau + \frac{t_{max}}{a}, \quad \tau < 0.52$$

$$Q_o = 1552 \frac{\rho c L}{a} \tau + \frac{t_{max}}{a}, \quad \tau \geq 0.52,$$

where $\tau = \sqrt{a\, t_{max}}/L$, the Fourier modulus, is a heat conduction property of the exposed fuel. The symbol t_{max} represents the time delay (in seconds) from the instant of explosion to the appearance of the principle thermal irradiance maximum at any distant target location. For purposes of these calculations (in which all burst heights are less than 15,000 feet), t_{max} is related to explosive yield in the following way:

$$t_{max} = 0.0417\, W^{0.44},$$

where W is the yield measured in kilotons.

It is estimated that the dependence of Q_{infl} on humidity is

$$Q_{infl} = Q_{0,infl} (1 + 0.005\ h) \quad ,$$

where h is the relative humidity in percent.

The practical ranges of the pertinent material properties are given in Table 4.5 .

Table 4 5 Applicable Properties of Ignitable Room Contents

Thicknesses:

$L = 0.02$ to 0.07 cm

Density of Kindling Material:

$\rho = 0.4$ to 0.5 g/cm^{-3}

Thermal Diffusivity

$\alpha = 0\ 95 \times 10^{-3}$ to 1.0×10^{-3} cm^2 sec^{-1}

Specific heat capacity.

$c = 0.3$ cal (°C)$^{-1}$ g^{-1}

Absorptivity·

$a = 0.5$ to 0.8 (nondimensional)

Critical Irradiance·

$H_c = 0.4$ cal/cm^2 sec^{-1}

Figure 4.2 illustrates the extrapolation procedure. It is important to note that the assumption has been made that transient ignition thresholds as exhibited by idealized (uniform, apertured exposures of small specimens) laboratory tests are more representative of fire initiating conditions in realistic situations than are the laboratory-determined thresholds of sustained ignition. This assumption has very

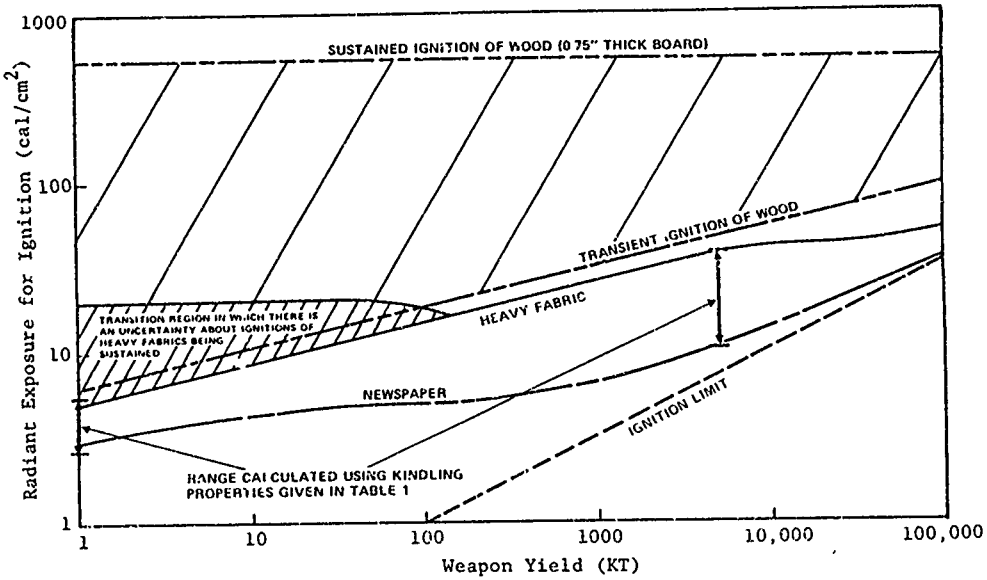

Figure 4.2. Radiant exposures to ignite materials (at 40-50% relative humidity) as a function of weapon yield.

little physical evidence to support it at the present time. The validity of this assumption will be seen to be of crucial importance to the outcome of the analysis.

Figure 4.3 shows the function dependence of (μ_i/M_i) on (Q/Q_{infl}) for two values of B. In the Five-City Study, B-values for residential occupancies were nearly constant for all conditions and classes, averaging about five Since B is a measure of the range in ignition thresholds, and for the short pulses of the kiloton range the spread is noticeably less than in the megaton range, it is appropriate to use a larger value of B in the kiloton region.

It is important to note that, in the calculation of probabilities of room fires, the level of exposure Q used for determining μ_i is not the free-field radiant exposure but rather is the radiant exposure of the kindling fuel in the room, which differs from the free-field level by a proportional constant $\bar{\alpha}$ which depends upon a number of factors and is not of uniform value for all rooms in any given building:

$$\bar{\alpha} = \bar{\alpha}_1 \cdot \bar{\alpha}_2 \cdot \bar{\alpha}_3 ,$$

where

$\bar{\alpha}_1$ = T_w, the window transmission,

$\bar{\alpha}_2$ = the fraction of the fireball not obscured by the general artificial horizon,

and $\bar{\alpha}_3$ = the fraction of the fireball not obscured by local objects (i.e , trees, nearby buildings).

The window transmission is treated as a two-level discrete distribution, namely 2/3 of the cases are assumed to have a transmission of 80% (averaged over the pertinent angles of incidence), corresponding to a single pane of glass, and

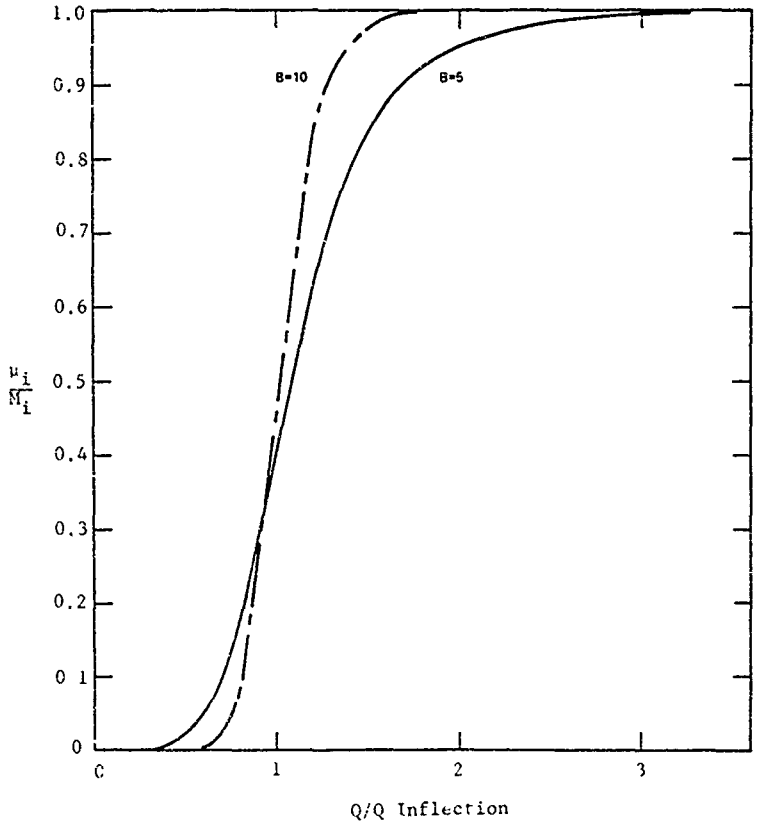

Figure 4.3. Mean number distributions.

1/3 are assumed to transmit only 70%, corresponding to two panes. The transmission values are adopted from recommendations (based on actual data) given in a 1966 Naval Applied Science Laboratory Technical Report (Ref. 4.13).

Window screens would further attenuate the transmitted radiation where they are used (NASL recommended a value of 50% transmittance (Ref. 4.13) for a single pane of glass combined with screen), but, noting the apparent infrequency with which insect screens are used in Central Europe, we have chosen to neglect this. The choice of 1/3 double-pane windows and 2/3 single-pane windows is purely an arbitrary one. Better statistical information could be readily obtained.

From the fraction of the fireball obscured by the artificial horizon, curves of the general form illustrated in Figure 4.4 can be constructed However, the artificial horizon should be treated as a scenario-dependent variable. Observations (including inclinometer measurements) made both here and in Germany give some indication of the general range of values of the artificial horizon. In U.S. cities, observations made from windows in one- and two-story buildings indicate a fairly consistent angle of inclination in the range 5° to 6°. In surburban areas and open country with nominal free coverage, such as one typically observes around the villages of Central Europe, the angle will average about 3° and rarely exceed 5° or fall below 2°. The principal exception is in heavily forested and mountainous areas such as the Black Forest where the artificial horizon (though it is often hard to define exactly) will range from about 10° to 15° and, surprisingly, even in the deepest canyons will rarely exceed 20°.

We have used a lognormal distribution of the artificial horizon with a mean of 3° and 95% confidence limits of 1.5° and 6°.

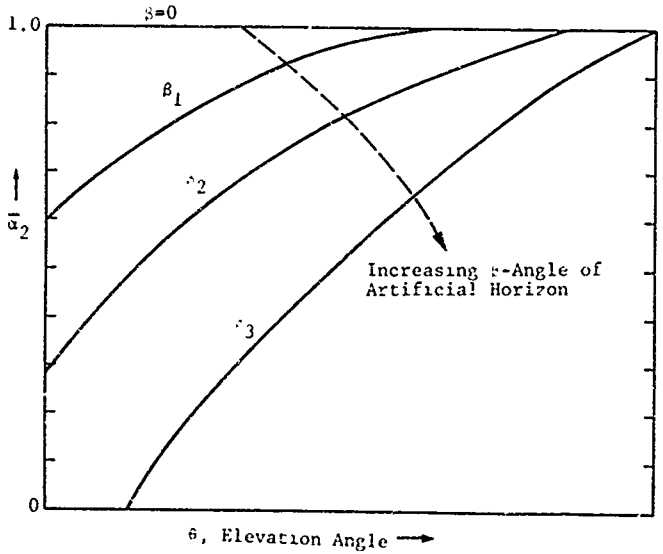

Figure 4.4. Trend of fireball obscuration vs. angle of artificial horizon.

The fraction of the fireball obscured by "local" objects is currently prescribed by the summer/winter distribution derived from the San Jose survey as part of the Five-City Study and shown here in Figure 4.5 . Obviously, this is another scenario-dependent variable.

Once the separate probabilities of significant room fires have been estimated with the distributed variables given, using the methods just described, these are then combined as

$$P_b = 1 - [1-P_{r(1)}][1-P_{r(2)}][1-P_{r(3)}]\cdots[1-P_{r(N)}]$$

to provide an estimate of the probability of significant (that is, self-sustaining and potentially life-threatening) fires in the exposed population of buildings (denoted P_b). The index $J = 1, 2, 3, \ldots, N$ designates the component exposed rooms contained by the structures in question. The number N should be determined (as a distributed variable) from a survey of West German villages. In the Five-City Study the mean value for single-family residences was found to be close to 5. It might be expected to increase somewhat linearly in proportion to the number of family units in a residential structure We have chosen to use three separate "flat" distributions of equal likelihood over the arbitrarily assumed range of values. The ranges are 4 to 8 exposed rooms in single-family residences, 6 to 12 in two-family residences, and 10 to 30 in larger multi-unit apartment houses.

Once we have estimated the function $P_b(0)$ we can readily calculate the ultimate burnout given (1) the number of buildings H_1 in a half-block (e.g., rows of 2 to 10 structures assumed to have an equal frequency of occurrence) and (2) the side-to-side fire-spread probability P_s. The empirical equations derived for this purpose are as follows:

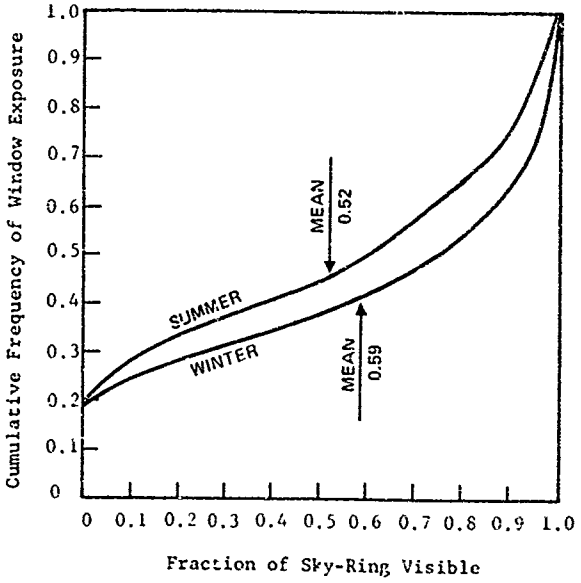

Figure 4.5. Exposure of first-story windows in San Jose residential area in summer and winter (based on survey of 300 windows).

$$\text{Fraction burned out} = \frac{P_b}{A + BP_b}$$

in which

$$A = 1 - 1.21(H_r - 1)^{0.096} P_s + 0.538(H_r - 1)^{0.038} P_s^2$$

and

$$B = 1 - A .$$

An example, taken from a URS study (Ref. 4.11) for a row of 5 structures, is shown in Figure 4.6. Single structures from which no spread is possible must also be accounted for. For single structures the fraction of ultimate burnout equals the probability of initial ignition.

Survey data are needed for these estimates, but for initial estimates we have used side-to-side spread probabilities based on the San Jose data from the Five-City Study.

A preliminary estimate of the number of buildings in rows was made for the study from aerial photographs of villages in the Niedersachsen Region of West Germany. Tallies were made of the frequency of observation of single (isolated) buildings and rows of 2, 3, 4 ... up to and including 10 and more. Although there were variations in the sums, no particular trends were found and we therefore decided to use a flat distribution (equal likelihood of occurrence of an isolated structure or any one row "length" up to and including the case of rows having 10 and more buildings). The terms "row" and "isolated building" are difficult to define precisely, but in practice the meaning is clear and unambiguous. Cases of isolated buildings have been included in the distribution function because, although they make no contribution to the fire spread, they are part of the population pool and must be accounted for in the burnout estimate.

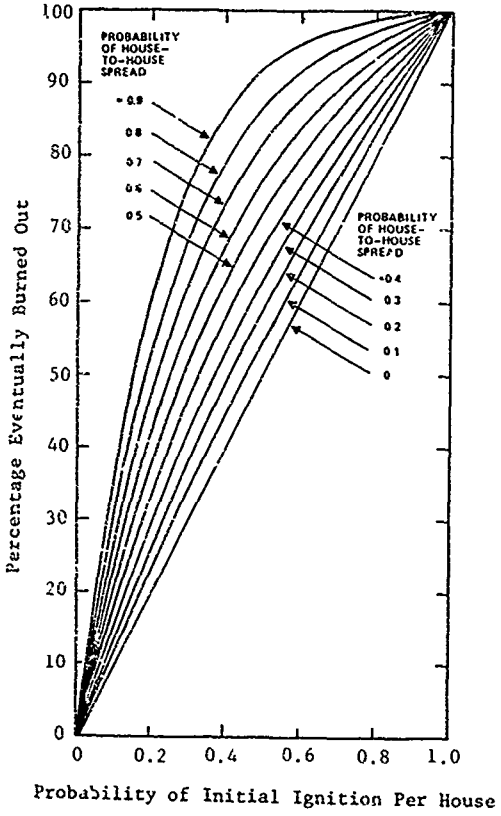

Figure 4.6. Average total burn for an isolated row of five houses.

The probability-of-spread distribution (only side-to-side, that is, along-the-row, spread events have been included) was derived from the statistical data of the Five-City Study (San Jose residential areas) illustrated in Figure 4.7 , making use of a physically plausible relationship between probabilities of fire spread and configuration factors utilized in the calculation of radiation intensities from burning (fully involved) buildings. (See Figure 4.8 .) Inasmuch as critical irradiances for spontaneous ignition of materials are in the range of about 0.2 to 0.6 cal cm^{-2} sec^{-1}, averaging about 0.4, while windows of rooms filled with flame radiate in the neighborhood of 4 cal cm^{-2} sec^{-1}, depending upon fuel loading, ventilation, and other factors, fire spread by radiation heating alone can be expected to occur in a large proportion of the cases when configuration factors (calculated for the burning building as "seen" by the as-yet-unignited building) exceed about $\phi = \frac{0.4}{4} = 0.1$. Thus, we expect the probability of spread to rise abruptly in the vicinity of $\phi = 0.1$ from small values that are representative of spread by spotting and piloting mechanisms (no more than a few-percent probable at distances where ϕ falls to 0.05 and below) to probabilities approaching unity at $\phi = 0.2$. This function is shown in Figure 4.8 . Combining this with the side-to-side spread probability statistics from the Five-City Study, we derived the frequency distribution function for fire-spread probabilities as shown in Figure 4.9 and used in this study.

EFFECTS OF BLAST

All the foregoing has ignored airblast and its effects on fires, which include (1) the interaction of the blast wave with the fire and (2) secondary fire ignitions. The effects of airblast and fire are inseparable, and their interactions

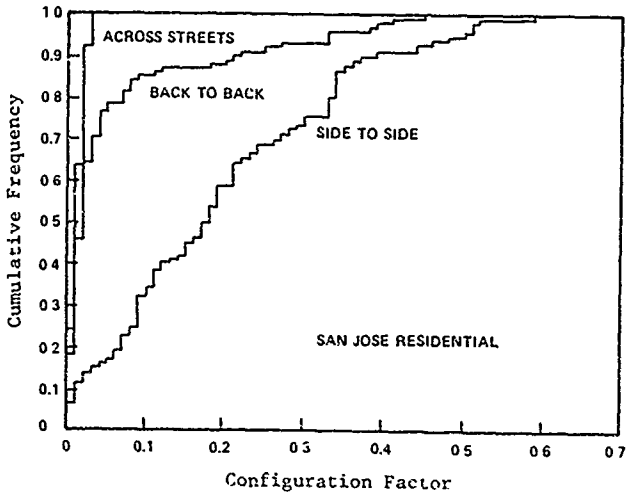

Figure 4.7. Distribution of configuration factors in San Jose residential areas.

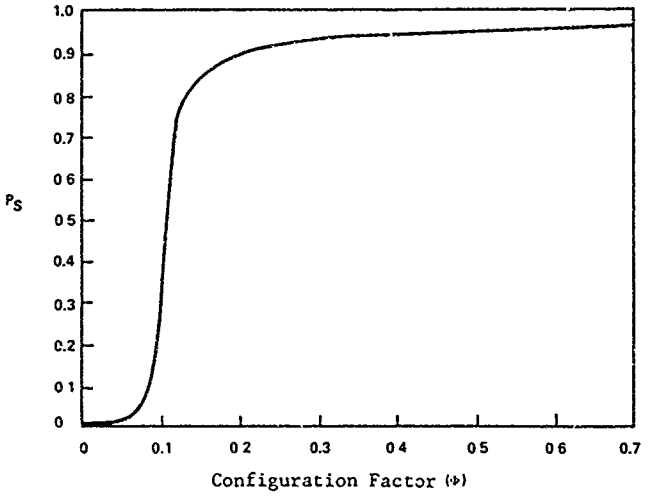

Figure 4.8. Probability of fire spread as a function of the configuration factor.

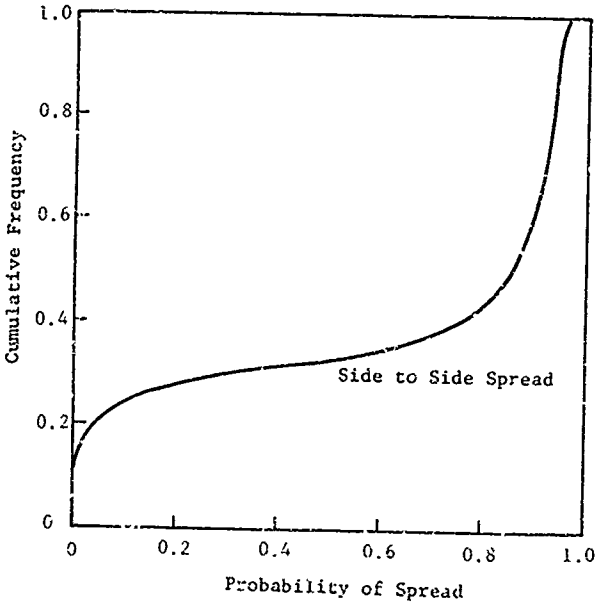

Figure 4.9. Probability of side to side fire spread.

are of great importance to the determination of population survival. Over those direct-effect areas where fire effects are important there will typically be substantial structural damage from blast. Even at large distances from ground zero, approaching the limit of incendiary reach, the effects of airblast on fires will be considerable. In most residential areas some structural damage, including partial collapse, accompanies fires of any practical consequence. This alters the environment in which the fires will develop and spread. Moreover, many fires may be extinguished by the airblast (or at least degraded from active flaming combustion to smoldering). The same applies to commercial and industrial occupancies except that, at the limit of incendiary reach, there will be, in general, less structural damage. Nevertheless, substantial change will be wrought by blast including (1) the loss of curtain walls and interior partitions, (2) the ejection of these structural components along with contents to form debris in the open spaces between buildings, and (3) some of the actively flaming initial fires will be extinguished or reduced to a less active smoldering state.

The question of whether (and how many) fires are extinguished by the blast wave is of extreme importance to survival and the planning of emergency operations to aid survival in the immediate period following attack. It cannot, as yet, be answered confidently. Studies of the effects in Japan and at various nuclear and high-explosive tests are contradictory and leave the question unresolved. Laboratory experiments that simulate blast loading of urban interiors show that the blast wave typically does extinguish flames but often leaves the material smoldering to reinitiate active flaming at a later time. It is not certain at present how universally

this behavior may extend to actual urban targets experiencing a nuclear explosion. Undoubtedly, some fires will survive the blast; others will be started by it. In all likelihood, the ultimate extent of damage will not depend nearly as heavily on whether or not blast extinguishment occurs as it will on how the blast either aids or impedes the effective application of self-help firefighting by the resident population. While blast damage may hinder this action, the blast wave may provide some additional time by snuffing out many actively flaming fires, leaving relatively slow-growing smoldering fires in their places.

Where blast overpressures are high enough to cause substantial structural collapse and to create deep, nearly continuous debris fields over much of the local area, the spread of fire and its threat to survival could be quite different in character from that modeled in this study. Where initial fire incidence is light, fires will burn in a spotty, sporadic fashion with little or no interaction. Basement spaces and structures still standing will usually provide fire-safe refuge. With proper precautions, a very high level of survival can result. Self-help firefighting can be important in the relatively infrequent circumstances where fires do start in (or quite near to) occupied buildings. Occupants have, perhaps, 1/4 to 1/2 hour to find and extinguish these fires. Air vents to underground shelter must be freed of debris that might subsequently become involved in a slow moving debris fire. Where the density of fire starts is high, fire spread plays a role in the fire threat for only a short period of time while the fires are merging. The threat is, therefore, determined by the intensity of the mass fire and the environment it creates, notably the air temperatures, and the atmospheric concentrations of CO and CO_2.

In typical residential areas where fuel loadings of 1.5 to 3 pounds/ft^2 will constitute the debris field, maximum burning rates will range from 0.1 to 0.2 lb/ft^2-min yielding about 2 lbs of CO per minute over each 100 sq ft of burning debris. The corresponding heat release rate will be 8×10^5 calories per minute per sq ft. This is comparable to the conditions generally ascribed to a fire storm and represents a substantial threat to survival, requiring special precautions such as closing air vents for a period of a half hour or so. The much heavier accumulations of debris in builtup commercial and industrial areas will cause burning to last for hours. Prospects for continued survival in these areas are bleak.

For such areas, crisis relocation of the resident population is the preferred planning option. After-the-fact, remedial movement of the surviving sheltered population at the earliest threat of fire will be imperative.

We were unable in this brief study to develop a model of fire spread for blast damaged urban areas. Additional fire research is required before such models can be developed.

Since these blast-fire interaction effects are not yet well defined, our estimates of them will necessarily have large dispersions. For nominal estimates we use an algorithm for blowout of fires that was previously used by URS, which states that below 2 psi peak overpressure no fires are blown out, above 5 psi only half of the primary ignitions survive the blast wave, and between 2 and 5 psi the survival of primary ignitions decreases linearly from 1 to 0.5.*

*A recently published URS report (Ref. 4.14) supports these earlier conclusions but points out the importance of fuel location in the room relative to the blast-induced air flow pattern.

The only definitive study that has been conducted to date (Ref. 4.15) on secondary-ignition fires per 1000 ft^2 of floor area in areas of the target experiencing 2 psi and higher overpressures. Additional insight, both with regard to secondary fires and casualty production by primary or secondary fires, may become available from studies of other World War II fire data analyzed under DNA Contract No. DNA001-76-C-0085, "Relative Collateral Damage."

To use the McAuliffe and Moll (Ref. 4.15) predictor of secondary-fire density, we require an estimate of floor area. In this study we estimated the average floor area of single-family dwellings to be 1667 ft^2 which yields a secondary-ignition-source building-fire probability of 0.01. For multiple-family dwellings we estimated the floor area to be 1000 ft^2 times the number of units per building.

According to a Dikewood survey of fire casualties in World War II (Ref. 4.16), fire fatalities rarely exceed 4%* of the population at risk unless the fire took on the extreme dimensions and the intense nature ascribed to firestorms. Based on this, the following casualty algorithm is proposed:

1. Three percent of the total population at risk, plus all of that portion of the population at risk which is either trapped or nonambulatory, will be killed by fire effects.

2. The population at risk is defined to be that fraction of the surviving population (all of those not killed by the prompt weapon effects) which is sheltered in burning buildings.

*Fires started by nuclear weapons will tend to be simultaneous and fewer people will have the opportunity to find refuge (compared to WW II fires).

EXAMPLE CALCULATIONS OF EXTENT OF FIRE

We illustrate here simple estimates of the extent of serious fires for a single set of scenario-dependent variables and without treating the dispersion of distributed variables. Moreover, no casualty production assumptions for fires are incorporated in this example, nor is the casualty production from other weapon effects included with these results. (Full, all-effects casualty calculations including distributed variables to establish confidence limits are given below in Section 6). As a rough indication of the potential seriousness of fires as a casualty production mechanism for low-yield weapons, however, the range of the effects of other mechanisms may be compared to the predicted extent of the burned-out region.

This example estimates the fraction of buildings burned for the following conditions:

(1) Weapon - (a) 1 kiloton, standard fission
(b) 10 kiloton, standard fission

(2) Height of burst - (a) 400 ft
(b) 895 ft*

(3) Residential area with 4 rooms per building exposed to the fireball and the following obscuration factors:

2 rooms with $\bar{\alpha}_1 = 0.8$, $\bar{\alpha}_3 = 1.0$

2 rooms with $\bar{\alpha}_1 = 0.8$, $\bar{\alpha}_3 = 0.5$

(4) Visibility of 10 miles

(5) Artificial horizon = 3°

*Height of burst scaled to give (at the second thermal maximum) a fireball line of sight equivalent to 1 kiloton at 400 feet.

(6) Total burn calculated for isolated rows of 5 houses with house-to-house spread probability of 0.67.

(7) Windows are not covered.

The calculations were made with and without a consideration of blast effects. When considering blast effects it was assumed:

(1) Below 2 psi peak overpressure the blast wave has no effect on fire.

(2) Above 2 psi peak overpressure (a) a fraction equal to the quantity (8 - P)/6, where P is the peak overpressure in psi, having a lower limit of 0.5, survive the blast wave blowout to rekindle active fires and (b) an additional 1% of the buildings have secondary ignition fires.

Results of these calculations are shown in Figure 4.10 for the 1 KT case and in Figure 4.11 for the 10 KT case. With or without the blast effects, there is a significant fraction, ∿10%, of the buildings completely burned out at a ground range of ∿0.5 mi from the 1 KT burst and 1.2 miles from the 10 KT burst. At these ranges, and with typical protection inside residences from the initial radiation, all other weapon effects produce no significant incidence of fatalities, although the creation of debris and the incidence of non-fatal, incapacitating injuries from other effects are not insignificant at this range. For these cases, then, the possibility exists that fire could be among the dominant fatality mechanisms at long ranges

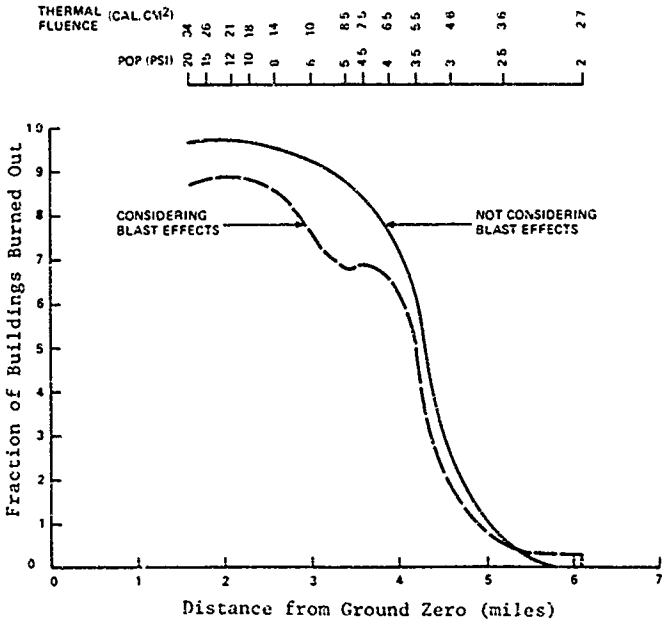

Figure 4.10. Fraction of buildings burned out for 1 KT weapon.

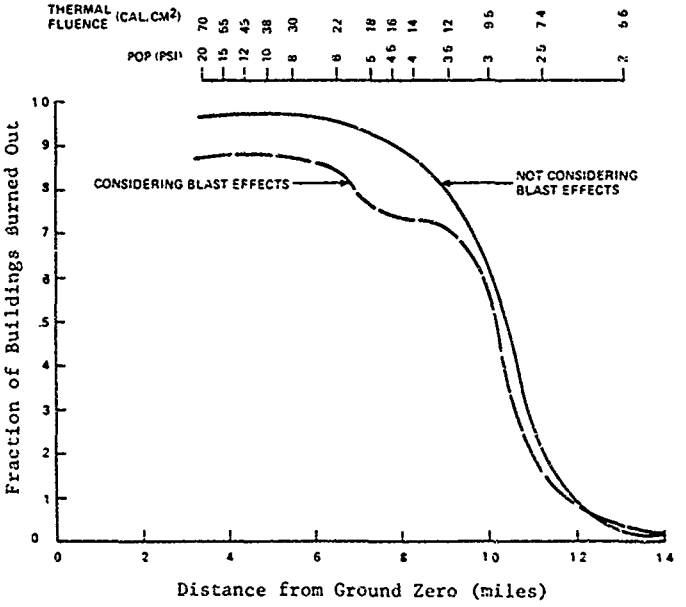

Figure 4.11. Fraction of buildings burned out for 10 KT weapon.

4.3.3 Conclusions and Recommendations

Recognizing some major weaknesses in the methodology and the physical-data base that underly it, this analysis still shows that, for tactical situations involving the use of nuclear weapons in Western Europe, collateral fire effects could be quite important. It also shows how strongly dependent the fire outcome is on scenario-related variables, and it implies that the threat to survival may be readily countered through civil preparedness.

The most serious deficiency in the methodology arises from its neglect or its inability to treat adequately the blast effects and their interaction with, and/or influence on, fire behavior. Yet these effects may drastically change the incendiary outcome--probably not to ameliorate its threat, but in still uncertain ways that may have important operational and decision-making ramifications.

Further work should be done to reduce these uncertainties. As a general and long-term recommendation, the unfinished research work on blast-fire interactions should be reactivated. At present, no DoD agency, to our knowledge, reactivated.* On the shorter term, several issues of direct relevance to collateral damage can be enumerated. For example: (1) the importance of exterior ignitions should be evaluated for situations where interior ignitions do not dominate the fire response of the target; (2) some consideration should be given to situations involving previous damage from either nuclear or conventional weapons, and how this could modify the conclusions

*Recently, the Defense Nuclear Agency and the Defense Civil Preparedness Agency have initiated new fire research programs.

regarding fire effects; (3) improved casualty algorithms should be developed from the historical and other retrospective sources of data (e.g., data from both wartime and peacetime experiences in which fire casualties followed explosions and/or structural collapse) in combinations with mathematical modeling of the dynamics of fire spread as it may impact survival (i.e., "fire trapping"); and (4) an effort should be made to resolve through experimentation the longstanding uncertainty about which laboratory-determined ignition threshold applies (or if neither does, what then?) to practical situations involving the exposure of mixed and geometrically complex fuel arrays.

The applicability of Five-City Study data to Western European situations is of questionable validity. Wherever we have shown that the results are sensitive to the assumed values of a particular target-description variable, an effort should be made to acquire data on-site to at least test the applicability of the U.S. data or, when practical to do so, to provide improved estimates of these variables and their statistics.

In fire predictions, there are numerous "scenario-related" variables that cannot, or should not, be treated in the same way as the usual physical variables having some natural effects, and provision must be made for analyzing their potential role. These include such factors as the following:

1. Burst height and yield
2. Sequence of two or more bursts

3. Warning of the population and its response to warning, e.g.,

   a. closing shutters and boarding up windows
   b. emergency housekeeping
   c. movement to shelter
   d. delegation of fire watch
   e. preparation for self-help fire fighting

4. Indirect threat due to wildland fires.

We discuss here the probable impact of some of these factors associated with sheltering conditions.

The height of burst critically affects (i.e., becomes the principal determinant of) the extent of primary fires of the airburst fireball. The range of 200 to 400 ft SHOB appears to be the main transition region, but a better measure of artificial horizons in typical West German villages is needed to verify this point.

A similar consideration applies to the probability of exposure of interior (room content) fuels. The probability is a strong function of the line-of-sight elevation angle, peaking at about 22° above the horizontal, but it is complicated by trees and buildings in the immediate vicinity of the exposed building (and considered separately from the artificial horizon). More survey information on building heights and separations would also help to better define this factor.

Moderate blast damage caused by one explosion can markedly increase the fire susceptibility of an urban target subjected to a second burst. This effect has not been considered in analyses to date. Other than its effect in removing shutters and other coverings from windows, it is not yet clear what analytical formalism would be applicable, nor what additional data might be needed.

A simple but very effective primary-fire countermeasure is the expendient covering of windows with opaque material. Simply closing a shutter can be quite effective in virtually eliminating all possibility of interior fire starts from a single explosion. This and other countermeasure options must be evaluated, both as a means of outlining the magnitude of the fire problem and to provide some quantitative measure of relative effectivenss for population defense planning.

The indirect threat due to wildland fires is properly treated in terms of such scenario-related variables as weather (current and recent past), proximity of the urban area to contiguous, heavily vegetated areas (e.g., forests), and the number, sequence, kinds, and locations of both nuclear and conventional weapon explosions in the wildland areas adjacent to urban interfaces. Ordinarily, such indirect effects will be unimportant, the threat is nonexistant. In a few circumstances, however, the potential threat should be recognized and an attempt made to evaluate it. In qualitative terms, the conditions accompanying the threat are the same as in any peacetime wildfire situation and much the same "spread/no-spread" rules will apply. The main differences will be magnitude and suddeness of threat development, and the phenomenon of crowning may occur in even the managed forest of Europe where it rarely if ever occurs under ordinary circumstances. Nevertheless, this is strictly a problem for limited localities and adds little to the overall evaluation of collateral damage.

Because of the potential for movement of both injured and uninjured people to avoid the threat of fire and the possibility of entrapment of survivors by fire, the dynamics of fire spread should be included in any comprehensive analysis.

Analytical models for fire dynamics and speed exist but have not been employed in this study because of the still uncertain nature of the overall fire start threat.

In conclusion, the fire threat to collateral damage must be considered due to its possible important outcome. However, the large uncertainties in the methodology and data base must be further refined.

4.4 INFERENCES ABOUT FIRE PREDICTION FROM THE JAPANESE EXPERIENCE

As a check on the prediction of fires, both to improve the methodology and to enhance the credibility of the results, some analytical estimates have been made, independently of the results of the postwar bombing surveys, of the fire damage in the Hiroshima and Nagasaki attacks of World War II. After establishing the scenarios, including relating free-field Q's to peak overpressures and distances from ground zero, we have successfully forecast the gross features of the incendiary damage within the uncertainties of the bombing survey results (see Tables 4.6 and 4.7). Despite the obvious differences between the 1945 atomic bombings and any tactical deployments contemplated for Western Europe in the future, this seemed to be a useful exercise because it represents a large extrapolation from the "Five-City Study" in the direction of tactical yields, and it offers the only real examples of urban targets impacted by the direct effects of a nuclear explosion.

The bombing survey estimates of fire damage resulting in Hiroshima and Nagasaki are shown in Figures 4.12 and 4.13 as functions of distance from ground zero. Our calculated predictions of burnout are shown in the same figures for purposes of comparison. Included also are the predicted initial fires, indicating by difference the contribution made by fire spread.

Table 4.6. Hiroshima Fire Data

Distances From GZ (ft)	No Fire	Primary Fires	Secondary Fires	Spread Fires	Total Fires	Total Buildings Surveyed	Fraction Burned (%)
0 - 999	0	5	3	7	15	15	100
1000 - 1999	0	5	5	10	20	20	100
2000 - 2999	1	4	3	5	12	13	92
3000 - 3999	2	5	3	7	15	17	88
4000 - 4999	5	1	2	13	16	21	76
5000 - 5999	6	0	1	10	11	17	64
6000 - 6999	10	0	2	9	11	21	52
7000 - 7999	12	0	0	4	4	16	25
8000 - 8999	19	0	1	0	1	20	5
9000 -	16	0	0	0	0	16	0

Table 4.7. Nagasaki Fire Data

Distances From GZ (ft)	No Fire	Primary Fires	Secondary Fires	Spread Fires	Total Fires	Total Buildings Surveyed	Fraction Burned (%)
1000 - 1999	7	68	7	30	105	112	94
2000 - 2999	20	30	3	15	48	68	71
3000 - 3999	26	5	6	12	23	49	51
4000 - 4999	46	1	3	5	9	55	16
5000 - 5999	33	1	6	11	18	51	35
6000 - 6999	18	0	4	9	13	31	42
7000 - 7999	2	0	0	0	0	2	0
8000 - 8999	8	3	0	8	11	19	58
9000 - 10,000	13	2	0	0	2	15	13
10,000 - 12,000	5	4	0	13	17	22	77
12,000 -	28	0	0	0	0	28	0

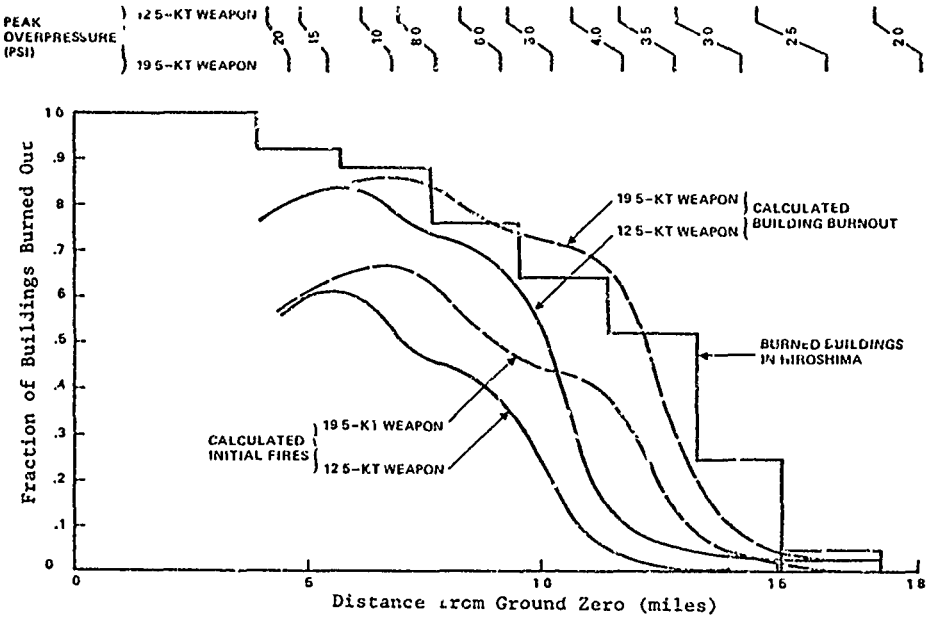

Figure 4.12. The Hiroshima fire data and predictions.

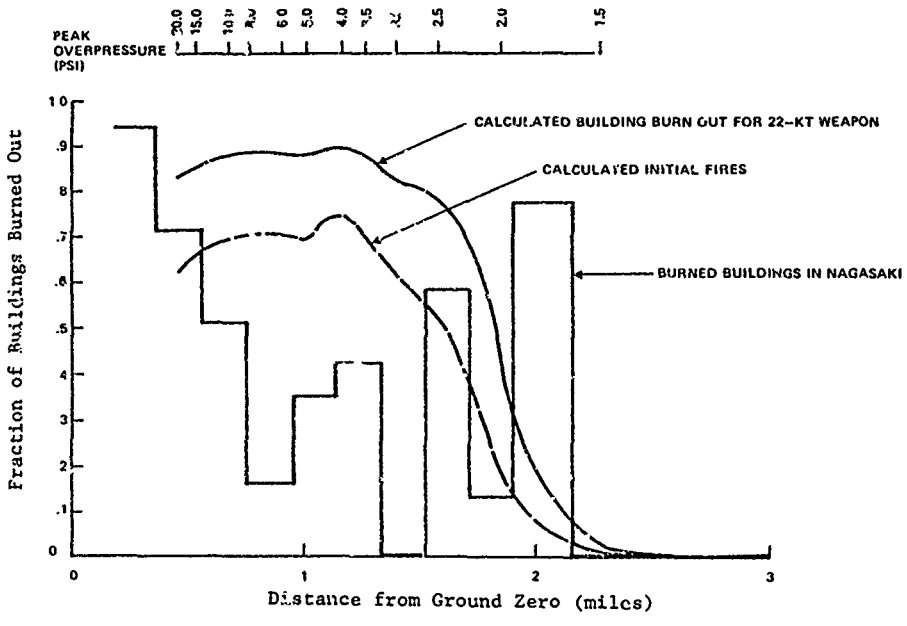

Figure 4.13. The Nagasaki fire data and predictions.

A detailed analysis of the two affected areas was not conducted We simply used average values of fire spread, building density, and structural variables for single-family residential areas as derived from the Five-City Study.

For the Nagasaki case, as shown in Figure 4.13, the predicted building burnout does not agree nearly as well with the fire data. It is felt especially that the characteristics of the structures, terrain effects, and other important scenario variables may have been much different than the "average residential area" variables that were used for predictions. The damaged area in Nagasaki was a heterogeneous complex of varied topography, containing a wide range of building use classes and structural types.

4.5 REFERENCES

4.1 Dolan, P.J., ed., "Defense Nuclear Agency Effects Manual Number 1, Capabilities of Nuclear Weapons," Vol. 2, EM-1 (July 1972).

4.2 "Physical Vulnerability Handbook - Nuclear Weapons," Defense Intelligence Agency, AP-550-1-2-INT, (1 June 1969), Change 3 (June 1976).

4.3 Scott, W.H., Jr., R.L. Faverty and R.E. Dietz, "Initial Radiation Protection in West German Villages," Science Applications, Inc. Report DNA 4340F (Oct. 1975).

4.4 Cohen, M.O., "Protection Afforded by West German Villages Against Initial Radiation from Tactical Nuclear Weapons (U)," Mathematical Applications Groups, Inc., DNA 4127F (Aug. 1975).

4.5 Daniels, R.D., "Investigation of Calculational Aids for Estimating the Effects of Nuclear Weapons on Targets," Lulejian and Assoc., Inc. Report DNA 4111F (Feb. 1976).

4.6 Wiehle, C.K., J R. Rempel and J.L. Beck, "Dynamic Response of Two Types of German House Construction," POR 6966, Stanford Research Institute Report (Sept. 1977).

4.7 Rempel, J.R. and C.K. Wiehle, "Collateral Air Blast Damage," Stanford Research Institute Report DNA 4609Z (April 1978).

4.8 Martin, S.B., et al., "The Impact of Fires Produced by Tactical Nuclear Weapons," Science Applications, Inc. Report DNA 4214 (Dec. 1976).

4.9 Five City Study - Guide for Participants, DOC.5X-XXXX-4000-1. Office of Civil Defense (May 1965).

4.10 John, F.I., and T.C. Passel "Evaluation of Nuclear Weapon Thermal Threat," OCD Work Unit 4311C. Stanford Research Institute Report (Aug. 1966)

4.11 Martin, S.B., R. Ramstad and C. Calvin, "Development and Applications of An Interim Fire - Behavior Model," OCD Work Unit 2538C, URS Report URS 674-3 (April 1968).

4.12 Martin, S.B., et al., "Effects of Air Blast on Urban Fire Response," URS Report URS 705-5 (May 1969)

4.13 Bracciaventi, J., "Window and Window Screens as Modifiers of Thermal Radiation Released in Nuclear Detonation," OCD Work Unit 2434B, U.S. NASL Project 9400-90 (Sept 1966).

4.14 Wilton, C., et al., "Blast/Fire Interaction, Blast Translation and Toxic Cases," OCPA Work Unit 2563A, URS Report URS 7239-11 (July 1966).

4.15 McAuliffe, J., and K. Moll, "Secondary Ignitions in Nuclear Attack," OCD Work Unit 2534A, Stanford Research Institute Report, Project 5106 (July 1965).

4.16 Keller, J.A., "A Study of World War II German Fire Fatalities," Dikewood Corp. Report DC-TN-1050-3 (April 1966).

5. PERSONNEL CASUALTY CRITERIA AND RELATED UNCERTAINTIES

5.1 RATIONALE FOR CONSISTENT CRITERIA

For air burst nuclear weapons, the principal injury mechanisms are

- ionizing radiation, both initial and from fallout
- blast
- thermal radiation,
- debris from buildings
- fires

with injury types generic to each of the above mechanisms as well as injuries from combinations thereof. Each of the basic injury types are considerably different, viz, cellular damage in the hematopoietic and gastrointestinal systems versus physical wounds and cellular disruption of the lungs versus external burns of varying severity. Inasmuch as when the effects of sheltering and injury severity are considered, no one injury mechanism or type predominates for the low yield tactical weapons we are considering in these civilian collateral damage studies, each injury mechanism (as well as combined injuries) must be considered.

It is incumbent on the analysts (of the extent of collateral damage to personnel from tactical nuclear weapons) to arrive at injury criteria that are consistent and intercomparable; like the old problem of counting apples and oranges, burns, broken limbs and depressed blood counts are not directly summable. Hence, in this section, we will arrive at some injury severity levels that are comparable and that can be used to give an overall estimate of the collateral damage suffered by the civilian personnel exposed to the effects of the low-yield tactical nuclear weapon.

5.2 IONIZING RADIATION

5.2.1 Introduction

The following discussion of the human response to ionizing radiation is based in part on the work and recommendations of the Armed Forces Radiobiology Research Institute (AFRRI) and from outher sources including analyses done at the Army Nuclear and Chemical Agency (ANCA), the School of Aerospace Medicine (SAM), the Oak Ridge National Laboratory (ORNL), the Brookhaven National Laboratory and at SAI. It will be limited to consideration of those factors pertinent to collateral damage estimates (viz., civilians) and hence will not address such topics as incapacitation, transient effects, nor supralethal levels. These effects of military interest are being considered in different contexts by other appropriate groups (e.g., AFRRI and ANCA).

We are limiting this discussion to acute effects over a relatively short-time (<60 days). Chronic and long term effects extending over years (and even generations) are equally important in order to consider the entire collateral damage picture, but analyses of these will need to be developed in detail at a later time. Moreover, we shall only consider the external radiation from weapons and shall defer a discussion of internal emitters (viz., fallout) to other reports.

As a further preface to the following, it should be noted that considerable uncertainty still exists with regard to the effects of ionizing radiation on humans. This is because radiation at any level is considered to be harmful thus preventing controlled human experimentation. Extrapolation of animal response data to man has inherent difficulties and inaccuracies. What human data that do exist have either uncertainties in dose (Japanese casualties) and/or non-uniformity of dose (radiation accidents). Where the dose is accurately known in the case of medical response data of very seriously ill patients who were partially or whole-body irradiated (either in single or multiple doses) in attempt to cure or palliate their disease, the nature of their disease also confuses the interpretation of radiation effects.

Respecting these difficulties in deriving human radiation response we shall strive to document some important dose/response data and their principal uncertainties in order to provide bracketing values for estimation purposes.

5.2.2 Basic Considerations

There are a few fundamentals of radiation exposure, energy deposition and biological response that should be considered prior to any detailed discussions of human response to ionizing radiation.

Radiation Units

The Roentgen (R) is a unit of air exposure, i.e., the quantity of ionization in air. Its application is particularly important with use of ionization chambers to measure the level of radiation exposure. The rad is a unit of absorbed dose (100 ergs/gm); it is related to the Roentgen by means of the mass energy absorption coefficients which are radiation, energy and material dependent. For x- or γ-rays of 0.1 to 4 MeV, 1 Roentgen of exposure produces about 0.95 rad of deposited dose in a small sample of muscle. Because most radiation is exponentially attenuated in matter with mean distances the order of human dimensions, the mass attenuation must be considered when converting from exposure to absorbed dose at depth; e.g., 1 Roentgen of photons from a weapon would produce about 0.65 rad of mid-line body dose (standard man) and about 0.70 rad of mid-head dose. For neutrons, air exposure has no meaning so that absorbed dose must be used. Moreover, the dose of secondary gamma rays produced by neutrons interacting with a body contributes to the dose at mid-line or mid-head so there is no simple relationship between these doses and the absorbed dose in a small tissue sample.

One quantity that is often used is the tissue kerma (units of rads) which is defined (Ref. 5.1) as the kinetic energy of all charged particles liberated by indirectly ionizing particles per unit tissue mass. Kerma and absorbed dose differ only slightly at depths where charged particle equilibrium exists and bremsstrahlung losses are negligible (Ref. 5.2). It is only at and near a tissue-air interface, where the dose buildup region

is located, that kerma and absorbed dose differ significantly. Its application is particularly useful in calculations involving complex, mixed spectra that might result from fission weapons. We shall use tissue kerma (free-in-air) as our basic calculational unit and, for our purposes, there is no significant difference between it and absorbed dose.

Relative Biological Effectiveness

All ionizing radiations produce the same types of biological effects, but the extent of response (or damage) in terms of absorbed dose varies with the tissue or organ irradiated, radiation type, total dose, dose rate, and magnitude of the effects (or damage) as well as other possible factors. The term relative biological effectiveness (RBE) is used to relate the radiation dose required to produce an effect to the dose of a reference radiation (Co^{60} or 200-250 kVp x-rays) required to produce the same effect. For the same radiation, there can be a variety of values for the RBE depending upon the variables noted above. It is further complicated by the shape of dose-survival curves and the phenomena of "recovery and repair".

A highly significant factor in determining the RBE of radiation in a particular circumstance is the linear energy transfer (LET) of the radiation. LET is most simply defined as the energy deposited "locally" per unit path length as the radiation interacts with the matter of interest. Its units are usually keV/μ or MeV-cm^2/g. From cellular and small animal radiobiological experiments, we know that RBE is a relatively complex function of LET. From cellular studies, the RBE has a maximum at a LET slightly above 1000 MeV-cm^2/g (carbon ions) (Ref. 5.3). The magnitude of this maximum decreases with severity of the injury. For weapon radiations, the gamma- and x-rays have an RBE of 1.0 (by definition); the neutrons interact with matter by elastic and inelastic collisions and other nuclear reactions

resulting in recoil protons and heavier ions - hence a very complex LET spectrum. High LET radiations (>35 MeV-cm^2/g) such as neutrons have RBEs of 2 to 4 for sub-lethal dermal responses (e.g., skin erythema) and small animal lethality with higher RBEs (10+) for long-term effects such as cataract formation (Ref. 5.4). However, there is some evidence that, for large-animal acute/lethal effects, the RBE of neutrons (Ref. 5.4) is closer to 1.0. For supralethal effects (Ref. 5.5), the neutron RBE (mixed fields with n/γ ratio of 0.4 and 3.0) is not different than 1.0. Conservative recommendations for neutron RBEs have been made for protection purposes (Ref. 5.6) which range from 2 to 11, depending on neutron energy. But for the acute, short-term effects we will be considering here, we will accept the recommendations of AFRRI (Ref. 5.7), ANCA (Ref. 5.8), the Space Radiation Study Panel (Ref. 5.9) and others (Ref. 5.10). These recommendations are that, in the absence of better data and analyses, the neutron RBE be considered 1.0, not because it is exactly 1.0 but because there is no more acceptable value.

Proper Dose Index

Because of the variation of deposited dose across a human (factor of 2 or more for 20 cm) and because the vital organs (i.e., marrow, GI track, cardiovascular system, brain, etc.) affected by radiation are located at different depths, it is nearly impossible to assign a single number (exposure, absorbed dose or otherwise) upon which all human radiation effects may be based. This effect is much larger for neutrons than gamma rays. However, some dose indices have been developed in an attempt to provide a means for inter-comparison and prediction. These include (Ref 5.10):

- Exposure in air - Roentgens
- Tissue dose or kerma free-in-air - rads
- First-collision dose - rads
- Mid-line body - rads

- Integral dose - grams-rads
- Specific organ dose (e.g., skin, marrow, gonads, etc.), integral or differential - gram-rads, rads, etc.

The use of any of these indices as a means to quantify radiation injury may only be appropriate under circumstances where other variables relating to the radiation exposure conditions are either known or within certain prescribed limits. For example, mid-line body dose is thought to be most appropriate when considering lethality. However, the mean lethal mid-line body dose for whole-body exposures for dogs is 20% higher for dogs irradiated unilaterally versus those irradiated bilaterally (Ref. 5.11). This effect would be even greater for human exposures. Likewise, exposure or kerma (free-in-air) cannot be used for children or extremely large adults without considering the radiation attenuation effects which would underestimate the mid-line dose in the former and overestimate the mid-line dose in the latter. Some work in progress to correlate the results of irradiation experiments to detailed calculations of the dose received by blood forming (red marrow) regions is described below in Section 5.5.

For neutrons or mixed neutron-gamma fields, the relationship between mid-line absorbed doses and tissue kerma (free-in-air) is not a single multiplying factor for several reasons (Ref. 5.8 and 5.10).

- Neutrons are more highly attenuated in tissue than gamma rays.
- Neutrons in interacting with tissue produce secondary gamma rays which produce mid-line dose.
- If the RBE for neutrons is believed different from 1.0 then the neutron and gamma dose at mid-line must be considered separately.
- Neutron spectrum differences affect both the attenuation and secondary gamma production, although these differences are less significant at larger ranges.

Hence, the conversion from mid-line doses to tissue kerma for neutrons must be done for each particular situation and not

ascribed a single factor as in the case for gamma-rays. For a simple fission spectrum at ranges beyond several hundred meters, mid-line dose is approximately 0.45 of the free-in-air tissue kerma. This factor includes the secondary gamma-rays. Without the secondary gamma-rays, the ratio would be approximately 0.27 (Ref. 5.10).

Non-uniform irradiations (e.g., half-body) can result in mean lethal integral doses (gram-rads) as much as four times larger (Ref. 5.12, 5.13) in dogs than for uniform whole-body doses. Indeed, some cancer patients are presently being given more than 3 times lethal whole-body doses in a treatment protocol that calls for a single dose of up to 1000 rads (mid-line delivered to one-half of the body followed 30 days later by 1000 rads (mid-line) to the other half) without severe side effects (Ref. 5.14).

Likewise a total treatment dose in excess of the 99% lethal single dose can be given to patients over a protracted period of several weeks without producing lethality (Ref. 5.15). Hence, it is extremely important to qualify the use of any one of these indices as the sole means to assess radiation injury. For the purposes of this discusison, we shall use mid-line body dose in rads or tissue kerma (free-in-air) in rads with the following constraints (unless otherwise noted):

- short irradiation period (<<1 day)
- nuclear irradiations (γ-rays and neutrons from conventional, low-yield, unenhanced fission weapons
- uniform, whole-body, unilateral irradiations.

Shielding Protection Factors

Structures can provide considerable protection from initial nuclear radiation. The degree of protection can vary substantially with the type of structure and the person's exact location within the structure. For a variety of structure types, protection factors have been developed (Ref. 5.16) as previously given in Table

4.1. A more recent analysis for European-type residential structures had derived variations in radiation protection factors (Ref. 5.17) as shown previously in Table 4.2. More analysis is required to refine the protection factors and derive realistic sheltering postures for people within these structures.

5.2.3 Radiation Injury

Radiation effects on man may be categorized in a number of different ways. Langham (Ref. 5.18) proposed dividing the effects into "somatic" and "genetic," where somatic effects appear in the individual irradiated and genetic only in progeny. As noted in Section 5 2.1, we are not considering genetic effects at this time. Somatic effects can be subdivided into early ($\lesssim$60 days) and late effects and each further categorized (Ref. 5.18).

Early Effects

- Skin erythema and moist desquamation
- Prodromal response (radiation sickness)
  - -gastrointestinal (anorexia, nausea, vomiting, diarrhea, intestinal cramps, salivation, dehydration and weight loss)
  - -neuromuscular (easy fatigability, apathy or listlessness, sweating, fever, headache, and hypotension followed by hypotensive shock)
- Hematological depression
- Early lethality
- Decreased fertility and increased sterility

Late Effects

- Permanent or delayed skin changes
- Increased incidence of cataract
- Increased incidence of leukemia and other neoplastic disease

Again, as noted above, we will not be considering late effects in this discussion.

The mean dose to cause skin erythema (reddening) is on the order of 575 rads (Ref. 5.19) and moist desquamation even higher. For the penetrating weapon radiations (excluding fall-out beta emitters) we are considering, this dose at mid-line is more than lethal. Hence, these skin effects -- although of medical interest -- are accompanied by the much more serious effect, lethality. We will not consider them further.

Decreased fertility and increased sterility are further effects we will not consider due to the lack of apparent manifestation of the condition in the irradiated individual.

Summarizing, we are left with the following early radiation effects to consider:

- Prodromal response
- Hematological depression
- Early lethality.

These are to be considered within the following injury hierarchy.

- non-apparent or latent injuries usually long-term or genetic - not considered here as noted above
- apparent (symptom) injuries but not serious enough to require intervention by another individual
- burdening (Ref. 5.20) injuries which require aid from another individual, especially the health care system
- lethal injuries.

Both apparent and lethal injuries have definitive symptoms and end-points, whereas a burdening injury level is a difficult quantity to develop but with immense import because of the implications it has on the quantity of health care necessary to care for the individuals irradiated. As an extreme example, 100 people inflicted with burdening radiation injuries in a city of 1,000,000 could be easily cared for One hundred thousand people in the same city with apparent symptoms of radiation injury but not requiring assistance could stay at home (and feel nauseous) without causing major stress on the city, but 100,000 inflicted with burdening injuries could not possibly be cared for in any organized, rational manner. The concept of burdening injuries thus has utility, although it has been properly criticized as being difficult to define (Ref. 5.21, 5.22).

Symptom Dose

Symptomatic manifestation of radiation effects has been of prime concern for the manned space program. Considerable studies and analyses have resulted from NASA encouraged work (e.g., References 5.19, 5.23, 5.24, 5.25, 5.26 and 5.27). Col. Stromberg (Ref. 5.21) of AFRRI suggests that the recommendations of symptom doses made by the Space Radiation Study Panel (Ref. 5.19) in 1967 are still valid (see Table 5.1). Collectively, the symptoms of anorexia (loss of appetite), nausea, vomiting, fatigue, diarrhea, etc., make up the prodromal response (Refs 5.25, 5.27 and 5.28) which, at a low enough dose, will be all the individual suffers but which at a higher dose, will be a prelude to acute radiation sickness and lethality.

It should be noted that a number of mean symptom doses (SD_{50}) given in Table 5.1 are the same order of magnitude as threshold lethality ($LD_{10/60}$), and lethality is nearly always accompanied by most of these symptoms. Hence, one should estimate the percentage of an irradiated group of individuals that

Table 5.1. Symptom dose levels[a].

	Mid-line Dose (rads)			Exposure Roentge. (R)[c]			Tissue Kerma[c] (free-in-air) (rads)		
	SD_{10}	SD_{50}	SD_{90}	SD_{10}	SD_{50}	SD_{90}	SD_{10}	SD_{50}	SD_{90}
Anorexia[a] (within 2 days)	1 $^{+62}_{-13}$	121 $^{+37}_{-64}$	241 $^{+52}_{-35}$	2	186	370	1	176	352
Nausea[a] (within 2 days)	25 $^{+52}_{-10?}$	172 $^{+??}_{-41}$	318 $^{+104}_{-53}$	38	265	489	36	251	464
Vomiting[a] (within 2 days)	50 $^{+48}_{-88}$	214 $^{+68}_{-43}$	379 $^{+164}_{-75}$	77	329	583	73	313	554
Fatigue[a] (within 6 weeks)	9 $^{+67}_{-163}$	181 $^{+79}_{-57}$	354 $^{+222}_{-83}$	14	278	544	13	265	517
Diarrhea[a] (within 6 weeks)	87 $^{+15}_{-15}$	238 $^{+122}_{-55}$	390 $^{+243}_{-95}$	134	366	600	127	348	570
Prodromal[a] derived from Langham et al. (Ref. 5 27)	78	111	143	120	170	220	114	162	209
Prodromal[b] Lushbaugh, (Ref 5.25)	37 $^{+15}_{-15}$	97 $^{+25}_{-25}$	239 $^{+150}_{-60}$	57	149	368	54	142	349
Prodromal[b] Aceto, et al., (Ref. 5.28)	$\frac{SD_{02}}{100}$	150	$\frac{SD_{80}}{200}$	$\frac{SD_{02}}{154}$	230	$\frac{SD_{80}}{308}$	$\frac{SD_{02}}{146}$	219	$\frac{SD_{80}}{292}$

Note. Derived from "Space Radiation Panel (Ref. 5.19), recommendations except as noted.

[a] Normal distribution.

[b] Non-normal distribution.

[c] Not appropriate for neutrons or mixed neutron-gamma fields. See Section 5.2.2.

would exhibit symptoms only, but not requiring medical assistance, by calculating the total number for a particular symptom and subtracting the number estimated to have either burdening or lethal injuries.

Burdening Injury

The concept of burdening injury was introduced years ago by civil defense authorities to enable defense planners to estimate a possible burden that would be placed on the health care system and survivors in general. Dr. White (Lovelace and now OMRF) and others suggested (Ref. 5.20) that the concept might have validity when considering collateral damage. A consideration of lethality alone lacks completeness, and the consideration of specific symptoms, although readily quantifiable, does not directly establish the stress placed upon the community, particularly if casualties are produced by several different weapon effects (which produce different symptoms). The difficulty of the burdening injury concept is the uncertainty in arriving at meaningful numerical values to describe it.

The dose required to produce a burdening injury is somewhat above the threshold of occurrence of the symptoms of radiation sickness and is obviously below lethality. Figure 5.1 shows probit plots of the radiation symptoms and prodromal responses given in Table 5.1 along with a lethality curve (derivation to be discussed in the next section). From this figure, the mean burdening level (BD_{50}) should lie somewhere above 100 rads (mid-line) and below 250 rads (mid-line).

Hematological levels are prime indicators as to the general well-being of individuals exposed to ionizing radiation in doses below about 1000 rads. Especially important are the depression of the neutrophils (help resist bacterial invasion), lymphocytes (help prevent infection) and platelets (assist with blood clotting) as well as the white blood count (WBC) in general. Moreover,

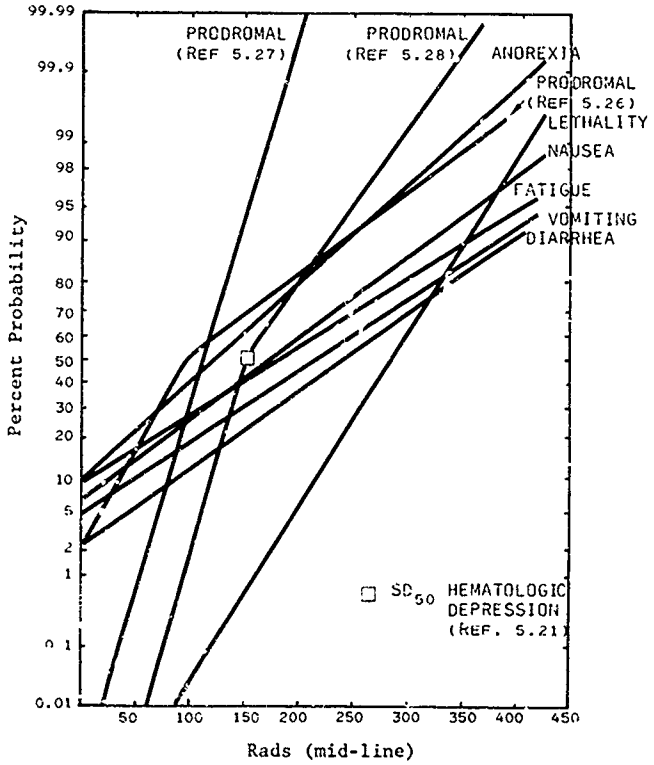

Figure 5 1. Probit plot of human radiation responses.

the survival of the stem cells (responsible for repopulation) is critical even though only a small fraction (~16%) of the total bone marrow is required to supply an adequate quantity of blood cells. Plotted in Figure 5.2 are the percentage hematologic nadirs (lowest points following an irradiation) for several peripheral blood elements (Refs. 5.4, 5.19, 5.26 and 5.29). Dr. Lushbaugh (Ref. 5.30) feels there may be significant inaccuracies in the data analysis of Langham (Ref. 5.19) as plotted in this figure. Dr. Lushbaugh's WBC data is based upon the multi-variant analysis of the clinical observations of 92 patients irradiated with whole-body exposures (Ref. 5.5, 5.26). Indicated also are a number of levels of seriousness for depression of blood levels (Ref. 5.4, 5.31). Clinical support may be required at doses above 75 rads (mid line) and certainly above 200 rads (mid-line).

The NCRP recommendations and analyses provide further insight as to the magnitude of the burdening level (Ref. 5.32). They indicate that less than 5% would require medical care for exposures between 50 R and 200 R, "most" would require medical care between 200 R and 450 R; and that 200 R is regarded as the dividing line between doses that will and will not require medical care.

In summary, the following statements may be made about the magnitude of burdening levels:

	Exposure (Roentgens)[a]	Mid-Line Dose (rads)	Tissue Kerma[a] (free-in-air)(rads)
Prodromal & symptoms:	$154<BD_{50}<385$	$100<BD_{50}<250$	$146<BD_{50}<365$
Hematological depression:	$BD_{10}>115$	$BD_{10}>75$	$BD_{10}>109$
	$BD_{90}<308$	$BD_{90}<200$	$BD_{90}<293$
Other.	$BD_{50}=200$	$BD_{50}=130$	$BD_{50}=190$
	$BD_{05}>50$	$BD_{05}>33$	$BD_{05}>48$
	$BD_{99}<450$	$BD_{99}<293$	$BD_{99}<428$

[a] Not appropriate for neutrons or mixed neutron-gamma fields. See Section 5.2.2.

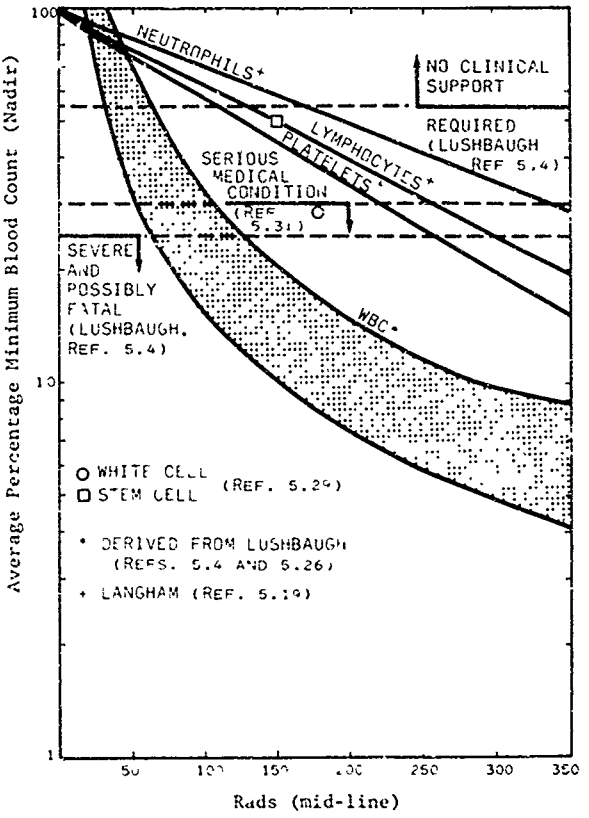

Figure 5 2. Hematologic nadirs versus dose

On the basis of the above and as plotted in Figure 5.3, we estimate the following characterization of radiation burdening levels:

	Tissue Kerma[a] (free-in-air) (rads)	Exposure (Roentgens)[a]	Mid-Line Dose (rads)
BD_{01}	150±75	158	103
BD_{10}	175	184	120
BD_{50}	200±50	211	137
BD_{90}	255	268	174
BD_{99}	300±50	316	205

[a] Not appropriate for neutrons or mixed neutron-gamma fields. See Section 5.2.2.

The BD probability curve shown in Figure 5.3 was skewed at low probabilities towards higher doses and at high probabilities towards lower doses in recognition of the fact that the prodromal response at higher doses will be a precursor to fatality and at the lowest doses non-burdening symptoms alone will appear. This is consistent with the statement that whole-body exposures of less than 100 R would not likely require medical attention (Ref. 5.33).

Lethality

The mean-lethal prompt radiation dose ($LD_{50/60}$) for a normal, healthy, young adult in the absence of medical treatment has been a subject of conjecture since shortly after radiation was discovered (see for example, refs. 5.4, 5.19, 5.32 and 5.33). As noted in the introduction, what human radiation biology that is known is principally the result of accidents, war and therapy of sick patients.

Mammalian radiation lethality is characterized by three syndromes depending upon dose (Ref. 5.34):

- Hematopoietic syndrome - whole-body doses of less than 500 rads
- Gastrointestinal syndrome - whole-body doses between about 500 and 2000 rads

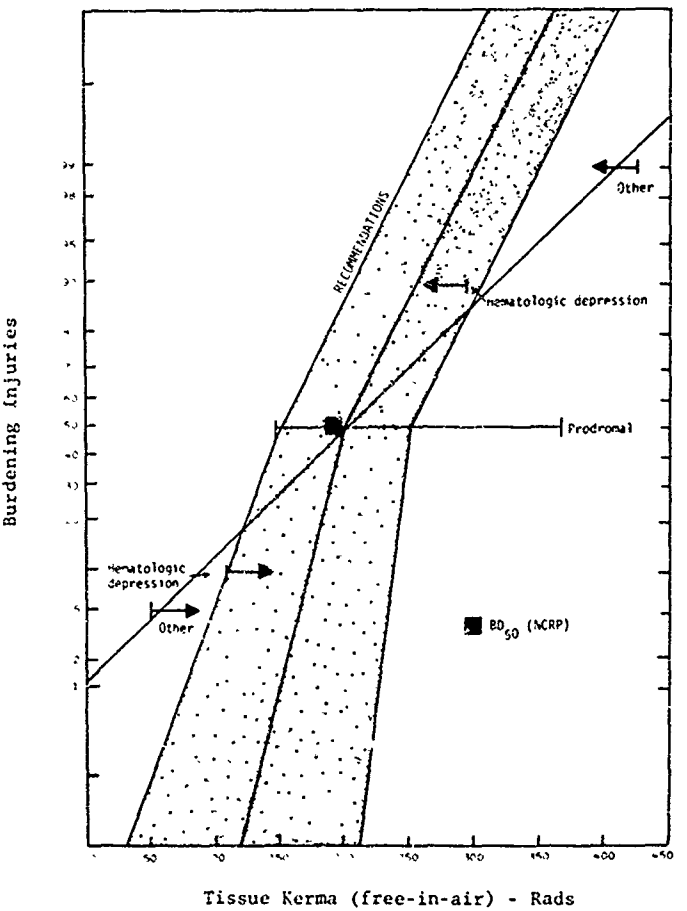

Figure 5.3. Burdening level probability (probit) analysis.

- "Central nervous system" syndrome - whole body doses above 2000 rads.

Although these syndromes are important considerations to the physician and are of fundamental interest to the radiobiologist, our present concern is not with the mechanisms of radiation lethality but rather quantification of lethality versus dose. Where the mechanisms of lethality can become important is when comparing radiations of differing quality, e.g., γ-rays versus neutrons and widely varying mixtures thereof. Then the dose to specific organs becomes important, e.g., bone marrow and spleen for the hematopoietic syndrome, GI tract for the gastro-intestinal syndrome and the cardiovascular and CNS systems for the "central nervous system" syndrome.

Col. Stromberg (AFRRI) has suggested (Ref. 5.21) that the Space Panel 1967 analysis (Ref. 5.19) of lethality for "normal man" is still valid and that there are no more recent analyses that would invalidate the earlier work. Their mid-life dose values for a normal distribution are:

LD_{10} = 220 rads
LD_{50} = 286 ± 25 rads
LD_{90} = 352 rads.

There is another recent study, the so-called "Rasmussen Report" on reactor safety (Ref. 5.35), that considered all lethality data to date including the medical whole-body irradiations. Their values for lethality with minimal medical care are

LD_{10} = 255 rads
LD_{50} = 340 rads
LD_{90} = 430 rads.

The mean lethal dose value is about 20% higher than the Space Panel values. We have chosen to use values slightly above the Space Panel's recommendations but below the reactor safety study.

Accordingly, we feel the errors should be increased somewhat and feel the confidence limits for the LD_{10} and LD_{90} are still not well justified due to the paucity of data at these levels. Our recommended values are:

	Mid-Line Dose (rads)	Exposure[a] (Roentgens)	Tissue Kerma[a] (Free-in-air) (rads)
LD_{10}	230±50	365±75	338±75
LD50	300±35	463±50	440±50
LD_{90}	370±35	570±50	540±50

[a]Not appropriate for neutrons or mixed neutron-gamma fields. See Section 5.2.2.

It should be emphasized that the above are for whole-body irradiations of a "normal man". There are a number of modifying factors which will be discussed below.

5.2.4 Modifying Factors and Special Considerations

There are considerable numbers of factors that modify the prompt, whole-body LD_{50} and BD_{50} estimates for "normal man" and many cases for which the specific values do not apply. In this section, we shall address a number of these factors but mostly as they relate to lethality. It has been nearly impossible to develop quantitative factors that would modify burdening levels. For the time being, we can only assume they are of the same magnitude as those for lethality.

Medical Care

The mean-lethal doses developed in Section 5.3 are for the case of no or "minimal" medical care. The reactor safety study (Ref. 5.35) defines three levels of medical care:

- minimal - little or none
- supportive - reverse isolation, large doses of antibiotics and blood transfusions to control infection and bacterial invasion
- heroic - extraordinary measures such as bone marrow transplantation.

"Supportive" care can be provided by most urban and some rural general M & S hospitals, especially those with facilities for kidney transplants. It is estimated (Ref. 5.35) that there are, within the US, over 400 hospitals that could provide this level of care. There are presently eight medical centers in the US doing bone marrow transplants and could provide "heroic" care. It should be noted that medical care for those irradiated individuals that have a chance for survival with quality medical care need not start for 5 to 20 days after their exposure. The details of treatment for radiation injury and bone marrow transplantation are found elsewhere (e.g., Refs. 5.35 5.36 and 5.37). The reactor safety study recommendations (Ref. 5.35) for lethal levels under the three levels of medical care are as shown in Figure 5.4. It is suggested that "supportive" care can increase the mean lethal dose ($LD_{50/60}$) by 50% and "heroic" care by a factor of 3. Stromberg (Ref. 5.21) of AFRRI also suggests that "supportive" or "heroic" medical treatment would probably increase the $LD_{50/60}$ by 2 to 4 times. Presumably, the LD_{10} and LD_{90} values would be similarly affected.

Partial Body Irradiation

The human body has the remarkable ability to repair injury and to recover from assault by external agents. The hematopoietic (blood forming) system is no exception. If the marrow stem cells are not completely destroyed by ionizing radiation, and if infection and bacterial invasion is controlled, the remaining stem cells can repopulate and the individual recover. Only some 16% of the stem cells are needed to supply sufficient blood cells. Moreover, stem cells in one portion of the body can repopulate areas in other portions of the body where the stem cells were irradiated.

Inasmuch as the blood forming marrow is distributed throughout the human skeleton (Ref. 5.38), a partial-body or a

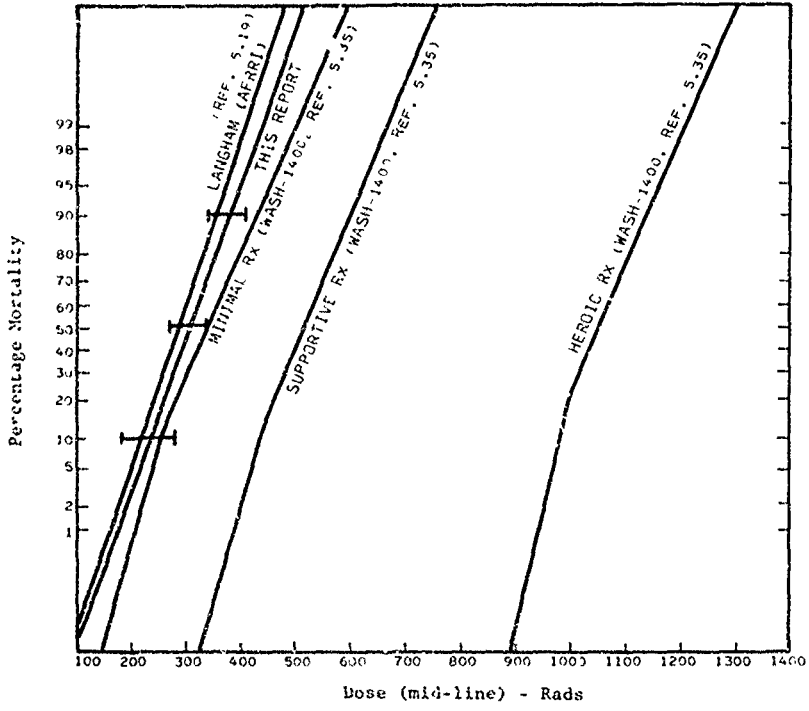

Figure 5-4. Radiation lethality - probit analysis.

non-uniform irradiation that left significant surviving portions of the bone marrow would not likely result in the hematopoietic syndrome and lethality. Indeed, dog experiments (Refs. 5.12 and 5.13) have shown that the $LD_{50/30}$ increases by a factor of 7.1 for partial-body irradiation above the xiphoid process and a factor 3.4 below. The unilateral versus bilateral irradiations (Ref. 5.13) increased the mean-lethal mid-line dose by 20%. In human radiation therapy trials (Ref. 5.14), individuals have been irradiated in single mid-line doses of 600-1000 rads to the upper body (above the xiphoid process or umbilicus) with non-fatal radiation sickness occurring usually within one hour. Irradiations to the lower half body with the same doses produce few or no side effects associated with the prodromal syndrome. In most instances the two irradiations (upper and lower) were separated by about 30 days.

On the basis of the above experiments and human radiation therapy, we conclude that the unilateral radiation would require $1.25\ ^{+0.3}_{-0.1}$ times the dose as bilateral (or uniform) exposure.

By comparison of the onsets of prodromal syndrome in those patients subjected to half-body irradiation (Ref. 5.14) with what would be expected in whole-body exposures, we can obtain some idea of the magnitude that partial body shielding might have for induction of radiation sickness. For the upper body irradiations, prompt radiation sickness was nearly always present; hence the 1000 rads (mid-line) might be equivalent to BD_{90} (174 rads mid-line for whole-body) or BD_{99} (205 rads). This would mean that about a factor of 5 increase in dose was required for approximately the same severity of radiation sickness.

For the lower-body irradiations, a similar analysis attributes the lack of severe radiation sickness to a BD_{10} (120 rads mid-line for whole-body or perhaps BD_{50} (137 rads). The gain would be about a factor of 7.5

The factors of 5 and 7.5 are roughly comparable to those observed for changes in the LD_{50}'s for the partial dog irradiations, although the anatomy is quite different and cannot be used as a good estimate for humans. Our best estimates of the effect of partial-body irradiation for radiation sickness are:

Mean-Burdening Doses (BD_{50})	Upper Body	Lower Body
Mid-line (rads)	700 ± 250	1000 ± 300
Exposure (Roentgens)[a]	1075 ± 400	1525 ± 450
Tissue kerma[a] (rads)	1025 ± 350	1450 ± 450

[a] Not appropriate for neutrons or mixed neutron-gamma field. See Section 5.2.2.

For lethality, very little information other than the partial dog work is known. Moreover, the partial body therapeutic irradiations of 1000 rads (Ref. 5.14) are obviously not lethal. Hence, with the lack of any further information, we assume the factors of 5 and 7.5 for radiation sickness are similar for lethality with large uncertainties. Our best estimates for lethality are.

Mean-Lethal Doses ($LD_{50/60}$)	Upper Body	Lower Body
Mid-line (rads)	1500 $^{+700}_{-300}$	2200 ± 900
Exposure (Roentgens)[a]	2300 $^{+1100}_{-500}$	3400 ± 1400
Tissue kerma[a] (rads)	2200 $^{+1000}_{-400}$	3200 ± 1300

[a] Not appropriate for neutrons or mixed neutron-gamma field. See Section 5.2.2

Obviously, irradiations over less than half-body would result in doses considerably higher than these figures, and irradiations greater than half-body would be closer to those for whole

What interpolation or extrapolation techniques should be used for these intermediate values are unknown.

Fractionation and Time Dependence

For cases where individuals receive multiple irradiations separated by periods of time, the radiation effects are not completely additive. The human body has the ability to initiate repairs in periods of less than a day. The Ellis formulation (Ref. 5.39) of normal tissue response to fractionated radiation is well founded in human therapy trials:

$$ED = NSD\ F^{0.24}\ T^{0.11}$$

where ED is the total dose given in F fractions over T days required to produce the same biological effect as the nominal single dose (NSD). The validity of this formulation for lethality is unknown but is not significantly different from formulations for the effectiveness of protracted continuous irradiations. For two equal doses separated by various periods the nominal single dose (NSD) is plotted in Figure 5.5.

Special Populations

In most species, females are slightly more radio-resistant than males. No quantification of this effect is available. However, it is known that in utero irradiation of a fetus has varying sensitivity throughout the period of gestation (see e.g. Refs. 5.34, 5.35, 5.40 and 5.41). Western European and U.S. birth rates are such that now only a little more than 2% of the female population is pregnant at any given time

For the first trimester of the pregnancy lethal doses to the fetus are quite low. The LD_{01} and LD_{50} as recommended by the Reactor Safety Study (Ref. 5.35) are plotted in Figure 5.6 Although the dose of LD_{50} is quite low shortly after

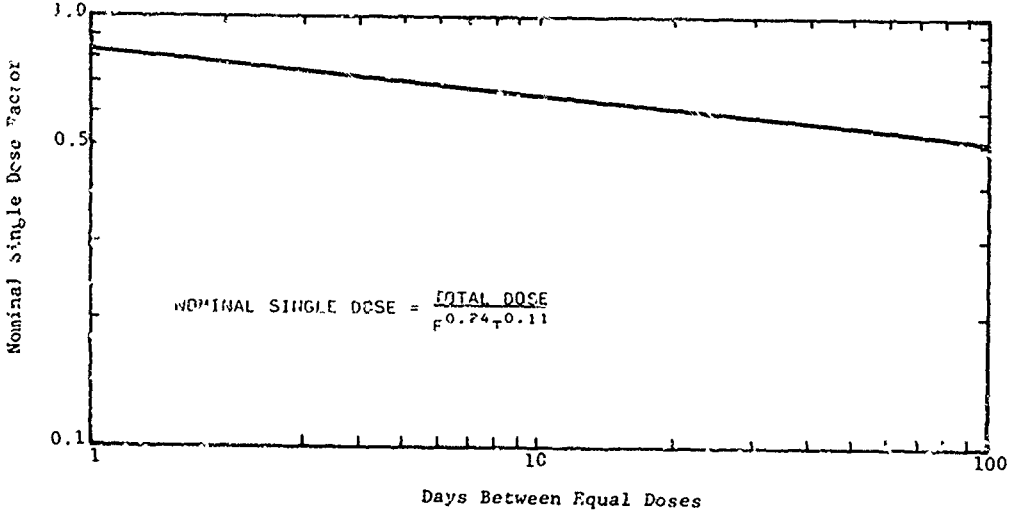

Figure 5.5. Fractional dose relationships.

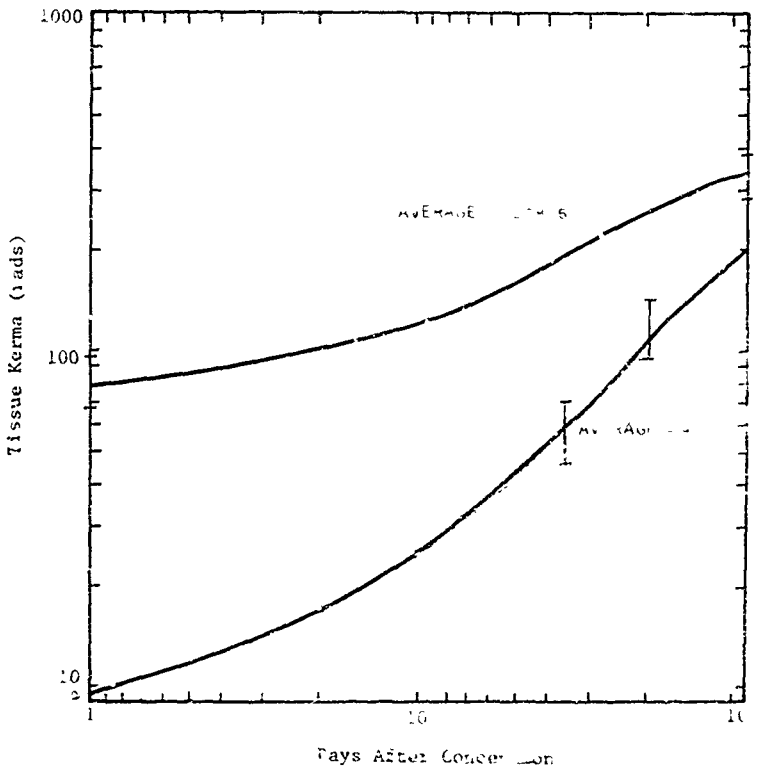

Figure [illegible] In utero [illegible]
(Ref [illegible])

conception, operational reality asks the question: "Who would even know if a day-old fetus was killed?" On the other hand, abnormalities and deformaties induced by radiation in fetuses that come to full-term will be readily apparent--not apparent will be genetic effects, increased mortality during the first year of life (Ref. 5.41), enhanced susceptibility to cancer, etc.

During organogenesis (3rd to 6th week of pregnancy) gross abnormalities of the human fetus can be produced by small radiation levels. Indeed, discussions regarding therapeutic abortions following exposures as little as 10 R have been made (Ref. 5.34). Quantitatively, reduced head size has been studied for Hiroshima and Nagasaki survivors irradiated in utero in the first 17 weeks of pregnancy (Ref. 5.42). The mean dose for 50% probability of reduced head size was about 150 rads, and 10% probability was between 10 and 20 rads. We thus assign to the production of non-fatal abnormalities the following in utero irradiation levels:

	Midline (rads)	Exposure[a] (Roentgens)	Tissue kerma[a] (rads)
ED_{10}	$15\ ^{+10}_{-5}$	$25\ ^{+15}_{-7}$	$20\ ^{+15}_{-7}$
ED_{50}	150 ± 25	230 ± 40	220 ± 35
ED_{90}	290 ± 75	450 ± 115	425 ± 110.

[a] Not appropriate for neutrons or mixed neutron-gamma fields. See Section 5.2.2.

Radio-sensitivity is higher in young and old mammals than in full adulthood (Ref. 5.34). This effect is thought to be present in man (Ref 5.43) but unverified by experimental data. The $LD_{50/30}$ in mice (Ref. 5.43) is about 25% less for young and old than for full adults. The $LD_{50/30}$ for young rats is about 70% less and for old rats about 30% less than for full

adults (Ref. 5.34). Extrapolation of small animal data to man is very risky, but some special consideration must be given to the children and aged of a civilian population.

The plots of the rat and mice lethality data versus effective human age are plotted in Figure 5.7. Our estimates for man are chosen to follow the general trend of the small-animal data. The distribution is for an entire population. In any given location it will be different; and, in a period of crisis, it is very likely to be different. Moreover, changes in birth rates in the U.S. and Western Europe will modify this age distribution in the future.

There are wide-ranging differences in LD_{50} between various species (contributing to the difficulty of extrapolating animal results to man), but there are even significant differences in radiation sensitivity between strains of the same species (Ref. 5.34). LD_{50} differences (Ref 5.44) in 6 strains of mice give a standard deviation of 7% and maximum deviation from the average of 13%. We have no way of relating this to human radiobiology but will assume that these differences are contained within the uncertainties of the $LD_{50/60}$'s developed earlier.

Other Modifying Factors

Health status, diet, endocrine status, fatigue and lowered temperature are factors (Ref. 5.34) that affect the value of LD_{50}, but the effects for man are unknown. Even for animal studies, there are very little data available. Hence, we will not at this time attempt to apply such data to man. There are, however, two effects that require some discussion -- reduced oxygen and chemical agents.

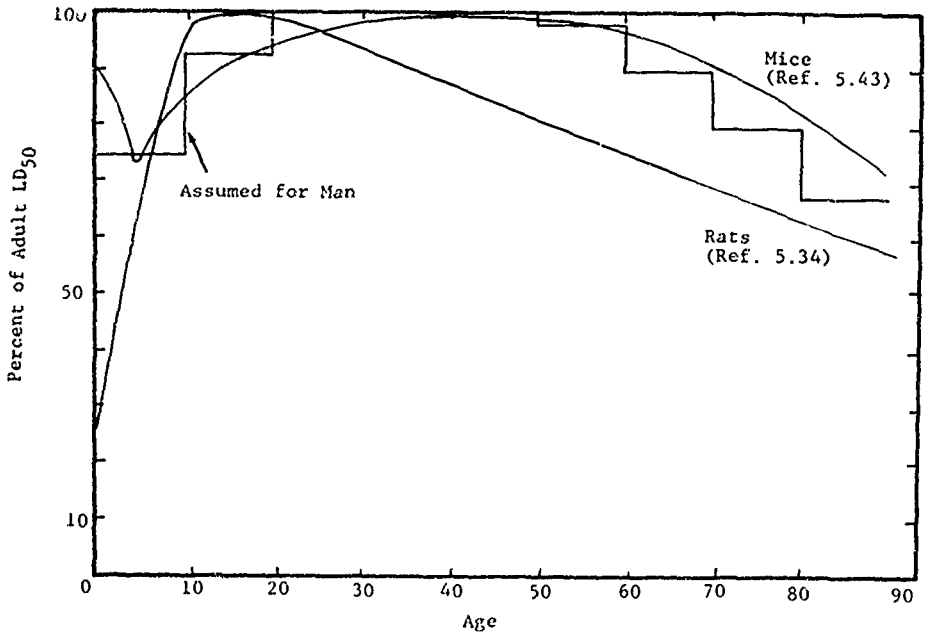

Figure 5.7. Age dependence of radiation lethality.

It is well known that reduced oxygen decreases radiation sensitivity (see e.g., Refs. 5.3 and 5.34) and that the oxygen effect is LET dependent; i.e., high LET radiations show less dependence upon oxygen tension. A decrease of oxygen pressures at 25% of the normal pressure results in an increase in LD_{50} for animals by a factor of two. This reduced pressure would correspond to an altitude of about 34,000 feet. Humans are not normally subjected to this amount of oxygen reduction. The functional dependence of the LD_{50} on oxygen pressure is unknown; but presumably the effect on mountain climbers, pilots and others at high elevations will probably be less than 30% (semi-log interpolation).

Chemical protective agents have been studied for some time (e.g., Refs. 5.3, 5.9, 5.34 and 5.45). Dose reduction factors DRF (defined as the ratio of the dose to produce an effect in the presence of the compound to the dose required to produce the same effect without the compound) as high as 2.7 have been noted for lethality (Refs. 5.29, 5 46). However, these compounds have not yet been approved for widespread use due to their high toxicity. Moreover, at this point in time, it is not reasonable to assume that a civilian population would be provided with protective agents prior to any irradiation. We will not consider this protection mechanism further at this time except to note that ethyl alcohol offers some protection from radiation (Ref. 5.34) -- human dose for significant protection would be about 1 liter of Vodka.

5.2.5 Summary

A summary of estimated radiation effects on men and uncertainties are given in Table 5.2.

Table 5.2. Summary radiation effects on man. (tissue kerma, free-in-air, rads) (a)

Symptoms	SD_{10}	SD_{50}	SD_{90}
Anorexia (within 2 days)	1^{+90}_{-1}	175^{+55}_{-95}	350^{+75}_{-50}
Nausea (within 2 days)	35^{+75}_{-35}	250 ± 60	456^{+150}_{-75}
Vomiting (within 2 days)	75^{+70}_{-75}	315^{+100}_{-65}	555^{+240}_{-110}
Fatigue (within 6 weeks)	15^{+100}_{-15}	265^{+115}_{-85}	515^{+325}_{-120}
Diarrhea (within 6 weeks)	125^{+65}_{-90}	350^{+180}_{-80}	570^{+355}_{-140}
Burdening	BD_{10}	BD_{50}	BD_{90}
Whole-body	175 ± 65	200 ± 50	255 ± 50
Partial-body (upper)	900 ± 450	1025 ± 350	1300 ± 350
Partial-body (lower)	1250 ± 600	1450 ± 450	1850 ± 450
Lethality	LD_{10}	LD_{50}	LD_{90}
Whole-body (min care)	338 ± 75	440 ± 50	540 ± 50
Whole body (supp care)	510 ± 150	660 ± 100	810 ± 100
Whole body (heroic care)	1110 ± 650	1320 ± 450	1620 ± 450
Partial-body (upper)	1700^{+1100}_{-500}	2700^{+1000}_{-400}	2200^{+1000}_{-400}
Partial-body (lower)	2450±1300	3200±1300	3900±1300
In-utero (1st trimester) (varies with time--see Fig 5 6)	40 - 250	80 - 325	115 - 405
Unilateral vs Bilateral		$\times 1.25^{+0.5}_{-0.1}$	
Age Distribution		x 0.68 - 1.0	
Sex		F > M	
Other	ED_{10}	ED_{50}	ED_{90}
Non-fatal abnormalities for in utero (1st 17 weeks of pregnancy)	20^{-15}_{-7}	220 ± 35	425 ± 110
Chemical Protective Agents		x 1.0 - 2.7	
Oxygen (14 000 ft)		$\times 1.3^{+0.1}_{-0.3}$	

(a) Not appropriate for neutrons or mixed neutron-gamma fields. Mid-line doses must be converted on basis of spectrum and neutron-gamma ratio to tissue kerma. See Section 5.2.2.

5.3 THERMAL RADIATION

5.3.1 Introduction

The following discussion of the human response to thermal radiation from nuclear weapons is based in part on the work and recommendations of a number of groups including the Naval Material Lab (Brooklyn), the Naval Surface Weapons Center (White Oak), the Army Nuclear and Chemical Agency (ANCA) and the Lovelace Foundation for Medical Education and Research as well as SAI. This discussion will be limited to consideration of the factors pertinent to collateral damage estimates (viz., civilians) and hence, will not address such topics as incapacitation. Effects of military interest are being considered in differing contexts by other appropriate groups (e.g., ANCA).

We are limiting this discussion to acute effects over a relatively short time ($\leq$ 60 days). Long-term disabilities and treatment (skin grafts, etc.) extending over years are equally important in order to consider the entire collateral damage picture, but analyses of these will need to be developed in detail at a later time. Moreover, in this section we shall only consider the thermal radiation effects from weapons resulting from flash burns or burns through clothing; burns caused by fires ignited by the nuclear weapon were discussed in Section 4.3.

The relative importance of thermal radiation in the production of nuclear casualties has been determined by analysis of the Hiroshima and Nagasaki Japanese casualties. For these particular cases (12.5 KT and 22 KT), the following distribution of casualties was noted (Ref. 5.47):

Burned	42%
Not burned but with other injuries	58%
Mortality in burned patients	19%
Mortality in unburned patients	6%.

However, there are considerable uncertainties in the production of casualties by thermal radiation from nuclear weapons. These will be discussed below. The latitude of variations due to shielding, clothing, etc. is such that the military does not use thermal criteria for nuclear weapons employment considerations and considers thermal casualties to be a "bonus effect" (Refs. 5.48, 5.49). Respecting the difficulties in predicting thermal casualties, we shall strive to document estimates of the primary effects and modifying factors, along with estimates of their principal uncertainties, in order to provide bracketing values for collateral damage predictions.

5.3.2 Basic Considerations

For the purposes of this report, a burn is defined as the irritation, injury, or destruction caused to tissue by exposure to excessive heat. In this case, the thermal energy component (20 to 40% of the total energy release) of the nuclear weapon causes either direct flash burns or contact burns due to heated/burning clothing. All effects discussed here are assumed to be independent of type of weapon, fusion or fission.

Burn severity is classified as first degree (1^{o}), characterized by immediate pain but reversible tissue injury similar to sunburn, second degree (2^{o}), characterized by pain with damage to only part of the skin thickness, thus allowing for scab formation and eventual full tissue regeneration; third degree (3^{o}), characterized by irreversible full-thickness skin damage, no pain except at the periphery due to damage of the nerve endings, and requiring skin grafts or resulting in scarring; and, sometimes considered, fourth degree (4^{o}), characterized by "charring".

Burns from nuclear weapons are either "flash burns" resulting from the direct interaction of the weapon's thermal energy with the skin's surface (or transmission through light clothing) or "flame" (or "contact") burns resulting from heat transfer through clothing, burning clothing or contact with burning materials. The flame burns are identical to those from industrial or domestic accidents. On the other hand, flash burns are very rare in accident cases. They are characterized by the quick rise of skin temperature and some transmission (skin is transparent to some wave lengths) before absorption, usually resulting in less damage at depth. The injured surface layers of the skin remain more intact than those from flame burns, which results in less susceptibility to infection (Ref. 5.50). The treatment is similar to other common thermal burns (Ref. 5.51) and possibly less fatal (Ref. 5.52). Experience in Hiroshima and Nagasaki give the following relative amounts of flash and flame burns among the 20-day survivors (Ref. 5.47):

	Flash Burn	Flame Burn	Both
Hiroshima	82.9%	1.9%	14.9%
Nagasaki	90.9%	3.4%	5.7% .

The flame burns tended to cover a larger area than the flash burns (Ref. 5.51).

5 3 3 Exposure

The extent and severity of flash burns depends directly on the total amount of the thermal radiation actually received or transmitted to the skin, its duration and, to some extent, its frequency spectrum The time-integrated irradiance, Q (expressed in cal/cm^2), is the radiant exposure energy per unit area.

For the purposes of this study, a cumulative lognormal distribution is most appropriate for the severity versus thermal energy relationship; some of the properties of this distribution are found elsewhere (Ref. 5.16). We shall be deriving Q_{50} (the integrated irradiance for a 50% probability of a particular degree burn under a determined set of circumstances) as well as mean-burdening (BD_{50}) and mean-lethality (LD_{50}) values of Q. An upper limit of the variance to mean ratio, σ/m, can be determined by analysis of the bare pig-skin burn threshold measurements of Henriques and Maxwell (Ref. 5.53). This analysis yields a $\sigma/m \leq 0.3$. The variance of laboratory experiments which, up to now, have been deliberately conducted with as uniform a sample as possible, denotes only how well the basic energy vs. burn severity relationship is known and does not reflect real population variances. A σ/m for an "average population" may be derived for burn data given in EM-1 (Ref. 5.16). This yields a value of 0.4, which may include addtional variations beyond the biological response (Ref. 5.54). Analysis of the Institute of Nuclear Studies study (Ref. 5.48), which intentionally "safe-sided" the data, yielded the following σ/m values: 1^o, 0.4; 2^o, 0.25, and 3^o, 0.19. For exposed skin burns, we have adopted the value 0.3 for σ/m.

For burns under clothing, experimental work on rats by Derksen and de Lhery (Refs. 5.55, 5.56) may be analyzed to give a σ/m near 0.2 for clothing in contact with the skin as well as separated by a gap of 5 mm.

Weapon spectrum differences result in ∿10 to 20% differences in values of Q for the same biological effect (Ref. 5.54). Infrared is less injurious than visible (Refs. 5.57, 5.58). Mean levels for complete transepidermal burns in swine versus spectrum have been measured by Berkeley, et al. (Ref. 5.59).

Carbon arc	4.9 cal/cm^2
Carbon arc + 2400 Å cutoff (some UV + visible + IR)	4.5 cal/cm^2
Carbon arc + 3600 Å cutoff (visible + IR)	5.0 cal/cm^2
Carbon arc + 5200 Å cutoff (part visible + IR)	7.0 cal/cm^2
Carbon arc + 6400 Å cutoff (mostly IR)	6.9 cal/cm^2

The thermal spectrum at a distance from a low-altitude nuclear explosion can be roughly approximated by a black body at a temperature of 6,000 to 7,000°K (Ref. 5.60). Its maximum occurs in the visible spectrum. Spectrum differences are unimportant at low altitudes. High-altitude explosions are richer in ultraviolet at the first portion of the thermal pulse. with a shift to mostly infrared in the long tail (Ref. 5.60). A content of ∿10% ultraviolet (greater for lower yields and higher altitudes) in the weapon spectra is not too important in the production of flash burns (Ref. 5.61). Ultraviolet is also readily attenuated in the air (Ref. 5.60).

Following Derksen (Ref. 5.54), we will adopt ± 15% in mean values of Q arising from spectrum differences.

5.3.4 Effects

The traumatic and physiological effects of human burns are becoming well understood due to the large number of accidental burns encountered each year. Besides the degree of the burn, the principal prognostic factor used is the percentage of the total skin area burned, as will be discussed below. However, the experience in whole-body flash exposures is limited to the Hiroshima and Nagasaki experiences. The resultant fire storm (Ref. 5.62) complicated the flash burn analysis (Ref. 5.47) in Hiroshima. There is a serious discrepancy in the thermal levels at Nagasaki; the Dikewood (Ref. 5.63) analysis gives a yield of 12.6 KT based upon burn levels versus the 22 KT derived from other yield analyses. Cloud cover could have attenuated the thermal radiation, but the height of burst was supposedly below the clouds (Ref. 5.63).

Excellent information exists on the Q required to produce a specific degree of flash burn; both animal and human experiments (small area) have been performed. But the real difficulty lies in determining the body area burned by the thermal radiation and to what degree it is burned. The controlled animal and human experiments use normal incidence on bare skin and clothed skin (both contact and spaced). Very little area of a human body will be normal to incoming thermal radiation, so that a cosine factor must be used; and the degree of protection by clothing (see below) is highly varied over the body (multiple layers versus single, contact versus spaced). Moreover, instinctive response to protect oneself from the pain assault may result in some amelioration of the burn for larger weapon yields.

In summary, there is considerable uncertainty in the Japanese casualty experience and additional uncertainties in projecting controlled laboratory experiments to field conditions.

The various factors that enter into the determination of the mean radiant exposure required to produce a specific biological effect will be discussed below along with a qualification of their uncertainties.

Burn Severity

The thermal energy from a nuclear weapon at a distance in the lower atmosphere is delivered over a period of time dependent upon yield. The time to maximum intensity, t_{max}, and the time for 80% of the integrated pulse, t_{80}, are (Ref. 5.60) as follows:

Yield (KT)	0.01	0.1	1.0	10	100	1000	10000
t_{max} (sec)	0.003	0.01	0.03	0.10	0.32	1.01	3.2
t_{80} (sec)	0.03	0.09	0.28	0.87	2.75	8.70	27.5

The thermal tail beyond the 80% point is mostly infrared and hence does not contribute significantly to the burn. The 80% time varies by two orders of magnitude with yield. At the higher yields (longer times), the absorbing skin has time to dissipate a considerable amount of the heat deposited; hence, the degree of burn is yield dependent.

For normal incidence on medium-colored exposed skin in moderate ambient temperature, the following (Refs. 5.53, 5.54) are the Q_{50} (cal/cm^2) values for pain and various degree burns which we have adopted for this study:

Yield (KT)	0.01	0.1	1.0	10	100	1000	10000
Pain - Q_{50}^{P}	1.0	1.0	1.1	1.4	1.8	2.6	3.8
1^{o} - $Q_{50}^{1^{o}}$	1.9	1.9	2.0	2.3	2.8	3.2	3.8
2^{o} - $Q_{50}^{2^{o}}$	3.8	3.8	4.0	4.6	5.2	6.1	7.0
3^{o} - $Q_{50}^{3^{o}}$	5.8	5.8	5.9	7.0	8.1	9.3	11.0

The errors in these mean Q's are on the order of 20% or less; but there are factors (e.g., clothing, skin color, external temperature, non-normal incidence, etc.) that considerably modify these nominal values as discussed below. It has been found, but not quantified, that the area of the burn alters the pain and 1^{o} mean values (Ref. 5.64).

Burn Area

The prognosis of a thermal injury is directly related to the degree of burn and the area of the body injured. The total area of the body in cm^2 is approximately equal to the product of 71.84, the height in cm and the weight in kg. First degree burns are not medically important, but there is a strong correlation of the prognosis of the thermal injury with area of second and third degree burns (Ref 5.51). A majority of the 20-day survivors with burns in Hiroshima and Nagasaki had burns covering less than 10% of the body, a considerable number had 10 to 20% burns and a few had more than 40% (Ref. 5.47). By geometric considerations, flash burns cannot cover more than 50% of the body, indeed, one-third might be a reasonable maximum (Ref. 5.51). For higher yields or moderately clothed individuals, large body burns are not probable except for unconscious persons (Ref. 5.54). Bull and Fisher (Ref. 5.65) suggest that the area of partial skin injury (i.e., 2^{o} or severe 1^{o}) be weighted by one-fourth and added to the area of 3^{o} burn.

Hence, in all cases, burns covering large areas of the body will generally consist of a combination of both 2^{o} and 3^{o} burns. In some approximation of the geometry of the human body, e.g., a cylinder (Ref. 5.48), it is necessary to determine for a given exposure the extent (area) of both 2^{o} and 3^{o} burns, inasmuch as there is a difference in the systemic reaction depending on the degree of the burn.

For a log-normal distribution with a σ/m of 0.3, an area correction factor that gives the area percentage of a specific degree burn for this assumed geometry versus what it would be for totally normal incidence as a function of Q_{inc}/Q_{50} has been developed (Ref. 5.66).

Q_{inc}/Q_{50}	Area factor
0	0
0.25	0.15
0.5	0.28
0.75	0.37
1.0	0.44
1.25	0.52
1.5	0.58
1.75	0.65
2.0	0.70
2.5	0.77
3.0	0.83
3.5	0.87
4.0	0.89
4.5	0.92
20	0 99

The total percentage of body area burned to 3^{o} is calculated from the 3^{o} area factor times 0.5 (a maximum of only 50% of the body surface area is exposed to a burst). This must be subtracted from the area burned to at least 2^{o} to obtain the area burned to 2^{o}, which is then weighted by one-quarter.

Injuries

Burns are one of the most highly feared injuries due to the nearly instantaneous intense pain and due to the nearly universal experience by everyone to burns of some level. Here

quantification of burn injuries and mortality may not present the entire picture. Success in burn therapy is not necessarily reflected in survival statistics. Hideous deformities, limiting contractures and scarred personalities may not reflect well in data which report only mortality. Hence, we are suggesting that three injury levels be considered:

- Threshold burn injury
- Burdening burn injury
- Lethal burn injury.

Each of these will be discussed below.

Threshold Injury

When considering civilian casualties, it may sometimes be important to know the total number of civilians affected in any way by the conflict. Hence, even a threshold injury that does not require hospitalization or aid from another person may be politically significant. For burns, threshold might be the induction of pain, a 1^{o} burn, or a small 2^{o} burn (that can be self-treated). Figure 5.8 shows the differential mixture of burns for 1 KT versus Q resulting from a probit analysis (σ/m = 0.3) of burn probabilities. For a Q of 2.5 cal/cm^2, at 1 KT, the following distribution gives an injury level that would be indicative of an injury threshold inasmuch as a 1^{o} burn might not always be recognized as an injury.

	Integral (%)	Differential (%)
Pain	100	27
1^{o} burn	77	71
2^{o} burn	6	6
3^{o} burn	0	0

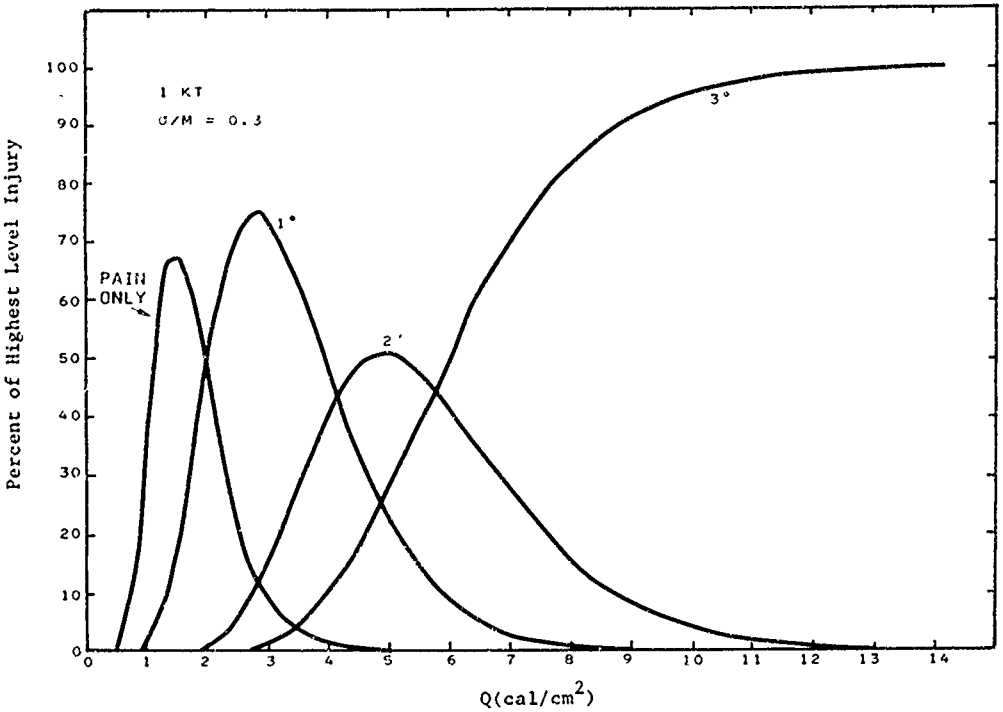

Figure 5.8. Injury levels versus Q (cal/cm^2).

Hence, the following Q's (cal/cm^2) are recommended as mean threshold injury levels:

Yield (KT)	0.01	0.1	1.0	10	100	1000	10000
Threshold Injury Q_2 (cal/cm^2)	2.4	2.4	2.5	2.9	3.4	3.9	4.6

Uncertainties would be on the order of $\pm$ 20%.

Burdening Injuries

As discussed above for the case of ionizing radiation, a consideration of lethality alone lacks completeness; and the consideration of specific burn levels, although readily quantifiable, does not directly establish the stress placed upon the community, particularly if casualties are produced by several different weapon effects (which produce different symptoms). The difficulty of the burdening injury concept is the uncertainty in arriving at meaningful numerical values to describe it. The Q required to produce a burdening injury is somewhat above the threshold injury and is obviously below lethality. There are several pieces of information that shed some light upon what mean radiance, Q, would be required to produce a mean burdening level.

Mixter (Ref. 5.67) suggests that 2° or 3° burns of body area in excess of 10% require hospitalization. Lyke, et al. (Ref. 5.68) suggests that no hospitalization is required and that treatment can be handled on an outpatient basis for burns of less than a 5% area. DNA EM-1 (Ref. 5.16) and the NATO Handbook (Ref. 5.69) both suggest hospitalization for 2° and 3° burns of area greater than 20%. But the NATO Handbook also suggests hospitalization for burns less than 20% if the hands, feet, neck, or face are involved (lips and eyelids are especially

sensitive) and requiring medical care for severe (1^{o}) burns. These areas could be as low as 5% or less. Shock resulting from burns is not important (Ref. 5.51) for burns of less than 10%. Shock is almost a certainty for 2^{o} burns exceeding 30% area and 3^{o} burns exceeding 25% area (Ref. 5.16). Summarizing, hospitalization is probably required for 10 to 20% area burns (2^{o} and 3^{o}). Outpatient treatment is probably required for 5 to 10% area burns (2^{o} and 3^{o}). The following are estimates of burn area percentage and probabilities using the area correction factors given above and the probability factors given in Figure 5.8 for 1 KT:

	2^{o} Burn		3^{o} Burn	
Q (cal/cm^2)	Prob. (%)	Area (if burned) (%)	Prob. (%)	Area (if burned) (%)
2	1	14	0	7
3	17	18	1	14
4	50	22	9	17
5	77	26	27	19
6	91	29	50	22
7	97	32	70	24
8	99	35	84	26
9	100	37	91	29
10	100	39	96	31

The mean 2^{o} level (4 cal/cm^2) produces, with about 50% probability, a burn in excess of 20% of the body area; hence, we shall adopt this value as the burdening level requiring hospitalization.

Of course, other factors enter into the burdening level determination: outpatient care, injury of sensitive/critical areas (e.g., extremities and head), protection by clothing, etc. The first two would require lower levels of Q; the last requires higher values of Q. It would be extremely difficult to

incorporate these opposing factors into an analysis; hence, we will assign 50% errors to the mean burdening levels. At the lower end of the range (2 cal/cm^2 for 1 KT), this would be at the threshold for 2^o burns, with a 50% probability of 1^o burns and nearly a 100% probability of pain. At the higher end of the range (6 cal/cm^2 for 1 KT), this would be near the 50% probability of 3^o burns. In summary, the mean burdening levels in cal/cm^2 for lightly dressed individuals would be (Ref. 5.70)

Yield (KT)	0.01	0.1	1.0	10.0	100	1000	10000
BD_{50} (cal/cm^2)	3.8	3.8	4.0	4.6	5.2	6.1	7.0

with uncertainties of $\pm$50% and the qualification that no evasive action (see below) is taken for the higher yields. As a check, ENW (Ref. 5.60) indicates that, for Hiroshima, "some" burns required treatment as far out as 12,000 to 14,000 feet from ground zero. The radiant exposure there was on the order of 2 cal/cm^2, which would be near the 1% burdening level.

In conjunction with burdening, some healing and hospitalization times have been analyzed. Butterfield, et al., (Ref. 5.71) reported the following empirical relationship for flash burns:

$$\text{healing time (days)} = 0.92\,Q^2 + 1.26\,Q - 4.26$$

$$\text{for } 2 < Q < 6 \text{ cal/cm}^2$$

where Q is the exposure in cal/cm^2.

White (Ref. 5.72) reported the following healing times for flash burns:

1^o	8 days
2^o (uninfected)	8-16 days
2^o (infected)	up to 42 days

3^{o} (uninfected, small burns)	20-30 days
3^{o} (larger burns with scar formation)	20-42 days
3^{o} (skin grafting)	"many months".

Bitke, et al., (Ref. 5.68) reported the following average hospitalization times:

	Survivors Only	All Patients
Group III (>30% 1^{o} and 2^{o} or >15% 3^{o})	130 days	73 days
Group II (15-30% 1^{o} and 2^{o} or 5-15% 3^{o})	113 days	90 days
Group I (<15% 1^{o} and 2^{o} or <5% 3^{o})	"substantially shorter"	

Blocker (Ref. 5.73) reports the following approximate hospitalization times:

Body Area	Hospitalization Time
<20%	6 weeks
20-50%	9-10 weeks
>50%	12-14 weeks (under most favorable conditions).

Second degree burns heal about twice as fast as third degree burns unless the lower extremities are involved.

Lethal Injuries

Several studies have been made of the mortality of flame burns versus area of the body burned. As noted earlier, Bull and Fisher (Ref. 5.65) suggest that the area of severe 1^{o} burns plus all 2^{o} burns be weighted by one-quarter and added to the area of the 3^{o} burns in order to estimate prognosis. Schwartz, et al., (Ref. 5.74) suggest that about 50% of the area of 2^{o} burns be added to the area of 3^{o} burns. The probit analyses of Bull and Fisher (Ref. 5.65) [confirmed by Bitke, et al., (Ref. 5.68)] in Figure 5.9 and those of Lynch (Ref. 5.75) (see Table 5.3) have shown that age is a highly significant factor in burn mortality, with the elderly being much more vulnerable and some indication that the very young might also be more vulnerable.

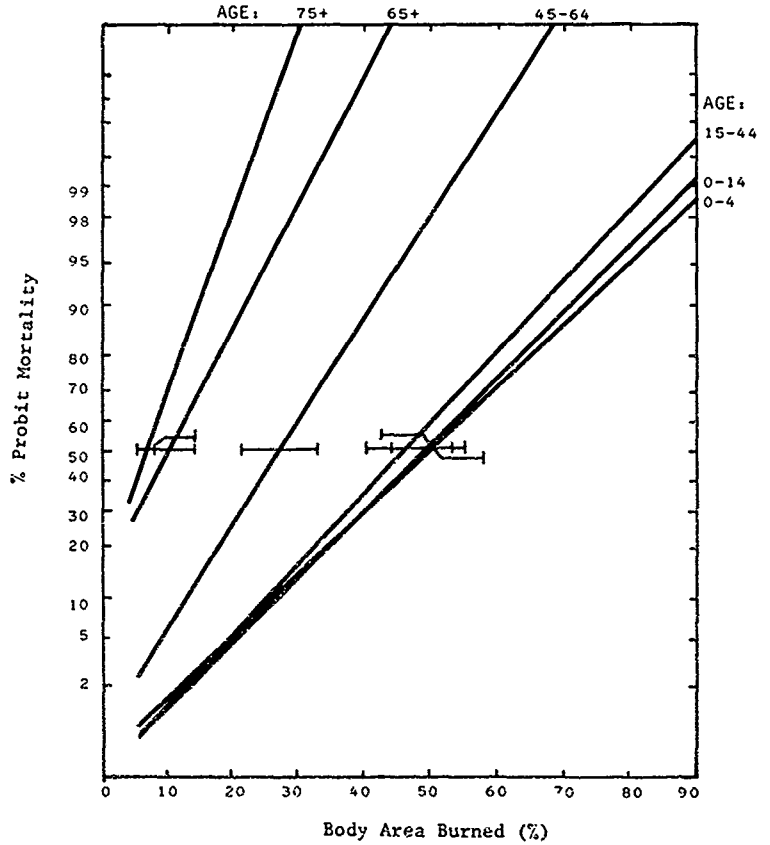

Figure 5.9. Mortality probability versus body area burned.

Table 5.3. Predicted mortality in males.

	Percent of Body Surface Burned									
Years	10	20	30	40	50	60	70	80	90	100
2	0	5	17	40	63	80	92	98	100	100
4	0	5	16	39	63	79	92	98		
8	0	4	14	37	60	78	91	97		
12	0	4	13	36	59	77	91	97		
16	0	3	13	35	59	77	90	97		
20	0	3	13	35	59	77	90	97		
24	0	4	14	37	60	78	91	97		
28	0	4	15	38	62	78	91	97		
32	0	5	17	40	63	80	92	98		
36	1	6	19	44	66	81	94	98		
40	1	7	22	47	69	84	94	98		
44	2	9	27	52	71	87	95	99		
48	3	11	32	56	75	89	96	99		
52	4	15	39	62	79	92	97	100		
56	6	20	45	67	83	94	98			
60	9	27	53	72	87	96	99			
64	13	36	59	77	91	97	100			
68	19	45	67	83	94	98				
72	29	54	73	88	96	99				
76	40	63	80	92	98	100				
80	51	71	86	95	99					
84	61	78	92	97	100					
88	71	86	95	99						
90	75	89	97	99						

Reference: Lynch, J.C., "Thermal Burns," 1968 (Ref. 5.75).

Even if the age variation is factored out, use of these flame burn mortality probit analyses to predict nuclear weapon flash burn lethality has real difficulties. Except for the aged, mean lethality as detailed for the flame burn data requires about 45% body burn; however, only a maximum of 50% of the body can be flash burned by a nuclear weapon unless there are burns from ignited clothing. In the cylindrical approximation, a 45% burn would require a Q five times Q_{50}, e.g., about 20 cal/cm^2 for low yields. Unfortunately, at this level, the percent area is a nearly non-invertable function of Q, i.e.:

Q (cal/cm^2)	Burn Area (2^o and 3^o)
4	22%
8	35%
12	42%
16	44%
20	45%
very large	~50% .

Hence, a shift of a few percent in mean-lethal burn area will result in considerable shift in Q

An alternative methodology is to look at the experience from Hiroshima and Nagasaki and to consider previous estimates of mean-lethal Q's. ENW (Ref. 5.60) reports that flash burns were fatal to "nearly all" persons in the open at Hiroshima out to 6,000 feet; this would correspond to about 9.5 cal/cm^2. Moreover, they estimate that 20 to 30% of all fatalities in Hiroshima and Nagasaki were caused by flash burns. Estimates have been made by White, (Refs. 5.76, 5.77), ANCA (Ref. 5.49) and Fricke (Ref. 5.70) as shown in Table 5.4. The log-log extrapolation by ANCA to lower yields is probably incorrect due to the lack of yield dependence for the shorter thermal pulses (see Burn Severity, Section 5.3.4).

Table 5.4. Lethal thermal radiation levels (cal/cm^2) for lightly clothed individuals.

	Yield (KT)	0.01	0.1	1.0	10	20	100	1000	100000	200000
White: (Refs. 5.76,5.77)										
	Threshold ($\sim LD_{01}$)					5	6	8	10	11
	Near 50% ($\sim LD_{50}$)					9	11	14	18	20
	Near 100% ($\sim LD_{99}$)					20	24	31	40	43
ANCA: (Ref. 5.49)										
	Latent Lethality ($\sim LD_{50}$)	4.4	5.2	8.8	12		18	26		
Fricke: (Ref. 5.70)										
	LD_{50}	7.8	7.8	8.0	8.6		10.8	14		

We will adopt recommendations of Fricke (Ref. 5.70) which were based in part on the data of White [Refs. 5.76, 5.77)] with estimated uncertainties of ±50%:

Yield (KT)	0.01	0.1	1.0	10	100	1000	10000
LD_{50} (cal/cm^2).	7.8	7.8	8.0	8.6	10.8	14	18

The σ/m from White's data is approximately 0.3, which is identical to that for the induction of the various degrees of burns.

If we compare these thermal exposure lethal levels with the burn area lethality, we find for 1 KT (8 cal/cm^2):

100% probability of pain
100% probability of 1^o burn covering 45% of body
99% probability of 2^o burn covering 35% of body
84% probability of 3^o burn covering 28% of body.

(Note: the percentage of body areas burned are not independent)

The total burn ($1^o + 2^o + 3^o$) area is near the mean-lethal levels observed in flame burn cases (Figure 5.9 and Table 5.3) but the areas of the less severe burns (1^o and 2^o) are not handled as recommended by Bull and Fisher (Ref. 5.65):

Special Anatomical Burn Injuries

Some consideration must be given to burns on specific anatomic sites. Experience at Hiroshima and Nagasaki showed the following for the 20-day burned survivors (Ref. 5.47):

98% involved head and/or limbs
87% involved limbs
9% confined to face and neck.

The high percentage of injuries on the head and extremities is due to their being unprotected by clothing (see below). Lips and eyelids are especially sensitive to burns, 1° burns at these sites usually require treatment.

Unexpectedly, few permanent eye burns were noted at Hiroshima and Nagasaki (Refs. 5.47, 5.62). Although there were a number of cases of temporary partial or total blindness, there was only one case of retinal injury (Ref. 5.60). This is because the chances of looking directly at the fire-ball are small, especially for low-yield weapons and the larger ranges. For high-yield weapons (longer thermal pulse), the blink response ($\sim$0.2 sec) will also limit the amount of energy deposited on retina (Ref. 5.16).

Modifying Factors

There are a considerable number of factors that modify the estimates for LD_{50} and BD_{50} for "normal man" and many cases for which the specific values do not apply. In this section, we shall address a number of these factors but mostly as they relate to induction of specific degrees of burns. We have not thus far been able to develop quantitative factors that would modify lethality and burdening levels and, for the time being, can only assume they are of the same magnitude as those for burn induction. These will be multiplicative factors that modify the Q for the "nominal" situation.

Warning and Evasion

If the civilian population is given sufficient prior warning along with proper training, there should be few casualties due to thermal effects from open exposure; i.e., shelter of some sort could be obtained by each person. Hence, in these cases, the specific shelter categories should be used.

However, for a very short prior warning (<<1 min), alert, exposed civilians (with considerable civil defense indoctrination) should be able to take a prone position with hands and face (the only exposed skin surfaces) covered. Hence, in the most optimistic case, it can be assumed that, for a short prior warning, no skin will be openly exposed, but that the personnel will still be subject to burns through their clothing. For larger yields (>100 KT), it is possible for individuals to evade a portion of the thermal pulse instinctively or on the basis of prior training. Such evasion may consist of dropping to a prone position and protecting any exposed skin surfaces (hands and face). The analysis of Lagerin, et al., (Ref. 5.78) suggests a 0.75-second evasion time for trained troops, which may or may not be appropriate for civilians. Without proper training, there is still an instinctive reaction (~0.5 sec) (Ref. 5.54) to evade the thermal pulse which produces immediate pain. Similarly Langerin, et al., (Ref. 5.78) suggest a value of 3.0 seconds for instinctive evasion. However, the effects of no evasion are also to be considered since, no matter how much training, some civilians will not properly evade the thermal pulse. Following the experimental work (Ref. 5.79) and analysis (Ref. 5.80) of Derkson, et al , time-dependent factors modifying Q_{50} were derived (Ref. 5.06) to account for evasion; these are given in Table 5.5. Thus, as an example for a 1-MT weapon, if protection/shelter is obtained within 1 second, it would require a thermal intensity 2.2 times greater than if no protection were obtained to produce the same injury level. For purposes of estimating civilian casualties we suggest that the following times for individuals exposed in the open might be appropriate:

Table 5.5. Evasion time factors.

Time to Cutoff (sec)	10[a]	Yield (KT) 100	1000	10000
0.5	1.0	1.6	15.0	high
0.75	1.0	1.2	3.2	high
1.0	1.0	1.1	2.2	15.0
1.25	1.0	1.1	1.8	5.3
1.5	1.0	1.0	1.6	4.5
1.75	1.0	1.0	1.5	3.8
2.0	1.0	1.0	1.3	3.3
2.5	1.0	1.0	1.2	2.6
3.0	1.0	1.0	1.1	2.2
3.5	1.0	1.0	1.0	1.8
4.0	1.0	1.0	1.0	1.6
5.0	1.0	1.0	1.0	1.4
10.0	1.0	1.0	1.0	1.1
30.0	1.0	1.0	1.0	1.0

[a]Factors for all yields below 10 KT are equal to 1.0.

Able to obtain shelter (where available).	3 → 30 sec
Protecting of exposed skin (some education required):	0.75 → 5 sec
Reactive pain avoidance (exposing larger area to less thermal energy):	0.5 → 5 sec
Unable to respond (very young, aged, crippled, etc.).	30 sec → hours

These times could be combined with the yield to produce protection factors as given in Table 5.5. Considerable analysis needs to be done in this area, especially on the effects of an active civil defense program.

Clothing

Under most circumstances, clothing plays a significant role in the protection/prevention of burns (except while swimming, at nudist camps, etc.). Large-area burns which contribute directly to lethality must be produced under clothing by either of two mechanisms

- Transmission - usually by heat conduction or the generation of hot volatile products, although for very light (weight and color) clothing, some direct transmission is possible
- Ignition of the clothing resulting in burns caused by flames and hot volatiles.

Several factors contribute to the extent that clothing protects the underlying skin from flash burns These include:

- Fabric material
- Fabric color
- Fabric weight
- Number of layers of fabric
- Spacing of the fabric from the skin.

Some analysis of these factors has been done for fabrics normally found in military uniforms. The greatest differences are exhibited by summer versus winter uniforms. A particular summer (hot-wet) uniform (cotton, poplin, shade 116, 5 oz/yd^2 plus bleached cotton sheeting, 4 oz/yd^2) has been studied for contact with the skin (Ref. 5.55) and separated from the skin by 5 mm (Ref. 5.56). A protective factor of ∿10% was found when the uniform was in contact and a factor of ∿100% when separated. Without a detailed analysis of the average separation distance of the uniform from the skin and consideration of the multiple layers of fabric at the yoke, collar, pockets, buttoned areas, seams, etc., we have assumed a protective factor of 1.5 $\pm$ 0.5 with a σ/m of 0.2. Certain other fabrics, because of the emission of volatile products, make the effects worse than for unprotected skin (Ref. 5.81), whereas smoke from some fabrics can form a protective barrier (Ref. 5.54 from the remainder of the thermal pulse.

Winter clothing offers considerably more protection. Experiments by Wilson and Drew (Ref. 5.81) showed that 21 cal/cm^2 delivered over 1 second (∿100 KT) to a human volunteer in contact with a winter uniform equivalent (wool-filled serge, 10.8 oz/yd^2, RCAF blue colour; cotton rayon twill, 3.5 oz/yd^2; cotton broadcloth, 3.4 oz, knitted cotton) produced only slight erythema even though the outer two fabrics were destroyed. However, multi-layer uniforms exhibit a complex behavior versus Q due to burning and falling away of the individual outer layers (Ref. 5.54). Moreover, it takes 5 to 30 seconds for the heat to transfer through the clothing (Ref. 5.54), thus allowing time for removal. We estimate and adopt a single protective factor of 10 $\pm$ 5 for transfer through winter clothing with a σ/m of 0.2

The second mechanism for burns under clothing is due to the ignition and burning of the fabric. Although there were few clothing fires noted in Hiroshima and Nagasaki (Ref. 5.62), those that did occur covered larger body areas than flash burns (>30-40%). The picture here is extremely complicated by the following factors:

- Various ignition thresholds depending on fabric characteristics (e.g., material, color, etc.)
- Higher thresholds for the support of combustion
- Some fabrics unable to support non-externally aided combustion
- The falling away from the body of burned fabric
- The deleterious effects of the decomposition products of the burning fabric including hot volatile products, and hot sticky residues (e.g., nylon)
- Moisture content of the fabric
- Flame spread analysis
- Heat transfer (5-30 seconds) allowing time for extinguishing or removal.

Data for sustained ignition thresholds for four fabrics (assumed to be Q_{10}) derived from URS data (Ref. 5.82) are shown in Figure 5.10, along with the measurements of Derksen and de Lhery (Refs 5.55, 5.56) for the summer uniform, ENW's value (Ref. 5.60) for 3 oz cotton khaki, and some theoretical values for 12 oz/yd cotton khaki derived by E. H. Smith and Company (Ref. 5.83). In the absence of a more detailed study, we have assumed the following Q_{50}'s, with a σ/m of 0.3 for clothing ignition.

Yield (KT)	0.01	0.1	1.0	10	100	1000	10000
Q_{50}(cal/cm^2)	8.8	9.3	11	16	22	30	60

Estimated uncertainties are ±50%.

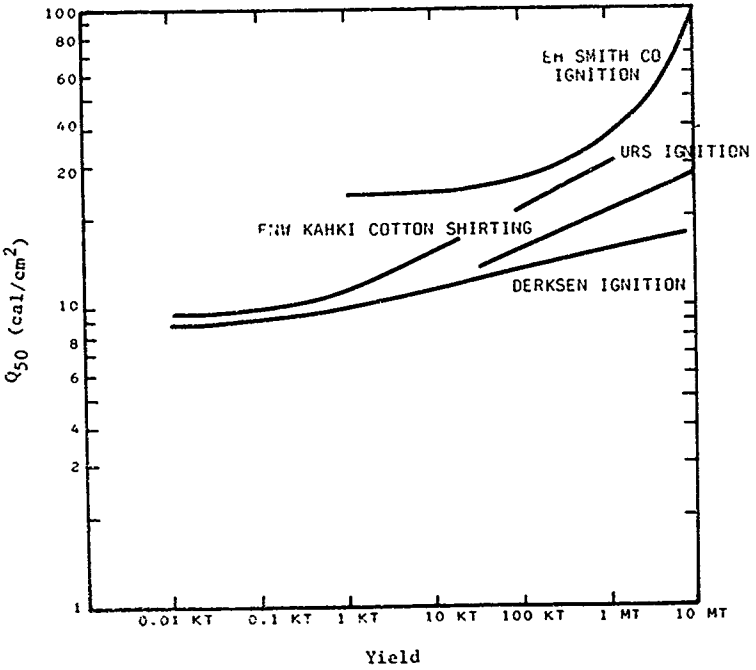

Figure 5.10. Clothing ignition.

Shelter

Virtually any solid shelter provides complete protection from flash burns. However, there are some special cases that can produce burns within a shelter:

- Hot dust-laden air (discussed elsewnere)
- Reflections into the shelter.

Albedos of construction materials vary considerably as well as configurations that would permit reflection into inhabitated areas. A single diffusive reduction of thermal radiation coming through a large window or door and impinging on an interior wall gives a factor of 20 (or more) reduction for a person located 3 meters from the reflecting wall. We shall assume this protective factor with large uncertainties: 20^{+30}_{-10}. The number of instances where this injury mechanism might be dominant are small due to the concomitant blast (glass especially) and radiation hazards.

Variations in Skin Conditions

The amount of thermal energy absorbed by exposed skin is dependent upon its color or level of pigmentation. Experimental work (Ref. 5.84) has measured absorptive differences for a wide range of skin colors from the Dutch and Europeans to the Yoruba and Aborigines. The correction factors (Ref. 5.80) to Q_{50} derived from these experimental results are given below for exposed skin flash burns:

Skin Color	Yield (KT) 0.01*	0.1	1.0	10	100	1000	10000
Very light	1.24	1.24	1.24	1.24	1.34	1.32	1.32
Light	1.10	1.10	1.10	1.10	1.15	1.16	1.16
Medium	1.00	1.00	1.00	1.00	1.00	1.07	1.08
Dark	0.89	0.89	0.89	0.89	0.92	0.94	0.95
Very dark	0.85	0.85	0.85	0.85	0.86	0.88	0.89

*Assumed same as 0.1 KT

Uncertainties are the order of ±10%.

The magnitude of the external ambient temperature affects the severity or extent of flash burns in two ways·

- Burn severity dependent upon initial skin temperature
- Transmission through clothing dependent on types and weight of clothing (see above).

Experimental work (Ref. 5.85) on rats for a simulated 100 KT pulse showed that cold skin (~20°C) required 45% more exposure for the same level of burn, and hot skin (~40°C) required 27% less when compared to moderate temperatures. However, it is postulated (Ref. 5.54) but unverified that this temperature dependence is negligible at yields below 1 KT. We have adopted these factors for yields of 100 KT and above and have log-log interpolated them to unity at 1 KT as given below:

Yield (KT)	0.01	0.1	1.0	10	100	1000	10000
Cold (freezing ambient)	1.0	1.0	1.0	1.0	1.45	1.45	1.45
Moderate	1.0	1.0	1.0	1.0	1.0	1.0	1.0
Hot (exposure to sun in hot ambient)	1.0	1.0	1.0	0.88	0.73	0.73	0.73

Estimated uncertainties are the order of ±20%.

Other Factors

Already discussed above in Section 5.3.3 were spectrum differences which might produce ±15% in the mean values of Q. (Figure 5.9 and Table 5.3). Using the data of Bull and Fisher (Ref. 5.65) and weighting the mortality for 50% body area burned versus a standard (US) population age distribution, we find that an average mortality is 70% as opposed to the approximately 50% mortality for young healthy individuals. Hence, on the average, age makes about a 40% difference with high mortality for moderate body burns (10-20%) for the very elderly.

Other factors affecting burn outcome are obesity (Ref. 5.86) (the greater the weight, the worse the outcome) and the presence of cardiovascular disease and renal disease (Ref. 5.87). For none of these is there any numerical quantification; hence, we must ignore them. Combined injury effects, particularly that of exposure to both thermal and ionizing radiation, are discussed in Section 5.6.

One modifying factor that has been noted (Ref. 5.57) in motion pictures taken during some of the above ground testing was that smoke, steam and products of combustion produced by the initial part of the thermal pulse tended to obscure/attenuate a portion of the rest of the pulse. Observations on "Operation Buster" ($\lesssim$20 KT) were that this effect might have reduced the thermal irradiance by 40%. The amount of attentuation would depend trememdously upon the nature and location of the nearby materials; e.g., asphalt roads, dry grasses and shrubs, curtains in windows, clothing, etc. At this time, there is no simple way of including this effect through the use of some gross correction factors for generic locales.

5.3.5 Summary

A summary of the estimated thermal effects on man, modifying factors and uncertainties is given in Table 5.6.

Table 5.6 Summary thermal effects on man.
(Q, integrated radiance, cal/cm^2)

	Yield (KT) 0.01	0.1	1.0	10	100	1000	10000	
Burn Severity								
Pain	1.0	1.0	1.1	1.4	1.8	2.6	3.8	±20% log-normal distribution σ/m = 0.3
1°	1.9	1.9	2.0	2.3	2.8	3.2	3.8	
2°	3.8	3.8	4.0	4.6	5.2	6.1	7.0	Pain and 1° function of burn area (?)
3°	5.8	5.8	5.9	7.0	8.1	9.3	11.0	
Injuries								
Mean Threshold	2.4	2.4	2.5	2.9	3.4	3.9	4.6	±20% log normal
BD_{50}	3.8	3.8	4.0	4.6	5.2	6.1	7.0	±50% distribution σ/m = 0.3
LD_{50}	7.8	7.8	8.0	8.6	10.8	14.0	18.0	±50%
Clothing	8.8	8.3	11	16	22	30	60	±50%
Modifying Factors								
Light Clothing	← × 1.5 ± 0.5 →							
Heavy Clothing	← × 10 ± 5 →							
Other Factors								
Skin Color								
Very light	← × 1.74 →				× 1.34	× 1.32	× 1.32	±10%
Light	← × 1.10 →				× 1.15	× 1.16	× 1.16	
Medium	← × 1.00 →				× 1.04	× 1.07	× 1.08	
Dark	← × 0.89 →				× 0.92	× 0.94	× 0.95	
Very dark	← × 0.85 →				× 0.86	× 0.88	× 0.89	
Skin Temperature								
Cold (freezing ambient)	← × 1.0 →		× 1.25		× 1.45	× 1.45	× 1.45	±20%
Hot (exposure to sun)	← × 1.0 →		× 0.88		× 0.73	× 0.73	× 0.73	
Spectrum Differences	← ±15% →							
Age Differences	← ∓40% →							
	← -0 →							
Shelter								
Optically tight	← $\times\infty$ →							
Single reflection	← × 20^{+30}_{-10} →							
Warning	← $\times\infty$ →							
Evasion	← no effect →				× $1\,1^{+5}_{-1}$	× 2^{+3}_{-1}	× 10^{+20}_{-9}	
Other								
Obesity	← severity increases with weight →							
Cardiovascular disease	← severity increases when present →							
Renal disease	← severity increases when present →							

5.4 AIRBLAST EFFECTS

5.4.1 Introduction

Studies concerning the effects of airblast on man have generally followed with commencement of major conflicts between nations. The Second World War produced considerable data for airblast effects generated by conventional weapons. Both the British, led by Zuckerman (Ref. 5.91), and the Germans, led by Desaga (Ref. 5.90), were active in this field. With the closing of the Second World War, a new dimension was added to the effects of airblast by the use of nuclear weapons. For nuclear weapons, the duration of the overpressure moves from the few millisecond regime to exposures lasting, in some cases, for more than a second.

The Lovelace Foundation for Medical Education and Research has been very much a leader in the investigation of the effects of blast waves of long duration. Contributors from this Foundation such as White (Ref. 5.76), Fletcher (Ref. 5.115), Bowen (Ref. 5.93), and Richmond (Ref. 5.121) have produced a number of extensive studies on the multiple aspects of this effect. Their studies have led to scaling methods for comparing animal casualties to man. They have also conducted extensive computer modeling and have developed the best estimates available on the tolerance of man to all forms of airblast effects.

Testing with human subjects has necessarily been limited to near or below burdening levels. Some studies of accident and suicide cases give criteria for lethal or burdening levels, but these do not scale directly to casualties produced by the blast from a nuclear weapon. This scaling has also presented a major problem in work with human cadavers or with animals.

Lethal and burdening levels for man exposed to airblast are still at a very tentative level. Much work has yet to be done, especially in the area of burdening and lethal decelerative tumbling and in injuries produced by blast energized penetrating debris and structural collapse.

5.4.2 Primary Airblast Effects - Direct Effects

Lethal Effects

In terms of physiological damage induced by a sudden change in air pressure, lung damage is of primary importance. Studies of cases of severe blast injury or mortality in both man and animals have indicated massive lung damage as the leading lethal mechanism (Ref. 5.88, 5.89, 5.90, 5.91).

Blast injury develops in complex organisms due to the difference in tissue density of the various organs that make up the individual. As the airblast wave distorts the body, movement of different tissue masses causes shear waves to be generated which accelerate parts of a same organ at different velocities. As a result, tears or ruptures occur. Gas-filled organs are especially susceptible to this damage, with the lungs being of greatest concern. As the lung tissue is disorganized, fat and air emboli can enter pulmonary veins. These emboli in turn can lead to further damage or death to an organism via coronary or cerebral damage. If the organism is sufficiently damaged, fibrin emboli may also be present, thus complicating the situation. All this is further complicated by the resultant degree of hypoxia due to lung damage. Age, health and predisposition all affect the response of the individual. These parameters, in turn, complicate the development of probabilities for mortality due to blast overpressure. The majority of information available on physiological response to overpressure is based on scaling data obtained from animal studies to what might be the expected response in a 70-kgm man.

Lung - Whole Body

Zuckerman (Ref. 5.91), working in England, carried out experiments during the Second World War in which small animals were tested for lethal overpressure. It was found at this time

that the pressure necessary to kill 50% of animals was related to the 2/3 power of the animals' body weight. Monkey and goat data were consistent with the relation. When the data were extrapolated to man, an LD_{50} of 400-500 psi peak overpressure was established and was considered to be of the right order when compared to actual air raid experience.

Desaga (Ref. 5.90), working in Germany during the Second World War, agreed with Zuckerman's blast tolerance of man, up to a point. Desaga showed that the tolerance was related to the duration of the overpressure. Desaga also indicated, from studies of gun emplacement casualties, that reflection of overpressure was highly additive and could cause a non-fatal overpressure to become fatal. This fact led to a redesign of the gun emplacements. For blast-caused casualties (from direct effects) inside structures, Desaga reports knowing of only one case during the entire war.

The Lovelace Foundation has produced extensive studies on the tolerance of animals and man to various blast waves. Richmond, et al., (Ref. 5.92), published a paper which demonstrated an apparent species difference in tolerance to duration of overpressure. In this paper, a grouping of data for large and small animals was demonstrated, with the large animals being more tolerant to overpressure than small animals. In a careful compilation of data, Bowen (Ref. 5.93) developed a set of curves for threshold peak overpressure values for lung damage as a function of its duration. In this study, man's tolerance to blast overpressure was also shown to be dependent on orientation to blast winds and adjacent buildings. The peak overpressure-duration data were also regenerated as survival curves for range versus weapon yield. These curves were subsequently employed in a number of publications of the Lovelace group.

Extrapolating from the data of Bowen, the LD_{50} value for man, exposed to a blast overpressure of 1-msec duration, is 450 psi. For exposures of long duration, 1000 msec or more, the LD_{50} value is 62 psi. In 1973, White (Ref. 5.94) indicated a threshold value for lethality (LD_{01}) as 40 psi, LD_{50} as 62 psi and LD_{99} as 92 psi. These values are in agreement with the Lovelace values of 1971 (Ref. 5.88), in which the probability of mortality was indicated for three different orientations to the blast wave (see Table 5.7, Figure 5.11). If orientation is considered, the LD_{50} peak overpressure for man ranges from 21 to 62 psi.

Burdening Effects

Lung

Minimal injuries of lung tissue result in disruption of alveolar walls. As overpressures are increased, hemorrhaging becomes more extensive to the point of major disruption of pulmonary tissue. As more tissue is disrupted, the subject suffers from increased hypoxia. From this point, air emboli can enter the bloodstream and lead to sudden death.

The investigations by Zuckerman (Ref. 5.91) during the Second World War, involving both animal and human experiences, lead to a tentative estimation of man's threshold for lung damage at 70 psi. Approximately the same period of time, Desaga estimated the lethal threshold of man at 100 psi. From these studies, it would appear, for short durations of overpressure, that man's burdening levels for lung damage from primary effects of overpressure are

BD_{01} = 70 psi

BD_{99} = 100 psi

Table 5.7. Probability of mortality from blast overpressures (PSI) surface bursts.

	Yield (KT)				
	0.01	0.1	1.0	10.0	100.0
A. Prone-long Axis Parallel Shock Wave					
1%	47	44	42	41	40
50%	74	68	64	63	62
99%	125	115	100	97	94
B. Long Axis Body Perpendicular to Blast Winds					
1%	30	29	28	27	27
50%	42	40	38	37	37
99%	60	55	53	52	51
C. Thorax Near a Reflecting Surface					
1%	17	16	15	15	14
50%	23	22	22	2[illegible]	21
99%	32	30	29	28	28

Note: These probabilities are based on data from White (Ref. 5.88), Bowen (Ref 5.93). They represent the closest approximations from available data.

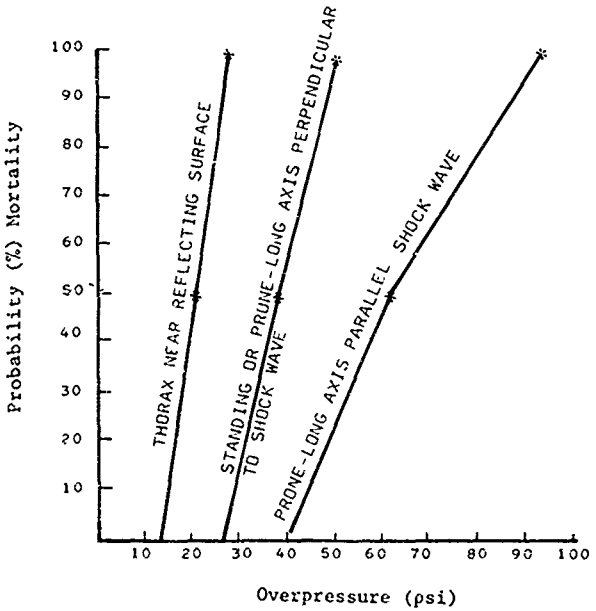

Figure 5.11. Probability of mortality from overpressure (psi of duration greater than 100 msec)

In 1966, Richmond (Ref. 5.92) published a paper in which he indicated the threshold for petechial lung hemorrhage in dogs occurred at approximately one-fourth the LD_{50} dose, and serious injury occurred at about three-fourths the LD_{50}. From these data, for short-duration overpressure exposures (~3 msec), lung damage occurred at the following levels:

Threshold = 30-40 psi
Severe = 80 psi and above.

White (Ref. 5.95) published a paper at the same time as Richmond and indicated the threshold and serious ranges for exposure to overpressure of long duration (400 msec). The results of this paper are the following peak overpressures:

Threshold = 12-15 psi
Severe = 37 psi and above.

Further animal studies by the Lovelace Foundacion (Ref. 5.94) have now established the following tentative peak overpresssure criteria for burdening lung damage due to direct effects of long-duration blast waves:

Threshold Lung Damage = 12 (8-15) psi
Severe Lung Damage = 25 (20-30) psi.

Eardrums

Early investigation (Ref. 5.96) of the effects of overpressure on the tympanic membrane indicated that an overpressure range between 5.4 and 44.1 psi (mean = 22.9 psi) was required for rupture. This work was performed on cadavers by slowly pumping air (slow-rising overpressure) into the external auditory canal. A study (Ref. 5.97) of World War II air raid casualties suggested that the lower and upper limits of peak overpressure at which human eardrum will burst in 50% of cases was 15 psi and 50 psi. The wide range in both studies was attributed to differences such as age, shape of ear and wax content.

In terms of probability of occurrence of eardrum injuries among casualty cases, in the Texas City Disaster (Ref. 5.98), of 2400 hospitalized patients, 11.5% (274 patients) had perforation of one or both eardrums. The incidence of ruptured eardrums among surviving casualties from the nuclear bombing of Japan was from 1% to 10% (Ref. 5.60, 5.99). The amount of damage to the tympanic membrane varies considerably, with slight tearing in some cases and complete removal in others. The main problem to avoid is infection to the ear following damage. If infection should occur, the amount of permanent hearing loss can be considerable. A new NATO Handbook (Ref. 5.69) advises evacuation of persons suffering from ruptured eardrums.

Studies (Ref. 5.100) of the effect of the duration of the blast wave indicate the tympanic membrane is not sensitive to this effect above 1 msec of pulse. Questions as to whether the positive overpressure or negative underpressure is the most damaging effect have not been completely settled. Relating membrane damage to positive overpressure, a compilation of dog data in 1965 (Ref. 5.101) indicated a threshold peak overpressure value of 5 psi and 50% failure at 15-20 psi. Due to reflection, the values are lowered for sheltering conditions such as covered foxholes to 1% at 2-3 psi and 50% at 6-8 psi. A 98-percent failure occurred for eardrums exposed to overpressures from 25-38 psi.

In summary, the burdening peak overpressure values for tympanic membrane casualty are tentatively indicated as:

BD_{01} = 5 psi

BD_{50} = 15-20 psi

$BD_{99} \geq$ 35 psi.

5.4.3 Secondary Airblast Effects - Debris and Missiles

Burdening and lethal casualties related to secondary blast effects are related to a number of parameters of both the target and the missiling material. The parameters of missiling include size, shape, density, mass and nature of the moving object. For the target, response parameters reflect whether the blow is piercing, penetrating, non-penetrating (sharp or blunt), and the tissue/organs involved (single organ, multiple organ, organs in one or more major body areas). From the science of wound ballistics, the velocity of a penetrating or piercing object is critical to the extent of physiological damage - this becomes especially evident in terms of very small missiles which obtain very high velocities which may result in massive disruption of tissue.

Of translating objects, the larger, more massive items are slower to gain velocity in blast winds. Small, light objects, such as glass splinters, reach maximum velocity in a relatively short period of time. Because of this, objects in a blast wind can change their velocities relative to each other. The longer the duration of the blast wind, the higher the velocity a large massive object can obtain. In contrast to this, small objects are not too greatly influenced by blast durations as they very quickly reach their maximum velocity.

The basic biomedical criteria for these effects are commonly expressed in units such as the kinetic energy at impact or the impact velocity of a particular type of missile (substance, weight, etc.). The physical phenomena (e.g., aerodynamics) of the missile's acceleration are then used to express the biomedical criteria in terms of blast-wave parameters.

Blunt Trauma

Blunt Trauma - Random Impact

An analysis of the wounding power of debris (Ref. 5.102), conducted by the British during the Second World War, indicates that lumps of hard crater debris, impacting with an energy of about 30 ft-lbs, would incapacitate 50 percent of the personnel crouched in slit trenches (see Table 5.8). Soft lumps of clay were found to produce incapacitation in 50 percent of personnel struck at a mean energy of 1800 ft-lbs. This research, performed on small animals and dried human skulls, contains extremely wide ranges of 95 percent confidence limits. The criteria for incapacitation in the British report were either death, unconsciousness, major bone fracture, or severe rupture or hemorrhage. The values are to some degree intended as combat ineffectiveness (CI), rather than burdening injuries (BD) as would apply to civilians.

Working from the British data, the United States Army Combat Developments Command (USACDC) (Ref. 5.103) redeveloped a probit analysis of the incidence of incapacitation (see Figure 5.12). Working from this probit analysis, the velocity required to produce a 50-percent incidence of incapacitation was developed by the USACDC (see Table 5.9) for three stone masses (1, 5 and 10 lbs). With the velocity values calculated, the overpressures as a function of yield were calculated for the three stone masses (see Figure 5.13). The overpressures from a 1-KT and 10-KT weapon which develop a CI_{50} for the three stone masses are shown in Table 5.10.

Table 5.8. Estimated LD_{50}'s in ft-lbs for human incapacitation. (95% confidence limits shown in brackets)

	Hard Strikers (metal)		Soft Strikers (Plasticine)	
Part of Body	"Fixed"	"Free"	"Fixed"	"Free"
Head	17 (11-27)	22 (12-43)	81 (42-158)	165 (85-323)
Thorax	55 (28-107)	56 (25-129)	95 (46-199)	331 (151-723)
Abdomen	102 (54-195)		151 (80-288)	
Upper Limb (Humerus)	20 (9-43)	c. 20	1240 (574-2685)	c. 3720
Lower Limb (Femur)	67 (25-182)		10198 (3616-28787)	
Random Impact		30		1800

"Fixed" - animal held firmly against metal anvil
"Free" - animal held lightly against air-filled rubber cushion
c. - estimate, no test run

Ref. 5.102

Table 5.9. Velocity for 50% incidence of CI resulting from random blunt impact.

Weight of Stones (lbs)	Velocity for 50% CI (ft/sec)
1	57
5	25
10	18

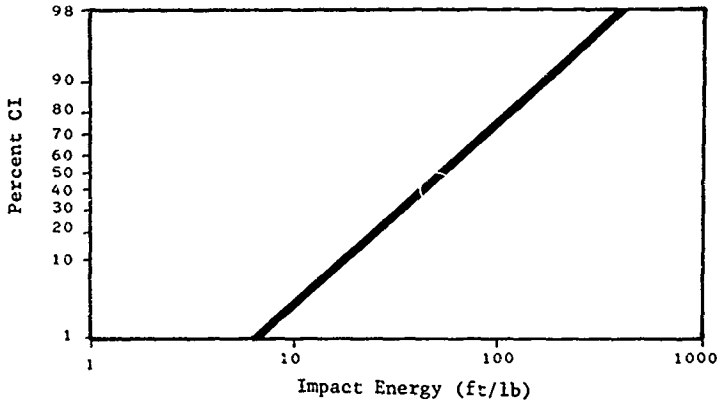

Figure 5.12. Incident of CI by blunt impact as a function of impact energy (Ref. 5.103).

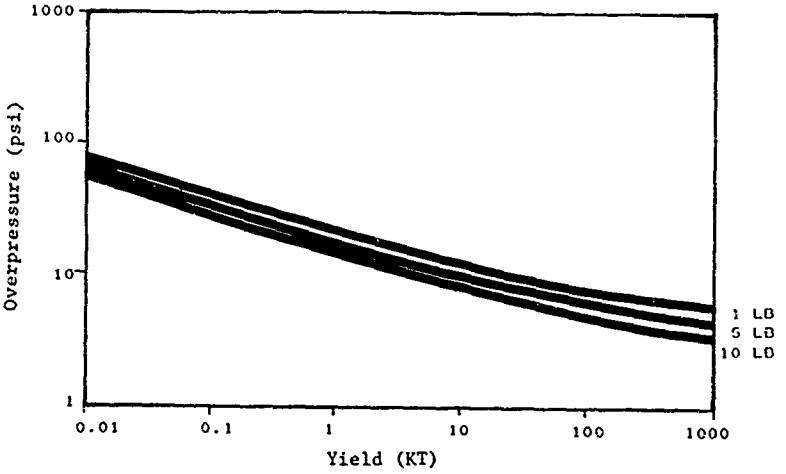

Figure 5.13. Overpressure for 50% CI from blunt impact for three stone masses (Ref. 5.103).

Table 5.10. Overpressures from specific weapons developing CI_{50} for various missile weights.

Lb	1 KT	10 KT
1	18.5	11.5
5	14.5	8.9
10	12.8	7.9

Blunt Trauma - Skull

The values for incapacitation, as developed from the British data, are intended for a mean probability of the event occurring to any portion of the body. If specific body regions were considered, the range of values would vary widely as indicated by the 95-percent confidence values of Table 5.8. As an example, for incapacitation due to head injury, the energy required of hard debris is 22 ft-lbs. From a probit analysis of the British data, the LD_{50} velocity for 1, 5, and 10 lb masses would be those shown in Table 5.11.

Table 5.11. 50% incidence of CI resulting from blunt impact to head.

Mass (lb)	Velocity for 50% CI (ft/sec)
1	37.5
5	16.8
10	11.9

From Table 5.8, the CI_{50} impact for skull fracture is about 22 ft-lbs. This value is based on experiments with human skulls which were filled with a 20-percent gelatin solution covered with thin rubber to simulate skin. In the Lovelace publications (Refs. 5.72, 5.76, 5.77, 5.99), impact velocity for skull fracture from a 10-lb mass has been indicated to range from 15-23 ft/sec for threshold to near 100-percent fracture (see Table 5-12). These data are based on reports of early British work (Ref. 5.104) employing monkeys and predate the British report used by the USACDC. The Lovelace data also employ engineering studies of skull fracturing (Refs. 5.105, 5.106) which support the British data. Although an apparent disagreement exists between USACDC and Lovelace as to what constitutes the critical impact velocity for a 10-lb object, the actual difference appears to be due to scaling and differences in experimental fracture development as employed in the original research. For skull fractures due to hard, blunt impact, the velocity data published by Lovelace is believed to be the best available at this time.

Table 5.12. Tentative critical impact velocities for blunt trauma due to hard, 10-lb object.

Skull Fracture	Velocity (ft/sec)
Mostly "safe"	10
Threshold	15
Near 100%	23

Blunt Trauma - Thorax

Lovelace research (Refs. 5.72, 5.107) on blunt trauma due to missile impact to the chest area has produced the data found in Table 5.13. These data were developed from research employing two sizes of blunt objects impacting with the lateral thorax of dogs. As evidence from Table 5.13, and as expected, the lighter

object requires more energy to produce a specific biological effect. Caution must again be expressed in scaling,animal data directly to human response.

Table 5.13. Effects of 0.4-lb and 0.8-lb missile impact on the chest.

Biological Effects	Threshold Velocities (ft/sec) 0.8 lb	0.4 lb
Lung Hemorrhages:		
Side of impact only (unilateral)	45	80
Impact side and opposite side (bilateral)	110	125
Rib fracture	60	120
Internal lacerations from fractured ribs	90	120
Fatality within 1 hour	155	170

From Table 5.13, the velocities required to produce unilateral or bilateral lung hemorrhage, or more complicating injuries, are fairly high. For the 0.8- and 0.4-lb strikers, minor hemorrhage threshold occurs at 45-80 ft/sec. The threshold for lethality is 155 to 170 ft/sec.

Blunt Trauma - Abdomen

A compilation of data by Clemedson (Ref. 5.108) has indicated that the abdomen (liver, spleen and kidney) is the most sensitive area to blunt trauma. The next most sensitive area is the head (central nervous system), followed thirdly by the heart. From civilian crash studies, the mortality rate for blunt trauma to the liver has been indicated by Clemedson to be about 40-60 percent. In a series of experiments on dogs by Hellström (Ref. 5.108), initial liver damage occurred at impact velocities as low as 5 ft/sec (see Figure 5.14). These experiments employed a

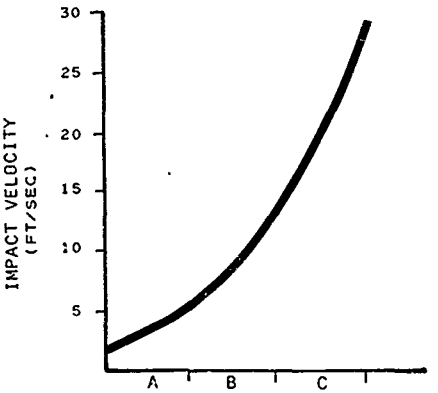

LIVER DAMAGE

A - NO INJURY VISABLE

B - HEMATOMAS TO SLIGHT RUPTURES

C - DEEPLY PENETRATING RUPTURES TO GREATER THAN 50 PERCENT LACERATED

NOTE: INJURIES IN 'C' ZONE ARE GENERALLY LETHAL.

Figure 5.14. Relation between impact velocity and degree of liver damage (15.5 kg mass striking liver area of dog abdomen).

15.5-kg mass impacting at known energies. Major damage to the liver, usually resulting in death, occurred at impact velocities above 12 ft/sec. From these data, a tentative velocity value for blunt injury to the abdomen indicates a threshold level for injury at 5 ft/sec and a near 100% level for fatality at 20 ft/sec (see Table 5.14).

Table 5.14. Tentative criteria for blunt impact (mass 15.5 lb) to abdomen (liver).

Injury Classification	Velocity (ft/sec)
Burdening	5-14
Lethal	12-20

Penetrating Trauma

The science of wound ballistics has investigated the effects of penetrating missiles and has developed much of our understanding of this form of injury. The physical wounding effects of a penetrating missile depend much upon the amount of kinetic energy available and upon the transfer of that energy to the tissue medium. The power available to generate a wound varies directly as the impacting area and shape of the missile, the density of the medium, the cube of the velocity, and varies inversely as the mass of the missile. The intervening tissue modifies a wound by such characteristics as elasticity, cohesiveness, brittleness, density, and length of missile tract.

Perforation or penetration wounds are lethal provided certain organs are involved or the area involved is large enough. For some injuries, mortality is almost entirely due to perforating wounds, as for example mortality of colon injuries (Ref. 5.109). From studies (Ref. 5.97) of civilians and military casualties of the Second World War, the British concluded only

penetrating splinter wounds of the head, neck and trunk are highly dangerous, and almost any such wound may be regarded as an incapacitating wound provided the missile concerned penetrates through the skin into the underlying tissue. In the case of limbs, single splinter wounds are not considered as dangerous, and the relative number of hits by small splinters which would prove incapacitating is clearly smaller.

A comparative study (Ref. 5.97) of the wounding power of steel balls and metal splinters produced the data of Figure 5.15. The mass of the missiles studied was 58 mgm. This was related to the average size of wounding fragments from the casing of a conventional gravity bomb. Although this does not necessarily relate to the size and velocity of penetrating fragments due to nuclear weapons, it does allow comparisons of the effect of missile shape on wounding ability. As shown in Figure 5.15, the random-shape 58 mgm missile requires 2600 ft/sec for a BD_{50}, while the same mass but uniform ball configuration only requires 1300 ft/sec for a BD_{50} level of incapacitation. These values are for clothed body surfaces (type of clothing unspecified) and random angle of impact (normal or oblique).

A more specific study of ballistic limits of tissue and clothing is that of Sperrazza and Kokinakis (Ref. 5.110). In this study, steel spheres of 1-, 2-, and 10-gram masses were impacted against military winter attire and human skin. From this study, a relationship of the V_{50} ballistic limit (fragment just penetrates in 50 percent of impacts) versus fragment area-mass was developed (see Figure 5.16). The information contained in Figure 5 16 was employed in USACDC studies (Ref. 5.103) to develop V_{50} values for stone masses of 0.1-, 1-, and 10-grams (see Table 5.15. From these data, the USACDC developed curves which illustrate overpressures as a function of yield (see Figure 5.17). These curves correspond to the 0.1-, 1.0-, and 10-gram stone velocities that produce a 50-percent incidence of severe wounds.

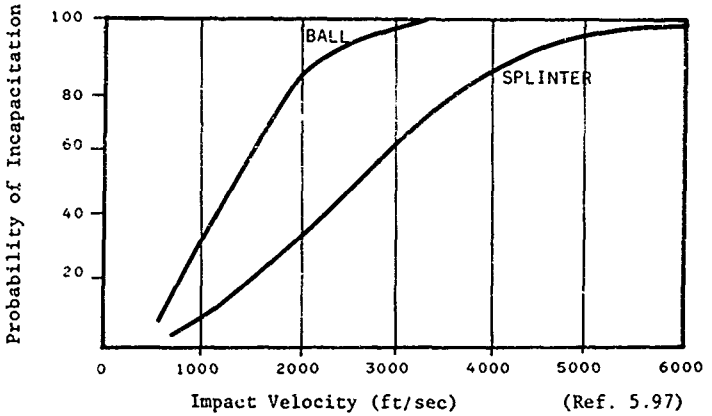

Figure 5.15. Wounding power of 58 mgm metal ball or splinter striking clothed body.

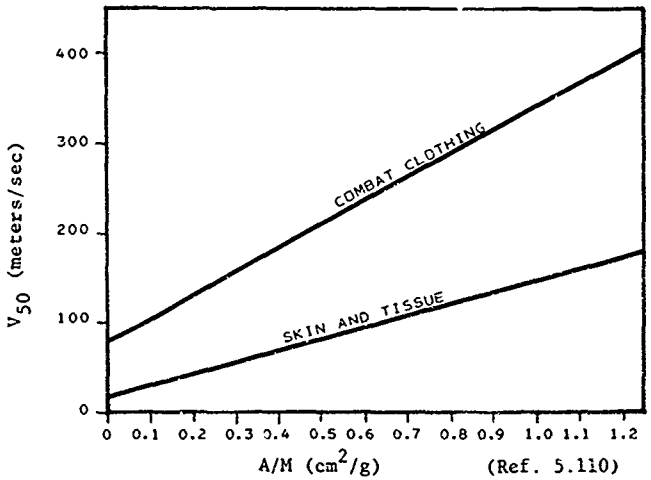

Figure 5.16. Ballistic limit (V_{50}) versus fragment area-mass for combat winter clothing and isolated human skin.

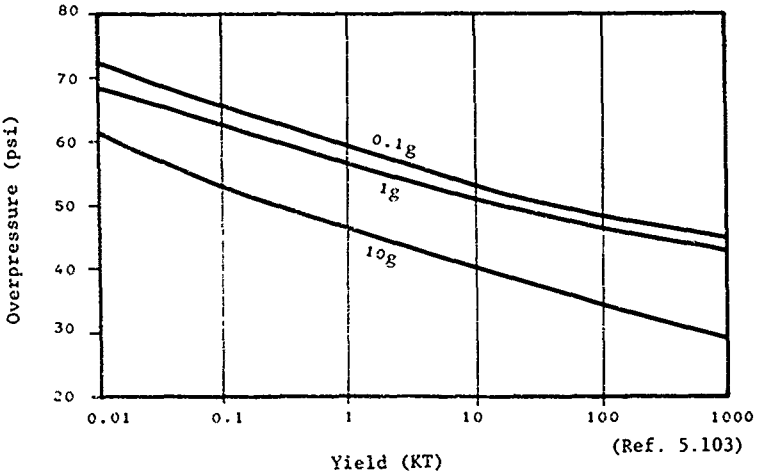

Figure 5.17. Overpressure for 50% CI from penetrating wounds for three stone masses.

For example, for a 1-KT weapon, the overpressures which produce a V_{50} for 0.1-, 1- and 10-gram stones are 59, 56.8 and 46.5 psi, respectively.

Table 5.15. Ballistic limits of skin and clothing.

Missile	Mass (grams)	Ballistic Limits (V_{50}) (ft/sec) Uniform	Skin
Steel Sphere*	1.0	502	197
	2.0	450	171
	3.0	364	131
Stone**	0.1	1340	617
	1.0	1160	340
	10.0	560	200

*Ref. 5.110
**Ref. 5.103

Cutting Mechanisms (Glass)

For determining lethal levels of glass fragments, the development of LD values becomes very difficult. In conventional bombing cases observed during the Second World War, glass was not the primary cause of death. Only in cases of severely lacerated arteries or organs could glass fragments be considered the lethal factor. Generally, glass lacerations were multifarious, superficial, and located on uncovered body surfaces. Superficial or not, glass laceration was a serious wound in that it carried with it contaminating dirt and debris which led to difficult complications in wound treatment. Where severe laceration was involved with a patient that eventually died, the patient also had other complications such as compound fractures and organ damage. Of civilian bomb casualties during the Second World War, the observed death rate, attributed to glass, was found in one British hospital to be approximately 0.3 percent (Ref. 5.111). When the nuclear bomb exploded over Hiroshima, windows were broken in places exceeding 10 miles distance (Ref. 5.112), and flying glass

caused a large number of casualties, even up to 15,000 feet from ground zero (Ref. 5.62). For very low yield nuclear weapons, where blast duration is insufficient to accelerate larger missiles to high velocities, the glass hazard may be a particularly important missile injury mechanism.

For personnel inside structures, the probability of being hit by glass fragments decreases rapidly as a person moves laterally from behind a window. At 25 degrees from the edge of a window pane, the density of glass fragments is approximately one-tenth the density of fragments measured directly behind the window. Since the lateral spread of fragments is not great, the probability of hit decreases rapidly. This was extremely evident in injuries of British civilians during World War II. As the people learned to quit looking out their windows during bomb raids, the number of glass casualties decreased dramatically (Ref. 5.111).

In one Nevada nuclear weapon effects study (Ref. 5.113), dogs were exposed to missiles from window glass as a result of an 11-KT explosion. The result of these tests indicated the weights of penetrating missiles increased exponentially with decreasing overpressure. At an overpressure of 3.9 psi, there was an average of 20 wounds per animal and about 2 severe wounds per animal.

To further quantify the glass missiles, tests were conducted (Ref. 5.114) using a series of styrofoam witnesses behind 0.125-inch thick windows. From these studies, it was determined that, at a distance of 10 feet behind a window pane, the probability of glass fragments penetrating tissue increased with increasing overpressure up to 3.8 psi. Beyond 3.8 psi, the probability of penetration decreased. This situation develops with glass in that, as overpressure increases above 3.8 psi (under conditions of tests), the size of the glass missiles decreases.

Figure 5.18 is an illustration of this situation. From Figure 5.18 at 5 psi and 10 feet from the window pane, 4 percent of the total missiles have sufficient energy to penetrate skin. Also, at this distance and overpressure, the expected penetration rate is 4 missiles per square foot. The following equation was designed to describe this relationship.

$$p = \frac{\log V - 2.5172 + \log(\log m + 2.3054)}{0.4842}$$

where

p = probability of penetration
V = missile velocity, ft/sec
M = missile mass, gm (Ref. 5.114)

During the above described experiment, in one test, the mean mass of fragments at 5 psi was 0.119-grams. The mean velocity of these fragments was 162 ft/sec, and there was an average of 88.3 fragments trapped per square foot at a distance of 9-13 feet behind the window. Overall the mean mass of the fragments in a series of seven tests ranged from 0.119-grams to 1.85-grams, and the mean velocities ranged from 99.2 ft/sec to 175 ft/sec (Ref. 5.115).

The probability of incapacitation from cutting mechanisms is proportional to the size of the cut area. A formula expressing this relationship in terms of combat ineffeciveness has been applicable to civilian casualties. For a first-order analysis of injury due to cutting mechanisms, White (Ref. 5.116) has indicated that 1) skin laceration may be anticipated at missile velocities on the order of 50 ft/sec and 2) serious wounds involving penetration of serous cavities may be predicted at velocities of about 100 ft/sec in a few cases and, in most cases, above 400 ft/sec.

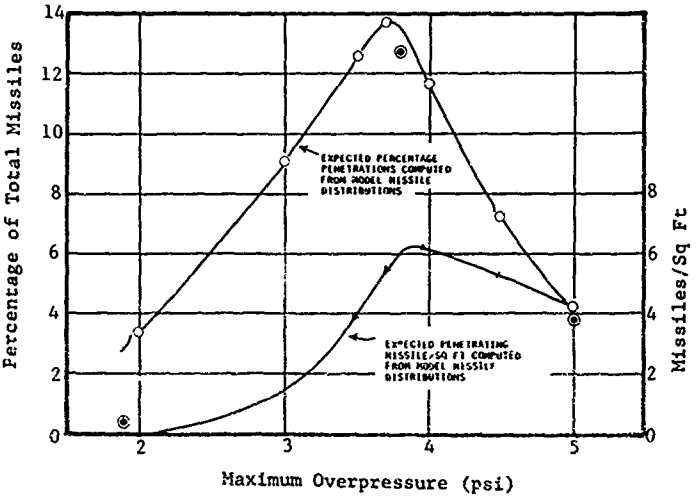

◉ Expected percentage penetrations computed from individual missiles

Figure 5.18. Expected frequency of penetration as a function of maximum overpressure computed for glass missiles occurring about 10 ft behind windows facing blast penetration criterion derived from dog abdomen penetration studies.

Lovelace studies (Ref. 5.101) have shown the probability of glass missiles producing serious wounds is a product of the mass-velocity relationship of the missiles. In their early studies, the BD_{99} velocity values for 1-gm and 10-gm glass missiles were tentatively set at 430 and 355 ft/sec. Employing the Lovelace data, the ITT Research Institute (IITRI) indicated that the mass-velocity relationship for glass laceration or penetration is approximately related to the MV^4 value of the glass missile. A recent Lovelace paper (Ref. 5.117) on glass penetration gives a 99-percent probability of penetration of the body wall, by a 2-gm mass, as 500 ft/sec (see Table 5.16).

Table 5.16. Velocity of glass fragments having probability of penetrating skin and body wall.

Probability of Penetration	Glass Fragment Mass (gram)				
	0.1	0.2	0.5	1.0	2.0
1%	190	150	125	110	90
50%	590	440	360	280	215
99%	1100	880	680	590	500

(Ref. 5.117, p. 8)

For the probability of mortality from glass penetration of the abdomen, IITRI scientists have estimated the single event has a 30-percent mortality factor. This would mean that, at a 99-percent probability of penetration, an event with a 30-percent mortality factor has a lethality equivalence of LD_{30}, while a 50-percent probability of penetration has an equivalence of LD_{15}. A ballpark number from a meeting with the Lovelace scientists (Ref. 5.118) has given glass penetration of the serous cavity a 50-percent mortality factor. This would indicate that a 99-percent probability penetration has an

equivalence of LD_{50}. From this, a very tentative estimate of lethality for glass is LD_{30-50} for 99-percent probability of penetration. From such penetration data and measurements of the velocity, mass and spatial distributions of glass fragments for various window constructions and blast-wave parameters, injury and fatality criteria are presently being developed in a way that they may be indexed to the yield, height-of-burst and peak overpressure of the blast. Highly preliminary results from Monte Carlo calculations indicate an effective (reflections included) peak overpressure, approximately independent of yield and burst height, of ∿5 psi for LD_{50} and a value on the order of the window breakage threshold (typically ∿1 psi) for BD_{50}. As expected, these preliminary results also indicate a reduction in the fatality probability with increasing overpressure (i.e., larger overpressures product less penetrating fragments) but the other air blast effects will have reached lethal levels.

5.4.4 Tertiary Airblast Effects--Whole Body Translation

Translation of objects due to blast winds from nuclear explosions can produce human casualties in a variety of ways. Either penetrating or non-penetrating debris energized by the airblast can induce wounds to the point of lethality. Whole-body translation results in an abrupt impact or a more gradual tumbling deceleration. The velocity-displacement relation of a translating object is different at the same overpressure value for weapons which are different in yield, and this difference can be related to the duration of the blast wave. In turn, the translation of different objects is related to their individual drag coefficients, acceleration coefficients, and motion characteristics when airborne.

Anthropomorphic dummies exposed to blast winds from nuclear explosions have been studied to estimate the translational characteristics of humans (Ref. 5.119). One significant finding from these studies involves orientations. As the blast winds overpower the standing dummy, its feet are knocked out from under it, and the dummy rotates through the air. With sufficient rotational movement, the head is the first part of the body to come in contact with the ground surface. As the dummy rotates through the air, its acceleration coefficient alters with its positional changes. Acceleration coefficients (α) are essential in predicting the velocity a translating object will obtain. Bowen (Ref. 5.120) tabulated the α-values for various positions of man as well as various sizes of stones, window glass fragments, and steel spheres. For man, an effective acceleration coefficient was estimated at 0.030 ft^2/lb. This was reasonably close to the 0.0268 ft^2/lb derived from studying film clips of a rotating dummy as it translated through air.

Lethal Injury

Impact

To calculate the overpressure vs. yield at which a human casualty will suffer a burdening or mortal injury from translation, the velocity required to generate the casualty must be determined. Initial research (Ref. 5.121) indicated probably lethal impact velocities for random impact orientations after a 10-foot translation distance of LD_{01} = 24 ft/sec and LD_{99} = 29 ft/sec. These values were scaled from experiments employing small animals. It was subsequently determined (Ref. 5.88) that small animals developed degrees of casualty at different velocities than larger animals, and a new LD_{50} velocity for man was tentatively set at 54 ft/sec. These data were modeled using information derived from studies employing dogs as test subjects. The latest values (Ref. 5.118) accepted by the Lovelace Foundation

for man's LD_{50} value for impact with random orientation, based on data derived from sheep, is 35 ft/sec. (See Table 5.17). This is still a tentative result requiring extensive testing and modeling.

TABLE 5.17. Impact velocity for a given probability of injury or mortality (ft/sec), impact at random orientation. (Data modified from Fletcher, Refs. 5.118, 5.122) $\sigma/m = 0.23$

	1%	50%	95%
Injury	6.5 ± 2	15.4 ± 2	$28.4\ ^{+6}_{-4}$
Mortality	$26.7\ ^{+3}_{-4}$	35.1 ± 2	$42.6\ ^{+7}_{-3}$

The initial orientation of human subjects is important to the maximum velocity developed in that different α-values are related to different surface areas. Fletcher, et al., (Ref. 5.122) ran a series of model computations of displacements for personnel initially prone and initially standing. For the initially prone exposure, velocity calculations were made for end-on, side-on, or random orientations to the airblast. For initially standing personnel, exposures to airblast were only considered for front-on or back-on orientations. These data were calculated for various overpressures developed for surface bursts, upper optimum HOB, and lower optimum HOB of different yields. From the modeled data a series of tables were developed which relate velocity and displacement, for personnel exposed to weapons ranging from 1 KT to 100 MT, to the blast-wave characteristics.

Applying the velocity data from Table 5.17 to the above described modeling results of Fletcher, the overpressures corresponding to different injury levels can be estimated. For 1- and 10-KT surface bursts, the resulting LD_{50} peak overpressure values for an

initially standing person are 14 psi and 9 psi, respectively (see Table 5.18). From the same results of Fletcher, a standing person who is hit, front-on or back-on, with blast winds of 14-psi peak overpressure from a 1-KT explosion, can be expected to be translated a distance of 28.7 feet, with a peak velocity of 35 ft/sec. The same person, if hit while in a random, prone position, would be translated 18.7 ft and attain a peak velocity of 27.1 ft/sec. (See Table 5.19).

Table 5.18. Overpressure (PSI from nuclear weapons developing LD_{50} impact velocity (35 fps) (impacting at 35 fps - random impact orientation)

Initial Orientation	0.1 KT		1 KT		10 KT		100 KT	
	S	HOB	S	HOB	S	HOB	S	HOB
Standing, Front or Back to Wind	22.6	21.6	14.1	16.1	8.6	11.1	6.2	7.2
Prone, Random Orientation	79.1	-	33.6	47.8	20.3	28.4	11.9	14.6

S = surface burst
HOB = upper optimum height-of-burst
Developed from displacement tables (Ref. 5.122)

Table 5.19. Differences in computed human translations by blastwinds from a surface burst nuclear weapon developing 14 psi overpressure.

Initial Orientation	0.1 KT		1 KT		10 KT		100 KT	
	V	D	V	D	V	D	V	D
Standing, front-on or back-on to wind	18.2	20.4	35.0	28.7	66.1	80.9	111.5	198.0
Prone, Random Orientation	13.8	5.99	27.1	18.7	50.9	54.0	87.5	138.8

V = maximum velocity, ft/sec
D = total displacement, ft

Table 5.20 is a further application of the Fletcher data by which yield dependence for displacement of a prone or standing person is calculated.

Table 5.20. Tertiary airblast criteria, surface burst.

	Yield (KT)				
	0.01	0.1	1.0	10.0	100.0
A. Displacement of Prone Person in Random Orientation					
Impact with Non-Yielding Surface after 10 ft of Body Travel	Overpressure (psi)				
Threshold	28.6	17.9	11.0	7.5	5.6
BD_{50}	68.4	31.3	19.8	12.6	7.8
LD_{50}	----	79.2	33.6	20.3	11.9
Decelerative Tumbling					
Threshold	----	58.5	29.1	18.0	10.6
BD_{50}	----	----	65.6	28.8	17.4
LD_{50}	----	----	>100.0	43.0	24.0
B. Displacement of Standing Person Front- or Back-On to Wind					
Impact with Non-Yielding Surface after 10 ft of Body Travel					
Threshold	10.8	6.6	4.5	3.3	2.6
BD_{50}	21.0	12.4	7.5	5.2	4.0
LD_{50}	37.7	22.6	14.1	8.6	6.2
Decelerative Tumbling					
Threshold	32.4	19.9	16.0	7.6	5.5
BD_{50}	94.9	35.6	22.1	14.3	9.4
LD_{50}	----	67.5	32.4	21.2	14.5

The LD_{50} velocities thus obtained are only for perpendicular impact with a hard, non-yielding surface. If softer surfaces were considered, a different impact velocity would be necessary. This in turn would develop a new set of overpressure values for the different weapons. In 1967 Schildt (Ref. 5.51) published a test in which fatal impact, based on data of Richmond, Bowen and White (Ref. 5.121), were calculated at 9 m/sec (29.5 ft/sec) for perpendicular impact with a hard, non-yielding surface. Schildt also considered the impact with elastic and soft material, e.g., snow, bushes. Schildt did not indicate velocities which were considered for the elastic or soft material, but for a 1-KT weapon, the LD_{50} overpressures were 11.0 and 29.4 psi, respectively (see Figure 5.19, Table 5.21).

Table 5.21. Peak overpressures (psi) developing lethal impact with various surfaces. LD_{50} velocity ≈ 29.5 ft/sec (from Figure 5.5).

	1 KT	10 KT	100 KT
Hard, Non-yielding	11.0	7.1	4.8
Elastic - decelerative force one-half of A	20.6	11.9	7.9
Soft - snow, bushes	29.4	19.1	11.8

An estimate of the LD_{50} velocities for impact with elastic material and soft material can be obtained from the overpressure data of Schildt and the velocity/displacement tables of Fletcher (Ref. 5.122). This yields LD_{50} velocities for perpendicular impact of 29.5 ft/sec for a non-yielding surface, 42 ft/sec for elastic material, and 102 ft/sec for soft material. The Lovelace LD_{50} perpendicular impact velocity value for non-yielding surfaces is 18.6 percent higher than that of Schildt (35 ft/sec vs. 29.5 ft/sec). If the Schildt velocity values are directly scaled from the single impact velocity value of Lovelace, the impact velocities become 35 ft/sec for a non-yielding surface, 50 ft/sec for elastic material

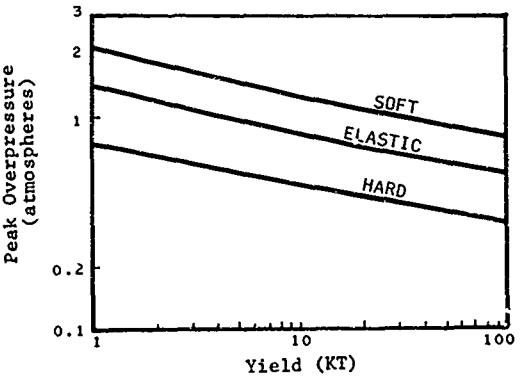

Figure 5.19. Variation of probability of death from tertiary blast effect with yield and peak overpressure (see Table 5.21).

and 120 ft/sec for soft material. For these velocities, a 1-KT yield will produce an LD_{50} for non-yielding surfaces at 14 psi, elastic material at 18 psi, and soft material at 34 psi (see Table 5.22).

Table 5.22. LD_{50} values for random impact with various surfaces. Calculated for surface burst.

	Velocity (ft/sec)	Peak Overpressure (psi) 0.1 KT	1 KT	10 KT	100 KT
Non-Yielding	35	22	14	9	6
Elastic Material	50	29	18	11	8
Soft Material	120	--	34	22	10.6

NOTE: This is Fletcher's data (35 ft/sec for LD_{50}) scaled to Schildt's data for impact with various surfaces.

Fletcher - Ref. 5.122
Schildt - Ref. 5.51

The complexity of the problem in determining lethal impact velocities can be illustrated by the following. For a random orientation upon impact, the lethal (LD_{50}) velocity is 35 ft/sec, if impact is made with a hard non-yielding surface. For a human subject to be accelerated to this velocity the required overpressure from a 1 KT surface burst weapon is 14.0 psi, if the subject were initially standing back- or front-on to blast wind. If the person were initially prone, in a random position, the overpressure necessary to accelerate him to 35 ft/sec would be 33.3 psi for a 1 KT surface burst. The problem thus becomes more complex in three ways: 1) If the person were initially standing sideways or reclining prone in a specific position, such as head-on to the advancing blast wave, the required overpressure to accelerate the person to 35 ft/sec would depend on the person's initial orientation; 2) if the person, impacting with a hard non-yielding surface, impacts with a specific orientation, the

required impact velocity would depend on final impact orientation of the person, 3) if the person impacted with a substance other than a hard non-yielding surface, the necessary velocity for lethality would be increased.

As an example result, a standing person hit by the blast winds of a 1 KT surface burst nuclear weapon would experience the following peak overpressure for a 50% probability of fatal impact due to translation, assuming the impact occurs within ~10 ft of body travel:

1 KT	10 KT
$LD_{50} = 14.1 \pm 0.6$ psi	$LD_{50} = 8.6\ ^{+0.5}_{-0.3}$ psi

Decelerative Tumbling

The response of man to impact is sensitive to the amplitude (kinetic energy of translating body) and time (suddenness of deceleration) characteristics of the impact. Because of this, man's burdening and lethal limits are much higher for decelerative tumbling than for impact. This relationship of casualties to amplitude and time characteristics has already been pointed out in the lethal impact studies of man against different surface hardnesses.

The relative tolerance of the human body, organs, or tissue, to injury is related to the mode of casualty production (Ref. 5.108). For tertiary blast injury (injuries resulting from whole-body translation), the head is the area most sensitive to trauma (see Table 5.23). Next would be the thorax (the heart and major veins and arteries), while the abdomen would be least sensitive. This categorization is under extremely ideal conditions. For the translating human body, the relative tolerance characteristics will depend upon the terrain over which the body is tumbling and the orientation(s) of impact. A blow to the abdomen due to the body striking a projecting object will mimic

a secondary blast injury (injuries due to debris impacting with the body), in which case the abdomen is more sensitive. If the angle of impact is low, the body will be able to "skip" along the surface, releasing kinetic energy in a number of impacts and thus minimizing the seriousness of each blow. These relationships tend to complicate any attempt to establish burdening or lethal limits to decelerative tumbling.

Table 5.23. Tolerance of organs to three types of blast effects. (Most sensitive organ first one in series.) Ref. 5.108

Primary : (blast overpressure)	1) lungs and circulatory system, 2) gut, 3) liver and spleen, 4) central nervous system
Secondary: (blast accelerated missiles)	1) liver, spleen, kidney, 2) central nervous system, 3) heart and great vessels
Tertiary: (whole-body) translation)	1) central nervous system,(brain and spinal column) 2) great vessels, 3) liver.

The Lovelace Foundation has estimated a peak velocity during displacement of 120 ft/sec would result in a 95% probability of burdening injury from decelerative tumbling (see Section 5.3.4 on Burdening Effects for burdening injuries). For impact, Fletcher (Ref. 5.122) has indicated a 95% probability of injury is approximately equivalent to a 5% probability of mortality. If the same correlation exists for decelerative tumbling, then 5% mortality would be in the region of 120 ft/sec. If a regression analysis is now performed in which the slope for the lethality curve for decelerative tumbling is assumed to be the same as that for lethal impact, the LD_{50} for decelerative tumbling falls at

148 ft/sec (see Figure 5 20). Peak overpressures which develop peak human translation velocities of 148 ft/sec are derived from the velocity/displacement tables of Fletcher, and the results are 39.6 psi for a 1 KT weapon and 25.4 psi for a 10 KT weapon.

From a study (Ref. 5.123) in which goats were translated from blast tubes, a LD_{50} peak velocity for decelerative tumbling was 80 ft/sec. Using this value and the slope of the lethality curve for impact, at 77% casualty the BD and LD curves for decelerative tumbling cross each other (see Figure 5 21). In other words, above 77%, or 88 ft/sec, all decelerative/tumbling casualties have a greater probability of being fatal injuries than serious injuries. It is interesting that these two curves would cross at 88 ft/sec in that this is the maximum velocity to which dogs and goats were subjected during decelerative tumbling investigations by the Lovelace Foundation (Ref. 5.118). During these investigations, no significant mortality was detected below 88 ft/sec.

Since the body is subjected to multiple impacts with decelerative tumbling, the slope of a line, which represents this effect, may not necessarily follow the same slope as that for a line which represents a single impact. On the basis of animal studies, the Lovelace Foundation (Ref. 5.122) has tentatively assigned the same value for burdening injuries whether the casualty is due to impact or decelerative tumbling. A source of possible error may be the animals employed (Ref. 5.118). The sheep are, to some degree, a round animal and tend to roll upon impacting with the surface. Also, sheep, goats, and dogs are all quadrupeds and give different structural/strain characteristics than would be found in a biped. For example, a difference in flight motion characteristics was noted between anthropomorphic dummies and goats during translation studies. When considering

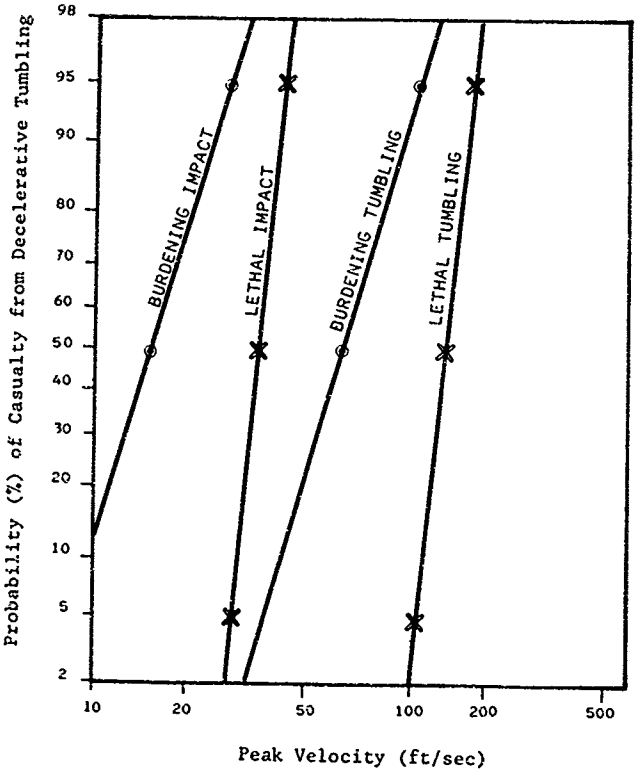

Figure 5-20. Probability of burdening and lethal velocities for casualties due to sudden impact (hard non-yielding surface) or decelerative tumbling.

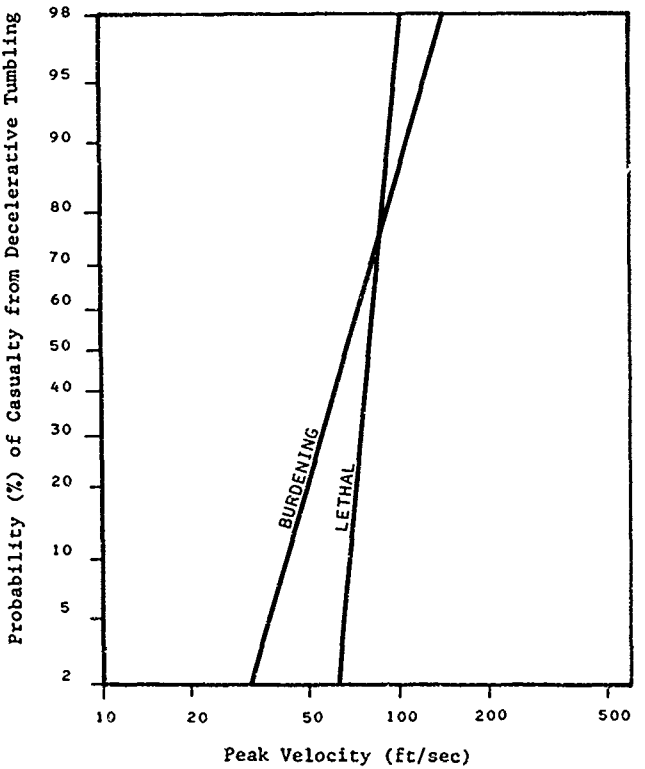

Figure 5.21. Probability of burdening and lethal velocities for casualties due to decelerative tumbling (LD_{50} based on 80 ft/sec).

the goat data that were originally employed to determine a LD_{50} of 80 ft/sec for decelerative tumbling, the animals did not remain low to the ground when air-blasted from shock tubes. Instead, they were observed to be lofted into the air. This lofting tends to result in an impact rather than decelerative tumbling. From this, it follows that the 80 ft/sec value for decelerative tumbling may not be the proper value for this casualty.

It would seem at this point that, for decelerative tumbling, LD_{50} occurs somewhere between peak velocities of 80 and 148 ft/sec. The arithmetic mean of this is 114 ft/sec. At 114 ft/sec, the peak overpressures from a 1 KT weapon which generate this peak velocity are 32.5 psi for a standing person and over 100 psi for a prone, randomly oriented person (Table 5.24). At a peak overpressure of 100 psi, the probability of death from the primary effect of overpressure is approximately 100% (see Table 5.7). From this, it appears that uncertainties in translational effects which occur at peak overpressures greater than 100 psi may not be critical since fatalities would also result from the direct effects of these overpressures.

Table 5.24. Probability of lethality from decelerative tumbling generated by blast overpressure - based on LD_{50} peak velocity of 114 ft/sec.

Initial Orientation	Peak Overpressure (psi) 0.1 KT	1.0 KT	10 KT	100 KT
Standing front-or back-on to wind	67.5	32.5	21.2	14.5
Prone, random orientation	>100	>100	42.8	24.0

Burdening Injury

Impact

For whole-body translation which terminates in impact with a solid, non-yielding sucface, the velocity which results in a burdening injury to 50% of a population (BD_{50}) has been estimated by the US Army Combat Development Command as 22 ft/sec (Ref. 5.103). The BD_{50} velocity was estimated from the velocity which produces a 1% mortality in animal population. This relationship was assumed from earlier animal studies by the Lovelace Foundation (Ref. 5.93), which indicated that impact with a non-yielding surface that resulted in 1% mortality within an animal population developed burdening injuries in approximately 50% of the surviving population. From a probit analysis of accident and suicide data, the human LD_{01} velocity was found to be 22 ft/sec (Ref. 5.124). Assuming the 1%/50% mortality/burdening relationship, the BD_{50} velocity for man is 22 ft/sec (Ref. 5.124). One problem arising from this study concerns the suicide data. The information used for this analysis was biased in that most of the victims landed feet first. If a more random impact situation is considered, the 22 ft/sec value would prove to be too high.

In 1968 Hirsch (Ref. 5.125) published a paper on the tolerance of man to impact. The data were based on studies of human volunteers and accident victims. It was found that at 20 ft/sec there was an almost certain probability of impact injury (BD_{99}) and a likelihood of some fatality (LD_{01}). The studies also indicated a BD_{01} value of 10 ft/sec. From these data, it is apparent that the mortality/burdening relationship ($LD_{01} = BD_{50}$) is not appropriate for human data. Based on the data of Hirsch (Ref. 5.125), Fletcher in 1975 (Ref. 5.122) found a BD_{50} value of 15.4 ft/sec. This information is in agreement with White's update to "Effects of Nuclear Weapons" (Ref. 5.94), where impacts were indicated to be mostly "safe" at 10 ft/sec. In terms of burdening injury,

Fletcher (Ref. 5.122) further refined the data of Hirsch and combined these data with those of experiments with sheep. The results from a probit analysis established BD_{01} as 6.5 ft/sec, BD_{50} as 15.4 ft/sec, and BD_{95} as 28.4 ft/sec (see Table 5.17).

The 1975 impact data of Fletcher in Table 5.17 are for combined orientations. If BD_{50} is considered for specific orientations at impact, the velocity values, based on sheep data, range from 12.1 ft/sec for a prone orientation at impact to 20.5 ft/sec for a supine orientation at impact (Ref. 5.122).

If the velocities for burdening injury are compared to the velocity/displacement data of Fletcher, the peak overpressure for a BD_{50} at 1 KT and 10 KT are 7.5 psi and 4.2 psi, respectively.

Decelerative Tumbling

In 1971, the USACDC (Ref. 5.103) indicated that a peak velocity of 63 ft/sec would produce a burdening injury from decelerative tumbling in at least 33% of the personnel involved. This estimate was derived from a direct scaling of goat data to human probabilities and is based on studies incorporating goats subjected to shock tube accelerations. The 63 ft/sec velocity was located on an impact probability table, and a regression line parallel to that for burdening impact drawn through the new velocity point. This new regression line indicated a BD_{50} value for decelerative tumbling of 76 ft/sec. From the same regression line, the BD_{50} peak velocity is 20 ft/sec, BD_{95} is 146 ft/sec, and BD_{99} is 192 ft/sec. When the peak velocity values were applied to USACDC overpressure curves for various weapon yields, the BD_{50} for 1 KT was 37 psi and for 10 KT was 33 psi.

Fletcher (Ref. 5.122) in 1975 determined translation characteristics for decelerative tumbling from studies of anthropomorphic dummies and goats subjected to blast winds of nuclear explosions and high explosive detonations. From the impact

studies of Hirsch (Ref. 5.125), a base value for decelerative tumbling was estimated. A regression line parallel to the impact regression line of the Fletcher study produced a set of casualty probabilities for decelerative tumbling over open terrain: BD_{01} = 28.8 ft/sec, BD_{50} = 66.4 ft/sec and BD_{95} = 120 ft/sec.

The data of Fletcher establish a BD_{50} peak velocity of about 10 ft/sec lower than the USACDC values. For BD_{50} peak overpressures, the data and graphs of USACDC indicate 37 psi for a 1 KT yield and 22 psi for 10 KT. The data of Fletcher indicate 22.1 psi at 1 KT and 14.3 psi at 10 KT (see Table 5.25).

Table 5.25. Decelerative tumbling resulting in burdening injury to 50 percent of a population.

Source	Peak Velocity (ft/sec)	Overpressure (psi) 1 KT	10 KT
Army Combat Developments Command	76	37	22
Fletcher, 1975	66.4	22.1	14.3

5.4.5 Structural Collapse and Debris

While the previously discussed, individual airblast effects are moderately well quantifiable, the causes of injuries and mortality to personnel located inside structures are extremely varied and interrelated. The possible effects include direct overpressure, glass, high-velocity debris, whole-body translation (with tumbling and/or impact), floor sweep, and structural collapse (low-velocity debris). Most of these effects are yield dependent. The higher overpressure vulnerabilities for some effects at smaller weapon yields reflect, among other things, the lower damage produced at a given overpressure level by dynamic impulse or drag loading due to the shorter blast wave duration of small yield weapons. (More generally, the yield dependence of

these damage functions implicitly reflects their dependence on other blast wave parameters, such as its duration, and accounts for the fact that few casualty producing mechanisms depend solely on peak overpressure.) The yield dependence of these damage mechanisms also illustrates that effective values for combined blast effects, which have been calculated at large yields (≥1 MT) and indexed to peak overpressure, will be likely to substantially overestimate blast casualties if they are adopted directly for low-yield weapons.

One method which has been frequently used to scale personnel blast vulnerabilities with weapon yield is to adopt the same scaling laws appropriate for blast damage to the structures within which the people are located. A basic weakness of this approach is that it does not treat in sufficient detail the actual, underlying mechanisms responsible for producing casualties which have different yield dependences For example, a person on an upper floor of a typical, weak walled multistory building may be swept out of the building by the first part of the blast wave and be killed by impact with the ground. The blast winds that then follow may or may not load the skeleton frame of the building left behind to an extent sufficent to bend or collapse the structural members. The latter effect is the one described by conventional data for damage to structures, not the first effect that, in this case, actually produces the fatality.

While each of the component effects can be handled, the combination requires a methodology such as the Monte Carlo approach of Longinow and Ojdrivich or the mechanistic probability approach of Fricke (Ref. 5.70). Since the Monte Carlo analysis is not appropriate for the lower yields, we will adopt Fricke's values recognizing that further refinements should be undertaken to reduce the large uncertainties, especially at the lower yields. Table 5.26 presents a summary of the airblast LD_{50} and BD_{50} values for personnel in various structures (glass to be considered separately).

Table 5.26. Airblast Casualty Criteria for Personnel Inside Structures (peak overpressure in psi) Glass injury to be considered separately.

	Yield (KT)					
	0.01	0.1	1.0	10	100	1000
Residences and Multistory Bldgs.						
LD_{50}	18	15	12	10	7	5
BD_{50}	8	8	7	5	4	3
Upper Floors of Multistory Bldgs.						
LD_{50}	18	15	12	10	7	4
BD_{50}	8	8	7	5	4	3
Basements and Strong-Walled Bldgs.						
LD_{50}	18	15	13	12	12	11
BD_{50}	10	10	10	10	10	10

Uncertainties are a factor of 3 at 0.01 KT and a factor of 2 for 0.1 to 10 KT with ±50% for higher yields.

5.4.6 Summary of Effects (Tentative Estimates)

Tables 5.27, 5.28, and 5.29 summarize the human response probability for personnel subjected to the various effects of airblast. The list is far from complete and most values are still tentative estimations from presently available data.

Table 5.27. Summary Primary Airblast Effects on Man (overpressure in psi).

		Yield (KT)					
		0.01	0.1	1.0	10	100	1000
Whole Body							
Prone (parallel to shock wave)	LD_{01}	47	44	42	41	40	40
	LD_{50}	74	68	64	63	62	62
	LD_{99}	125	115	100	97	94	93
Standing or Prone (perpendicular to shock wave)	LD_{01}	30	29	28	27	27	27
	LD_{50}	42	40	38	37	37	37
	LD_{99}	60	55	53	52	51	51
Thorax Near Reflecting Surface	LD_{01}	17	16	15	15	14	14
	LD_{50}	23	22	22	21	21	21
	LD_{99}	32	30	29	28	28	28
Lung							
Threshold	BD_{01}	←		12^{+3}_{-4}			→
Severe	BD_{85}	←		25 ± 5			→
Eardrums	BD_{01}	←		5			→
	BD_{50}	←		15-20			→
	BD_{99}	←		$\gtrsim 35$			→

Unless otherwise noted, estimated uncertainties are of the order of $\pm$15% for 1.0 KT and above, and $\pm$20% for 0.1 KT and below.

Table 5.28. Summary of Secondary Airblast Effects on Man (peak overpressure in psi).

		Yield (KT)					
		0.01	0.1	1.0	10	100	1000
Blunt Trauma							
Whole Body-Standing Solid Object							
1 pound	LD_{50}	157	76	31	19	11	9
	BD_{50}	74	40	18	12	7	6
5 pound	LD_{50}	134	61	24	15	9	6
	BD_{50}	63	32	14	9	6	4
10 pound	LD_{50}	106	53	20	13	8	5
	BD_{50}	50	28	12	8	5	5
Penetrating Trauma							
Whole Body							
Metal Sphere (58 mg)	LD_{50}	89	78	69	61	54	50
	BD_{50}	76	68	62	56	50	47
Metal Fragment (58 mg)	LD_{50}	97	85	75	65	58	54
	BD_{50}	83	74	67	60	54	51
Stone Masses							
0.1 gm	LD_{50}	84	75	66	58	51	48
	BD_{50}	72	65	59	53	48	45
1.0 gm	LD_{50}	80	71	64	56	50	46
	BD_{50}	68	62	57	51	47	43
10.0 gm	LD_{50}	73	61	52	45	37	32
	BD_{50}	62	53	46	41	35	30
Cutting Trauma							
Glass	LD_{50}		← 3 →				
	BD_{50}		← 1 →				

- Uncertainties are ±1 ·00% for secondary airblast effects at all yields.
- LD_{50} data for blunt trauma is BD_{50} data scaled same as Impact-Lethal data.
- LD_{50} data for Penetrating tauma is BD_{50} level if Medical Care not available or vital organ hit (e.g., heart) - Otherwise LD values are related to probability of number of penetrations and/or velocity of missile.

Table 5.29. Summary of Tertiary Airblast Effects on Man (peak overpressure in psi).

		Yield (KT)					
		0.01	0.1	1.0	10	100	1000
Whole Body Impact							
Standing							
Non Yielding Surface	LD_{01}	51	19	11	7	5	4
	LD_{50}	38	22	14	9	6	5
	LD_{99}	53	27	17	11	7	6
	BD_{01}	11	7	5	3	3	2
	BD_{50}	21	13	8	4	4	3
	BD_{99}	35	21	13	8	6	5
Elastic Material	LD_{50}	59	29	18	11	8	6
Soft Material	LD_{50}	--	74	34	22	11	8
Prone-Random Orientation							
Non Yielding Surface	LD_{50}	--	79	34	20	12	3
	BD_{50}	68	31	20	13	8	6
Decelerative Tumbling (open terrain)							
Standing	LD_{01}	--	55	29	19	13	8
	LD_{50}	--	68	33	21	15	10
	LD_{99}	--	97	38	24	17	12
	BD_{01}	32	20	16	8	6	4
	BD_{50}	95	36	22	14	9	7
	BD_{99}	--	74	34	22	15	11
Prone	LD_{50}	--	--	>100	43	24	16
	BD_{50}	--	--	66	29	17	11

Uncertainties are of the order of ±15% for 0.1 KT and above, and ±30% for 0.01 KT.

5.5 DETAILED DOSE CALCULATIONS

A study is in progress to produce a methodology for determining the probability of early radiation mortality in reference man resulting from a single acute exposure to nuclear weapons radiation. Early radiation mortality is defined as death attributable to specific high-intensity exposures within 60 days after irradiation. This phenomenon results from the collapse of the blood forming (red marrow) regions of the body.

The approach used to attain the above objective is to correlate the probability of early radiation mortality in man and laboratory animals on the basis of dose to the red marrow. Miniature pigs and rhesus monkeys have been exposed to photon and mixed neutron-photon radiation at the Armed Forces Radiobiological Research Institute (AFFRI) and the effects reported as a function of midline tissue dose (Refs. 5.126, 5.127, 5.128) This project makes use of the MORSE Monte Carlo radiation transport computer code (Ref. 5.129) to duplicate these experiments analytically, thereby enabling the determination of the doses received by the red marrow, a quantity not measured in the original experiment. Experimental environments are determined from previously reported calculations and measurements applicable to the AFRRI TRIGA reactor (Refs. 5.130, 5.131, 5.132) and x-radiation (Ref. 5.133) sources. Physical models of the miniature pig and rhesus monkey are based on the gross descriptions of the subjects as given in the experiment reports. This material has been augmented by the study of frozen section of specimens similar to those used in the actual experiment (Ref. 5.134). No attempt is made to obtain absolute red marrow dose values from these calculations, instead, calculated values are normalized to dose values measured at specific points within the subjects in the actual

experiments. In one experiment (Ref. 5.126) rhesus monkeys were exposed to both pure photon and mixed neutron-photon radiation under otherwise identical experimental conditions. Analysis of this experiment is intended to serve the additional goal of estimating the relative biological effectiveness (RBE) of neutrons versus photons for producing the early radiation mortality phenomenon.

This project makes use of the MORSE code (Ref. 5.129) in its adjoint mode to calculate dose to the red marrow resulting from exposure to nuclear weapons radiation. In such a calculation all nuclear cross section matrices are inverted, allowing the code to follow neutrons and photons in reverse direction, i.e., from deposition region to radiation source rather than vice versa.

Particles are sampled from the appropriate response function for depositing dose in the region of interest (in this case the red marrow) and are followed through all reactions which may occur until they pass through a spherical surface surrounding the man, where particle energy and direction are recorded. This process effectively modifies the initial response function to account for transport through the system. Thus, the result is also a response function which may be combined with any arbitrary radiation field to obtain a dose value for that field. This may be done providing that man does not significantly perturb the radiation field by his presence. In the case of man standing on an open plane this is a good assumption. For the purpose of this study a model of an adult male has been produced in Combinatorial Geometry. This model has been adapted from one reported earlier by W.S. Snyder, et al., (Ref. 5.135) and is based on international reference man (Ref. 5.136). The exterior configuration of the male model is shown in Figure 5.22.

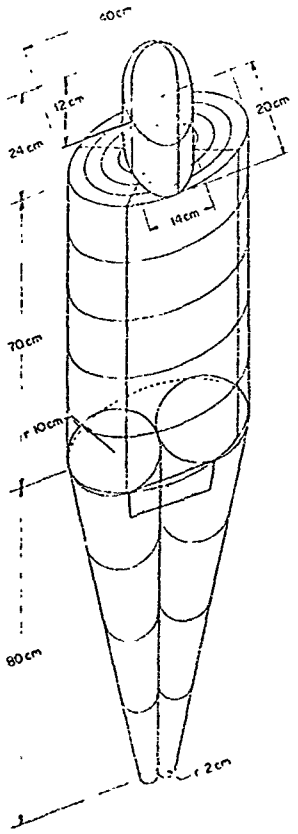

Figure 5.22. The adult human phantom.

Progress under this project to date consists of the completion of calculations of photon dose-response for 98.4% of the red marrow in man. The distribution of red marrow in the body is shown in Figure 5.23. Response values thus obtained have been followed by energy group with radiation environment data consisting of the angle-integrated neutron-induced gamma-ray fluence calculated at the air-ground interface 1200 meters from an unmoderated (Watt) fission neutron source located at a height of 50 ft (Ref. 5.137). This secondary gamma-ray field approximates that produced by a low-yield boosted fission weapon at a similar range and results in an average marrow dose of 4.0E-23* rad(marrow) per source neutron. In the absence of man the neutron-induced gamma dose at the same point is calculated to be 5.83E-23 rad (tis, free-in-air) per source neutron. Therefore, for this particular environment the dose/exposure conversion factor is 0.686 rad (marrow) per rad (tis, free-in-air).

Published estimates of the exposed population fraction succumbing to a lethal dose to the red marrow give the 50 percentile (LD_{50}) value as 350 rads (marrow) (Ref. 5.35), assuming the availability of only minimal medical treatment. This means that for an environment having the characteristics of the one described above, exposure to the secondary gamma-ray component alone would require a level of 495 rad (tis, free-in-air) to produce an average marrow dose having the LD_{50} value.

Efforts are now underway to calculate the marrow dose produced by incident neutrons. This problem has some rather unique features in that man is essentially a column of water and as such can trap neutrons, rapidly reducing them in energy by scatter with hydrogen, then allow them to scatter many times

*Read as 4.0×10^{-23}.

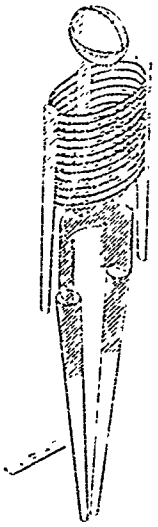

SKULL	13.1%
VERTEBRAE	28.4%
RIBS + STERNUM	10.2%
SCAPULAE	4.8%
HEAD AND NECK OF BOTH ARMS	1.9%
BOTH CLAVICLES	1.6%
HEAD AND NECK OF BOTH LEGS	3.8%
PELVIS	36.2%

TOTAL AMOUNT OF RED BONE MARROW: 1500 g

RED BONE MARROW

ORNL-DWG 70-4810R

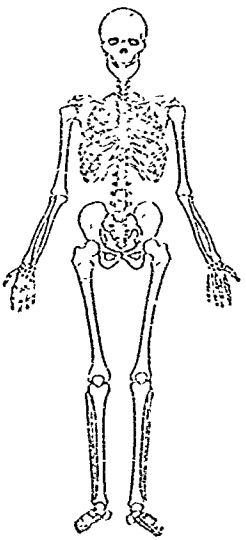

Figure 5.23. Idealized model of the skeleton for computer calculations (left) and a more realistic representation (right) with percentages of red bone marrow found in the shaded portions of the bones. Clavicles and scapulae not shown in phantom.

before they are captured. Following particles in the adjoint mode, this translates into the problem of having to follow a low-energy neutron through many scattering events before it finally escapes the system and is counted. Several schemes for reducing the statistical variance of the calculated neutron response are being tested; however, initial estimates indicate that, in terms of converting free-in-air dose to marrow dose, neutrons are somewhat more effective than gamma rays.

All results obtained to date are preliminary with significantly more study required to fully understand the already large body of data amassed. In the meantime work is underway to complete the skeletal detail of the miniature pig and rhesus monkey models. On completion of these models marrow dose received by the experimental subjects will be determined and correlated with their response. Further correlation of these dose/response relationships with weapons radiation deposited dose in reference man will fulfill the goals originally set for this project.

5.6 COMBINED INJURIES

Studies are now in progress, primarily at AFRRI, on the effects of combined injuries. Results from these studies are not yet available; however, we have made some highly preliminary estimates of the potential impact of combined injuries on damage functions for civilian personnel. These estimates will be appropriately refined as the results of more thorough studies become available.

Selected references (Refs. 5.52 and 5.138-5.154 were consulted for these preliminary estimates. Many of the papers showed adaptation (or "antagonistic") effects, where small trauma increased resistance to subsequent larger trauma; and the majority of the studies involving ionizing radiation showed very large synergistic effects when other trauma were introduced later (periods of days) than the exposure to ionizating radiation. Here, we concern ourselves only with untreated and essentially simultaneous ("same day") injuries, the different injuries usually being inflicted within about 2 hrs. A brief indication of the major results of a few of these articles is given below. These results, together with general impressions obtained from the other references listed, have formed the basis for some combined injury criteria used in the present examination (Sections 5.6.5 and 5.6.6)

5.6.1 Hot, Dust Laden Air

A cursory examination of data (Ref 5.140) from seven weapons tests (low air bursts with yields from 10 to 37 KT) involving a variety of shelter types suggests that this effect will not be a dominant casualty mechanism for the weapon yields and sheltering situations of greatest present interest Viz at ranges where significant burns might be expected, supra lethal doses of ionizing radiation would also be expect-

Consequently, we do not pursue this further here with regard to combined injuries. However, for deep shelter situations, such as tunnels or subways, this effect may well deserve further examination.

5.6.2 Airblast and Thermal Radiation

Most of the data reviewed on the combination of these trauma indicates little, if any, "combined injury" effect; by combined injury we mean any addition of casualty probabilities P other than the usual one that assumes the effects (i) are independent, $P_{tot} = 1 - \pi_i(1 - P_i)$. Indeed, in one experiment (Ref.5.140) on rats, where a sub-lethal flash burn (6 cal/cm^2, 30% area) was combined with direct (lung damage) blast injury in the lethal range (~30-35 psi), a general antagonistic trend (a reduction in mortality) was observed.

5.6.3 Airblast and Ionizing Radiation

Direct, or Primary, Blast Effects (Lung Damage)

R.K. Jones, et al., (Ref. 5.141). Sheep exposed to HE blast (145 psi) plus reactor radiation (422 rad, n/γ = 5).

- No fatalities in 60 days from radiation alone
- 25% fatalities from blast alone
- 50% fatalities from both blast and radiation.

Lovelace Data, (Ref. 5.140). Sheep exposed to blast (40 psi) plus ^{60}Co gamma radiation (325 rad).

- 25% fatalities in 60 days from radiation alone
- 15% fatalities from blast alone
- 15% fatalities from both blast and radiation.

Lovelace Data (Ref. 5.140). Swine exposed to blast (50 psi) plus reactor radiation (350-400 rad).

- No fatalities in 60 days from radiation alone
- 30% fatalities from blast alone
- 33% fatalities from both blast and radiation.

D.R. Richmond, et al. (Ref. 5.142). Sprague-Dawley rats exposed to shock tube blast (16 psi, 370 msec) and x-rays (30 day LD_{46} level).

- 46% fatalities in 30 days from radiation alone
- 5% fatalities from blast alone
- 51% fatalities from both blast and radiation.

Indirect, or Secondary and Tertiary, Blast Effects (Impacts, debris, and other sources of open or closed wounds)

L. Koslowski and D. Messerschmidt (Ref. 5.142). NMRI mice exposed to open wounds (5% body area, skin removed) and x-rays (510 rad).

- 26% fatalities from radiation alone
- 6% fatalities from wound alone
- 32% fatalities from both wound and radiation.

W.H. Moncrief, Jr. (Ref. 5.145). General review article; comments follow on closed wounds:

"Clinically, soft-tissue wounds are relatively unaffected by radiation if wound infection is not a problem, that is, in the closed wound.... Closed fractures heal uneventfully when complicated by whole-body irradiation.... The problem of the compound fracture is the problem of the soft-tissue wound."

(This article, along with many others, emphasizes that surgical procedures carried out during the response to radiation will add to the patient's morbidity. This affects studies concerned with the load on medical care facilities, since surgery may be restricted for considerable periods of time.)

5.6.4 Thermal and Ionizing Radiation

Flash Burns

R.K. Jones (Ref 5.141) Swine exposed to thermal flash (30 cal/cm^2, 15-20% body area) and reactor (n + γ) radiation

- No fatalities in 60 days from burn alone
- 13% fatalities in 60 days from 554 rad alone
- 67% fatalities in 60 days from 612 rad alone
- 29% fatalities from both burn and 554 rad
- 54% fatalities from both burn and 612 rad.

H. Baxter, et al. (Ref 5.152) Yorkshire swine exposed to thermal flash (10-15% body area) and x-rays (400 rad)

- No fatalities from burn alone
- 20% fatalities in 30 days from x-rays alone
- 90% fatalities in 30 days from both burn and x-rays

H. Baxter, et al (Ref 5.153) Above result for exposure to both burn and x-rays (90% fatalities) reduced to (20%) fatalities expected from x-rays alone by treatment with streptomycin.

J.D Reid, et al. (Ref 5.147) Dogs exposed to thermal flash (8 cal/cm^2, 1 sec per application, 20% body area, deep second-degree burn) plus 100 rad x-rays; order to exposures (thermal or x-rays first) produced no difference

- 12% fatalities from burn alone
- 72% fatalities from both burn and x-rays
- Conclusion was that x-rays did not predispose animals to bacteremia but by depression of defense mechanisms, as evidence in part by leukopenia, allowed more virulent organisms to enter and produce a fatal septicemia. The site of the tissue injury, and the local flora therein, appeared to determine the type of invading bacteria.

Flash Burns, with Direct Airblast

Lovelace Data (Ref. 5.140). Rats exposed to flash burn (6.3 cal/cm^2 over 25-30% body area) plus reactor (n/γ = 5) radiation. Variation in mid-lethal (shock tube, long duration) overpressure observed:

- Blast only, LD_{50} (blast) = 30.9 psi
- Blast and burn, LD_{50} (blast) = 34.7 psi
- Blast and burn plus 250 rad, LD_{50} (blast) = 27.7 psi
- Blast and burn plus 350 rad, LD_{50} (blast) = 19.8 psi.

Lovelace Data (Ref. 5.140). Experiment as per above with constant blast of 27 psi.

- Blast only, no fatalities
- Burn only, no fatalities
- 250 rad only, 17% fatalities in 30 days
- 350 rad only, 55% fatalities in 30 days
- Burn plus 250 rad, 12% fatalities in 30 days
- Burn plus blast, 19% fatalities
- Blast plus 250 rad, no fatalities in 30 days
- Burn plus blast plus 250 rad, 42% fatalities in 30 days
- Burn plus blast plus 350 rad, 94% fatalities in 30 days.

Contact Burns

J.W. Brooks, et al. (Ref. 5.52). Dogs exposed to conditions of Ref. 5.147 (indicated above) and compared to previous studies of contact burns of comparable depth and extent.

- Conclusion was that from both blood culture and mortality studies, flash burns produced a less fatal outcome. This was throught to be greatly influenced by the initial ascar formation in the flash burn, which acted as a protective coat to prevent the purulent suppuration seen in contact lesions.

E.L. Alpen and G.E Sheline (Ref. 5.151). Sprague-Dawley rats exposed to dip burn (water at 80°C, 25 seconds, 16-3% body area) and x-rays (100-500 rad).

- No fatalities from 100-250 rad alone
- 20% fatalities from 500 rad alone
- Sub-lethal burns (16-20% area) plus 500 rad produce 75% fatalities
- Burns that, alone, produce 50% fatalities (31-35% area) produce 65% fatalities when combined with 100 rad and 100% fatalities with 250 rad.

J.W. Brooks, et al. (Ref. 5.154). Dogs exposed to contact burn (brass plate at 60°C, 1 min per application, 20% body area) and x-rays (up to 100 rad); no differences observed in order of exposures.

- 12% fatalities from burn alone
- 20% fatalities from both burn and 25 rad
- 75% fatalities from both burn and 100 rad
- Above reduced to 14% fatalities by treatment with penecillin.

5.6.5 Trial Criteria

The above "sample" results vary widely in statistical accuracy and, even with regard to general trends, are not satisfyingly consistent. For this brief study, we define below two sets of combined injury fatality criteria, one thought to be fairly "pessimistic" (high mortality) and one thought to be more "optimistic." Both sets pertain to multiple effects received at nearly the same time and the assumption that no treatment with antibiotics is available.

Pessimistic Criteria

At and below a yield ~10 KT, a dominant blast casualty mechanism for people in built-up areas is expected (Ref. 5.70) to be debris resulting from structural failures. This, in turn,

can be expected to produce a sizable incidence of external wounds. Open wounds together with ionizing radiation, both in the lethal range, tend to show an additive (not independent) combination of fatality probabilities. To be on the pessimistic side, we consider this to hold true for wounds in the sub-lethal (but serious) range. Namely, our "pessimistic" assumptions are that all blast injuries produce open wounds and that "burdening" (sub-lethal) blast injuries (Ref. 5.70) lead to the same additive fatality probabilities as those in the lethal range.

In combination with ionizing radiation, flash burns appear to be considerably less hazardous than contact burns but, for the pessimistic case, we will not make this assumption. Also, we will adopt the general trends of the strongest synergism (Ref. 5.154) reported in the references examined.

The Pessimistic Criteria are then defined as follows.

- Blast and thermal radiation without ionizing radiation: blast P_K revised as follows for ionizing radiation exposures $\geq$200 rad

  $$P_K^{BLAST} \rightarrow P_K^{BLAST} + P_K^{INITIAL}, \; P_K^{BLAST} \leq 1 ,$$

  where P_K^{BLAST} is the burdening injury probability for blast (Ref. 5.70) and $P_K^{INITIAL}$ the fatality probability for ionizing radiation ($\sim$0 at 200 rad).

- Thermal exposure to flash with ionizing radiation: thermal P_K revised when free-field level is >2 cal/cm^2 (approximate threshold for second degree burn):
  - Initial <25 rad, no change
  - 25 rad $\leq$ initial $\leq$ 100 rad,

    $$P_K^{THERMAL} \rightarrow P_K^{THERMAL} + 0.50, \; P_K^{THERMAL} \leq 1$$

  - Initial >100 rad, $P_K^{THERMAL} \rightarrow 1.0$

These <u>revised</u> P_K values are then combined in the usual fashion, $P_K^{TOTAL} = 1 - (1 - P_K^{BLAST})(1 - P_K^{THERMAL})(1 - P_K^{INITIAL})$.

Optimistic Criteria

For blast and ionizing radiation, we still assume that the blast hazards produce a high incidence of external wounds but that combined injury effects (additive instead of independent probability combinations) are seen only in the lethal region.

For thermal and ionizing radiation, we still take the general indications of Ref. 5.154 but now assume that only contact burns produce a combined injury effect. The probability of producing contact burns from radiant exposure of clothing worn by civilians is quite complicated and has not been completely analyzed to date. Several factors are involved in determining whether the burn is due to transmission through, or ignition of, the fabric. In transmission burns the factors include fabric material, color, weight, number of layers and spacing. Ignition burns are further complicated by additional considerations including a variety of possible ignition thresholds, different thresholds for transient or sustained ignition, the falling away of burning fabric, and secondary fabric products such as hot vapors and hot-sticky residues (which also produce contact burns).

Some pertinent data are given in Refs. 5.55, 5.56, 5.81, 5.82, 5.155, and 5.156. Mixter, et al. (Ref. 5.155) studied fabric contact burns of white pig skin in which the animal was placed next to fabric clamped in a 1.7 cm, water cooled exposure port. The results were scaled to 2^{o} human burns, and the exposure (cal/cm^2) necessary for a contact burn was found to increase by about 300% when going from black to white material or from material in contact with skin to material about 5 mm from the skin. The experiments of Mixter and other investigators used exposure times ranging from 250 msec to 30 sec, which presents additional problems when scaling to yields of 10 KT or less. From

our analysis to date, the best estimate for averagely dressed civilians in the summer would be about 6 cal/cm^2 for a significant probability of producing a 2^o contact burn from exposure to the thermal flash of ∿1-10 KT weapons.

The Optimistic Criteria are then defined as follows:

- Blast and thermal radiation without ionizing radiation: no change
- Blast with ionizing radiation: blast P_K revised as follows:

  $P_K^{BLAST} \rightarrow P_K^{BLAST} + P_K^{INITIAL} \cdot P_K^{BLAST}$ ≤ 1
- Thermal exposure to flash with ionizing radiation: thermal P_K revised as follows when free-field level ≥ 6 cal/cm^2:
  - Initial <25 rad, no change
  - 25 rad $\leq$ Initial $\leq$ 100 rad

    $P_K^{THERMAL} \rightarrow P_K^{THERMAL} + 0.5$, $P_K^{THERMAL} \leq 1$
  - Initial >100 rad,

    $P_K^{THERMAL} \rightarrow 1.0$.

5.6.6 Effects Produced by Assumed Combined Injury Criteria

One example of the effects produced by the trial combined injury criteria defined here is shown in Figure 5.24. Damage functions, as discussed in Section 7 are shown in this figure. Both the expectation values and 90% confidence limits are shown for the "nominal" (no combined injury effects) fatalities produced by a 10 KT weapon and a sheltering category of aboveground portions of typical residences with 10% of the occupants fully exposed to the thermal flash and flying glass from broken windows. Using the "Optimistic" combined injury criteria produces essentially no difference from the nominal expectation values, whereas the

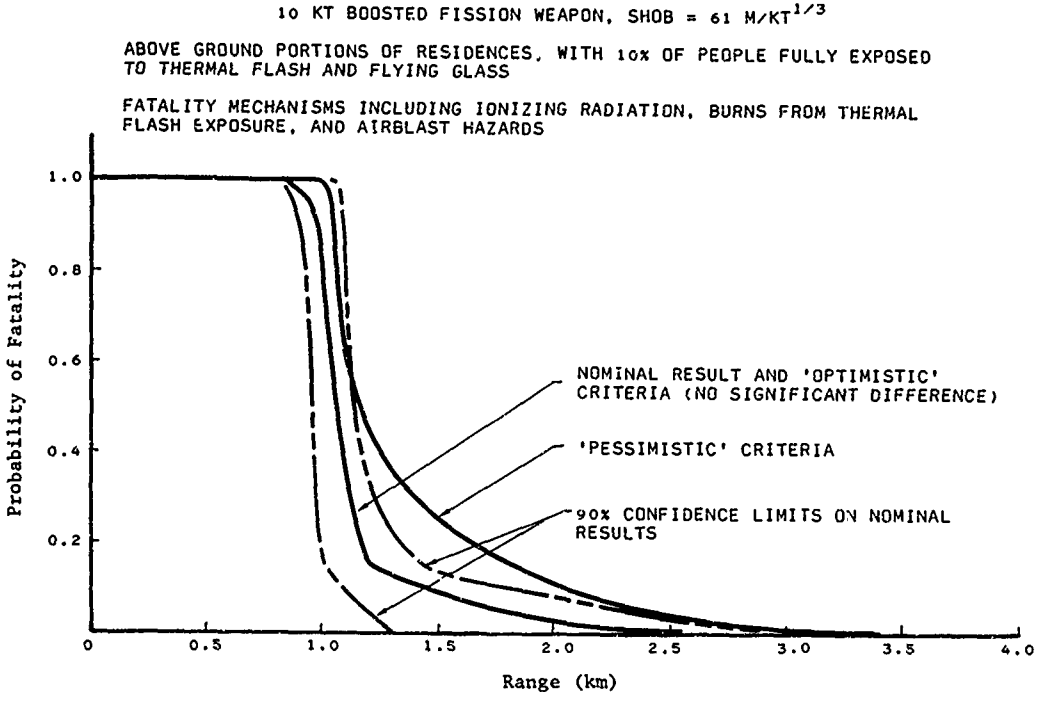

Figure 5.24. Example of effects produced by combined injury criteria.

"Pessimistic" criteria give higher fatality probabilities than the upper 90% confidence limit of the nominal criteria when the latter produce p_ks in the range ∿0.1 to 0.5 (between about 1.2 and 2.0 km in range). The Optimistic Criteria make little difference in this case because (1) the P_k for initial radiation greatly dominates that for airblast out to ranges where both are small, and thereafter the P_k from the glass hazard dominates the rapidly falling P_k from initial radiation; and (2) for the 10% of people exposed to thermal radiation, the difference in range between the thermal criterion (6 cal/cm^2) for contact burns and the mid-lethal (8.6cal/cm^2) value is fairly small and occurs where the ionizing radiation exposure is low (∿10-40 rad). The Pessimistic Criteria produce the greatest difference from the nominal criteria at a range ∿1.1 - 1.2 km. There, the thermal radiation is lethal but in this sheltering case contributes only a $P_k \leq 0.1$. The effect is due, rather, to satisfying the Pessimistic Criteria for airblast (P_B = 50% near 4 psi) and ionizing radiation ($P_k > 0$ near 200 rad), since between 1.1 and 1.2 km the airblast varies from ∿5 to 4 psi and the ionizing radiation (inside) from ∿450 to 200 rad.

This preliminary study has resulted in no clear indication of the possible significance of combined injuries. Consequently, as improvement in the criteria for combined injuries becomes available, several burst conditions and sheltering situations should be examined more closely for a better assessment of the potential impact of combined injuries on the damage functions. The available biomedical data will probably limit this to an examination of the damage functions for fatalities, not of those for non-fatal injuries.

5.7 REFERENCES

5.1 International Commission on Radiation Units and Measurements, "Radiation Quantities and Units," ICRU Report No. 19, 1971.

5.2 Johns, H.E. and J.R. Cunningham, The Physics of Radiology, Third Edition (Charles C. Thomas, Springfield, 1969), p. 278.

5.3 Todd, P. and C.A. Tobias, "Cellular Radiation Biology" in Space Radiation Biology and Related Topics, C.A. Tobias and P. Todd, editors (Academic Press, New York, 1974), p. 141.

5.4 Lushbaugh, C.C., "Human Radiation Tolerance" in Space Radiation Biology and Related Topics, C.A. Tobias and P. Todd, editors (Academic Press, New York, 1974), p. 475

5.5 Verrelli, D.M., et al., "Biological Effects of Prompt Supralethal Radiation," Paper presented at 34th MORS meeting, 1974.

5.6 National Council on Radiation Protection and Measurements, "Protection Against Neutron Radiation," NCRP Report No. 38, 1971.

5.7 AFRRI Recommendations (1976).

5.8 U.S. Army Nuclear Agency, "The Calculation of Absorbed Dose and Tissue Transmission Factors," ANA Technical Memorandum 1-74, November 11, 1974.

5.9 Langham, W.H., editor, Radiobiological Factors in Manned Space Flight, NAS/NRC Publication 1487 (NAS/NRC, Washington, 1967), p. 119.

5.10 Tate, P.A., "Dosimetry for Initial Radiation from Nuclear Weapons," DREO Memo 20/72 (NBC), June 1972.

5.11 Bond, V.P. and C.V. Robinson, "Bone-Marrow Stem-Cell Survival in the Non-Uniformily Exposed Mammal," in Effects of Ionizing Radiation on the Haematopoietic Tissue (IAEA, Vienna, 1967), p. 69.

5.12 Hansen, C.L., Jr., et al., "Lethality of Upper Body Exposure to X-radiation in Beagles," Public Health Reports 76, 245 (1961).

5.13 Michaelson, S.M., et al., "Mechanisms of Injury and Recovery from Whole and Partial Body Exposure to Ionizing Radiation," University of Rochester Report No. UR-615, 1962.

5.14 Fitzpatrick, P.J. and W.D. Rider, "Half Body Radiotherapy," Int. J. Radiation Oncology 1, 197 (1976).

5.15 Cohen, L., "Radiation Response and Recovery, Radiobiological Principles and Their Relation to Clinical Practice," in The Biological Basis of Radiation Therapy, E.E. Schwartz, editor (J.B. Lippincott, Philadelphia, 1966), p. 208.

5.16 Dolan, P.J., editor, "Capabilities of Nuclear Weapons," DNA EM-1, July 1972.

5.17 Scott, W. (SAI) and M. Cohen (MAGI), "Initial Radiation Protection in West German Villages", SAI Rpt. SAI-75-652-LJ, Sept. 1975 and best estimates made by E. Straker (SAI) 1976.

5.18 Langham, W.H., "Radiobiological Factors in Space Conquest," Aerospace Med. 40, 834 (1969).

5.19 Langham, W.H., editor, "Radiobiological Factors in Manned Space Flight," NAS/NRC Publication 1487 (NAS/NRC, Washington, 1967).

5.20 White, C.S., (Lovelace Foundation), Private Communication, 1974, and M.P. Fricke (SAI), Private Communication, 1975.

5.21 Stromberg, L.R. (AFRRI) Private Communication, 1975.

5.22 Still, E. (AFRRI) Private Communication, 1976.

5.23 Tobias, C.A. and P. Todd, editors, Space Radiation Biology and Related Topics (Academic Press, New York, 1974).

5.24 Reetz, A. and K. O'Brien, editors, "Protection Against Space Radiation," NASA SP-169 (ANS-SD-5), 1968.

5.25 Warman, E.A., editor, "Proceedings of the National Symposium on Natural and Manmade Radiation in Space," NASA Technical Memorandum NASA TM X-2440, January 1972.

5.26 Ricks, R.C. and C.C. Lushbaugh, "Studies Relative to the Radiosensitivity of Man Based on Retrospective Evaluations of Therapeutic and Accidental Total-Body Irradiation," NASA Final Report, Oak Ridge Associated Universities, September 1, 1975.

5.27 Langham, W.H., P.M. Brooks and D. Grahn, editors, "Radiation Biology and Space Environmental Parameters in Manned Spacecraft Design and Operations," Aerospace Medicine 36 (entire issue No. 2), February 1965.

5.28 H. Aceto, et al., "Mammalian Radiobiology" in Space Radiation Biology and Related Topics, C.A. Tobias and P. Todd, editors (Academic Press, New York, 1974), p. 375.

5.29 Baum, S. (AFRRI) Private Communication, 1976.

5.30 Lushbaugh, C.C. (ORAV), Private communication, Sept. 1976.

5.31 Stromberg, L.R., Chairman, Meeting at AFRRI, November 11, 1975.

5.32 National Council on Radiation Protection and Measurements, "Radiological Factors Affecting Decision-Making in a Nuclear Attack," NCRP Report No. 42, 1974.

5.33 Bond, V.P., T.M. Fliedner and J.O. Archambeau, Mammalian Radiation Lethality (Academic Press, New York, 1965).

5.34 Casarett, A.P., Radiation Biology (Prentice-Hall, Englewood Cliffs, New Jersey, 1968).

5.35 U.S. Nuclear Regulatory Commission, "Reactor Safety Study," WASH-1400 (NUREG 75/014), October 1975.

5.36 Berdjis, C.C., Pathology of Irradiation (Williams and Wilkins, Baltimore, 1971).

5.37 Thomas, E.D., et al., "Bone-Marrow Transplantation," Parts 1 and 2, New England Journal of Medicine, 292, 832 and 895 (1975).

5.38 Wilson, J. and J.A. Carruthers, "Measurement of Bone-Marrow Dose in a Human Phantom for Co^{60} γ-Rays and Low-Energy X-Rays," Health Phys. 7, 171 (1962).

5.39 Ellis, F. "Relationship of Biological Effects to Dose-Time-Fractionation Factors in Radiotherapy" in Current Topics in Radiation Research, Volume 4, M. Ebert and A. Howard, editors (North-Holland, Amsterdam, 1968), p. 357.

5.40 National Academy of Sciences/National Research Council, "The Effects on Populations of Exposure to Low Levels of Ionizing Radiation (BEIR)," NAS/NRC, November 1972.

5.41 Kato, H., "Mortality in Children Exposed to the A-Bombs While in Utero, 1945-1969," Am. J. Epidemiology 93, 435 (1971).

5.42 Miller, R.W. and W.J. Blot, "Small Head Size Following in Utero Exposure to Atomic Radiation," Lancet 2, 784 (1972).

5.43 Bacq, Z.M. and P. Alexander, Fundamentals of Radiobiology, Second Edition (Pergmon Press, Oxford, 1961).

5.44 Kohn, H.I. and R.F. Kallman, "The Influence of Strains on Acute X-ray Lethality in the Mouse, I. LD_{50} and Death Rate Studies," Radiation Res. 15, 309 (1956).

5.45 Gus'Kova, A.K. and G.D. Baysogolov, "Radiation Sickness in Man," Translation AEC-tr-7401, 1971.

5.46 Yuhas, J.M., et al., "Some Pharamacologic Effects of WR-2721: Their Role in Toxicity and Radio Protection," Radiation Res. 54, 222 (1973).

5.47 Oughterson, A.W. and S. Warren, editors , Medical Effects of the Atomic Bomb in Japan (McGraw-Hill, New York, 1956).

5.48 U.S. Army Combat Development Command, Institute of Nuclear Studies, "Personnel Risk and Casualty for Nuclear Weapons Effects," August 1971.

5.49 Warshawsk, A.S. and C.N. Davidson, "Addendum to Personnel Risk and Casualty Criteria for Nuclear Weapons Effects," U.S. Army Nuclear Agency Report, ACN 22744, March 1976.

5.50 NRC and Office of Civil Defense "Mass Burns" (NAS, Washington, 1969).

5.51 Schildt, E., Jr., Nuclear Explosion Casualties (Almqvist and Wiksell, Stockholm, 1967).

5.52 Brooks, J.W., et al., "A Comparison of Local and Systemic Effects Following Contact and Flash Burns," Ann. Surg. 144, 768 (1956).

5.53 Henriques, F.C., and R.A. Maxwell, "The Applicability of the Skin Damage Integral to the Prediction of Flash Burn Injury Threshold, Including Those Caused by Atomic Detonations," TOI 54-19, February 1, 1956.

5.54 Derksen, W.L. (Naval Surface Weapons Center), Private Communication, January 1975.

5.55 Derksen, W.L., et al., "Protection by a 'Hot-Wet' Uniform in Contact with Skin for Nuclear Weapon Pulses of Thermal Radiation," AFSWP-1071, April 1958.

5.56 de Lhery, G.P., "The Burns Under a 'Hot-Wet' Uniform Spaced from Skin for Nuclear Weapon Pulses of Thermal Radiation," DASA-1148, May 1959.

5.57 Brooks, J.W., et al., "Operation Buster - Thermal Effects on Animals (Dogs)," AISWP Project 4.2, June 1952.

5.58 Evans, E I., et al., "Flash Burns Studies on Human Volunteers," Surgery 34 (2), 291 (February 1955).

5.59 Berkley, K.M., et al, "The Effect of Spectral Distribution on the Production of Cutaneous Burns," Surg. Gyne. & Obstetrics 114, 163 (1962).

5.60 Glasstone, S., editor, The Effects of Nuclear Weapons, U.S. Atomic Energy Commission, April 1962.

5.61 Pearse, H.E. and H.D. Kingsley, "Thermal Burns from the Atomic Bomb," University of Rochester Report, UR-254 (Rev.), April 30, 1953.

5.62 The U.S. Strategic Bombing Survey Committee, "The Effects of Atomic Bombs on Hiroshima and Nagasaki," (USGPO, Washington, June 1946).

5.63 Davis, L.W., et al., "Analysis of Japanese Nuclear Casualty Data," Dikewood Corporation Report DC-FR-1054, AD-653922, April 1966.

5.64 Butterfield, W.J.G., "High Temperature," in Symposium on Burns, NAS/NRC (Washington, D.C., 1951).

5.65 Bull, J.P. and A.J. Fisher, "A Study of Mortality in a Burn Unit: A Revised Estimate," Ann. Surg. 139, 269 (1954).

5.66 Groce, D.E., "Thermal Incapacitation from Nuclear Weapons," Science Applications Report SAI-76-779-LJ, June 1976.

5.67 Mixter, G., Jr., "The Medical Burden from Skin Burns at Nagasaki: A Reappraisal," U.S. Naval Applied Science Laboratory Project 9400-12, Progress Report 11, DASA Subtask 03.062, October 1965.

5.68 Bitke, G, et al., "Studies on Burns," Acta Chirargica Scandinavia, Supplement 228, 1957.

5.69 NATO, Emergency War Surgery, (USGPO Washington, 1975), NATO Handbook Number 740600139.

5.70 Fricke, M.P., "Preliminary Civilian Casualty Criteria for Low-Yield Nuclear Weapons," Science Applications Report SAI-74-560-LJ, October 1974.

5.71 Butterfield, J.H., et al., "Flash Burns from Atomic Weapons," Surg. Gynecol. Obstet. 103, 655 (1956).

5.72 White, C.S., et al., "Comparative Nuclear Effects of Biomedical Interest," USAEC Report CEX-58.8, January 1961.

5.73 Blocker, T.G., Jr., "The Acute Burn as a Catastrophic Illness," Bulletin ACS 50, 141 (1965).

5.74 Schwartz, M.S., et al., "An Evaluation of the Mortality and the Relative Severity of Second and Third Degree Injuries in Burns," Brooke Army Medical Center Report MEDEW-RS-12-56, December 1956.

5.75 Lynch, J.C., "Predicted Mortality in Males," in Plastic Surgery, W.C. Grabb and J.C. Smith, editors (Little, Brown, Boston, (1968).

5.76 White, C.S., "Tentative Biological Criteria for Assessing Potential Hazards from Nuclear Explosions," Lovelace Report DASA-1462, December 1963.

5.77 White, C.S., "The Nature of the Problems Involved in Estimating the Immediate Casualties from Nuclear Explosions," USAEC Report CEX-71.1, July 1971.

5.78 Langerin, R.A., R. Greenstone and C.O. Elder, "The Distribution of Thermal Ineffectiveness," Technical Operations, Inc. Report TOI W56-2, May 1957.

5.79 Derksen, W.L. and J. Mongiola, "An Experiment on the Avoidance of Thermal Radiation Burns from Nuclear Weapons by Evasive Action," Lab. Project 940-12, Report 21, U.S. Naval Applied Science Laboratory, October 1969.

5.80 Derksen, W.L., et al., "Output Intensities and Thermal Radiation Skin Injury for Civil Defense Shelter Evaluation," Special Report for Blast and Thermal Subcommittee, National Academy of Sciences, 1967.

5.81 Wilson, L.G., and G. Drew, "Threshold Values for Thermal Radiation Burns on Human Subjects," Projects No. D49-74-70-18, Report 320, Defense Research Chemical Laboratories, Ottawa, May 1960.

5.82 Martin, S.B., "The Role of Fire in Nuclear Warfare," DNA 2692F/URS-784, August 1974.

5.83 Smith, E.H., and Company, "Nuclear Weapon Casualties - Effects on Personnel," AD 261739, May 1961.

5.84 Derksen, W.L., "The Variation of Skin Absorptance with Skin Color for Several Radiant Sources," Draft Report for DASA, U.S. Naval Applied Science Laboratory, July 1968.

5.85 Derksen, W.L., M. Mazarella, and J. Mongiola, "The Influence of the Inital Skin Temperature on Thermal Radiation Burns from Nuclear Weapons," Lab. Project 940-12, Report 22, U.S. Naval Applied Science Laboratory, May 21, 1969.

5.86 Bennett, J., "Significant Factors in Burn Mortality," J. Trauma 5, 599 (1965).

5.87 Rittenbury, M.S., et al., "Factors Significantly Affecting Mortality in the Burned Patient," J. Trauma 5, 587 (1965).

5.88 White, C.S., R.K. Jones, E.G. Damon, E.R Fletcher, and D.R. Richmond, "The Biodynamics of Airblast," DNA Report 2738T, 1971.

5.89 Chiffelle, T.L., R.K. Jones, D.R. Richmond, E.G Damon, "The Biologic and Patholcgic Effects of Blast Injury," Accident Pathology - Proceedings of an International Conference, K.M. Brinkhous, Editor, University of North Carolina, p. 90-105, 1968.

5.90 Desaga, H., "Blast Injuries," in German Aviation Medicine - World War II, Vol. II, Scholium International Inc., Pelham Manor, N.Y., Reprinted 1971.

5.91 Zuckerman, S., "The Biological Effects of Explosion," in History of the Second World War - Medical Research, F.H.J. Green, Editor, Ministry of Home Security, London, p. 339-359, 1953.

5.92 Richmond, D.R., E.G. Damon, E.R. Fletcher, I.G. Bowen, and C.S. White, "The Relationship betweet Selected Blast Wave Parameters and the Response of Mammals Exposed to Air Blast," Anuls N.Y. Acad Sci. 152, 103-121 (1968).

5.93 Bowen, I.G., E.R. Fletcher, and D.R. Richmond, "Estimate of Man's Tolerance to Direct Effects of Air Blast," DASA Report 2113, 1968.

5.94 White, C.S., Comments on Report SRI 72-453 Draft Material for Revision of Chapter XII Entitled "Biological Effects" in the Effects of Nuclear Weapons, Lovelace Foundation, Albuquerque, N.M., 87108, 1973.

5.95 White, C.S., "The Scope of Blast and Shock Biology and Problem Areas in Relating Physical and Biological Parameters," DASA Report 1856, 1966.

5.96 Zalewski, T., "Experimentelle Untersuchgen Veber Die Resistheitshigheit Des Trommelfells, Ohren 52:109-128 (1906 Aeitscr).

5.97 Textbook of Air Armament, Part 2, Chapter 12, "Vulnerability of Human Targets to Fragmenting and Blast Weapons," Ministry of Defense, London, 1952.

5.98 Blocker, T.G., Jr., V. Blocker, J.E. Graham, H. Jacobson, "Follow-up Medical Survey of the Texas City Disaster," Am J. Surg. 97, 604-623 (1959).

5.99 White, C.S., I.G. Bowen, and D.R. Richmond, "Comparative Analysis of Some of the Immediate Environmental Effects at Hiroshima and Nagasaki," Health Physics 10, 89-150 (1964).

5.100 Hirsch, F.G., "Effects of Overpressure on the Ear - A Review" DASA Report 1858, 1966.

5.101 White, C.S., I.G. Bowen and D.R. Richmond, "Biological Tolerance to Air Blast and Related Biomedical Criteria," USAEC Report CEX-65.4, 1965.

5.102 Zuckerman, S., B.D. Burns, P.M. Black, "The Wounding Power of Debris," Report R.C. 423, Ministry of Home Security, Oxford, England, 1944.

5.103 "Personnel Risk and Casualty Criteria for Nuclear Weapons Effects," Institute for Nuclear Studies Report AD516440, 1971.

5.104 Zuckerman, S., A.N. Black, "The Effect of Impact on the Head and Back of Monkeys," Report R.C. 124, Ministry of Home Security, Oxford, England, 1940.

5.105 Lissner, H.L. and F.G. Evana, "Engineering Aspects of Fractures," Clin-Orthop. 8, 310-322 (1958).

5.106 Gurdjian, E.S., J.E. Webster, and H.L. Lissner, "Studies on Skull Fracture with Particular Reference to Engineering Factors," Am. Jour. Surg. 78, 736-742 (1949).

5.107 Bowen, I.G., E.R. Fletcher, D.R. Richmond, F.G. Hirsch, and C.S. White, "Biophysical Mechanisms and Scaling Procedures Applicable in Assessing Responses of the Thorax Energized by Air-Blast Overpressures or by Nonpenetrating Missiles," DASA Report 1857, 1966.

5.108 Clemedson, C.J., G. Kellström, S. Lindgren, "The Relative Tolerance of the Head, Thorax and Abdomen to Blunt Trauma," Annls. N.Y. Acad. Sci. 152, 18-198 (1968).

5.109 Nahum, A.M. "Early Management of Acute Trauma," C.V. Mosby Company, 1966.

5.110 Sperrazza, J. and W. Kokinakis, "Ballistic Limits of Tissue and Clothing," Annls. N.Y. Acad Sci. 152, 163-167 (1968).

5.111 Bell, R.C., "An Analysis of 259 of the Recent Flying Bomb Casualties," Brit. Med. J. 2, 689-692 (1944).

5.112 Tsuzuki, M., "Report of the Medical Studies on the Effects of the Atomic Bomb," Medical Report on Atomic Bomb Effects. The Medical Section, the Special Committee for the Investigation of the Effects of the Atomic Bomb, the National Research Council of Japan, 1953.

5.113 Goldzen, V.C., D.R. Richmond, T.L. Chiffelle, I.G. Bowen, and C.S. White, "Missile Studies with A Biological Target," Operation Plumbob Report WT-1470, 1961.

5.114 Bowen, I.G., D.R. Richmond, M.B. Wetherbe, and C.S. White, "Biological Effects of Blast from Bombs, Glass Fragments as Penetrating Missiles and some of the Biological Implications of Glass Fragmented by Atomic Explosions," AECU-3350, Oak Ridge, Tenn., 1956.

5.115 Fletcher, E.R., D.R. Richmond, and R.K. Jones, "Velocities, Missiles, and Spatial Distribution of Glass Fragments from Windows Broken by Airblast," Lovelace Foundation - unpublished, 1972.

5.116 White, C.S., "Biological Effects of Blast," DASA Report 1271, 1961.

5.117 Fletcher, E.R. and D.R. Richmond, "Characteristics and Biological Effects of Fragments from Glass and Acrylic Windows Broken by Airblast," Research Report 22, Technical Summary, DCPA All-Effects Research Contractors Meeting, Pacific Grove, CA, 1974.

5.118 Fletcher, E.R., private communications, 1976.

5.119 Taborelli, R.V., I.G. Bowen, and E.R. Fletcher, "Tertiary Effects of Blast-Displacement," USAEC Report WT-1496, 1959.

5.120 Bowen, I.G., R.W. Albright, E.R. Fletcher, and C.S. White, "A Model Designed to Predict the Motion of Objects Translated by Classical Blast Waves," USAEC Report CEX-58.9, 1961.

5.121 Richmond, D.R., I.G. Bowen and C.S. White, "Tertiary Blast Effects: Effects of Impact on Mice, Rats, Guinea Pigs and Rabbits," DASA Report 1245, 1961.

5.122 Fletcher, E.R., J.T. Yelverton, R.A. Hutton, and D.R. Richmond, "Probability of Injury from Airblast Displacement as a Function of Yield and Range," DNA Report 3779T, 1975.

5.123 Jones, R.K., D.R. Richmond, and E.R. Fletcher, "A Reappraisal of Man's Tolerance to Indirect (tertiary) Blast Injury," Minutes of the Eleventh Meeting of Panel N-2, (Blast, Shock, and Thermal), Subgroup N, the Technical Cooperative Programme, Part II, Ministry Defense, London, pp. 41-56, 1969.

5.124 Lewis, W.S., A.B. Lee and S.A. Grantham, "Jumpers Syndrome," The Journal of Trauma 5 (#6),(1965)

5.125 Hirsch, A.E., "The Tolerance of Man to Impact," Annls. N.Y. Acad. Sci.,168-171 (1968).

5.126 AFRRI SP66-23,"The Acute Mortality Response of Monkeys (MACACA MULATTA) to mixed Gamma-Neutron Radiations and 250 KVP X-Rays", December 1966.

5.127 AFRRI SR68-17, "The Acute Mortality Response of Monkeys (MACACA MULATTA) to Pulsed Mixed Gamma-Neutron Radiations", July 1968.

5.128 AFRRI SR69-10, "The Acute Mortality Response of the Miniature Pig to Pulsed Mixed Gamma-Neutron Radiations", July 1969.

5.129 Straker, E.A. et al., "The MORSE Code With Combinatorial Geometry," DNA2860T, May 1972.

5.130 AFRRI CR66-2, "Fast Neutron Spectrum of the AFRRI TRIGA Reactor," January 1966.

5.131 Chapman, G.T., and Burus, W.R., "Spectrum of Gamma Rays Emitted by a Stainless Steel Clad, Pool Type Reactor" (BSR-II), Nuclear Science and Engineering, 34, 169-180, (1968).

5.132 Verrelli, D.M., Private Communication, 11 June 1976.

5.133 National Bureau of Standards Handbook 85 (ICRU Report 106).

5.134 Measurements made at AFRRI, 23 June 1976.

5.135 Snyder, W.S., et al., "A Tabulation of Dose Equivalent Per Microcurie-Day of Source and Targe Organs of an Adult for Various Radioactive Nuclides," ORNL-5000, November 1972.

5.136 Inter-Commission on Rad. Protection, Report of the Task Grour on Reference Man, ICRP 23 (Pergamon Press, 1975).

5.137 Straker, E.A., "Time-Dependent Neutron and Secondary Gamma-Ray Transport in an Air-Over-Ground Geometry," ORNL-4289, September 1968.

5.138 Baum, S., "The Postirradiation Hematopoietic Syndrome," AFRRI Draft Report, May 1976.

5.139 Messerschmidt, O., "Combined Injury Caused by Nuclear Explosions," Tech. Univ. of Munich and Lab. for Expl. Radiology, Neuherberg; trans. for Lovelace Biomedical and Environmental Research Institute, May 1976.

5.140 Miscellaneous data (yet unpublished) from the Lovelace Foundation, D.R. Richmond and E.R. Fletcher, private communication, May 1976.

5.141 Jones, R.K., "The Biomedical Effects of Combined Injuries," Problems des Baulichen Schutzes (Proceedings: Kolloquim des Fauchausschusses I der Innern, June 15-16, 1971, Weil/ Rhein, pp. 37-90, Ernst-Mach-Instituts, Aussenstelle, Weil, Germany, 1971)

5.142 Schildt, B. and Thoren, L., eds., "Proc. of the Symp. on Combined Injuries and Shock," June 3-7, 1967, Uppsale; Research Institute of National Defense, Stockhold, 1968.

5.143 "Tripartite Technical Cooperation Program, Sub-Group N, Panel NI (Biomedical)" May 10-14, 1965, USNRDL, 1965.

5.144 Kinnamon, K.E., and Sutter, J.L., "Radiation and Wound Healing: A study of the Role of Sulfur Amino Acides," Rad. Res. 25, 566 (1965).

5.145 Moncrief, W.H., Jr., "Experimental and Theoretical Aspects of Severe Trauma," Jour. Bone and Joint Surgery 44-A, 747 (1962).

5.146 McKenna, J.M., and Zweifach, B.W., "Comparative Study of the Physiological Effects of X-Irradiation and Resistance to Traumatic Shock," Rad. Res. 6, 126 (1957).

5.147 Reid, J.D., et al., "The Influence of X-Radiation on Mortality Following Thermal Flash Burns: The Site of Tissue Injury as a Factor Determining the Type of Invading Bacteria," Ann. of Surgery 142, 844 (1955).

5.148 Davis, W.M., et al., "The Combined Effects of Thermal Burn and Whole-Body X-Irradiation: III. Study of Blood Coagulation," Ann. of Surgery 142, 66 (1955).

5.149 Alpen, E.L., et al., "Combined Effects of Total Body X-Irradiation and Radiant Energy Thermal Burns. III, Osmotic and Mechanical Fragility of the Erythrocyte," USNRDL-419, 1954.

5.150 Davis, A.K., et al., "The Combined Effects of Thermal Burns and Whole-Body X-Irradiation. II. Anemia," Ann. of Surgery 140, 726 (1954).

5.151 Alpen, E.L. and Scheline, G.E., "The Combined Effects of Thermal Burns and Whole Body X-Irradiation on Survival Time and Mortality," Ann. of Surgery 140, 113 (1954).

5.152 Baxter, H., et al., "Blood Histamine Levels in Swine Following Total Body X-Radiation and a Flash Burn, "Ann. of Surgery 139, 179 (1954).

5.153 Baxter, H.L., et al., "Reduction of Mortality in Swine from Combined Total Body Radiation and Thermal Burns by Streptomycin," Ann. of Surgery 137, 450 (1953).

5.154 Brooks, J.W., et al., "The Influence of External Body Radiation on Mortality from Thermal Burns," Ann. of Surgery 136, 533 (1952).

5.155 Mixter, G., et al., "The Sub-Fabric Flash Burn: Quantitative Effect on Protectivity of Fabric Reflectance Fabric Weight and Exposure Time: University of Rochester Report UR-368, 1955.

5.156 "Synopsis of the Ad Hoc Committee on Thermal Ineffectiveness", TM-23-200(1), 1954.

6. METHODOLOGY FOR GENERATING DAMAGE FUNCTIONS

This section describes the methodology that was developed to generate the damage functions and their confidence limits. This methodology has been incorporated in a Monte Carlo simulation code, WEREUA, (Weapon Responses Uncertainty Analysis) which was used to generate the casualty damage functions given in Section 7 of this report.

Basically, the WEREUA code accepts as input the weapon environments and their uncertainty parameters, shelter protection factors and their uncertainty parameters and personnel response criteria and their uncertainties The code then utilizes a Monte Carlo simulation to estimate the damage function as well as to perform an error propagation analysis.

6.1 OVERVIEW OF THE METHODOLOGY

WEREUA has been used to estimate the overall uncertainties in weapon environments and the responses to such environments. This was done by taking a base environment and applying correction factors. If only two independent factors existed, the environment E was

$$E = F_1 \cdot F_2 \cdot E_{BASE}$$

The correction factor approach was used for all nuclear radiation and airblast environments. This approach was adopted to minimize the time required to regenerate the various environments for each Monte Carlo sample. However, for the thermal radiation environment, a small SAI code THERMX (Ref. 6.1) was used to obtain an estimate of the thermal radiation environment for each sample.

The calculational flow of WEREUA is shown in Figure 6.1. Uncertainties and other parameters were input into the code, from which the correction factors are calculated for the nuclear radiation or airblast environments. If a thermal radiation environment was required, a set of parameters for THERMX were input. The base environment was interpolated from tables or calculated (thermal) and the correction factors were applied. The modified environment value was then stored as a sample value. After the required number of samples had been collected, the statistics were calculated and the results were output to both disk and printer. This output included the environment probability density function as a function of range and parameters which characterized it (e.g., mean value, standard deviation and confidence levels). The above procedure was carried out for selected ranges for each environment.

After all of the environment distributions had been determined and stored on disk, the weapon response calculations were made. The environments were read, in INPUT2, along with the parameters for finding the shelter protection and response for each environment. For every range and all environments, the protection factors for the shelter were calculated. Each environment was modified by these factors to determine the environment inside the shelter. The response to the modified environment was then determined. When this had been completed, a combined response due to all environments was found. As above, this value was stored as a sample and statistics were collected, with the final result was a response distribution for each range. Mean values and confidence levels versus range were found from these distributions.

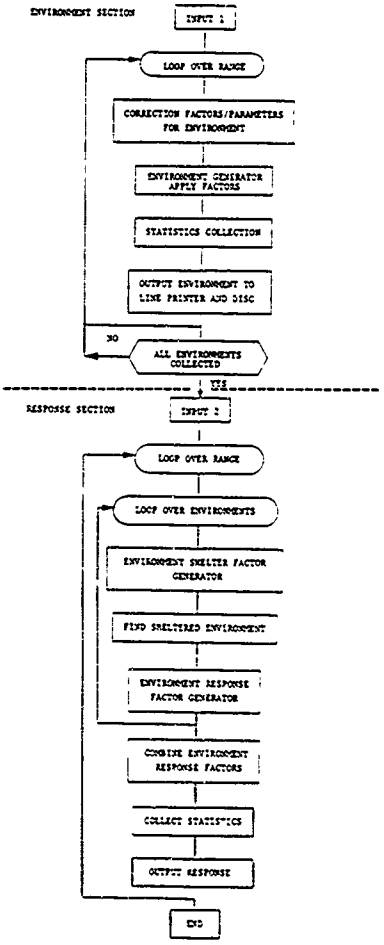

Figure 6.1. WEREUA flow diagram.

6.2 DESCRIPTION OF WEAPON ENVIRONMENT MODULES

In this section the blocks shown in the Environment section in Figure 6.1 will be described in greater detail, along with examples of results.

6.2.1 INPUT 1

INPUT 1 is the input section for the weapon environment calculation. Along with housekeeping parameters and range step information, it reads the uncertainties to be used in determining the correction factors. Table 6.1 lists these uncertainties, many of which may not be required for any given problem.

The uncertainties are specified by the following parameters:

Uncertainty identification	HUM for humidity, etc.
Type of distribution	Constant, one-dimensional, range dependent, joint two-dimensional, etc.
Name of distribution	Constant, Gaussian, Johnson SB, etc.
Four parameters which define the distribution. Generally different for different distributions.	For a Gaussian, these would be mean, standard deviation, minimum and maximum.

Table 6.2 gives examples of some of the values used for the uncertainties. Once read in, the uncertainties are stored and modified for use in the subsequent calculations.

6.2.2 Correction Factors/Parameters

For each uncertainty considered, the program picks a value randomly from its distribution. This value is used directly as a correction factor or a parameter value, as in the case of the neutron yield, or is used to calculate the correction factor, as in the case of temperature for the humidity correction. All factors are used as multipliers of the environment.

Table 6.1. Uncertainties for weapon environment calculations.

Neutron transmission through air
Secondary γ transmission through air
Primary γ transmission through air
Fission γ transmission through air

Neutron spectra correction
Secondary γ spectra correction
Primary γ spectra correction
Fission γ spectra correction

Neutron asymmetry correction
Secondary γ asymmetry correction
Primary γ asymmetry correction
Fission γ asymmetry correction

Neutron air ground correction
Secondary γ air ground correction
Primary γ air ground correction
Fission γ air ground correction

Terrain correction
Humidity correction (for transmission)
Range correction (for pressure)
Weapon yield (Kt)

Neutron yield (number/Kt)
Primary γ yield (number/Kt)
Fission γ yield (number/Kt)
Thermal partition

Height of burst
Elevation
Temperature
Pressure

Humidity (for density calculations and ρ-r scaling)
Meteorlogical range
Height of cloud cover
Percentage of cloud cover
Percentage of days of cloud cover
Ground albedo
Thermal partition
Miscellaneous special parameters

Table 6.2. Example weapon environment uncertainty parameters.

Parameter	Mean Value	Standard Deviation	Distribution Type	Truncation Values Low	High
Energy Yield	1.0 KT	0.075 KT	Normal	0.0	1.5
Thermal Partition	0.33	0.033	Normal	0.0	0.7
Air Pressure	1015 MB	10 MB	Normal	900	1115
Relative Humidity	79%	10%	Normal	0	100
% Cloudy Days	53%	15%	Normal	0	100
Elevation	76 M	8 M	Normal	0	140
Ground Albedo	----	----	Uniform	0	1.0
Height of Burst	61 M	12 M	Normal	0	150
Temperature	8.3°C	11.0°C	Johnson SB	-25	37
Meteorological Range	10.5 KM	5 KM	Joint-Tabular	0	10
Cloud Ceiling	2.1 KM	1.3 KM			
Range Uncertainty Factor	1.0	0.125	Normal	0.0	2.0

The selection of the random quantities followed the methods given by McGrath, et al. (Ref. 6.2) for probability distribution functions. If an uncertainty was range-dependent and did not exist at a desired range, a new distribution was constructed from the existing ones by interpolation. This was done once at the start of each new range. The program can also pick from joint distributions as was done for cloud ceiling versus visibility.

Importance sampling is also available. This permits picking of values from a biased distribution in order to enhance the statistics in a desired region, such as the tails of the calculated distributions. This was accomplished by entering both the biased and unbiased distributions and calculating a weight such that

$$W_{UB}P_{UB} = W_BP_B$$

where

W_{UB} = unbiased weight - set to 1

P_{UB} = probability of choosing from unbiased distribution

W_B = biased weight

P_B = probability of choosing from biased distribution

These weights were carried along during the calculation and multiplied together to form the final weighting factor. It was implicite in this multiplication that the probabilities were independent. In fact, after the value was picked for each uncertainty, the program considered them independent.

6.2.3 Neutron Radiation Correction Factors

The uncertainties used in determining the neutron dose correction factors, which were used directly as factors, were:

Weapon energy output
Weapon neutron yield
Neutron transport
Neutron spectra
Neutron asymmetry
Air ground correction

Uncertainties which were used to calculate factors were:

Temperature
Pressure
Atmospheric relative humidity
Ground elevation
Hydrogen content of soil
Height of burst

The atmospheric uncertainties were used to find changes in the neutron transport due to atmospheric density changes and water vapor content.

The base neutron dose was calculated for sea level and standard atmospheric conditions. To account for the dose variations due to the atmospheric density difference between standard conditions and those selected by the program, ρ-r scaling was used. For a time-dependent flux, the ρ-r scaling was formulated as

$$\phi_2(r_2) = K^2\phi_1(r_1)$$

$$\rho_2 = K\rho_1$$

$$r_2 = r_1/K$$

where

ϕ_1 = base flux

ρ_1 = standard sea level atmospheric density

ρ_2 = atmospheric density (see Section 6.2.9)

r_1 = slant range at sea level

r_2 = current slant range

ϕ_2 = flux scaled for the density change.

ρ_1 and r_2 were known, ρ_2 was calculated and K was found. r_1 was then calculated, and the base dose found from the dose tables (it was assumed that dose and flux scale the same way). This dose was then multiplied by K^2 to give the scaled dose.

The dose correction factor for atmospheric humidity was obtained by first estimating the water vapor density. This was based on the relative humidity and temperature (see Section 6.2.9). The data given in Table 6.3 was used to obtain the dose correction factor. A linear interpolation was performed using the calculated water density to find the dry (ATR) dose ratio to the current required value. The corrected dose was

$$D_{correct} = D_{dry}/ratio$$

The hydrogen content of the soil was used to find a correction factor. Figure 6.2 shows the distribution of hydrogen content of European soils. This distribution was then folded with a curve similar to Figure 6.3, taking a hydrogen content of 9×10^{-3} gm/cm^3 as base case (this value was used in ATR to generate the base environment). Figure 6.4 shows a representative distribution of the correction factor used for conditions listed in the figure.

6.2.4 Secondary Gamma Correction Factors

The same uncertainties as given in Section 6.2.3 were used except for the neutron specific ones. Those were replaced by:

Secondary gamma transport
Secondary gamma spectra
Secondary gamma asymmetry

6.2.5 Primary Gamma Correction Factors

The same uncertainties as given in Section 6.2.3 were used except for the neutron specific ones. Those were replaced by:

Table 6.3. Ratio of dose calculated for dry air to dose calculated for wet air.

Ground Range (m)	Neutron	Prompt Gamma Ray	Secondary Gamma Ray
	Ratio $\frac{\text{(Humid Air Dose } 2 \times 10^{-6} \text{ gm/cc Water Vapor)}}{\text{(Dry Air Dose } 0 \text{ gm/cc Water Vapor)}}$		
100	0.98	0.99	1.23
250	0.82	0.98	1.09
500	0.67	0.96	0.97
750	0.58	0.94	0.91
1000	0.52	0.93	0.87
1500	0.44	0.9	0.84
2000	0.4	0.88	0.82
2500	0.38	0.86	0.815
3000	0.35	0.84	0.81
	Ratio $\frac{\text{(Humid Air Dose } 5 \times 10^{-5} \text{ gm/cc Water Vapor)}}{\text{(Dry Air Dose } 0 \text{ gm/cc)}}$		
100	0.85	0.99	1.46
250	0.63	0.95	1.27
500	0.42	0.9	0.94
750	0.31	0.85	0.82
1000	0.25	0.82	0.76
1500	0.17	0.76	0.7
2000	0.14	0.73	0.67
2500	0.11	0.71	0.66
3000	0.1	0.7	0.66

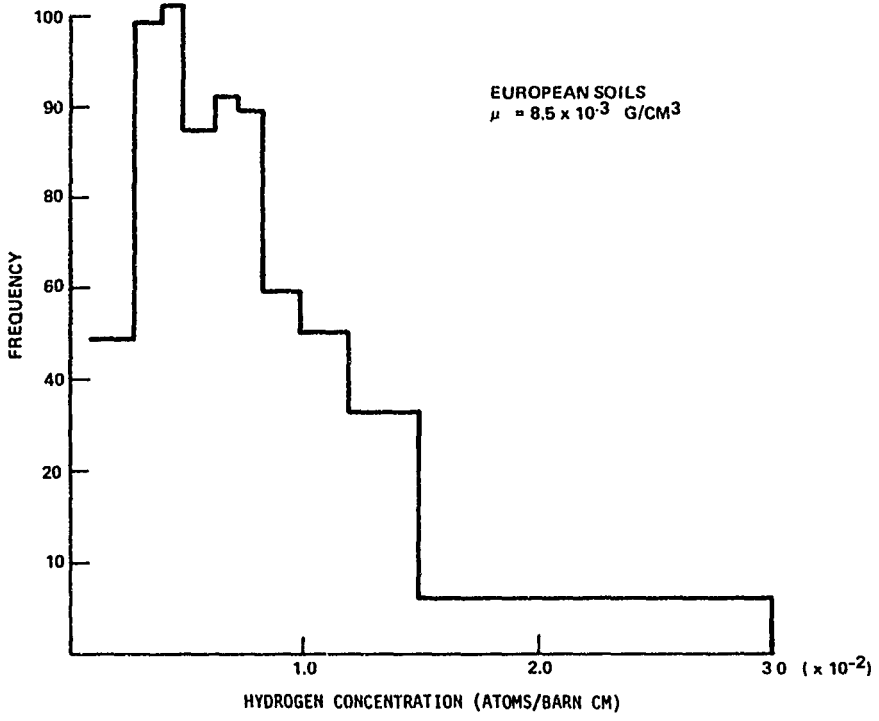

Figure 6.2. Frequency distribution of hydrogen content of soils.

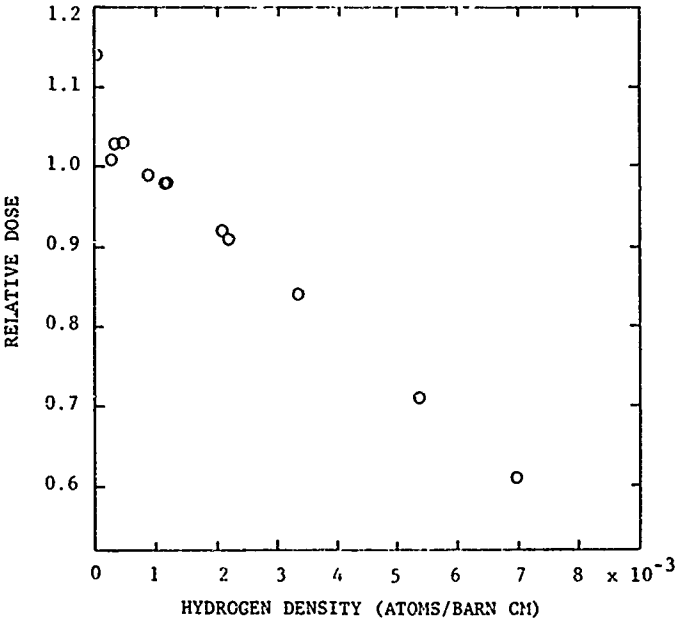

Figure 6.3. Sensitivity of tissue dose to hydrogen content of soil.

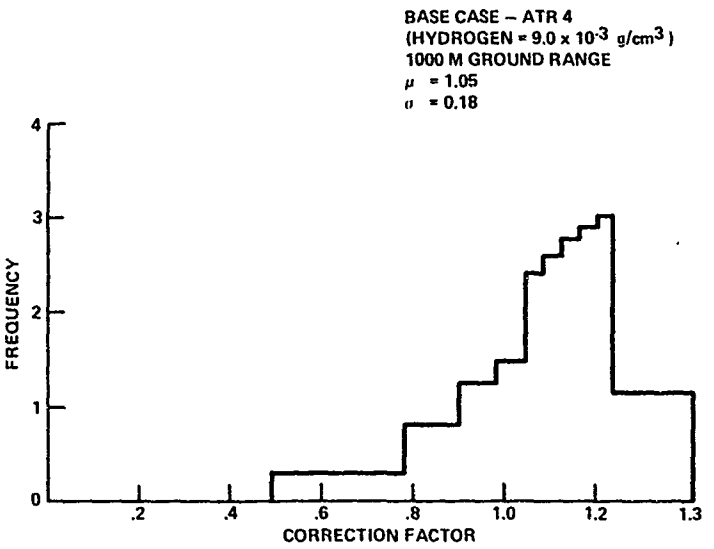

Figure 6.4. Dose correction factors for water in soils.

Primary gamma transport
Primary gamma spectra
Primary gamma asymmetry
Weapon primary gamma yield

6.2.6 Fission Gamma Correction Factors

The same uncertainties as given in Section 6.2.3 were used except for the neutron specific ones. Those were replaced by:

Fission gamma transport
Fission gamma spectra
Fission gamma asymmetry
Fission fraction for primary gamma yield

6.2.7 Overpressure Correction Factors

The basic overpressure environment was generated for sea level and standard atmospheric conditions. The uncertainties associated with this environment were:

Weapon yield
Height of burst
Range error to an overpressure level
Atmospheric pressure
Terrain

6.2.8 Thermal Radiation Parameters

There were no correction factors for the thermal environment. The uncertainties were used as input parameters for the thermal radiation generation module for calculating the environment for each sample. The uncertainties used were:

Weapon yield	Cloud ceiling
Weapon thermal partition	Cloud height
Height of burst	Cloud optical thickness
Temperature	Percent cloud cover
Pressure	Percent cloudy days
Relative humidity	Ground albedo
Meteorological range	Ground elevation

6.2.9 Calculation of Atmospheric Properties

The atmospheric density was calculated for a given temperature T(^{o}K), pressure and relative humidity by using the equation of state,

$$\rho = \frac{Pmd}{RT^*}$$

where

md = dry air mass 28.9644 gm/mole

R = ideal gas constant 8.3143×10^{7}

T* = virtual temperature

P = atmospheric pressure

T* is defined by

$$T^* = \frac{T}{1-3/5q} = \frac{T}{1-3/8\ \frac{e}{p}}$$

where

q = specific humidity

e = water vapor pressure

The relative humidity is approximately

$$RH \approx \frac{q}{qs} \times 100$$

where

qs = the saturated specific humidity and is given by

$$qs = \frac{.622\ e_s}{p - .378\ e_s}$$

where

e_s = the saturated vapor pressure.

e_s is approximated by

$$\ln e_s = 1.80957 + 0.079447t - 4.2899610^{-4}t^2$$

where t is the temperature in ^{o}C. This fit is good to within 10 percent over the range $-50^{o}C$ to $49^{o}C$ to the data given in the "Handbook of Chemistry and Physics."

To determine the water vapor content, the equation of state for water vapor was used,

$$\rho_w = \frac{em}{RT} w$$

where

m_w = 18.01 gm/mole, and

ρ_w = the water vapor density.

The relative humidity was defined as

$$RH = \frac{\rho_w}{\rho_{ws}} \cdot 100$$

where

ρ_{ws} is the saturated absolute humidity given by

$$\rho_{ws} = \frac{e_s m_w}{RT}$$

and e_s is given above. The water density was then

$$\rho_w = \frac{RH \cdot P_{ws}}{100} .$$

6.3 BASIC WEAPON ENVIRONMENTS

WERUA requires the use of the basic weapon environments (nuclear radiation, airblast and thermal radiation). Because of the time involved in generating the nuclear radiation and overpressures for each sample, a set of basic environments were generated. The correction factors described above were used to approximate the effects that the uncertainties would have on these environments. This section describes how the basic environments were obtained.

6.3.1 Nuclear Radiation Environment

ATR (Ref. 6.3) (Air Transport of Radiation) was used to generate the nuclear radiation environments for given yields, source spectra, HOB's and ranges for sea level and standard atmospheric conditions:

$T = 288.15^{o}K$

$P = 1013.25$ Mb

$\rho = 0.001225$ gm/cm^3

If the weapon is boosted or is a thermonuclear device, then a second step which combines the ATR outputs with the correct normalizing factors for each spectral component (fission, fusion) is carried out.

A set of data containing the dose as a function of range for several heights of burst, and yields, constitutes the basic radiation environment. These data were stored on disk and was the input to WEREUA whenever the nuclear radiation was required.

6.3.2 Airblast Environment

The basic airblast environment was a tabulated representation of Brode's (Ref. 6.4) peak overpressure for overpressure >70 psi, and EM-1 (Ref. 6.5) data for <70 psi. The tables were arranged by HOB and are scaled by $(\text{yield})^{1/3}$. The overpressure was found by interpolating the tables on HOB

and range, given the weapon yield, HOB and range. Overpressure was assumed to be independent of weapon type.

6.3.3 Thermal Radiation Environment

THERMX, a code which calculates the thermal radiation for low altitude nuclear bursts, was used to generate thermal environments for each sample. The required parameters for THERMX were those listed in Section 6.2.8.

6.3.4 Application of Correction Factors

After the correction factors had been determined, they were applied to the appropriate environment as given by the following equation.

$$E_c = \left(\prod_{i=1}^{N} CF_i\right) E_B$$

where

E_c = corrected environment

E_B = basic environment

CF_i = correction factor

N = number of correction factors

If a truncated distribution, or importance sampling was requested, a weight was also assigned to each sample environment. Weights were calculated by the formula:

$$W_c = \prod_{i=1}^{n} (W_i)$$

where

W_c = weight corresponding to environment E_c,

W_i = individual uncertainty weights, and

n = number of uncertainties used.

6.4 STATISTICS ANALYSIS

Each sample of an environment was stored along with its weight. When all samples had been collected, they were ordered by value in a monotonically increasing sequence. The mean value, standard deviation and confidence levels were determined. Distribution functions in 5 percent and 10 percent probability bins were generated. Figure 6.5 shows a 10 percent probability bin neutron dose distribution along with the error bars that indicate the statistical significance of the sampling. This sampling error was assumed to have binomial distribution with a value

$$\text{Error}_B = \left[N_B \left(1 - \frac{N_B}{N} \right) \right]^{1/2}$$

where

N = total number of samples, and

N_B = number of samples in bin B.

6.5 WEAPON ENVIRONMENT OUTPUT

The output from the weapon environment section consisted of distributions at predetermined range values. These distributions were represented as histograms along with the error associated with each bin due to the sampling procedure. There was a set of distributions for each of the six weapon environments.

Table 6.4 shows a distribution for the peak overpressure environment at 1000 meters, as generated with the uncertainties in Table 6.2. The environment distributions were stored on disk by weapon type, yield, HOB and range for use in the response section of the calculation.

The printed output consisted of listing the mean values, standard deviation, confidence limits and the distributions for each environment and range. An example is given in Figure 6.6 for the case shown in Table 6.4.

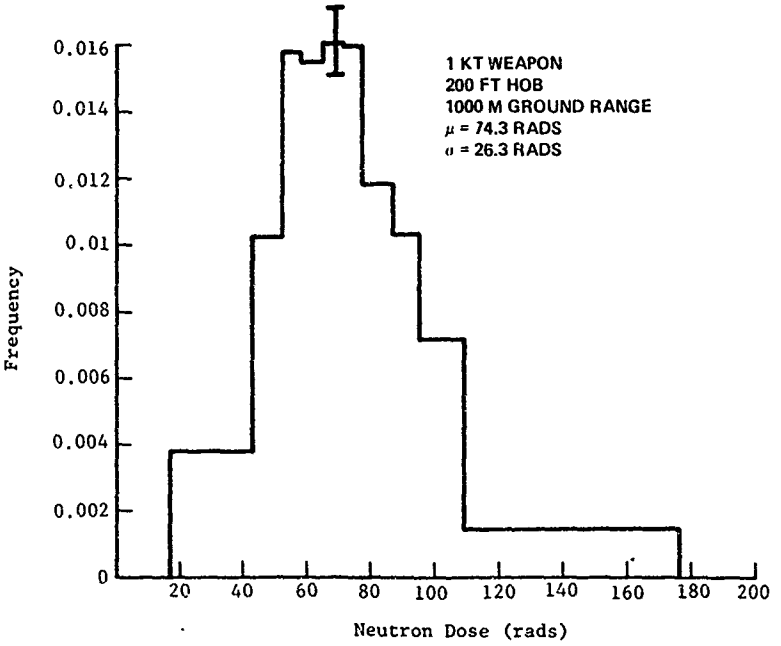

Figure 6.5. Frequency distribution of neutron dose.

Table 6.4. Output for a 1-KT weapon overpressure environment at a range of 500 meters.

DISTRIBUTION FOR A RANGE OF 5.0000E+02
NUMBER OF TRIAL 2000

DISTRIBUTION PARAMETERS. MEAN = 5.02626 STANDARD DEVIATION = 1.07148

DISTRIBUTION CONFIDENCE LIMITS

CONFIDENCE (PER CENT)	FUNCTION VALUE
0 5	3.25003
1.0	3.32079
2.5	3.51825
5.0	3 69884
10 0	3.91676
20.0	4.19524
25.0	4.29399
30.0	4.39662
40.0	4.57921
50.0	4.76054
60.0	4.91926
70.0	5.32717
75.0	5.67257
80.0	6.00463
90.0	6.55197
95.0	7.04174
97.5	7.47857
99 0	8.08619
99.5	8.87940

Table 6.4. Output for a 1-KT weapon overpressure environment at a range of 500 meters (continued).

THE FREQUENCY DISTRIBUTION IN 10 PER CENT INCREMENTS
(PER CENT ACCURACY FOR EACH INTERVAL = 11.0)

END VALUE	CUMULATIVE PROBABILITY	INTERVAL SPREAD		FREQUENCY VALUE
3.91676	0.10	2.87948	3.91676	0.964057E-01
4.19524	0.20	3.91676	4.19524	0.359093
4.39662	0.30	4.19524	4.39662	0.496581
4.57921	0.40	4.39662	4.57921	0.547679
4.76054	0.50	4.57921	4.76054	0.551480
4.91926	0.60	4.76054	4.91926	0.630056
5.32717	0.70	4.91926	5.32717	0.245148
6.00463	0.80	5.32717	6.00463	0.147611
6.55197	0.90	6.00463	6.55197	0.182701
11.5354	1.00	6.55197	11.5354	0.200666E-01

THE FREQUENCY DISTRIBUTION IN 5 PER CENT INCREMENTS
(PER CENT ACCURACY FOR EACH INTERVAL = 16.0)

END VALUE	CUMULATIVE PROBABILITY	INTERVAL SPREAD		FREQUENCY VALUE
3.69884	0.05	2.87948	3.69884	0.610230E-01
3.91676	0.10	3.69884	3.91676	0.229443
4.07234	0.15	3.91676	4.07234	0.321367
4.19524	0.20	4.07234	4.19524	0.406855
4.29399	0.25	4.19524	4.29399	0.506333
4.39662	0.30	4.29399	4.39662	0.487159
4.48220	0.35	4.39662	4.48220	0.584271
4.57921	0.40	4.48220	4.57921	0.515400
4.66386	0.45	4.57921	4.66386	0.590665
4.76054	0.50	4.66386	4.76054	0.517171
4.83521	0.55	4.76054	4.83521	0.669644
4.91926	0.60	4.83521	4.91926	0.594887
5.04225	0.65	4.91926	5.04225	0.406523
5.32717	0.70	5.04225	5.32717	0.175487
5.67257	0.75	5.32717	5.67257	0.144761
6.00463	0.80	5.67257	6.00463	0.150576
6.24662	0.85	6.00463	6.24662	0.206619
6.55197	0.90	6.24662	6.55197	0.163746
7.04174	0.95	6.55197	7.04174	0.102089
11.5354	1.00	7.04174	11.5354	0.111269E-01

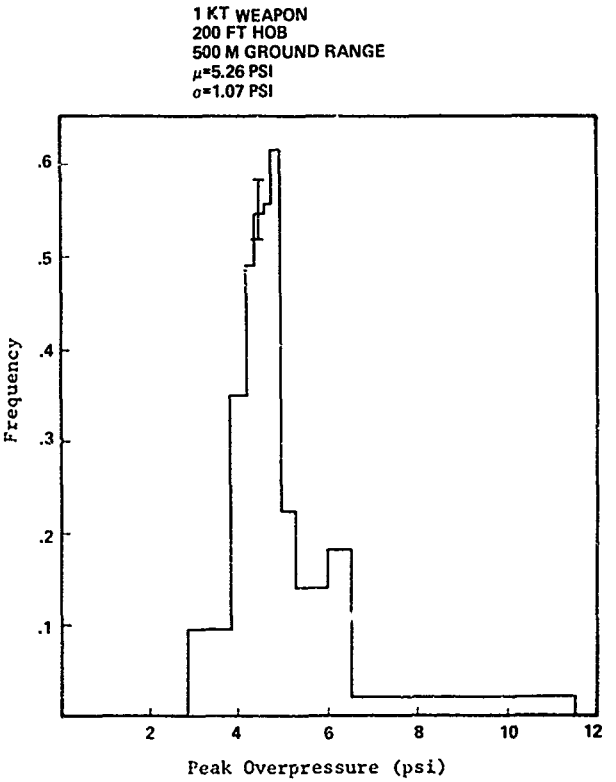

Figure 6.6. Frequency of peak overpressure.

6.6 DESCRIPTION OF RESPONSE SECTION MODULES

The response section used the environment distributions, modified them by the shelter factors, and with a given response function, determined the response. The response functions and shelter parameters were input.

6.6.1 INPUT 2

A set of weapon environment probability distributions, e.g., thermal radiation, was generated as described above. These were generated at a set of range points and were for a specific weapon type, yield, and height of burst. These distributions were read as input into INPUT 2 along with shelter protection data and personnel response data (and uncertainty data).

A new set of weapon environment probability distributions were generated at a different set of range points, which were selected to adequately define the shape of the damage function. The new environment distributions were based on the assumption that the environment was proportional to the logarithm of the slant range between the old environment range points.

6.6.2 Shelter Protection Factors

A provision was made to allow each of the weapon environments to be reduced according to the protection afforded by shelters. This was done by reducing the free-field weapon environment by a given protection factor (this was a user input). The code accepted the following protection factors:

- Neutron Dose
- Prompt Gamma-Ray Dose
- Air Secondary Gamma-Ray Dose
- Fission Product Gamma-Ray Dose
- Peak Overpressure
- Thermal Radiation

Uncertainties in the shelter protections factor were treated by specifying a fraction of the population that would have a given protection factor. An example for nuclear radiation protection factors are shown in Table 6.5.

6.6.3 Personnel Response

Personnel response was treated in a manner similar to that for shelter protection. As with the shelter module this was user defined. An example of some of the different uncertainties used for the nuclear environment are shown in Table 6.6. The response was calculated using a cumulative lognormal function which for $P \geq 0.5$ is

$$P\left(\frac{D}{D_{50}},\frac{\sigma}{m}\right) = \frac{1}{\sqrt{2\pi}} \int_{-1/\beta}^{\infty} \ln\left(\frac{D}{D_{50}}\right) e^{-t^2/2}\, dt$$

where P is the probability of damage. D_{50} is the LD or BD value, given in Table 6.6, $\frac{\sigma}{m}$ the variance to mean ratio (an input parameter and β given by

$$\beta = \left\{\ln\left[\left(\frac{\sigma}{m}\right)^2 + 1\right]\right\}^{1/2}$$

for $P < 0.5$

$$P\left(\frac{D}{D_{50}}, \frac{\sigma}{m}\right) = 1 - P\left(\frac{D_{50}}{D}, \frac{\sigma}{m}\right)$$

A response distribution was generated at each of the ranges for a specific environment-response combination. These distributions were then used to obtain the mean value, standard deviation and confidence limits of the response. All of the environment response combinations were then calculated. The range dependent mean values were taken to be the contribution to the damage functions for a specific environment-response combination. All of the

Table 6.5. Variation in nuclear radiation protection factors.

	ABOVEGROUND PORTIONS OF RESIDENCES		BASEMENTS	
PER CENT POPULATION	PROMPT NEUTRONS AND SECONDARY GAMMA RAYS	PROMPT AND FISSION PRODUCT GAMMA RAYS	PROMPT NEUTRONS AND SECONDARY GAMMA RAYS	PROMPT AND FISSION PRODUCT GAMMA RAYS
	(PROTECTION FACTORS)			
20	2	2	4	4
20	3	6	7	12
20	4	10	10	20
20	6	15	15	30
20	8	20	20	40

Table 6.6. Personnel response uncertainties.

	PARAMETER	UNCERTAINTY (2σ)	COMMENT
NUCLEAR RADIATION	LD_{10}	± 25% IN TOTAL DOSE	HEALTHY, YOUNG ADULT
	LD_{50}	± 10% IN TOTAL DOSE	HEALTHY, YOUNG ADULT
	BD_{10}	± 50% IN TOTAL DOSE	HEALTHY, YOUNG ADULT
	BD_{50}	± 25% IN TOTAL DOSE	HEALTHY, YOUNG ADULT
	AGE DEPENDENCE	+ 0% - 25% IN TOTAL DOSE	VERY YOUNG AND ELDERLY MORE VULNERABLE
	PROPER DOSE INDEX	± 25% IN TOTAL DOSE	ANALYSIS BEING MADE
	RBE OF NEUTRONS (60 DAY MORTALITY)	+ 0% - 50% NEUTRON DOSE	UNITY COMMONLY USED
	PARTIAL EXPOSURE	+ ?% - 0%	IMPACT NOT KNOWN

contributions were then calculated. An example is shown in Figure 6.7 of the various contributions to the overall damage function.

6.6.4 Combine Response

The individual contributions were combined to formulate the damage function (mean value as well as confidence limits). Figure 6.8 shows an example for the combined damage function for people in residences, given the separate responses as shown in Figure 6.7. The combining module for this example placed 90 percent of the population at risk to initial nuclear radiation and airblast effects, with the individual responses combined as

$$P_{90} = 1 - (1 - P_{\substack{\text{BLAST} \\ \text{DEBRIS}}})(1 - P_{\substack{\text{INITIAL} \\ \text{RADIATION}}})$$

The remaining 10 percent were at risk to initial nuclear radiation, thermal radiation and glass hazards. Individual responses were combined by

$$P_{10} = 1 - (1 - P_{\text{GLASS}})(1 - P_{\text{FLASH}})(1 - P_{\substack{\text{INITIAL} \\ \text{RADIATION}}})$$

A total response curve was formed by taking P_{90} and P_{10} and combining as

$$P_{TOT} = 0.9\ P_{90} + 0.1\ P_{10}$$

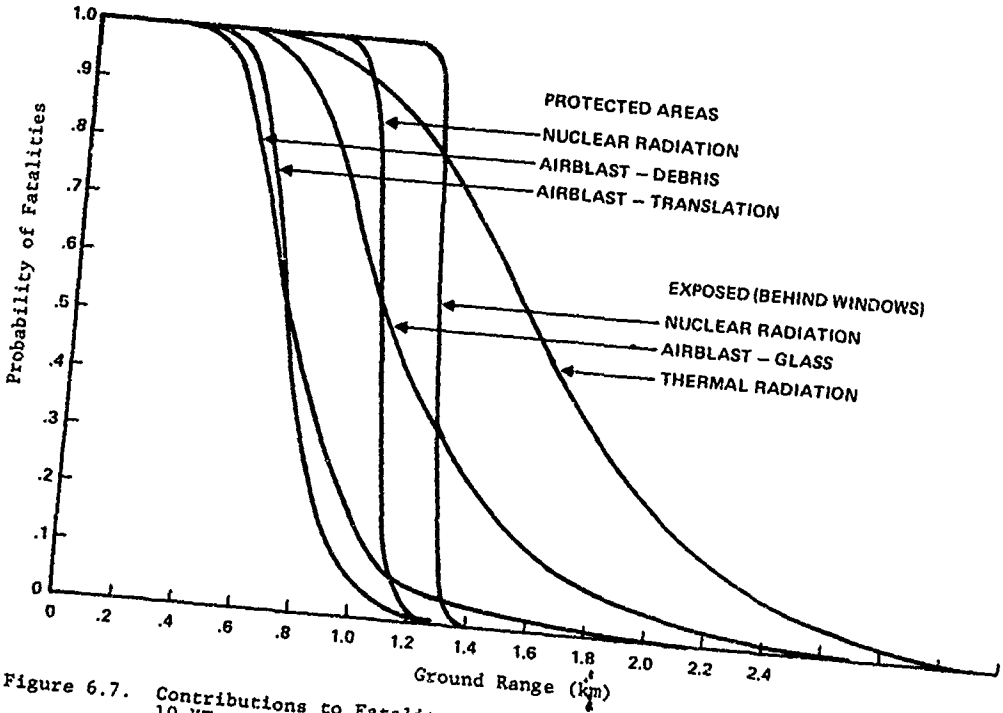

Figure 6.7. Contributions to Fatality Damage Function Residences (Aboveground) - 10 KT - 60 M Fission Weapon.

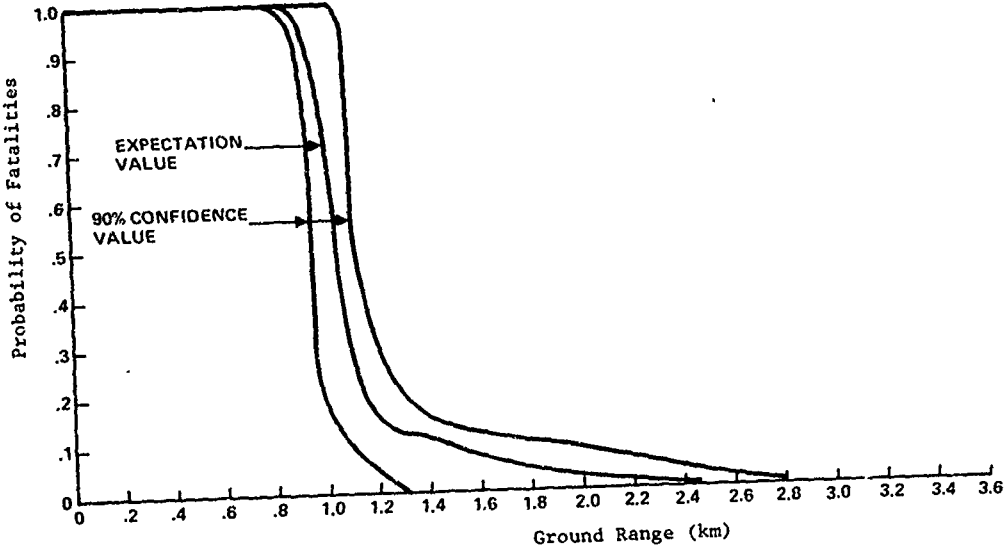

Figure 6.8. Damage Function for Fatalities. Residences (Aboveground) - 10 KT Fission Weapon 60 Meter SHOB.

6.7 REFERENCES

6.1 Drake, M.K., C.J. Rindfleisch, and D.C. Shreve, "Collateral Damage Methodology and Vulnerability Representation," Monthly Progress Report, DNA Contract DNA001-76-C-0039, SAI-76-507-LJ, (Jan. 1976).

6.2 McGrath, J, et al., "Techniques for Efficient Monte Carlo Simulation, Vol. 1, Selecting Probability Distributions," ORNL-RSIC-38 (Vol. 1), (April 1975).

6.3 Huszar, L. and W.A. Woolson, "Version 4 of ATR (Air Transport of Radiation), DNA 3995, SAI-76-561-LJ, (Jan. 1976).

6.4 Brode, H.L., "Height-of-Burst Effects at High Overpressures," DASA 2506, (July 1970).

6.5 Dolan, P.J., "Capabilities of Nuclear Weapons," DNA EM-1, Part I, (July 1972).

7. COLLATERAL DAMAGE ESTIMATION

This section contains the basic data for estimating casualties produced by nuclear weapons, i.e., the damage functions for fatalities and injuries. The damage functions were obtained using the biomedical effects data (casualty criteria and uncertainties) given in Section 5, the sheltering data given in Section 4 and the weapon environment data given in Section 3. Section 7.1 contains damage functions for weapons in the yield range from 0.1 to 10 KT. Each graphical display of a damage function contains data for five weapon yields (0.1, 0.3, 1.0, 3.0 and 10 KT), for a specified height of burst (three are given, surface, 200 and 600 ft/$KT^{1/3}$), for either injuries or fatalities and for one of three shelter categories (in the open, residences or basements). Section 7.2 contains graphical displays of damage functions and upper and lower confidence bounds (90%) on the damage function. Also shown are the dominant weapon effects (nuclear radiation, thermal radiation and airblast. Although several airblast effects were used in the analysis (direct effects on body organs, secondary effects caused by debris and tertiary effects - whole-body translation), only the most important effects are shown.

7.1 DAMAGE FUNCTIONS - LOW YIELD WEAPONS

Figures 7.1 through 7.18 show damage functions for weapon yields between 0.1 and 10 KT. The graphical displays are organized as follows.

Figure	Casualty Type	Shelter	Height-of-Burst SHOB ($ft/KT^{1/3}$)
1	Injury	open	Surface
2	"	"	200
3	"	"	600
4	Fatality	"	Surface
5	"	"	200
6	"	"	600
7	Injury	Residences	Surface
8	"	"	200
9	"	"	600
10	Fatality	"	Surface
11	"	"	200
12	"	"	600
13	Injury	Basements	Surface
14	"	"	200
15	"	"	600
16	Fatality	"	Surface
17	"	"	200
18	"	"	600

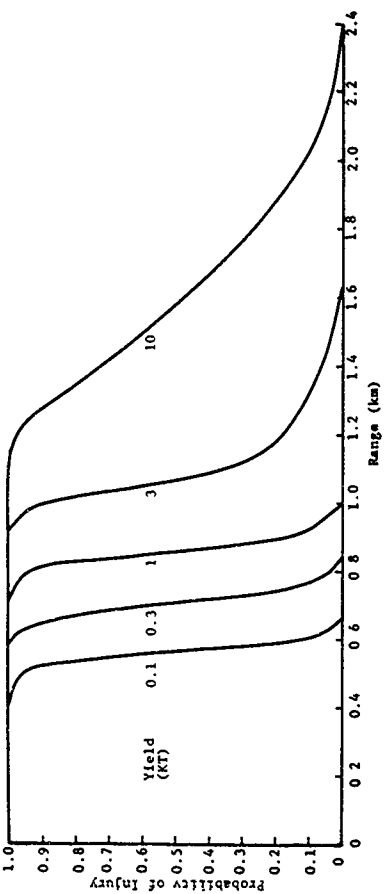

Figure 7.1. Injury Damage Function, People in the Open, Surface Burst.

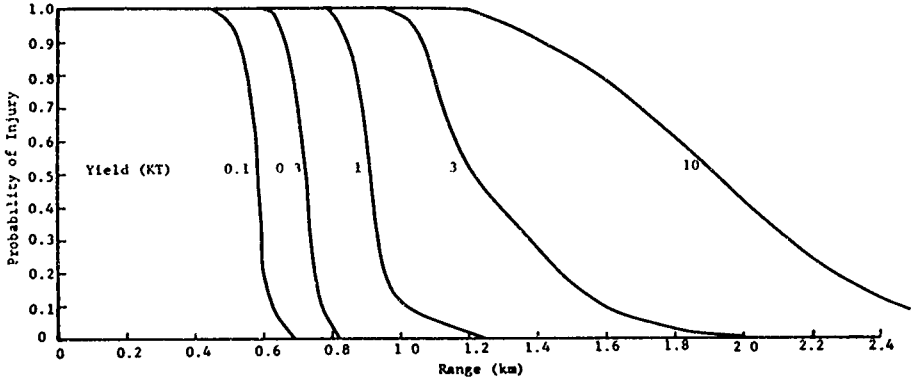

Figure 7.2. Injury Damage Function, People in the Open, 200 ft/$KT^{1/3}$ Scaled Height of Burst.

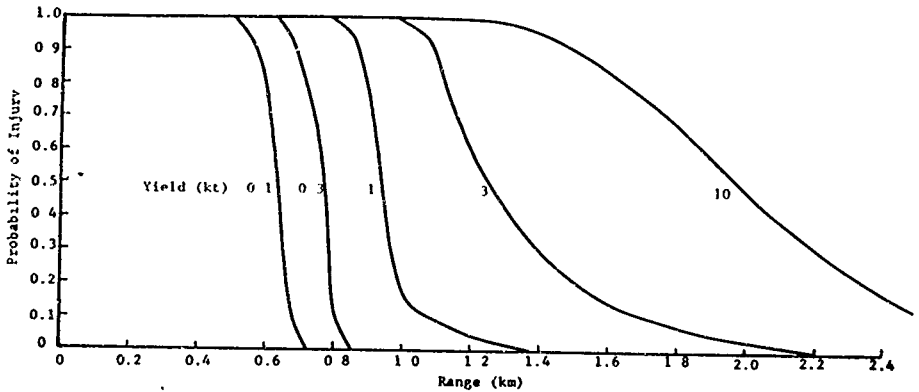

Figure 7.3. Injury Damage Function, People in the Open, 600 ft/$KT^{1/3}$ Scaled Height of Burst.

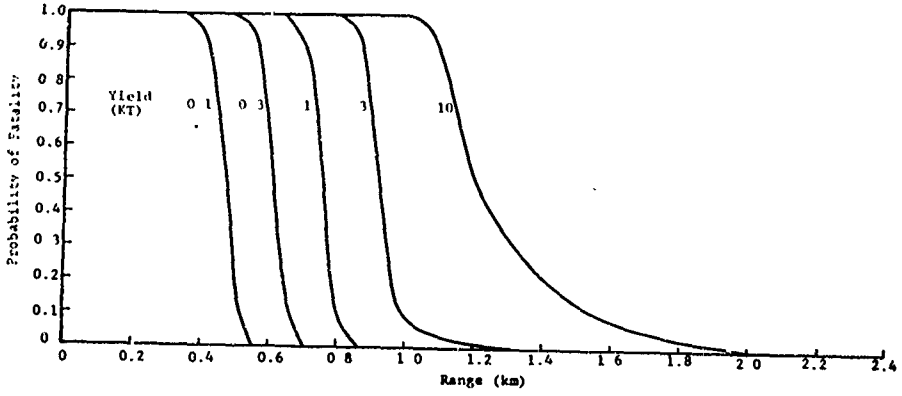

Figure 7.4. Fatality Damage Function, People in the Open, Surface Burst.

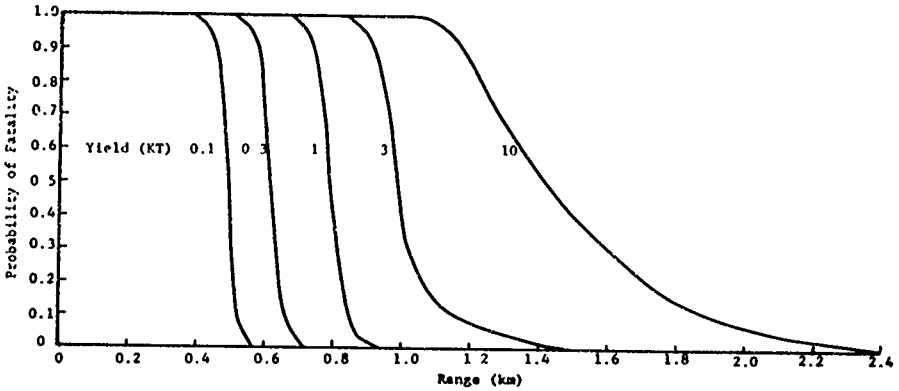

Figure 7.5. Fatality Damage Function, People in the Open, 200 ft/$KT^{1/3}$ Scaled Height of Burst.

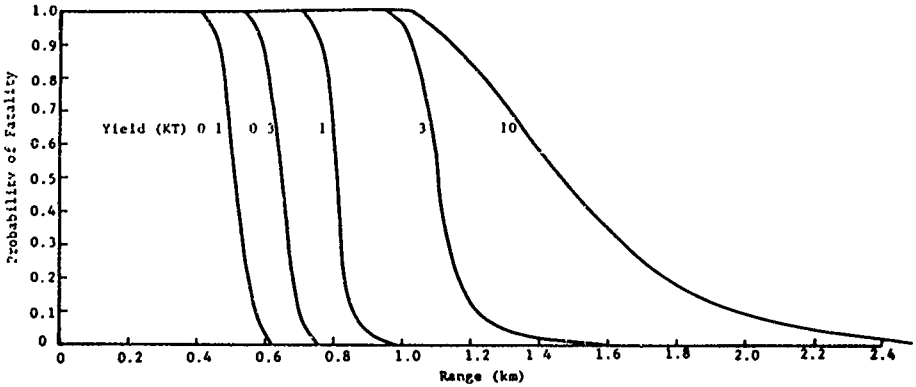

Figure 7.6. Fatality Damage Function, People in the Open, 600 ft/$KT^{1/3}$ Scaled Height of Burst.

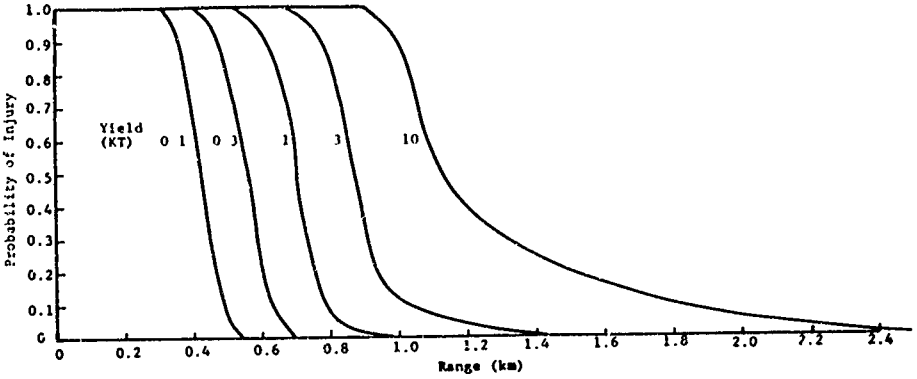

Figure 7.7. Injury Damage Function, People in Residences, Surface Burst.

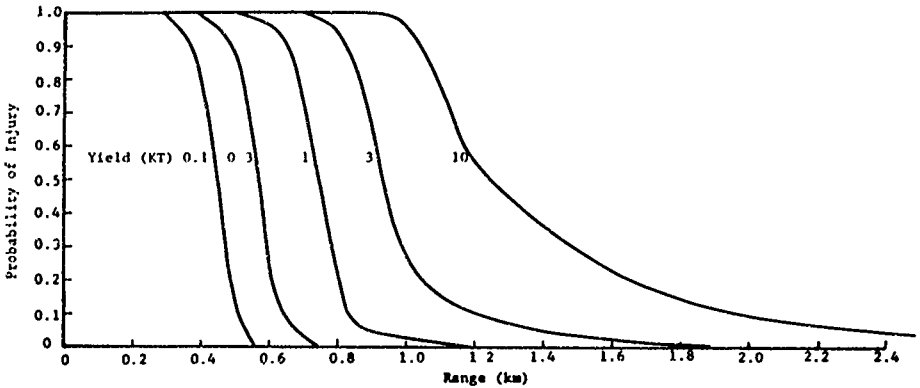

Figure 7.8. Injury Damage Function, People in Residences, 200 ft/KT$^{1/3}$ Scaled Height of Burst.

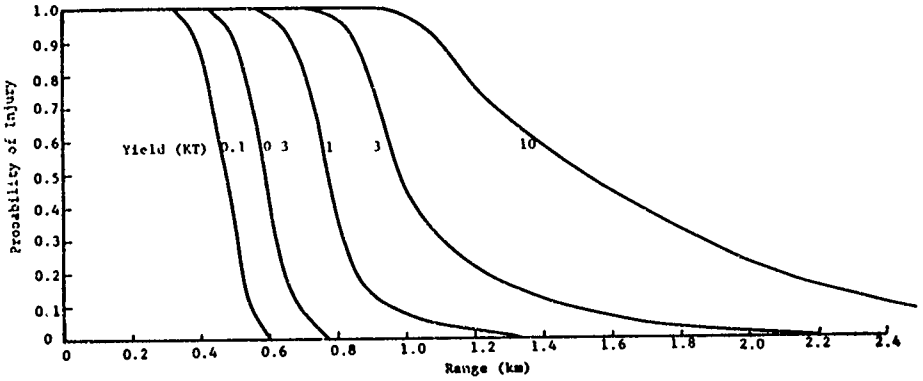

Figure 7.9. Injury Damage Function, People in Residences, 600 ft/KT$^{1/3}$ Scaled Height of Burst.

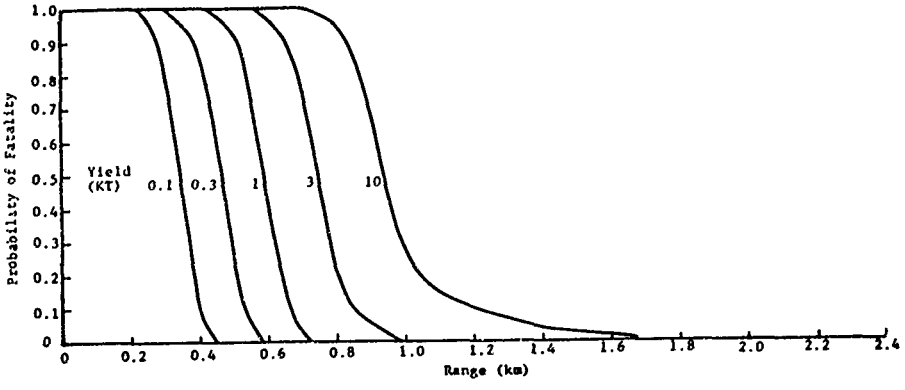

Figure 7.10. Fatality Damage Function, People in Residences, Surface Burst.

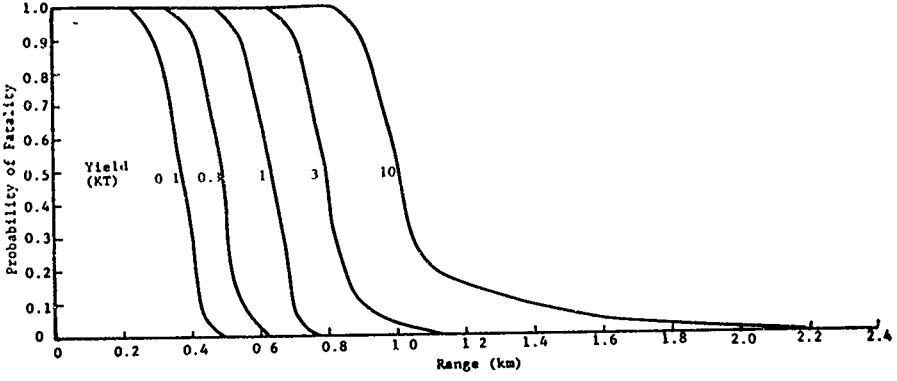

Figure 7.11. Fatality Damage Function, People in Residences, 200 ft/KT$^{1/3}$ Scaled Height of Burst.

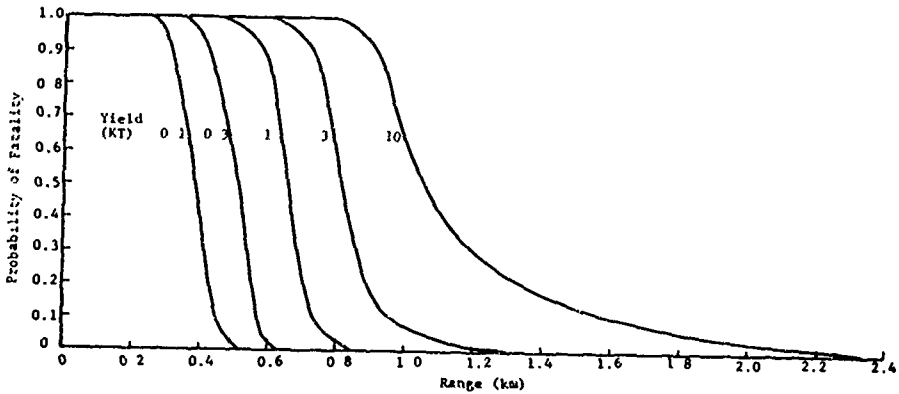

Figure 7.12. Fatality Damage Function, People in Residences, 600 ft/KT$^{1/3}$ Scaled Height of Burst.

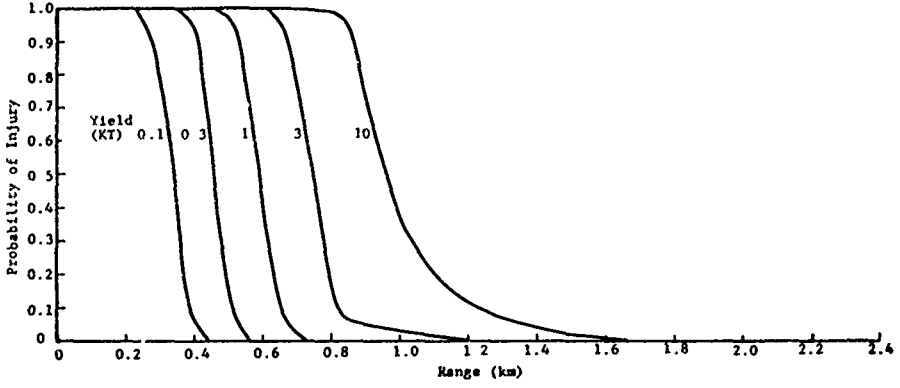

Figure 7.13. Injury Damage Functions, People in Basements, Surface Burst.

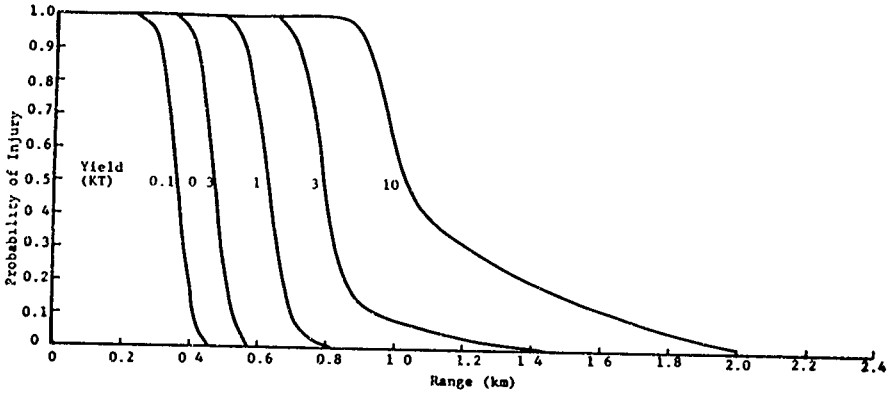

Figure 7.14. Injury Damage Function, People in Basements, 200 ft/$KT^{1/3}$ Scaled Height of Burst.

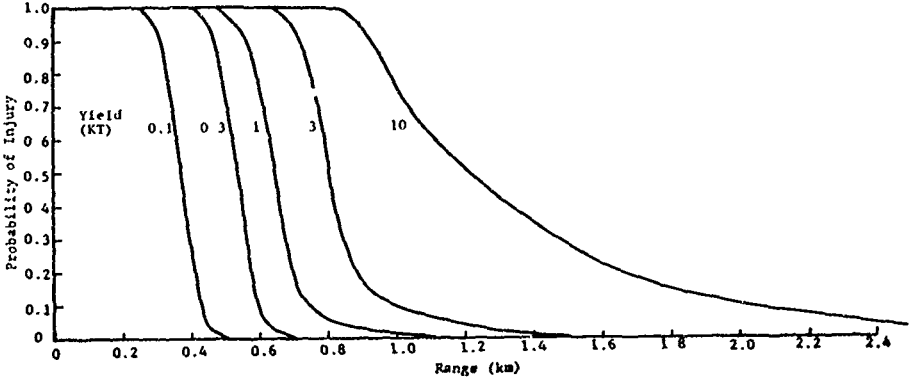

Figure 7.15. Injury Damage Function, People in Basements, 600 ft/KT$^{1/3}$ Scaled Height of Burst.

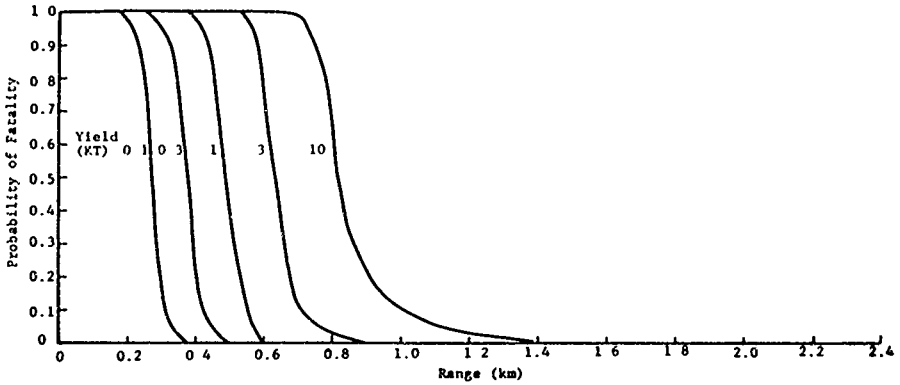

Figure 7.16. Fatality Damage Function, People in Basements, Surface Burst.

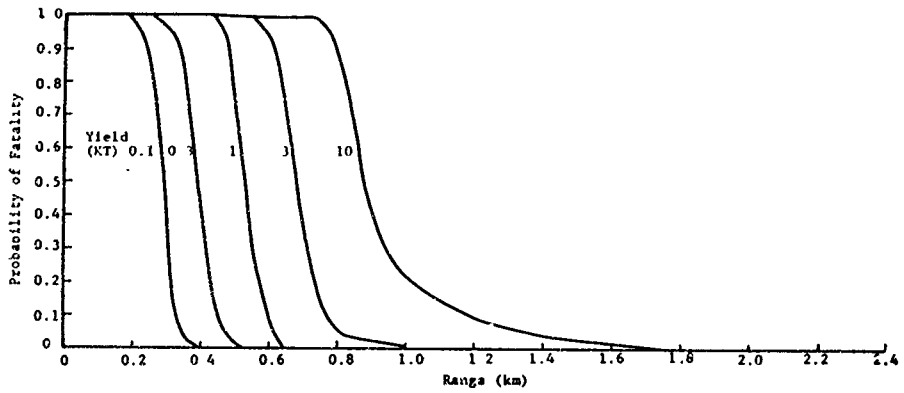

Figure 7.17. Fatality Damage Function, People in Basements, 200 ft/$KT^{1/3}$ Scaled Height of Burst.

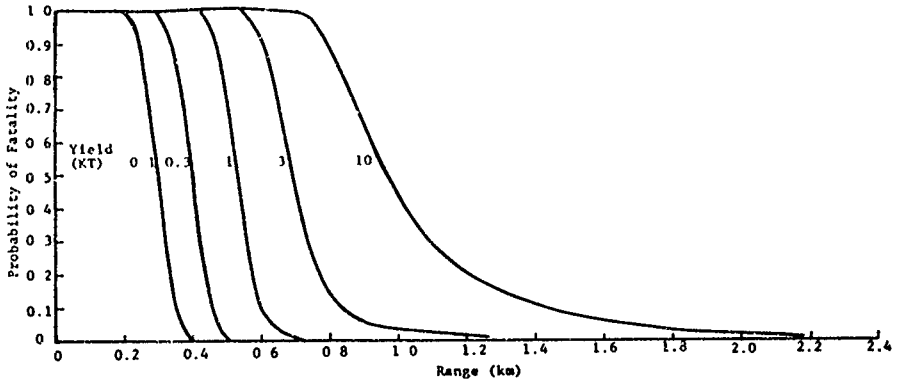

Figure 7.18. Fatality Damage Function, People in Basements, 600 ft/$KT^{1/3}$ Scaled Height of Burst.

7.2 DAMAGE FUNCTIONS AND CONFIDENCE BOUNDS

7.2.1 Injury Damage Functions, People in the Open

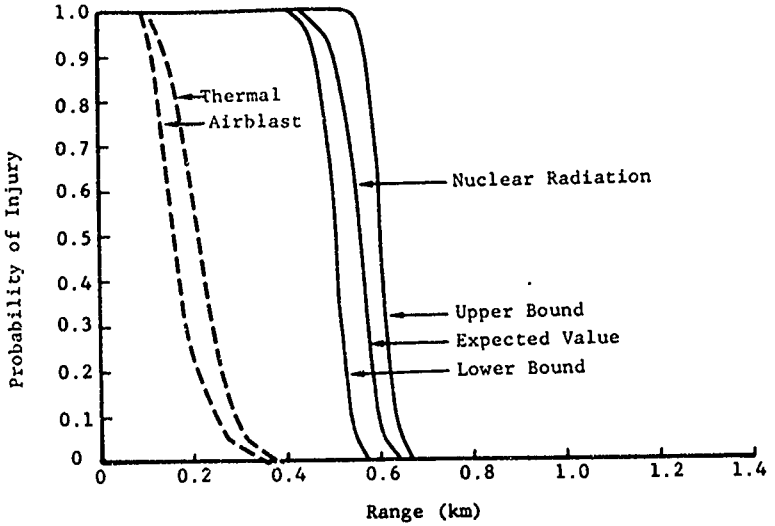

Figure 7.19. Injury Damage Function, People in the Open, 0.1 KT, Surface Burst.

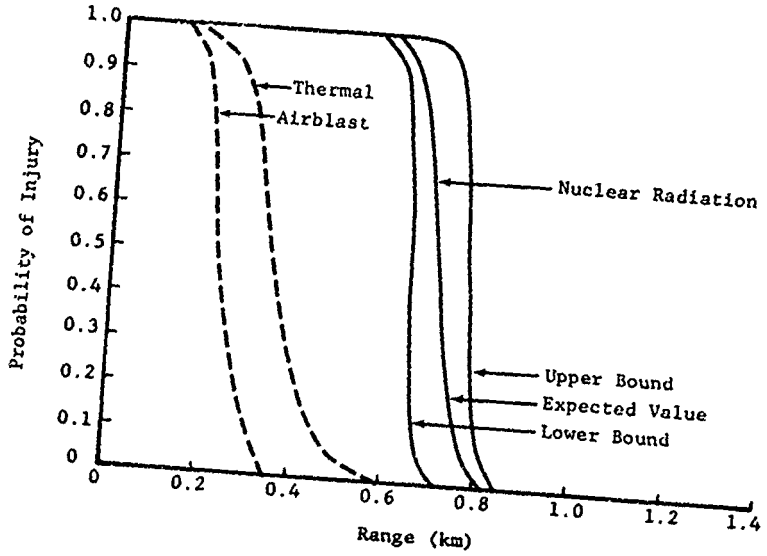

Figure 7.20. Injury Damage Function, People in the Open, 0.5 KT, Surface Burst.

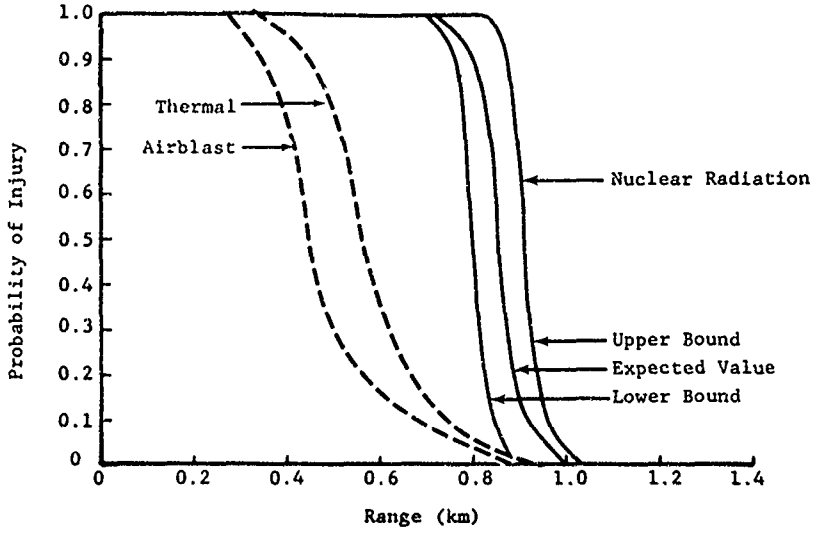

Figure 7.21. Injury Damage Function, People in the Open, 1 KT, Surface Burst.

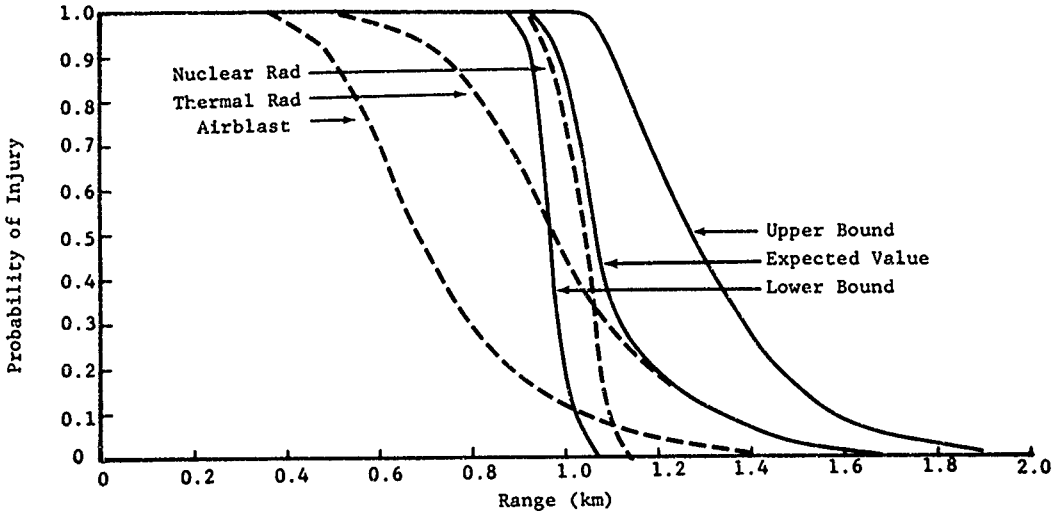

Figure 7.22. Injury Damage Function, People in the Open, 3 KT, Surface Burst..

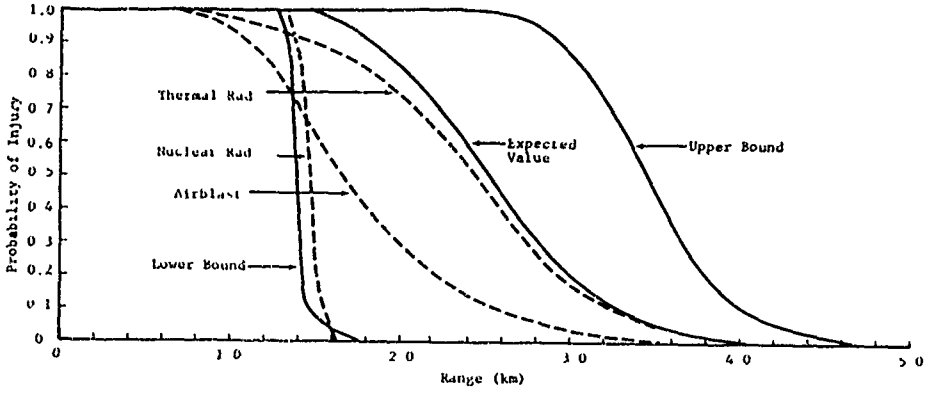

Figure 7.23. Injury Damage Function, People in the Open, 10 KT, Surface Burst.

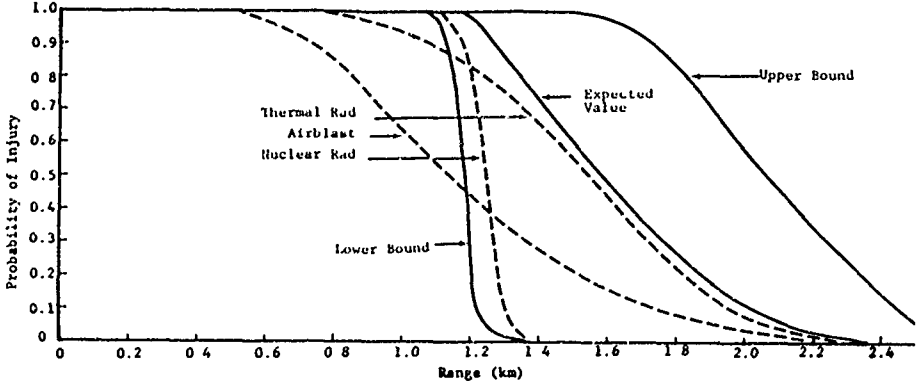

Figure 7.24. Injury Damage Function, People in the Open, 30 KT, Surface Burst.

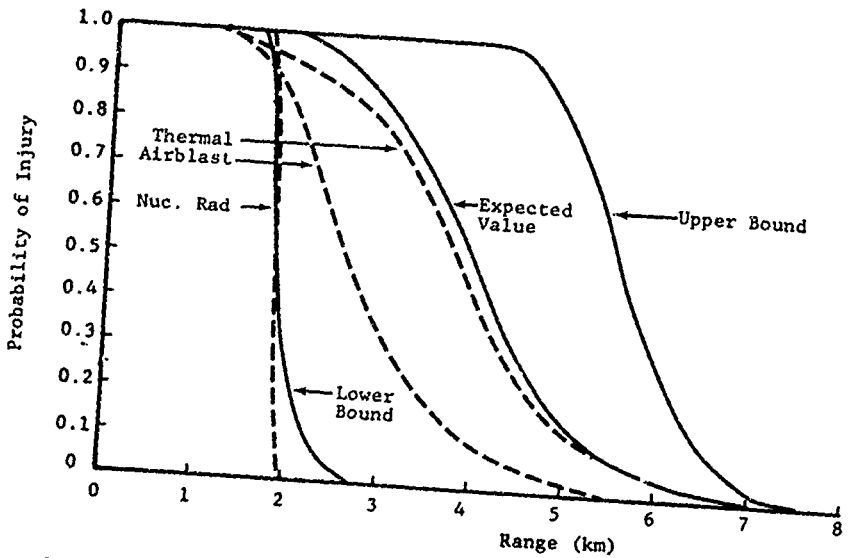

Figure 7.25. Injury Damage Function, People in the Open, 100 KT, Surface Burst.

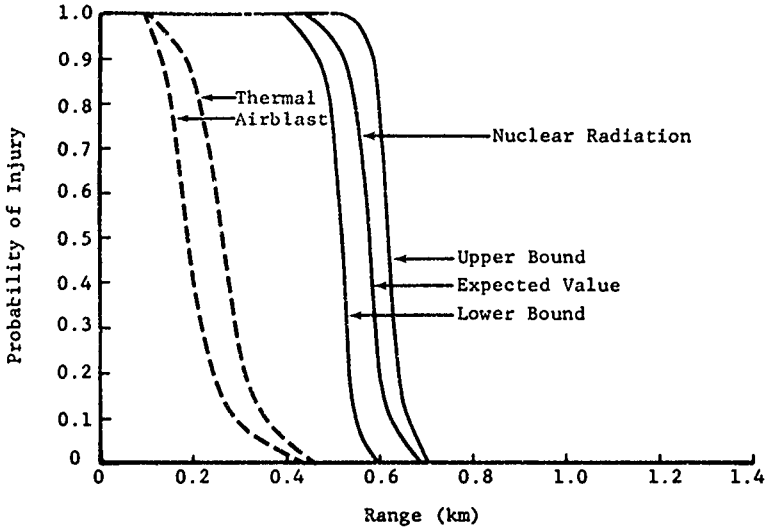

Figure 7.26. Injury Damage Function, People in the Open, 0.1 KT, 200 ft/KT$^{1/3}$ Scaled Height of Burst.

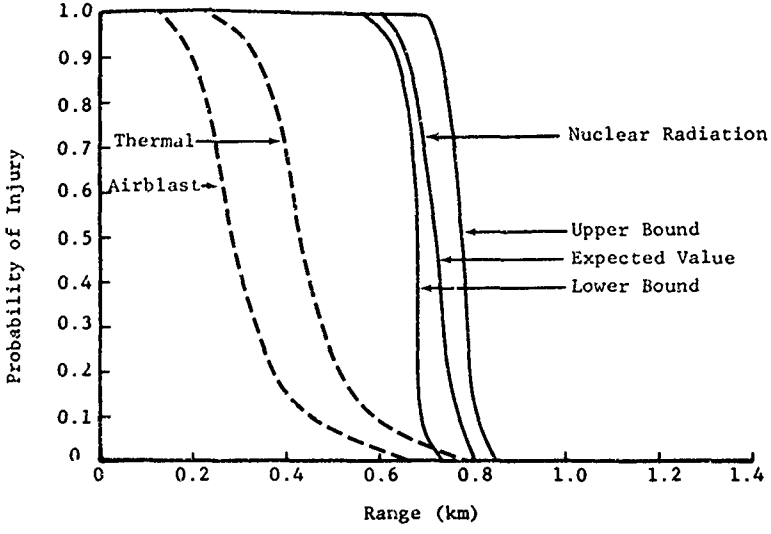

Figure 7.27. Injury Damage Function, People in the Open, 0.3 KT, 200 ft/KT$^{1/3}$ Scaled Height of Burst.

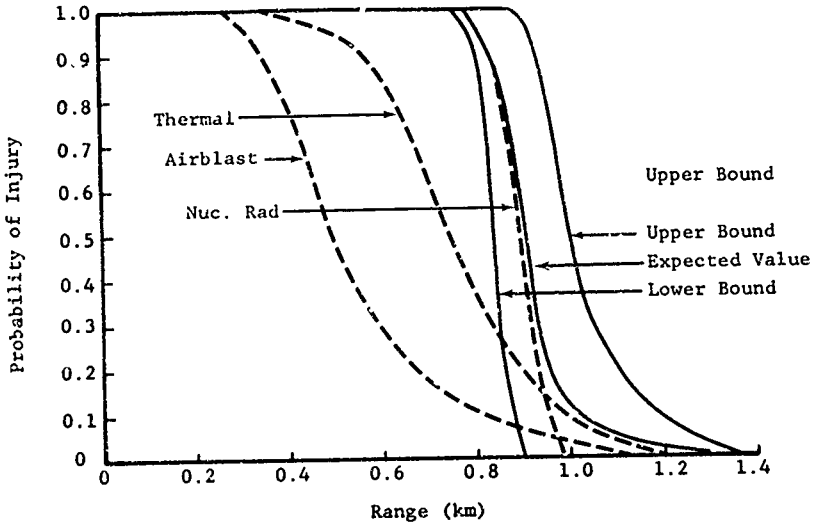

Figure 7.28. Injury Damage Function, People in the Open, 1.0 KT 200 ft/KT$^{1/3}$ Scaled Height of Burst.

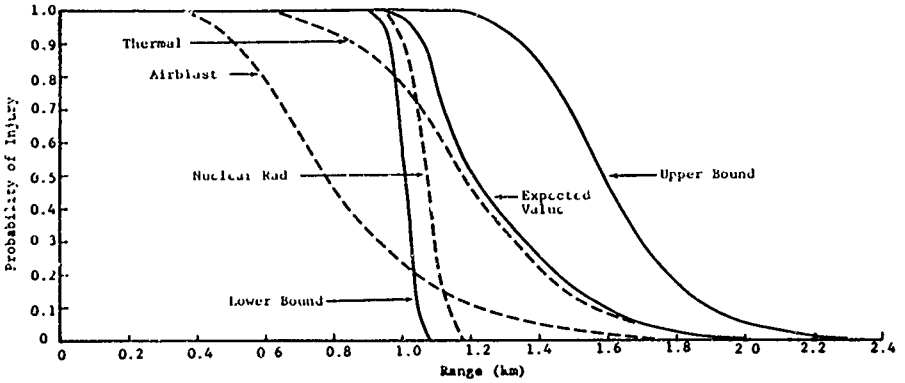

Figure 7.29. Injury Damage Function, People in the Open. 3 KT, 200 ft/KT$^{1/3}$ Scaled Height of Burst.

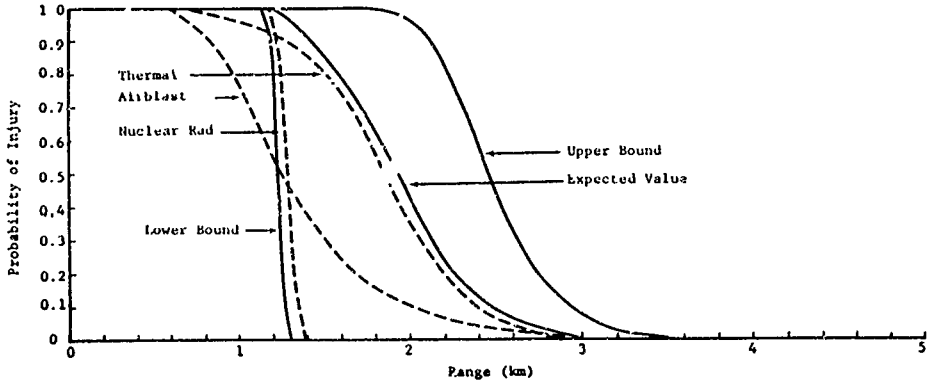

Figure 7.30. Injury Damage Function, People in the Open, 10 KT, 200 ft/KT$^{1/3}$ Scaled Height of Burst.

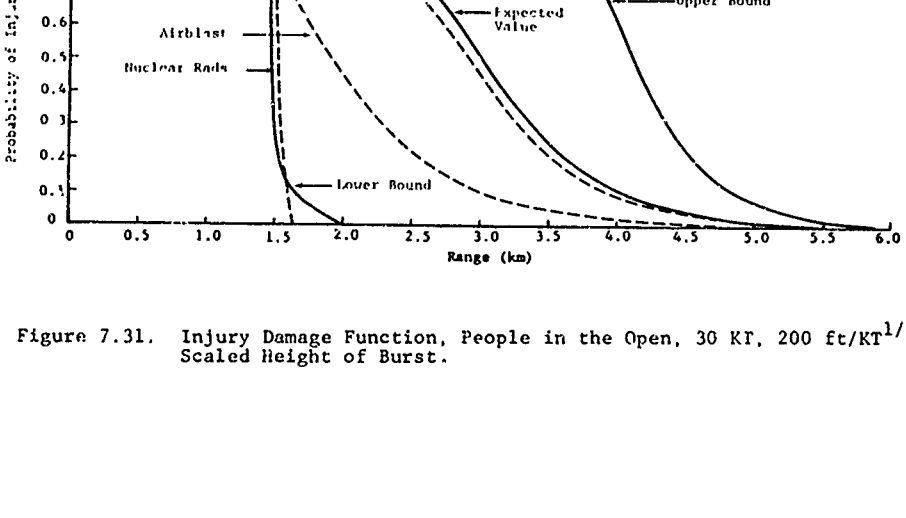

Figure 7.31. Injury Damage Function, People in the Open, 30 KT, 200 ft/KT$^{1/3}$ Scaled Height of Burst.

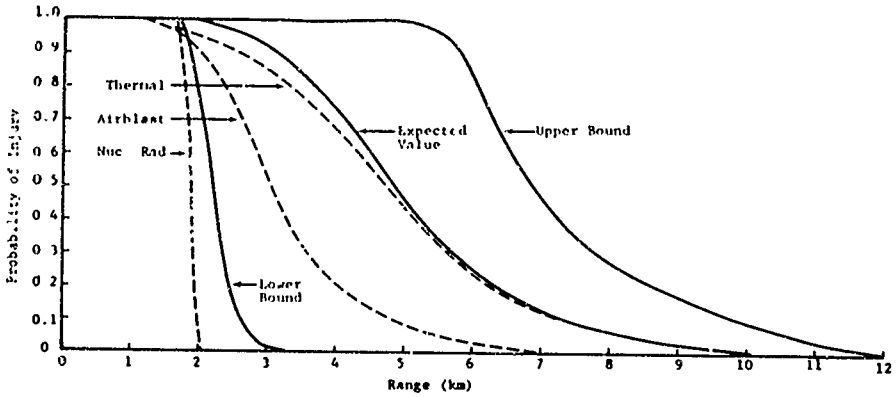

Figure 7.32. Injury Damage Function, People in the Open, 100 KT, 200 ft/KT$^{1/3}$ Scaled Height of Burst.

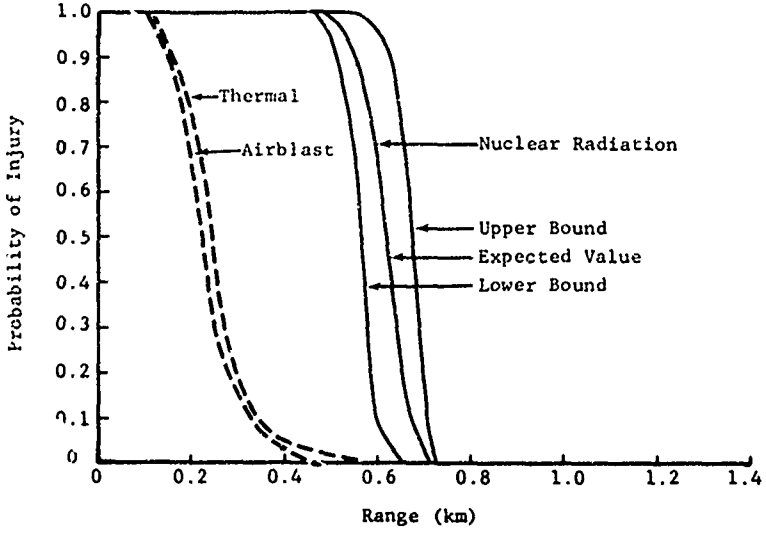

Figure 7.33. Injury Damage Function, People in the Open, 0.1 KT, 600 ft/KT$^{1/3}$ Scaled Height of Burst.

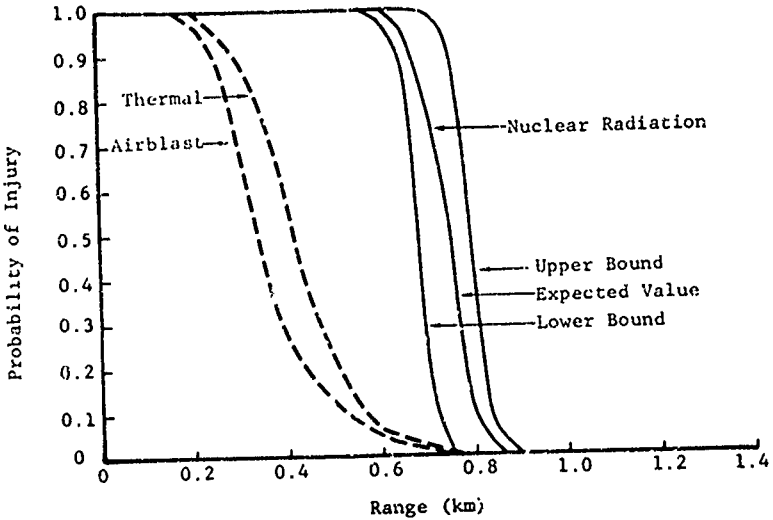

Figure 7.34. Injury Damage Function, People in the Open, 0.3 KT 600 ft/KT$^{1/3}$ Scaled Height of Burst.

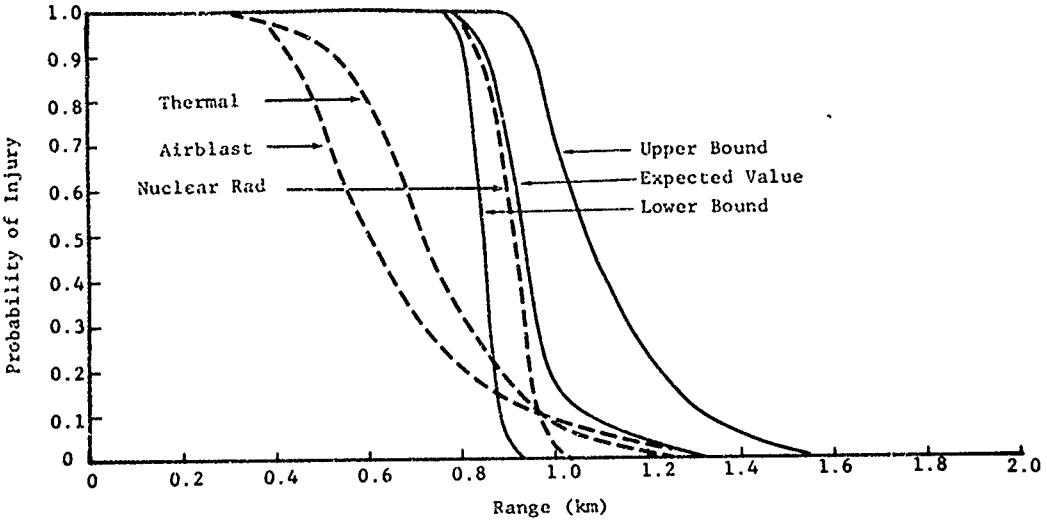

Figure 7.35. Injury Damage Function, People in the Open, 1.0 KT, 600 ft/KT$^{1/3}$ Scaled Height of Burst.

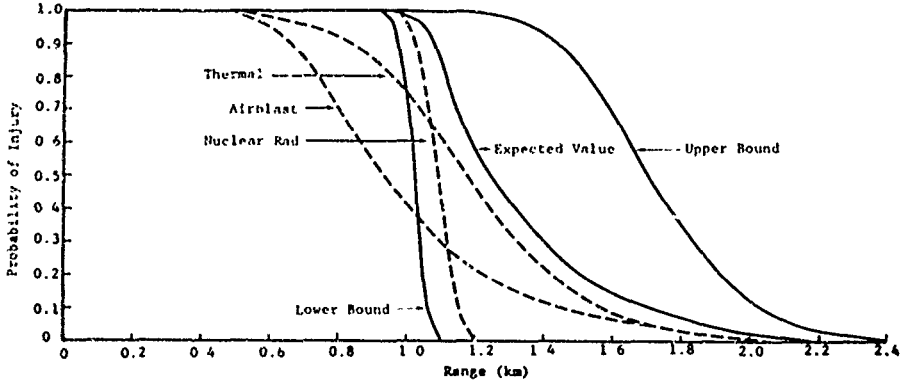

Figure 7.36. Injury Damage Function, People in the Open, 3 KT, 600 ft/KT$^{1/3}$ Scaled Height of Burst.

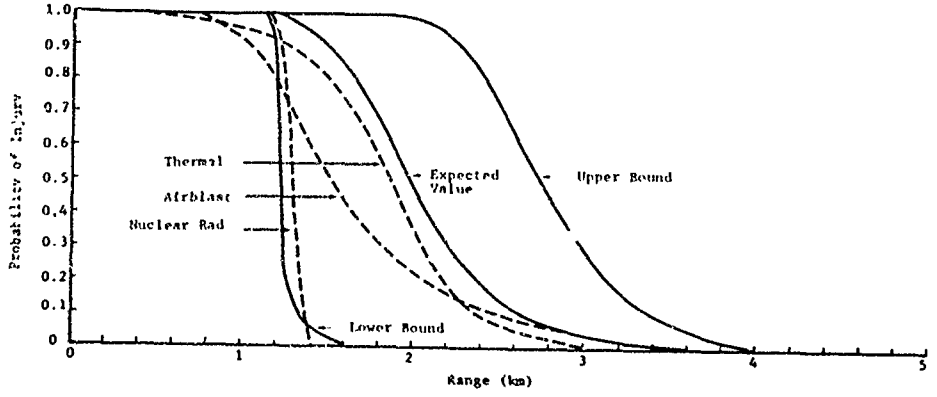

Figure 7.37. Injury Damage Function, People in the Open, 10 KT, 600 ft/KT$^{1/3}$ Scaled Height of Burst.

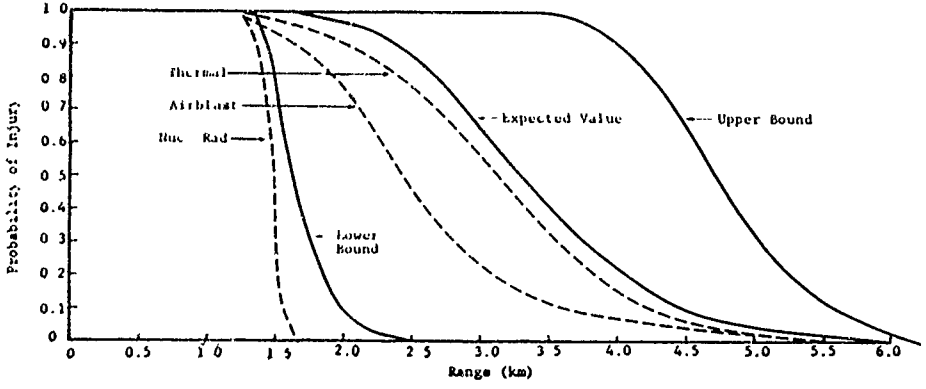

Figure 7.38. Injury Damage Function, People in the Open, 30 KT, 600 ft/KT$^{1/3}$ Scaled Height of Burst.

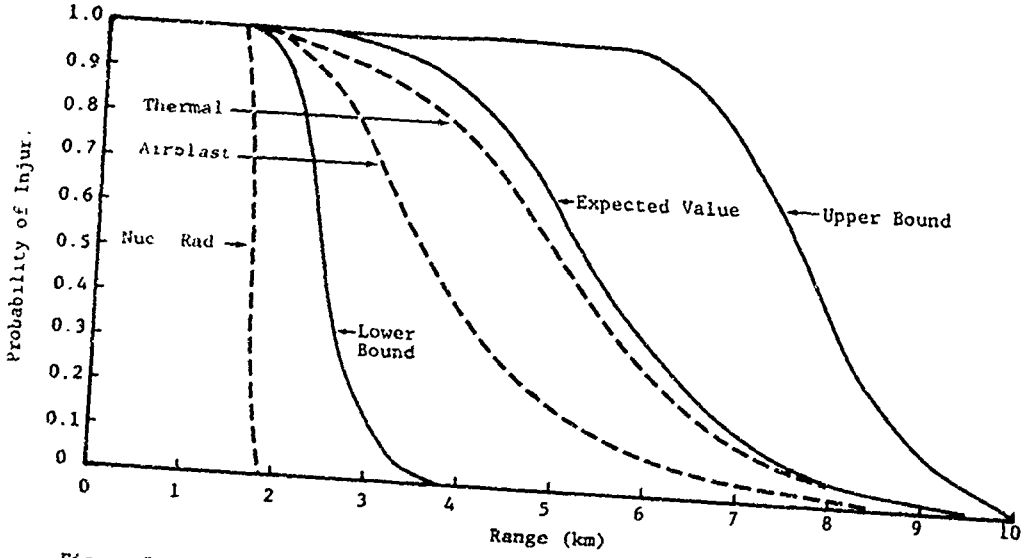

Figure 7.39. Injury Damage Function. People in the Open, 100 KT, 600 ft/KT$^{1/3}$ Scaled Height of Burst.

7.2.2 Fatality Damage Functions, People in the Open

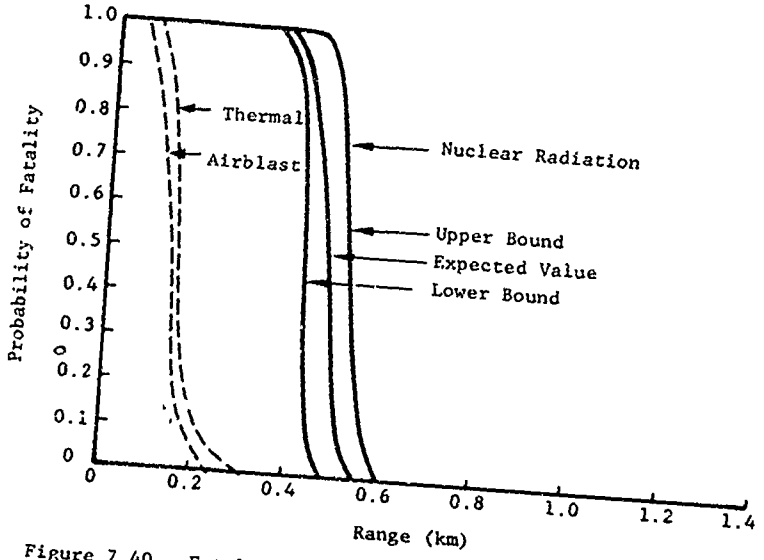

Figure 7.40. Fatality Damage Function, People in the Open, 0.1 KT, Surface Burst.

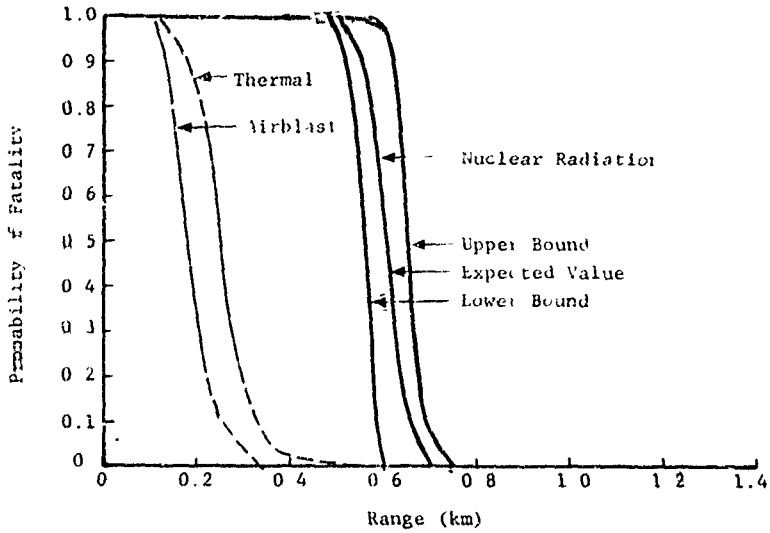

Figure 7-41 Fatality Damage Function, People in the Open, 0.3 KT, Surface Burst.

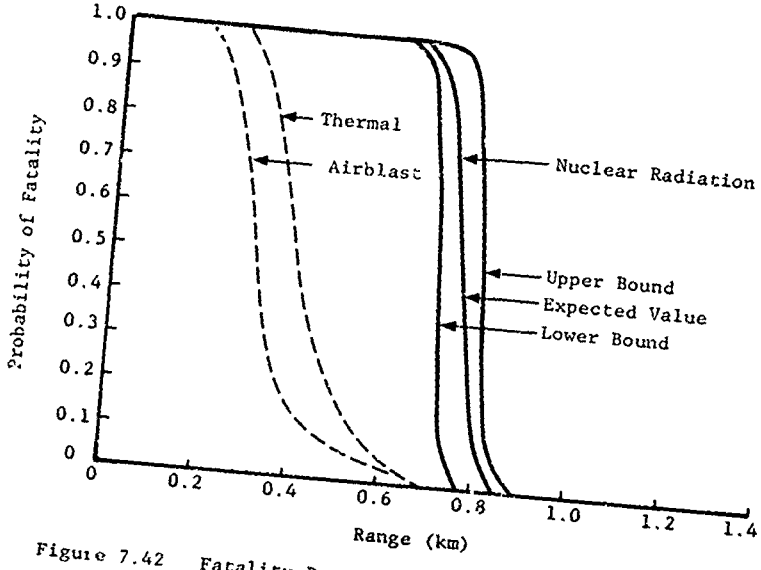

Figure 7.42 Fatality Damage Function, People in the Open, 1 KT, Surface Burst.

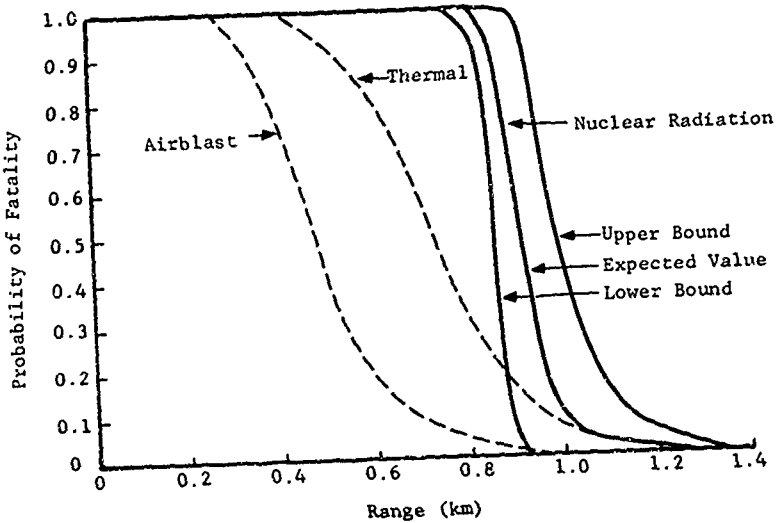

Figure 7.43. Fatality Damage Function, People in the Open, 3 KT, Surface Burst.

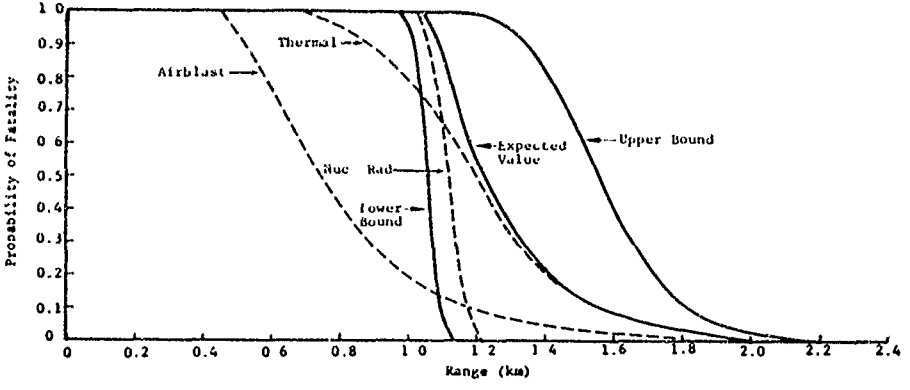

Figure 7.44. Fatality Damage Function, People in the Open, 10 KT, Surface Burst.

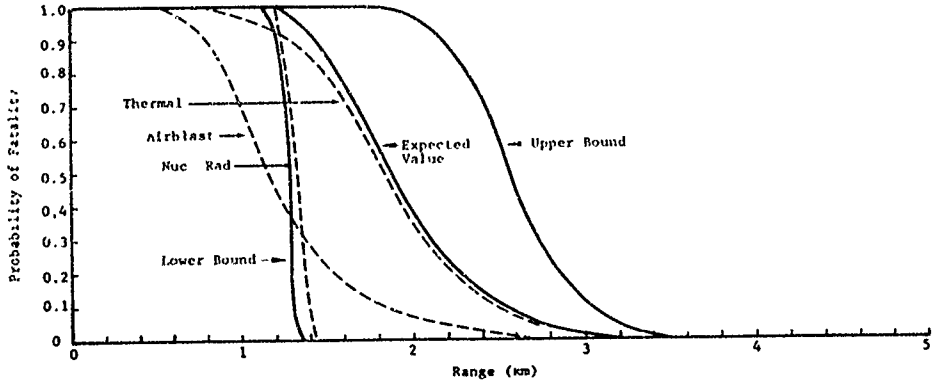

Figure 7.45. Fatality Damage Function, People in the Open, 30 KT, Surface Burst.

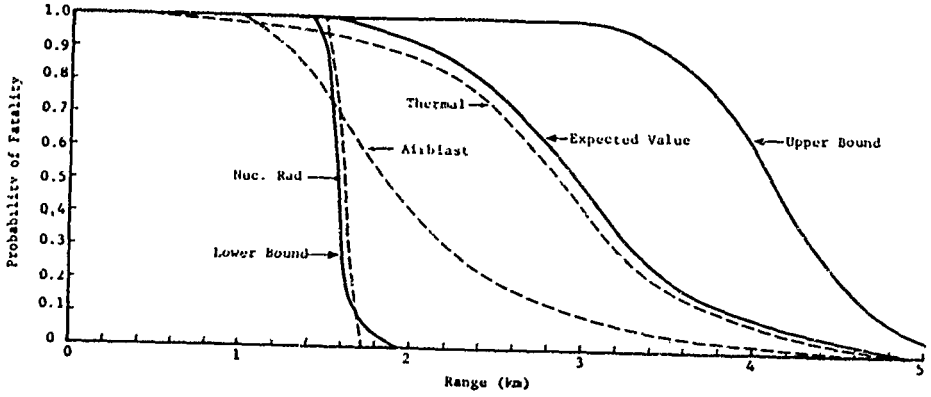

Figure 7.46. Fatality Damage Function, People in the Open, 100 KT, Surface Burst.

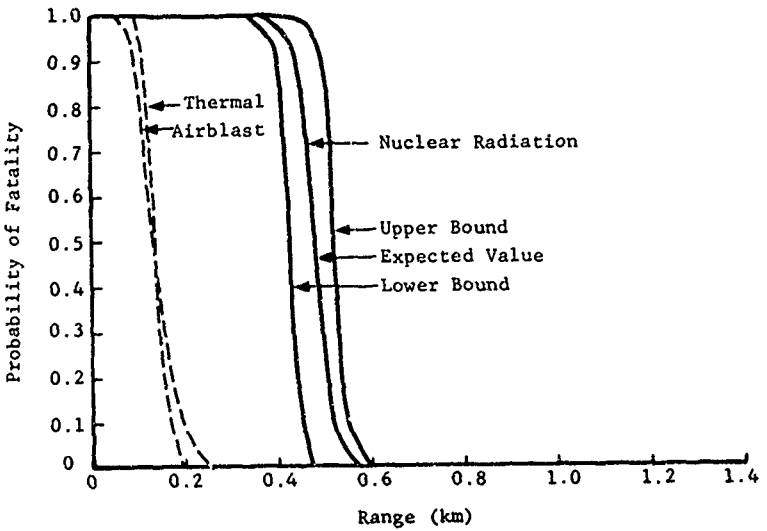

Figure 7.47. Fatality Damage Function, People in the Open, 0.1 KT, 200 ft/KT$^{1/3}$ Scaled Height of Burst.

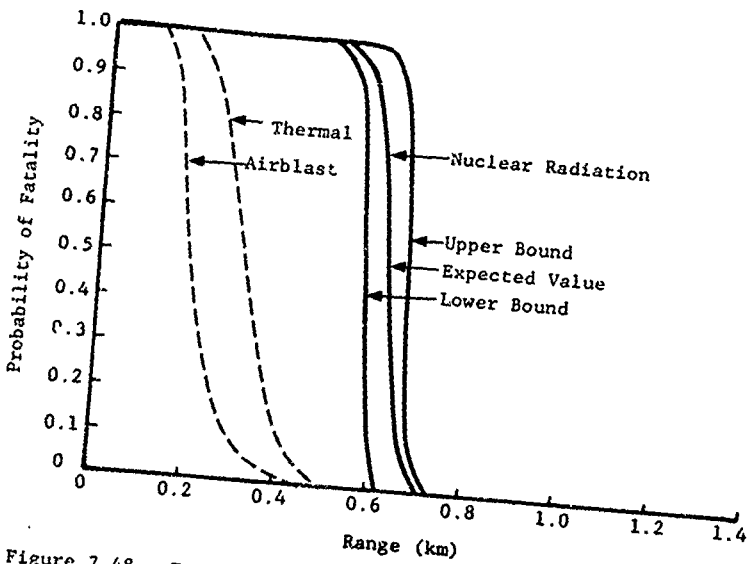

Figure 7.48. Fatality Damage Function, People in the Open 0.3 KT, 200 ft/KT$^{1/3}$ Scaled Height of Burst.

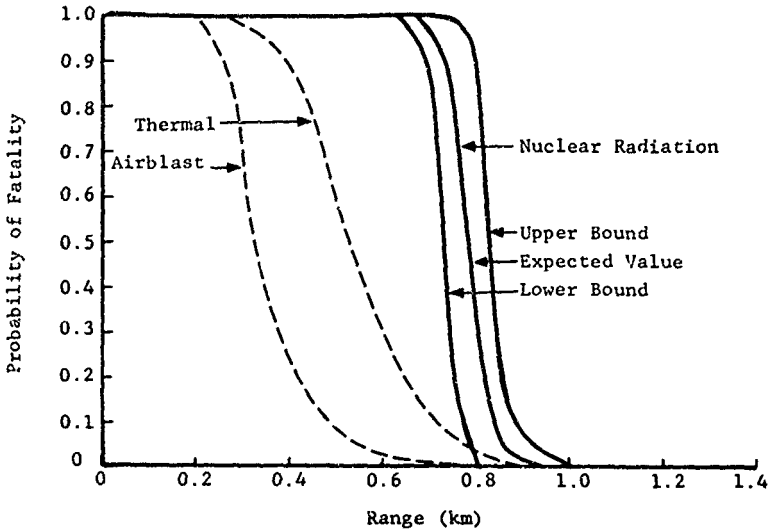

Figure 7.49. Fatality Damage Function, People in the Open, 1 KT, 200 ft/KT$^{1/3}$ Scaled Height of Burst.

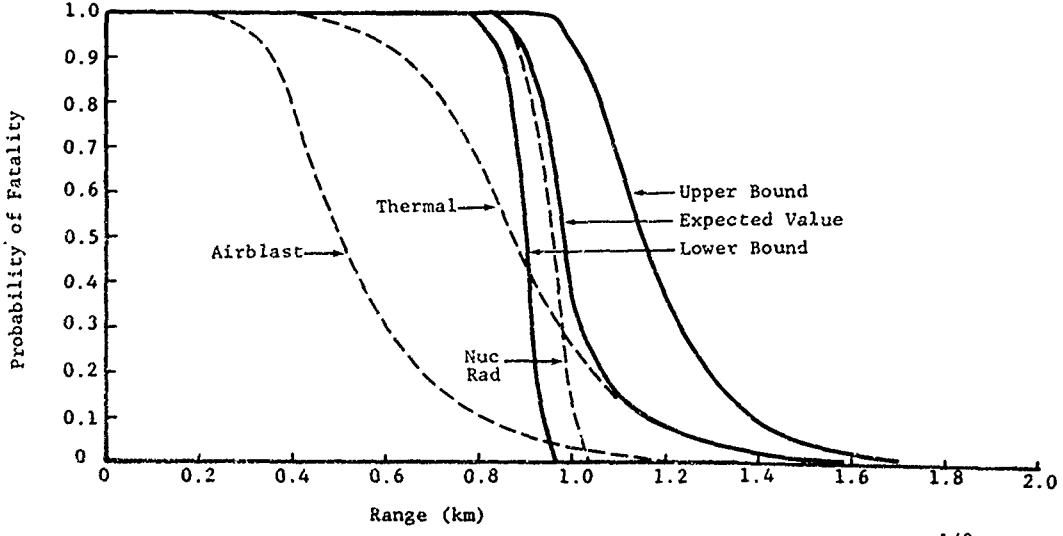

Figure 7.50. Fatality Damage Function, People in the Open, 3 KT, 200 ft/KT$^{1/3}$ Scaled Height of Burst.

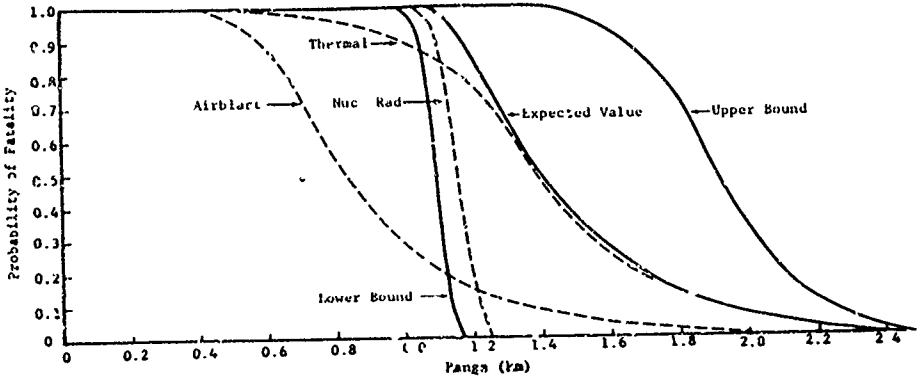

Figure 7.51. Fatality Damage Function, People in the Open, 10 KT, 200 ft/KT$^{1/3}$ Scaled Height of Burst.

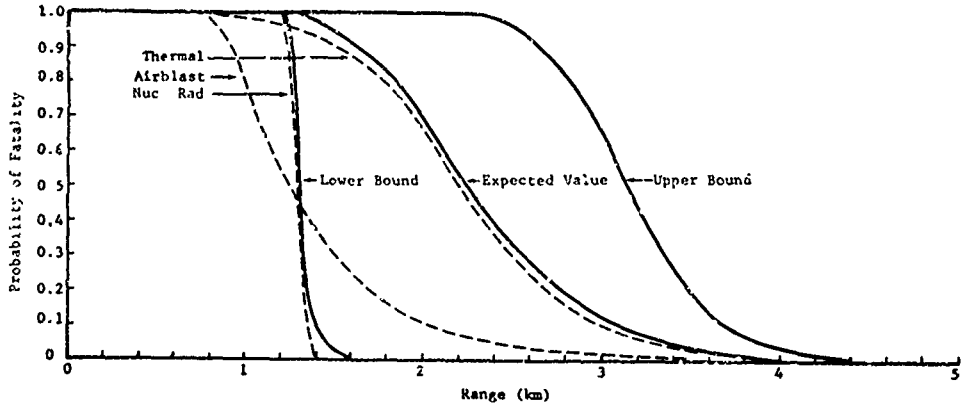

Figure 7.52. Fatality Damage Function, People in the Open, 30 KT 200 ft/KT$^{1/3}$ Scaled Height of Burst.

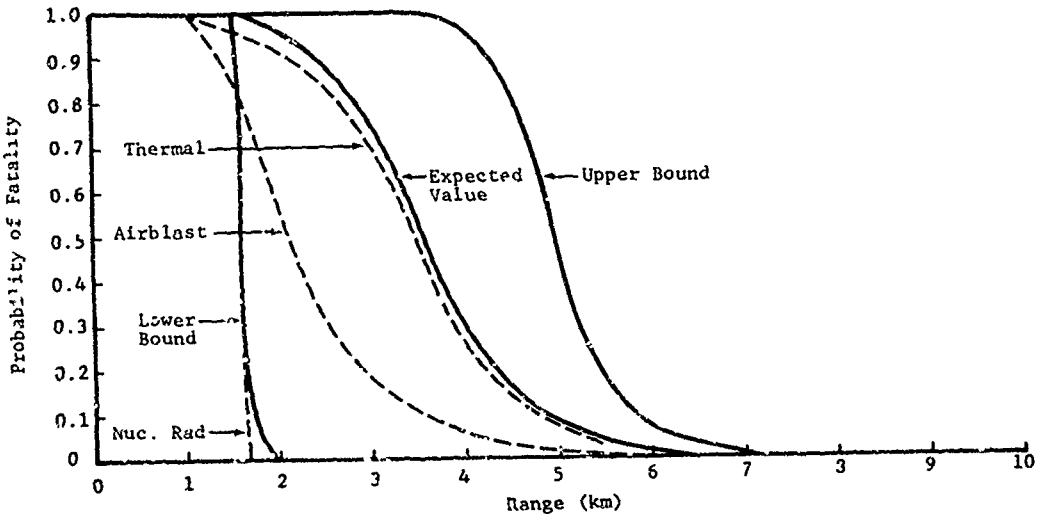

Figure 7.53 Fatality Damage Function, People in the Open, 100 KT, 200 ft/KT$^{1/3}$ Scaled Height of Burst.

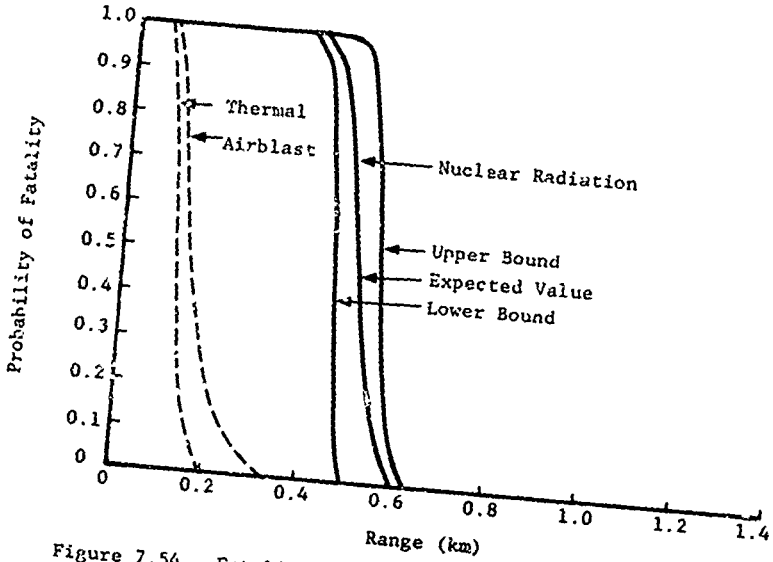

Figure 7.54. Fatality Damage Function, People in the Open, 0.1 KT, 600 ft/KT$^{1/3}$ Scaled Height of Burst.

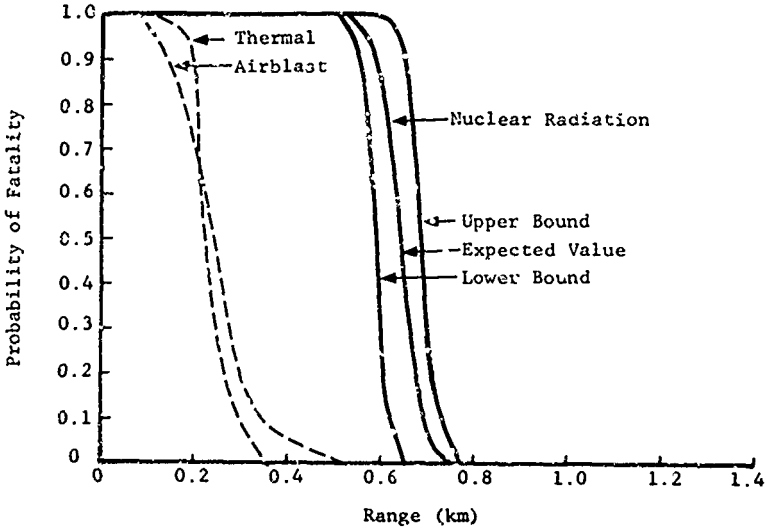

Figure 7.55. Fatality Damage Function, People in the Open, 0.3 KT, 600 ft/KT$^{1/3}$ Scaled Height of Burst.

Figure 7.56. Fatality Damage Function, People in the Open, 1 KT, 600 ft/KT$^{1/3}$ Scaled Height of Burst.

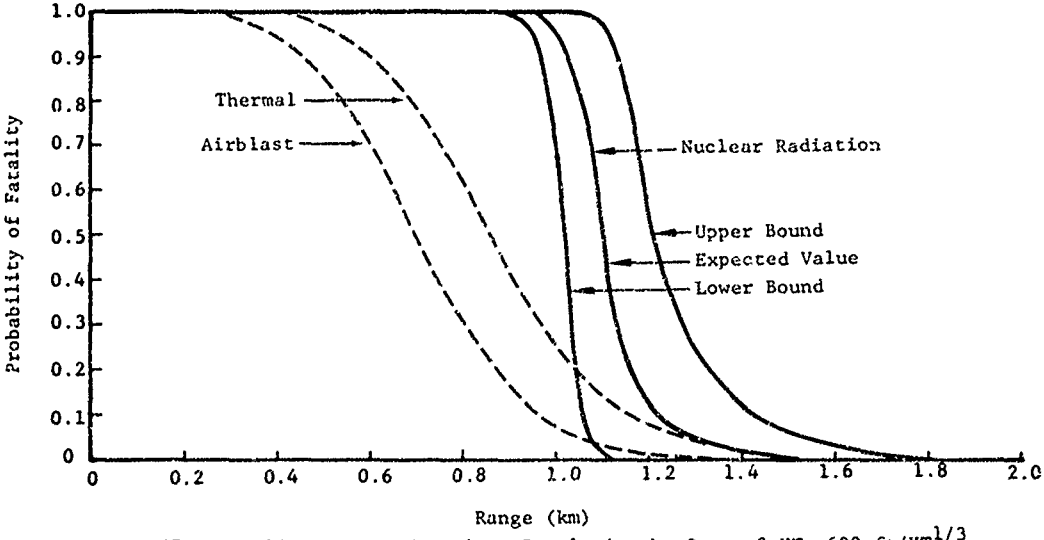

Figure 7.57. Fatality Damage Function, People in the Open, 3 KT, 600 ft/KT$^{1/3}$ Scaled Height of Burst.

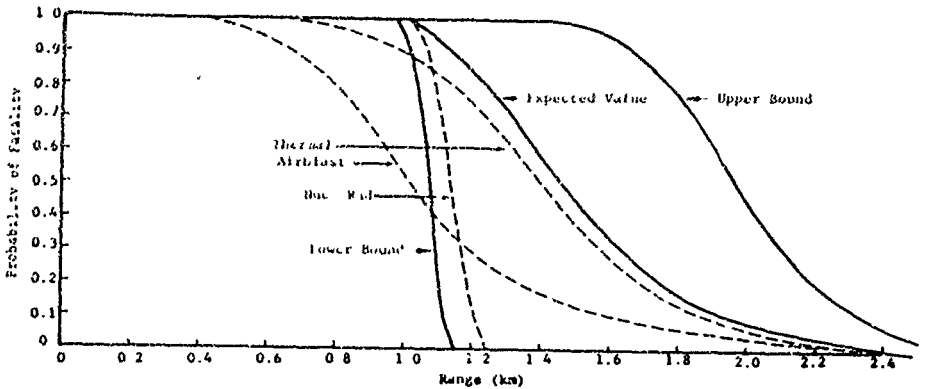

Figure 7.58. Fatality Damage Function, People in the Open, 10 KT, 600 ft/KT$^{1/3}$ Scaled Height of Burst.

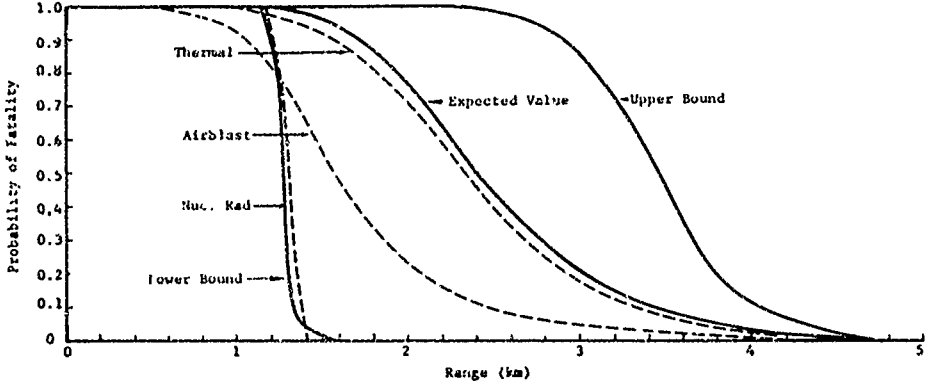

Figure 7.59. Fatality Damage Function, People in the Open, 30 KT, 600 ft/KT$^{1/3}$ Scaled Height of Burst.

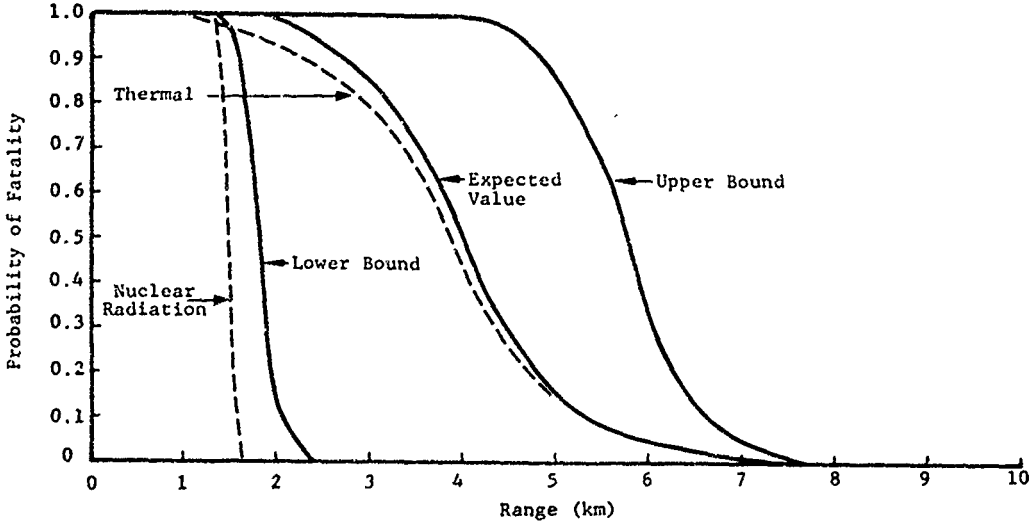

Figure 7.60. Fatality Damage Function, People in the Open, 100 KT, 600 ft/KT$^{1/3}$ Scaled Height of Burst.

7.2.3 Injury Damage Functions, People in Residences

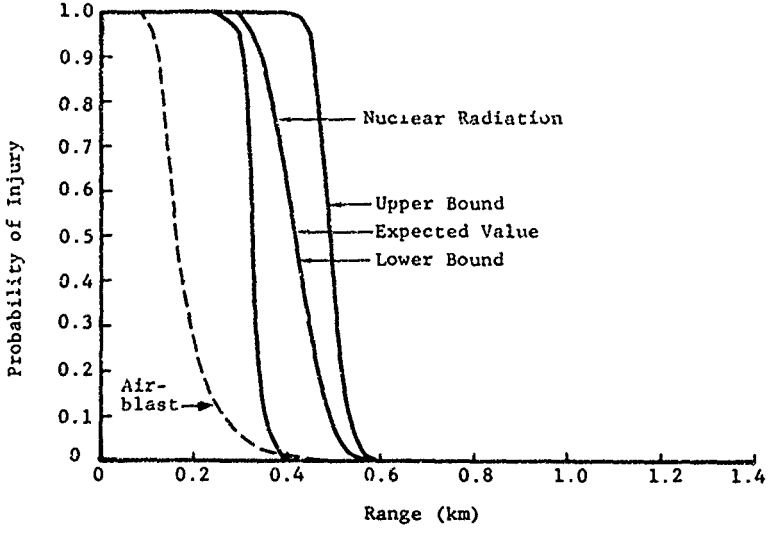

Figure 7.61. Injury Damage Function, People in Residences, 0.1 KT, Surface Burst.

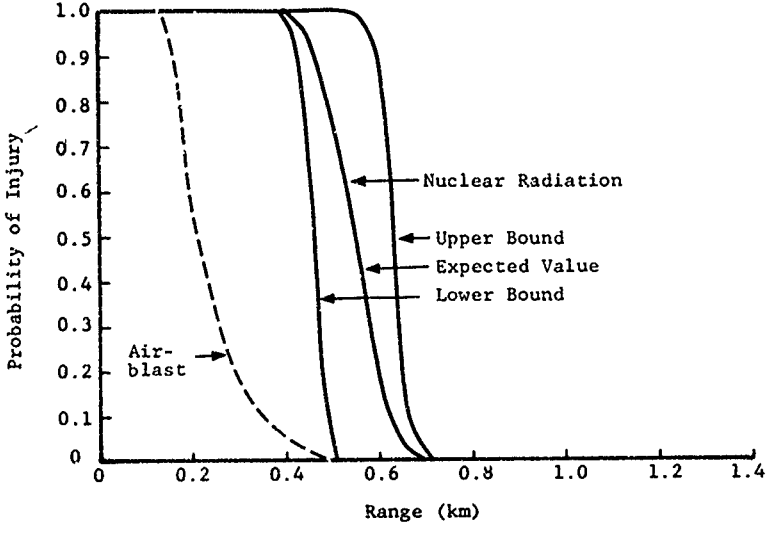

Figure 7.62. Injury Damage Function, People in Residences, 0.3 KT, Surface Burst.

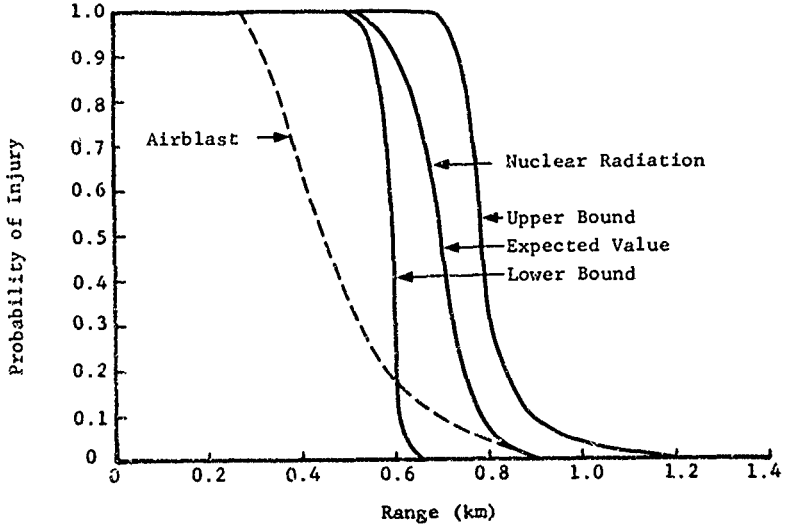

Figure 7.63. Injury Damage Function, People in Residences, 1 KT, Surface Burst.

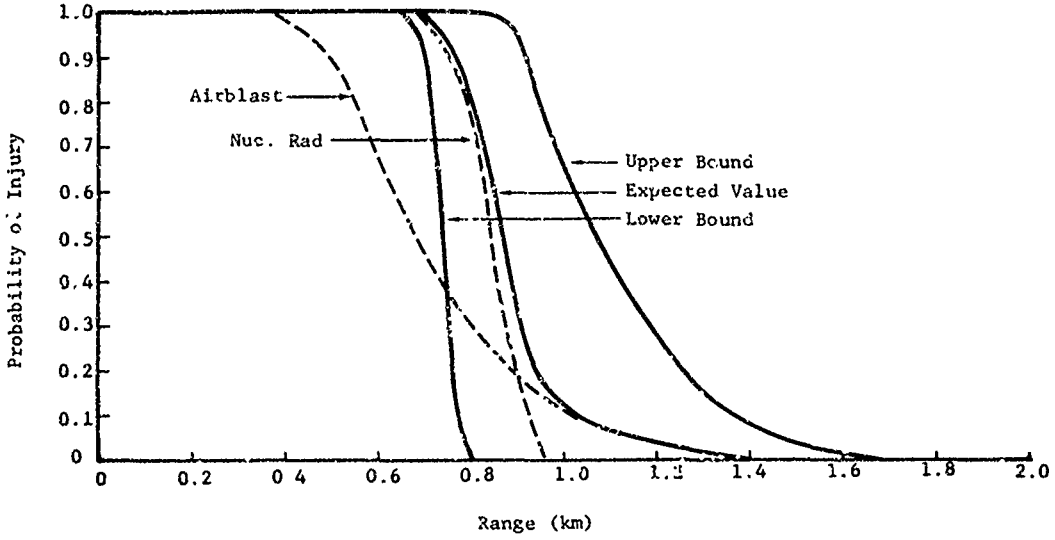

Figure 7.64. Injury Damage Function, People in Residences, 3 KT, Surface Burst.

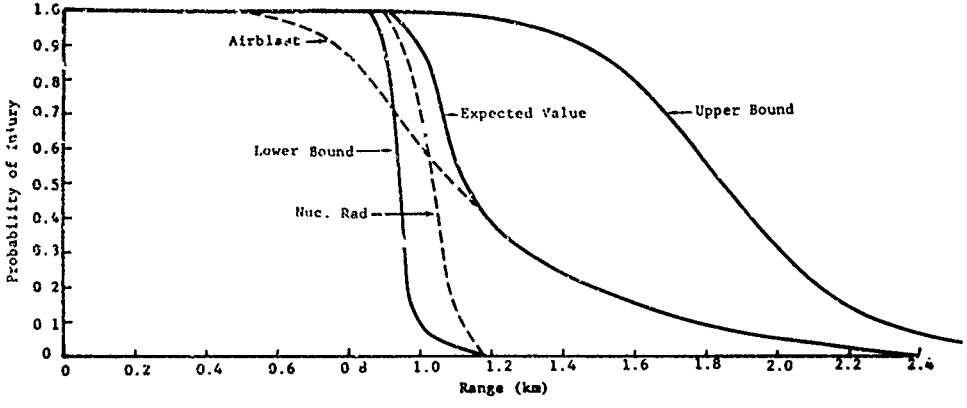

Figure 7.65. Injury Damage Function, People in Residences, 10 KT, Surface Burst.

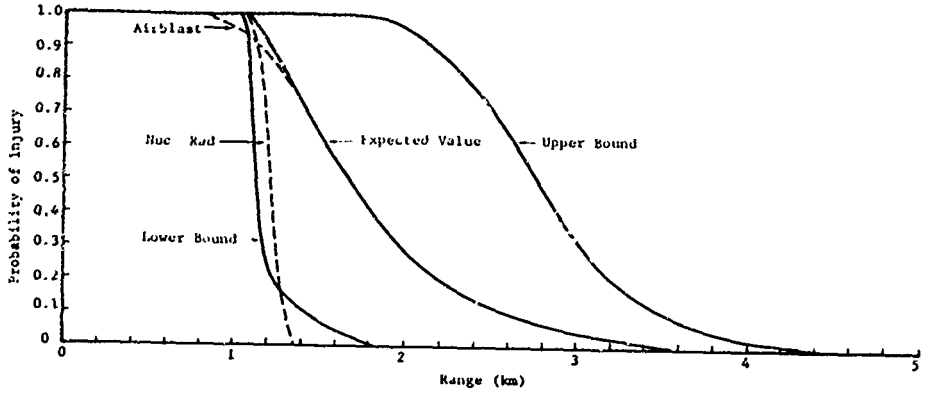

Figure 7.66. Injury Damage Function, People in Residences, 30 KT, Surface Burst.

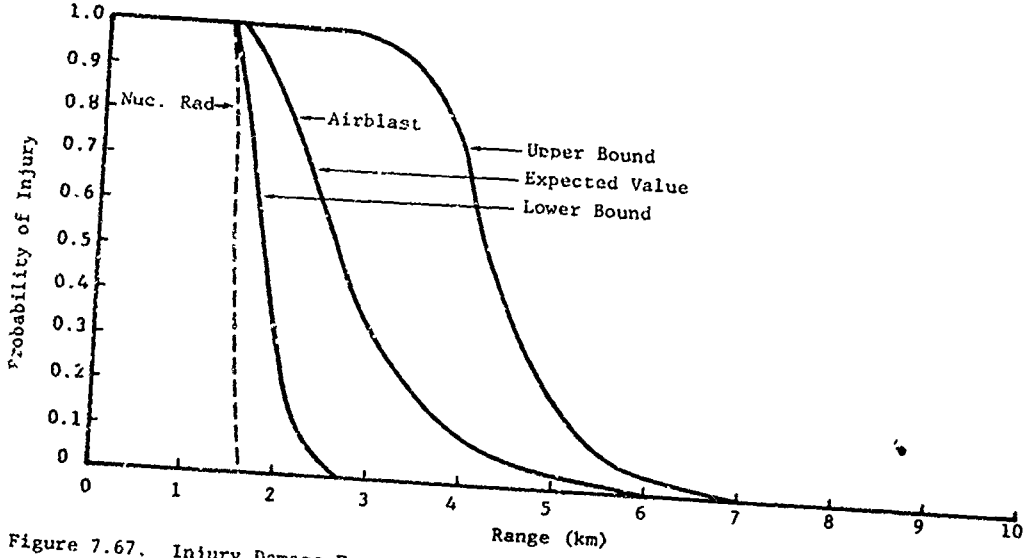

Figure 7.67. Injury Damage Function, People in Residences, 100 KT, Surface Burst.

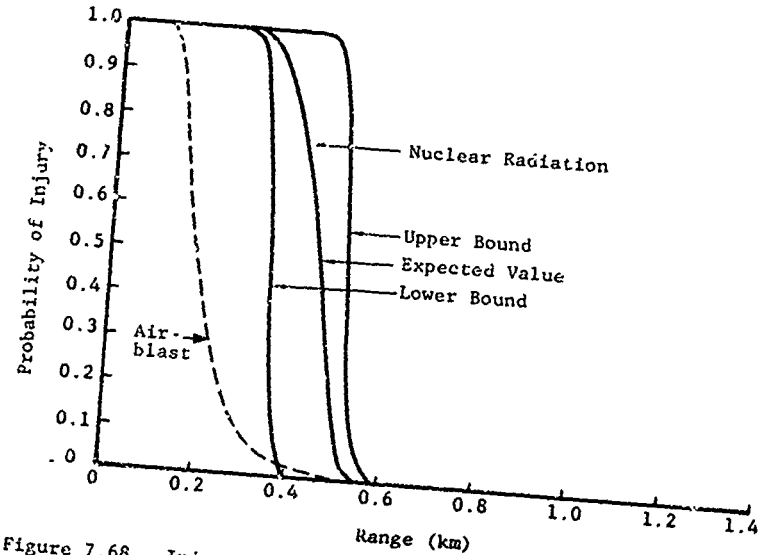

Figure 7.68. Injury Damage Function, People in Residences, 0.1 KT, 200 ft/KT1/3 Scaled Height of Burst.

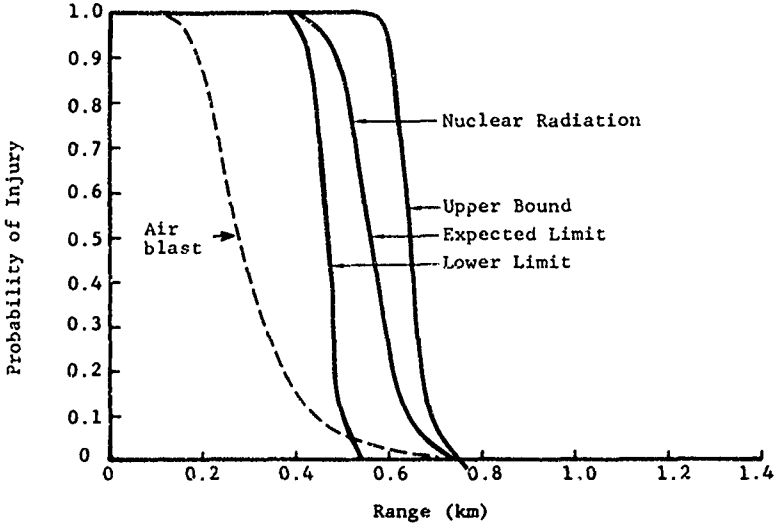

Figure 7.69. Injury Damage Function, People in Residences, 0.3 KT, 200 ft/KT$^{1/3}$ Scaled Height of Burst.

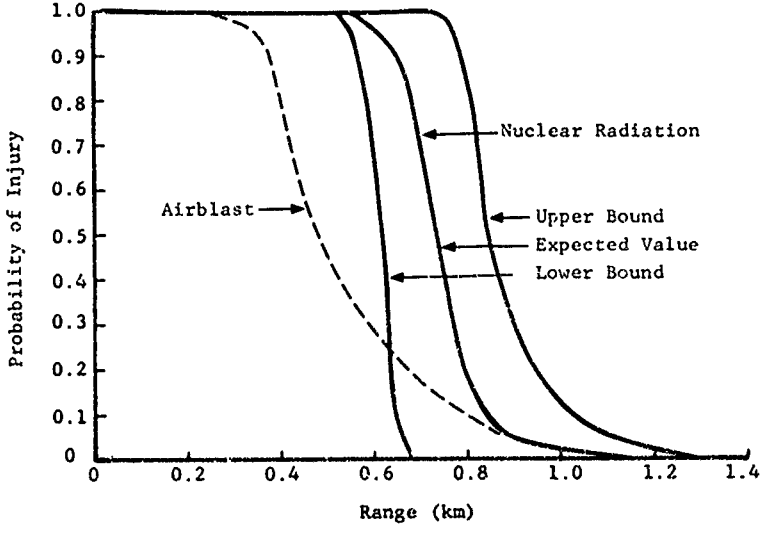

Figure 7.70. Injury Damage Function, People in Residences, 1 KT, 200 ft/KT$^{1/3}$ Scaled Height of Burst.

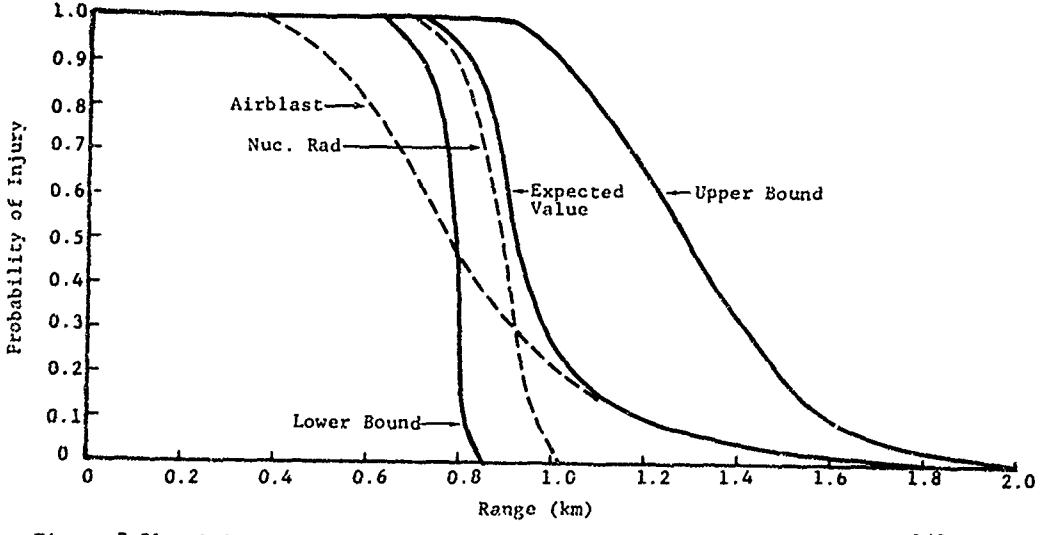

Figure 7.71. Injury Damage Function, People in Residences, 3 KT, 200 ft/KT$^{1/3}$ Scaled Height of Burst.

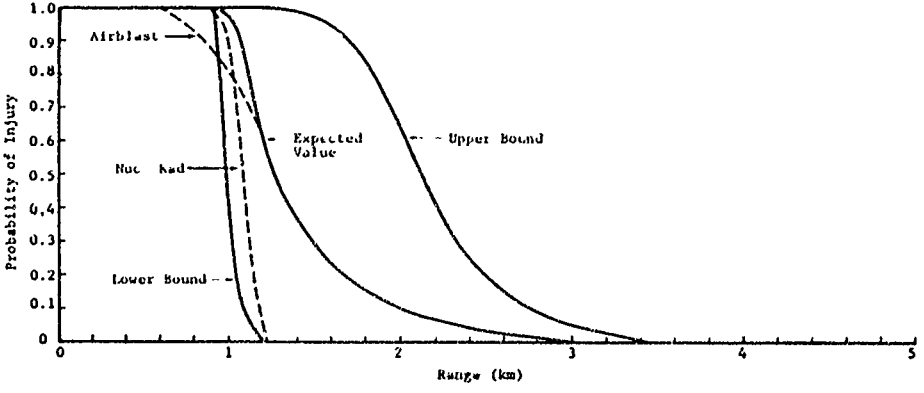

Figure 7.72. Injury Damage Function, People in Residences, 10 KT, 200 ft/KT$^{1/3}$ Scaled Height of Burst.

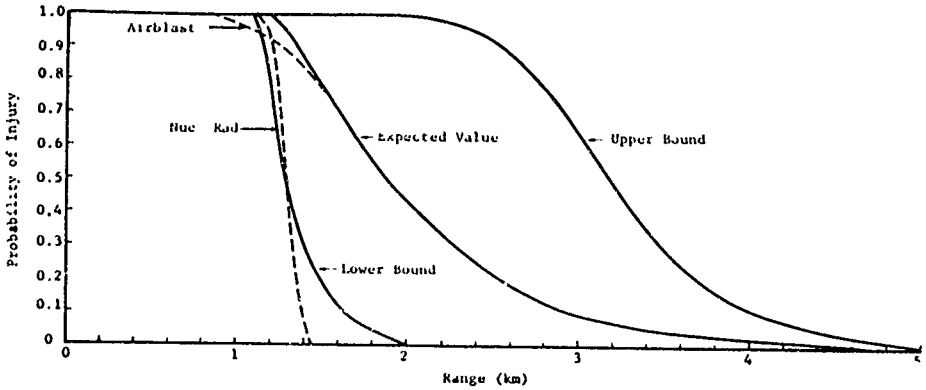

Figure 7.73. Injury Damage Function, People in Residences, 30 KT, 200 ft/KT$^{1/3}$ Scaled Height of Burst.

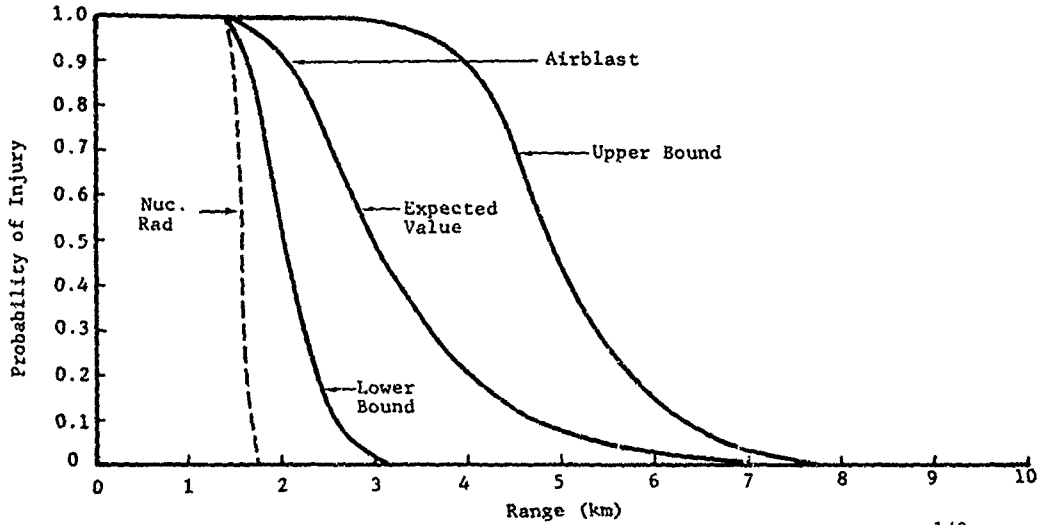

Figure 7.74. Injury Damage Function, People in Residences, 100 KT, 200 ft/KT$^{1/3}$ Scaled Height of Burst.

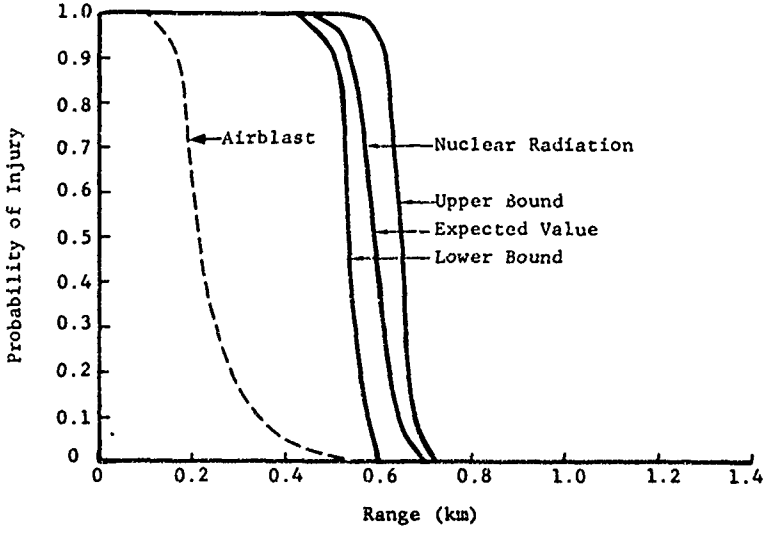

Figure 7.75. Injury Damage Function, People in Residences, 0.1 KT, 600 ft/KT$^{1/3}$ Scaled Height of Burst.

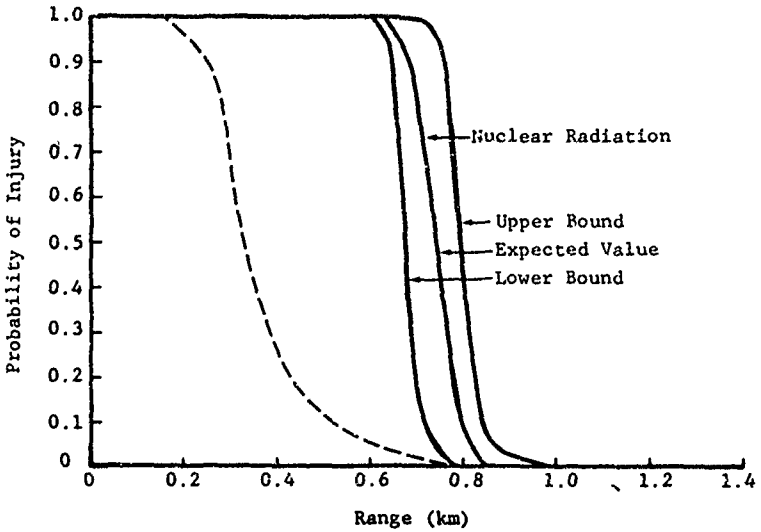

Figure 7.76. Injury Damage Function, People in Residences, 0.3 KT, 600 ft/$KT^{1/3}$ Scaled Height of Burst.

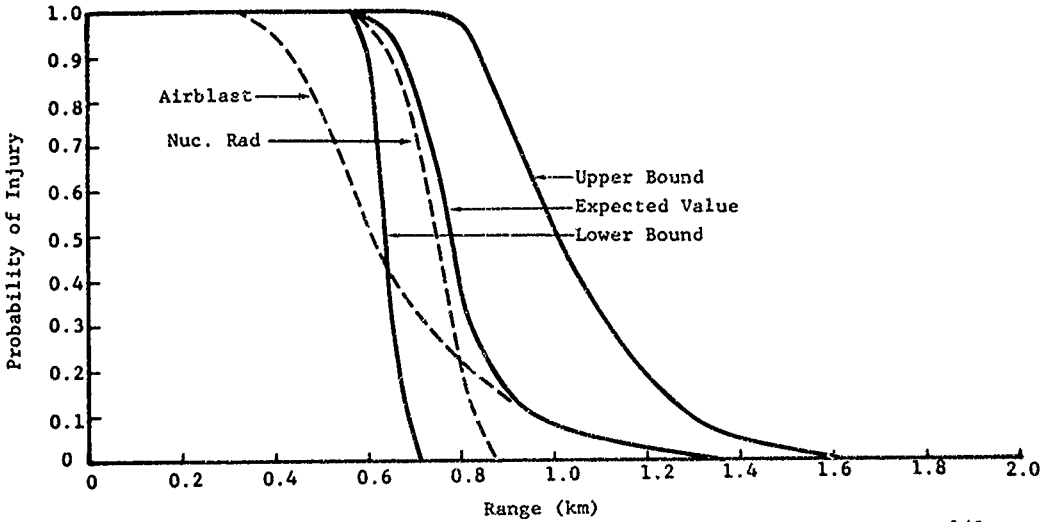

Figure 7.77. Injury Damage Function, People in Residences, 1.0 KT, 600 ft/KT$^{1/3}$ Scaled Height of Burst.

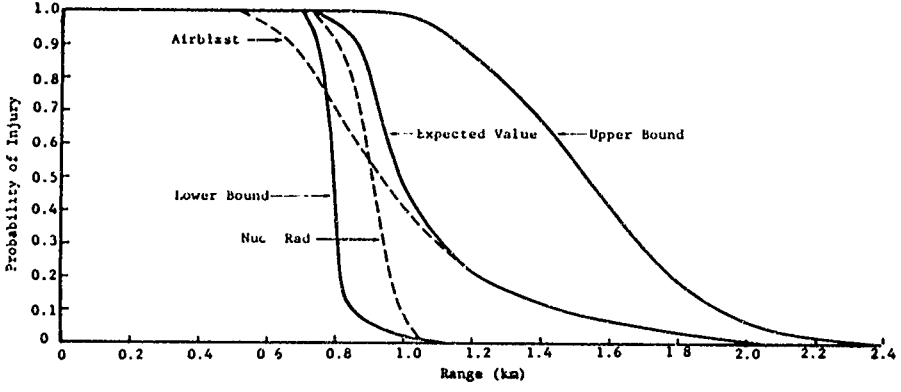

Figure 7.78. Injury Damage Function, People in Residences, 3 KT, 600 ft/$KT^{1/3}$ Scaled Height of Burst.

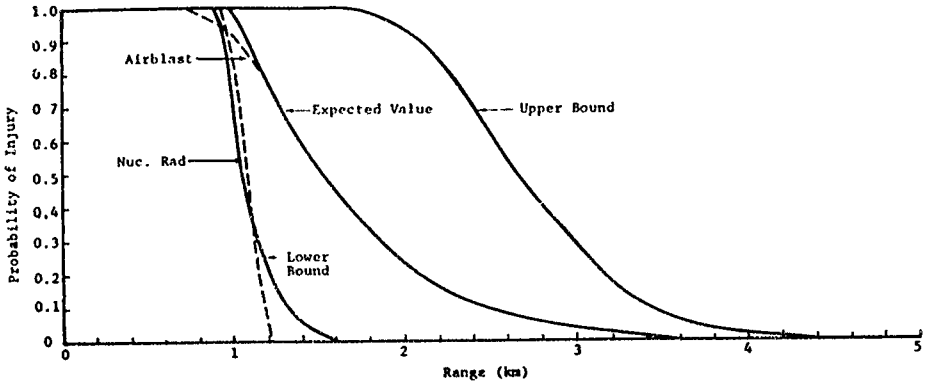

Figure 7.79. Injury Damage Function, People in Residences. 10 KT, 600 ft/KT$^{1/3}$ Scaled Height of Burst.

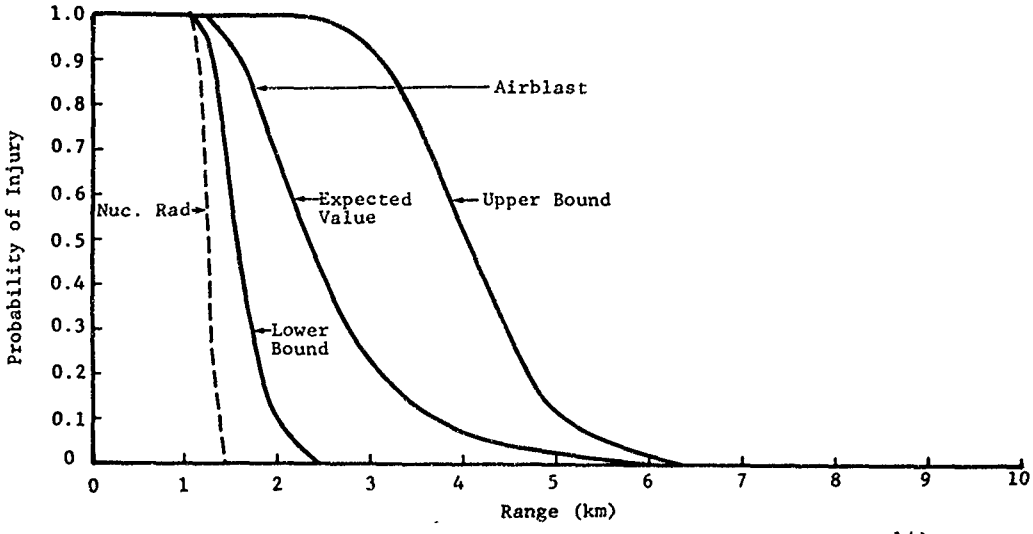

Figure 7.80. Injury Damage Function, People in Residences 30 KT, 600 ft/KT$^{1/3}$ Scaled Height of Burst.

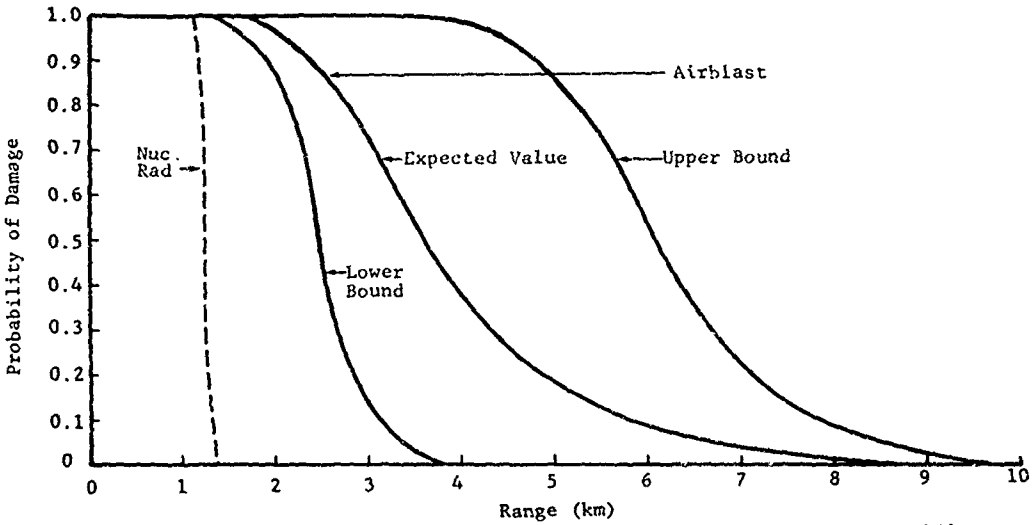

Figure 7.81. Injury Damage Function, People in Residences, 100 KT, 600 ft/KT$^{1/3}$ Scaled Height of Burst.

7.2.4 Fatality Damage Functions, People in Residences

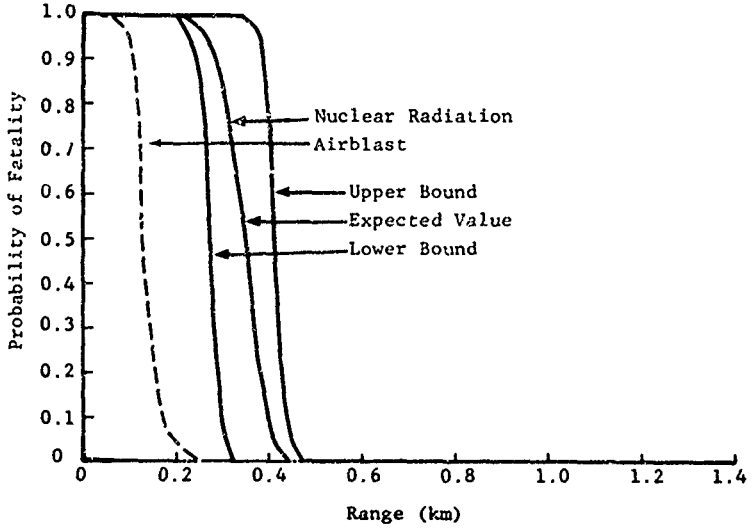

Figure 7.82. Fatality Damage Function, People in Residences, 0.1 KT, Surface Burst.

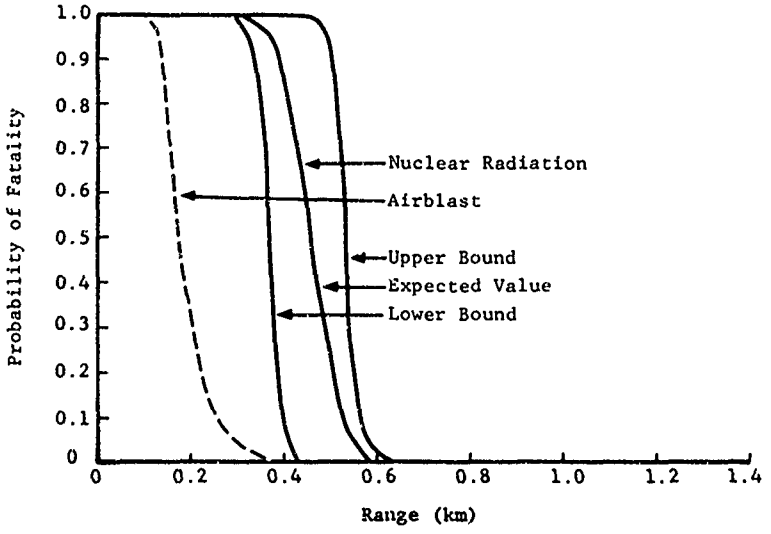

Figure 7.83. Fatality Damage Function, People in Residences, 0.3 KT, Surface Burst.

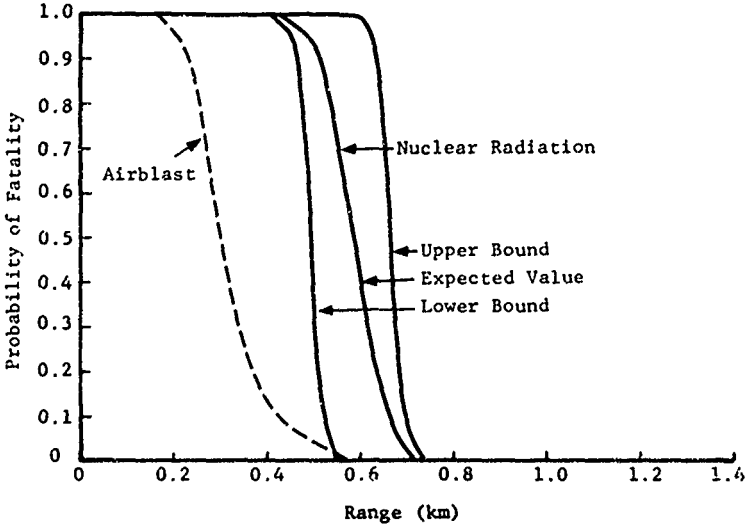

Figure 7.84. Fatality Damage Function, People in Residences, 1 KT, Surface Burst.

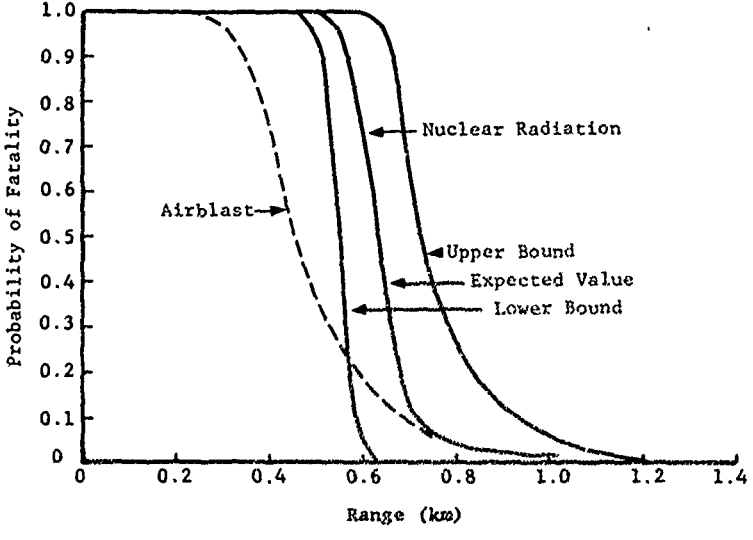

Figure 7.85. Fatality Damage Function, People in Residences, 3 KT Surface Burst.

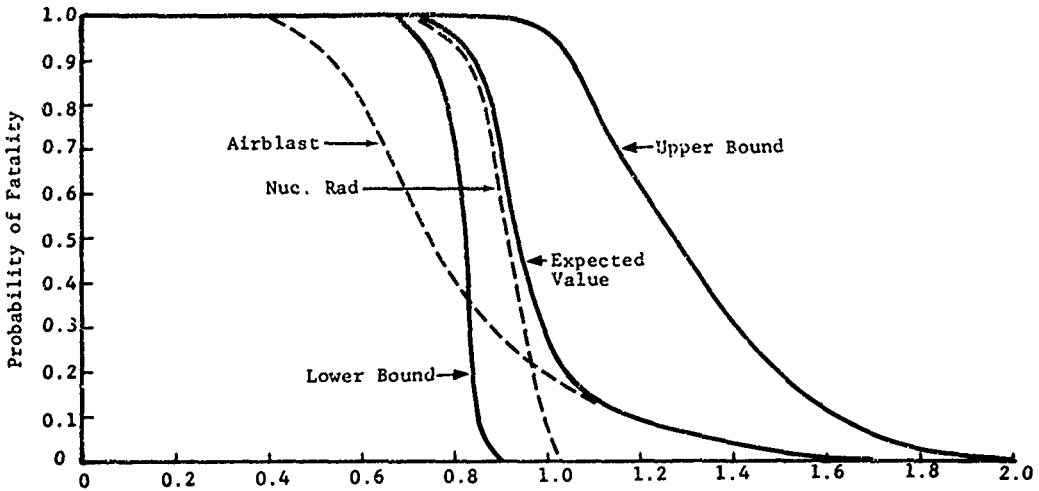

Figure 7.86. Fatality Damage Function, People in Residences, 10 KT, Surface Burst.

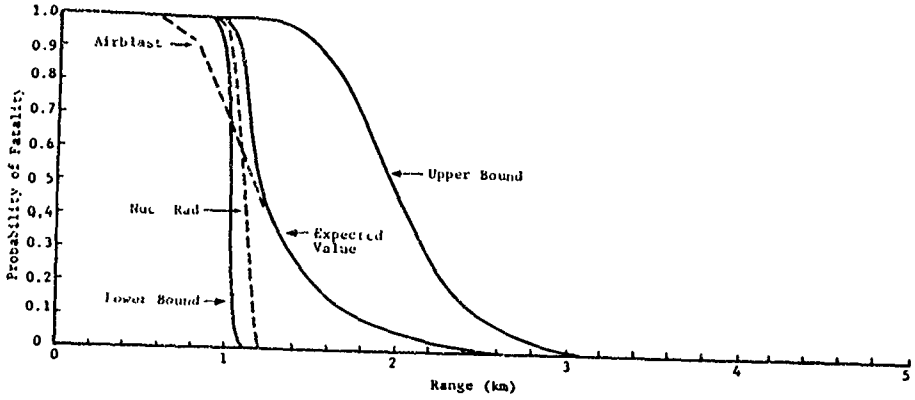

Figure 7.87. Fatality Damage Function, People in Residences, 30 KT, Surface Burst.

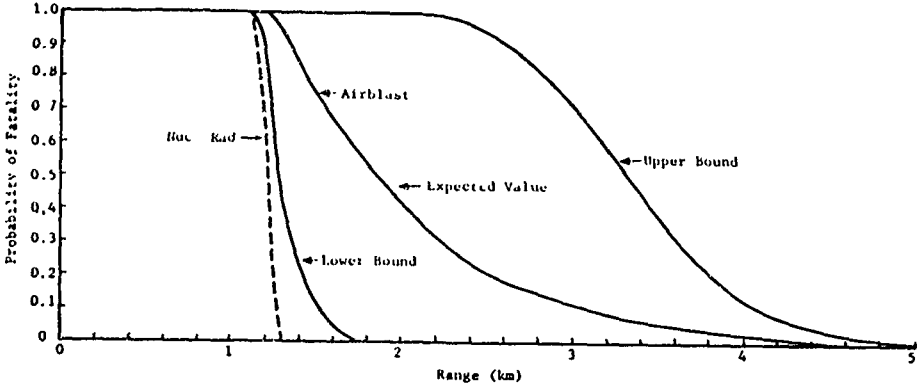

Figure 7.88. Fatality Damage Function, People in Residences, 100 KT, Surface Burst.

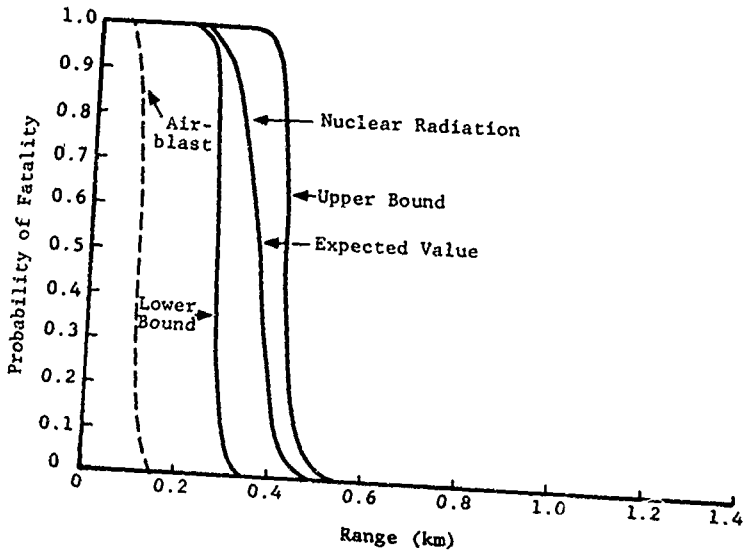

Figure 7.89. Fatality Damage Function, People in Residences, 0.1 KT, 200 ft/KT$^{1/3}$ Scaled Height of Burst.

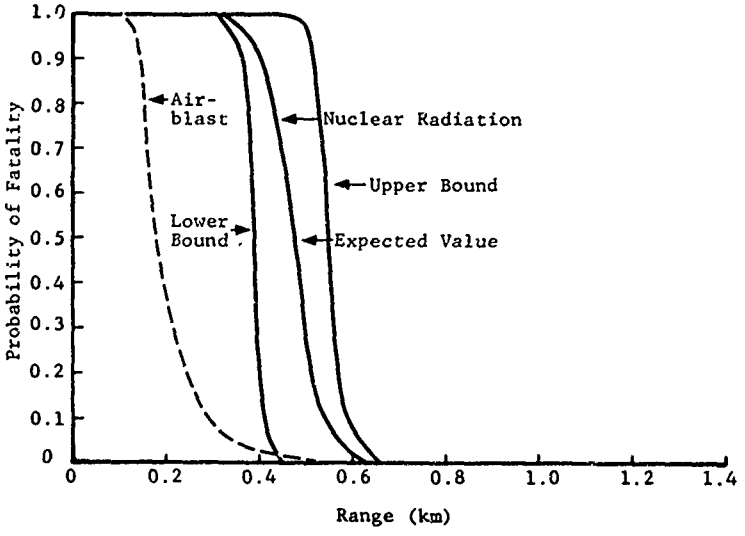

Figure 7.90. Fatality Damage Function, People in Residences, 0.3 KT, 200 ft/KT$^{1/3}$ Scaled Height of Burst.

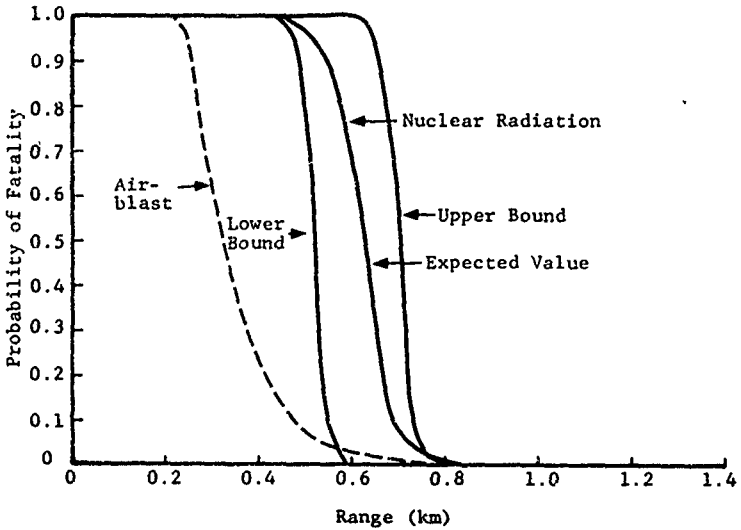

Figure 7.91. Fatality Damage Function, People in Residences, 1 KT, 200 ft/KT$^{1/3}$ Scaled Height of Burst.

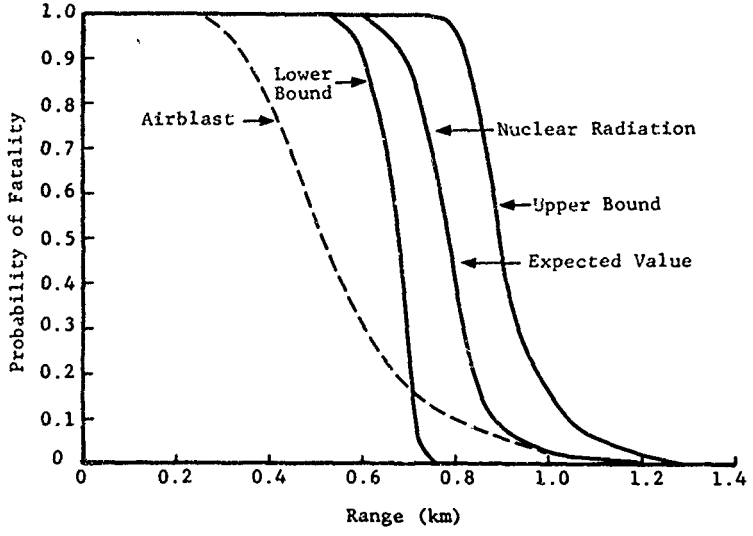

Figure 7.92. Fatality Damage Function, People in Residences, 3 KT, 200 ft/KT$^{1/3}$ Scaled Height of Burst.

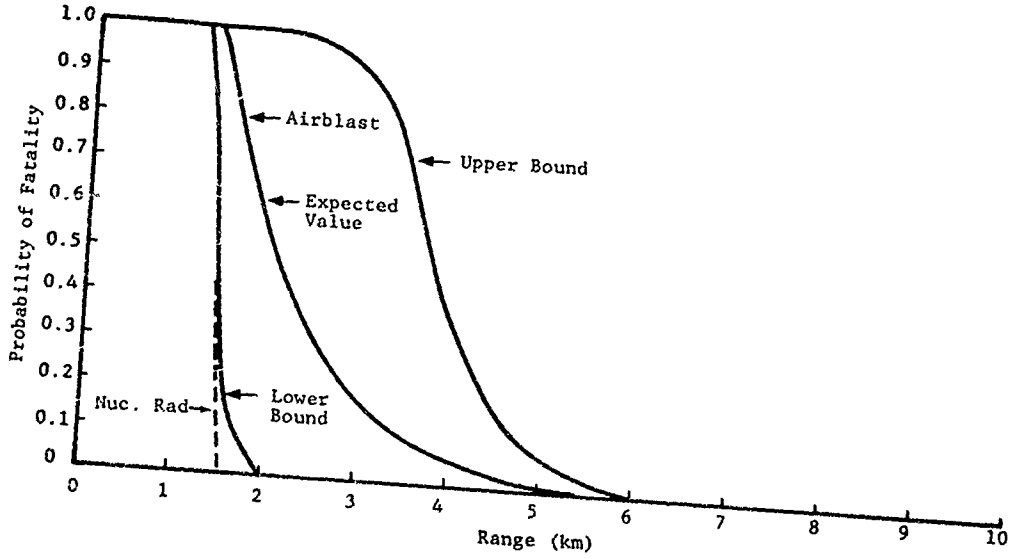

Figure 7.93. Fatality Damage Function, People in Residences, 10 KT, 200 ft/KT$^{1/3}$ Scaled Height of Burst.

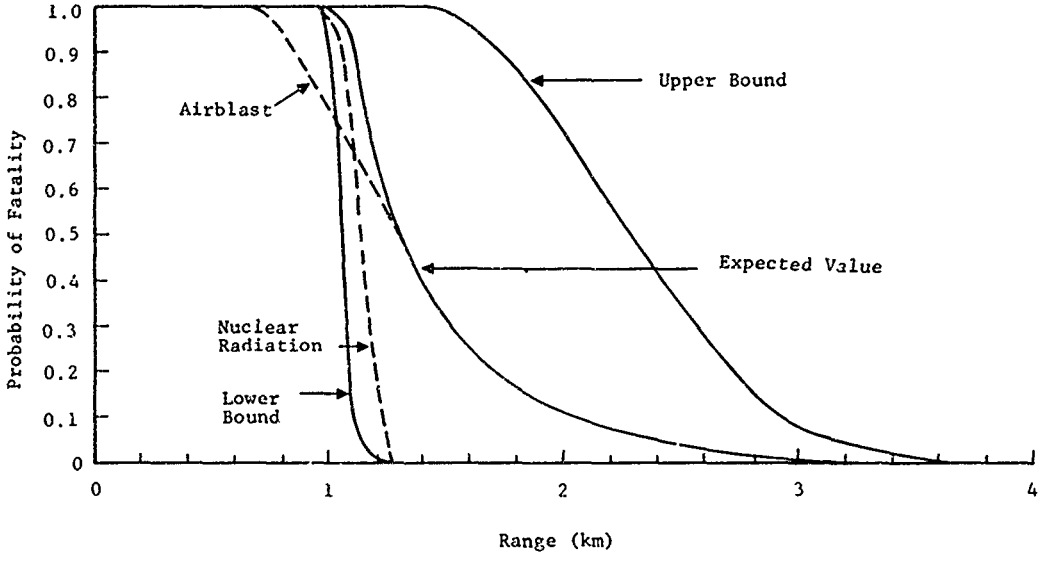

Figure 7.94. Fatality Damage Function, People in Residences, 30 KT, 200 ft/KT$^{1/3}$ Scaled Height of Burst.

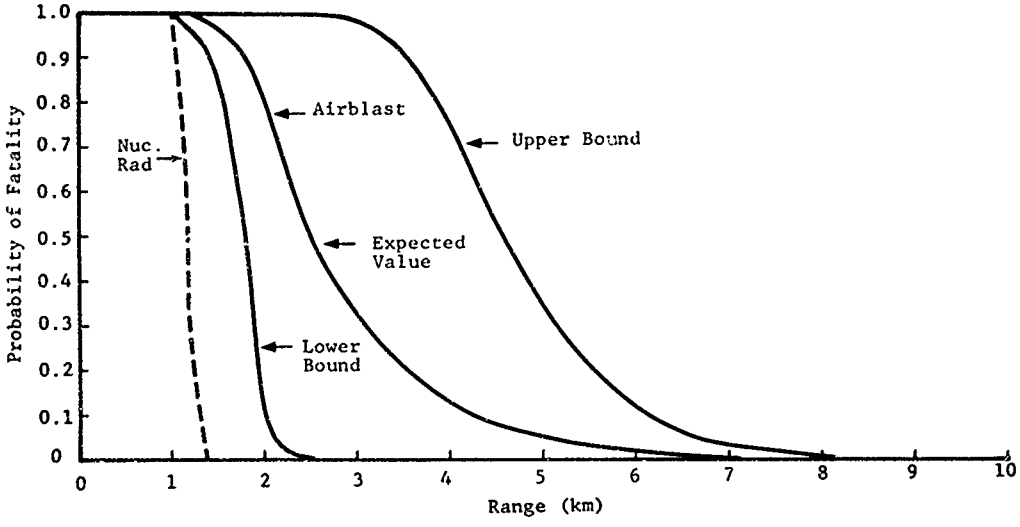

Figure 7.95. Fatality Damage Function, People in Residences, 100 KT, 200 ft/KT$^{1/3}$ Scaled Height of Burst.

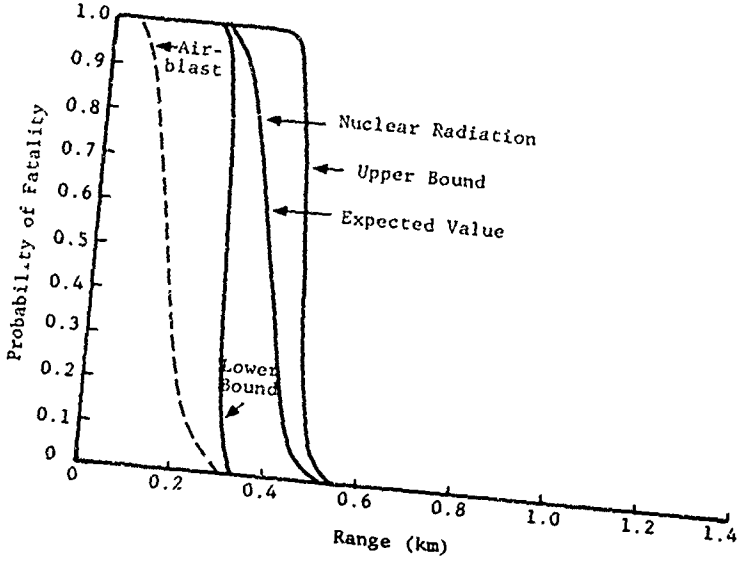

Figure 7.96. Fatality Damage Function, People in Residences, 0.1 KT, 600 ft/$KT^{1/3}$ Scaled Height of Burst

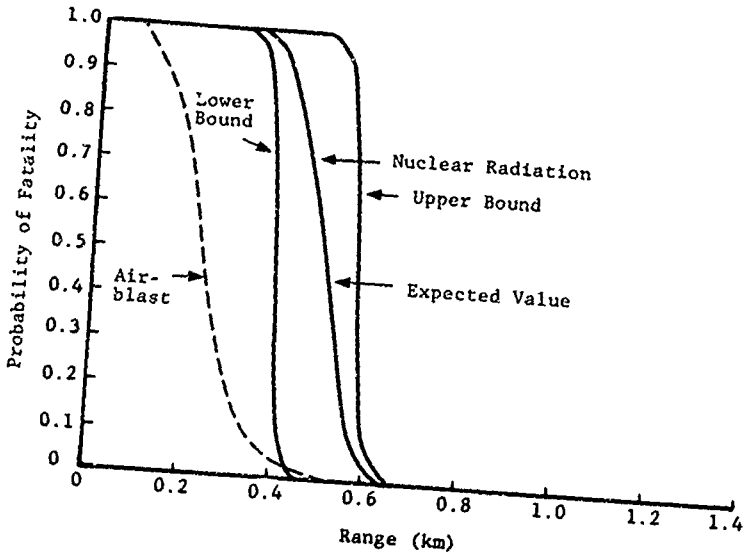

Figure 7.97. Fatality Damage Function, People in Residences, 0 3 KT, 600 ft/KT$^{1/3}$ Scaled Height of Burst.

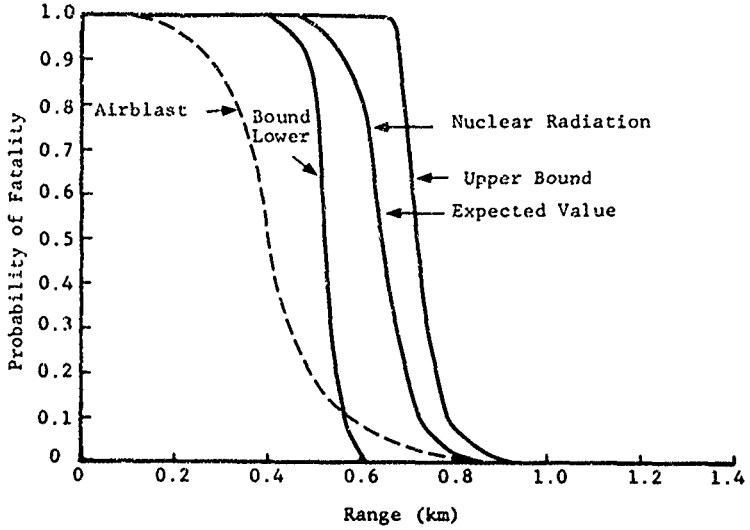

Figure 7.98. Fatality Damage Function, People in Residences, 1 KT, 600 ft/KT$^{1/3}$ Scaled Height of Burst.

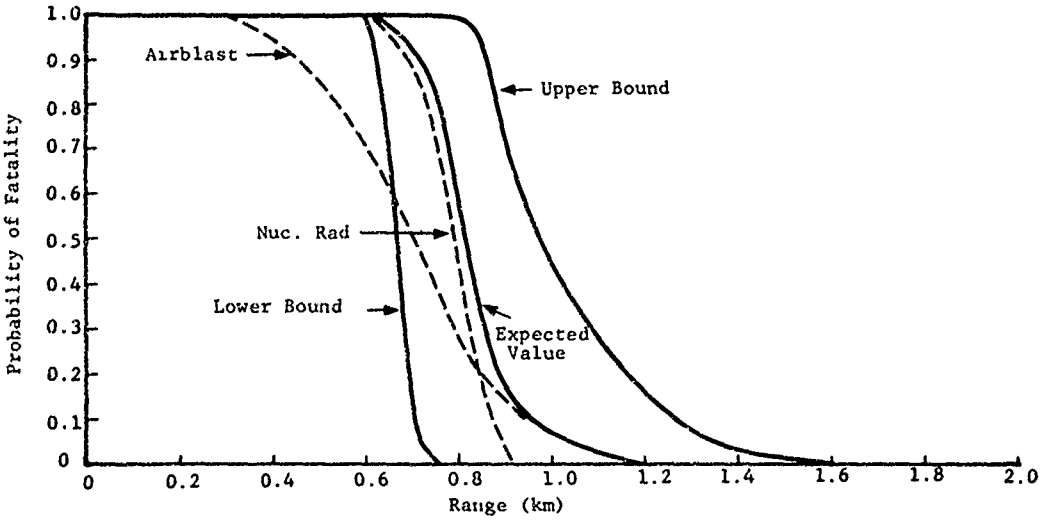

Figure 7.99. Fatality Damage Function, People in Residences, 3 KT, 600 ft/$KT^{1/3}$ Scaled Height of Burst.

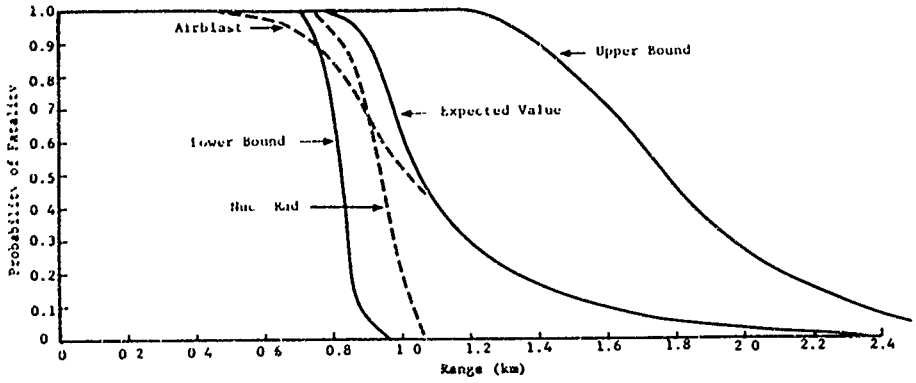

Figure 7.100. Fatality Damage Function, People in Residences, 10 KT, 600 ft/KT$^{1/3}$ Scaled Height of Burst.

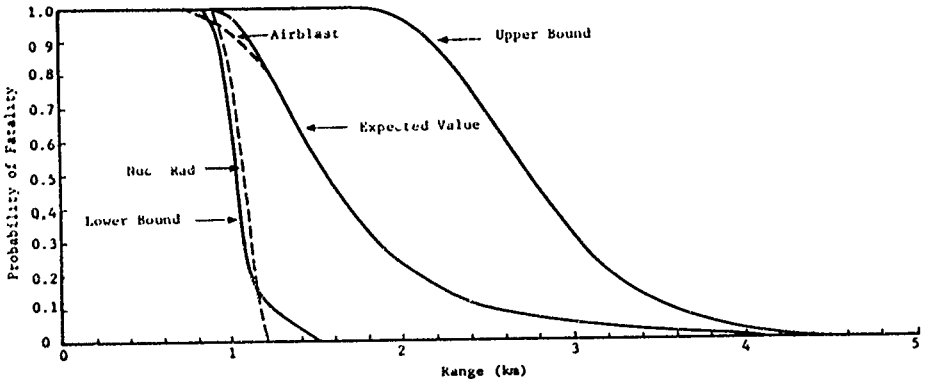

Figure 7.101. Fatality Damage Function, People in Residences, 30 KT, 600 ft/KT$^{1/3}$ Scaled Height of Burst.

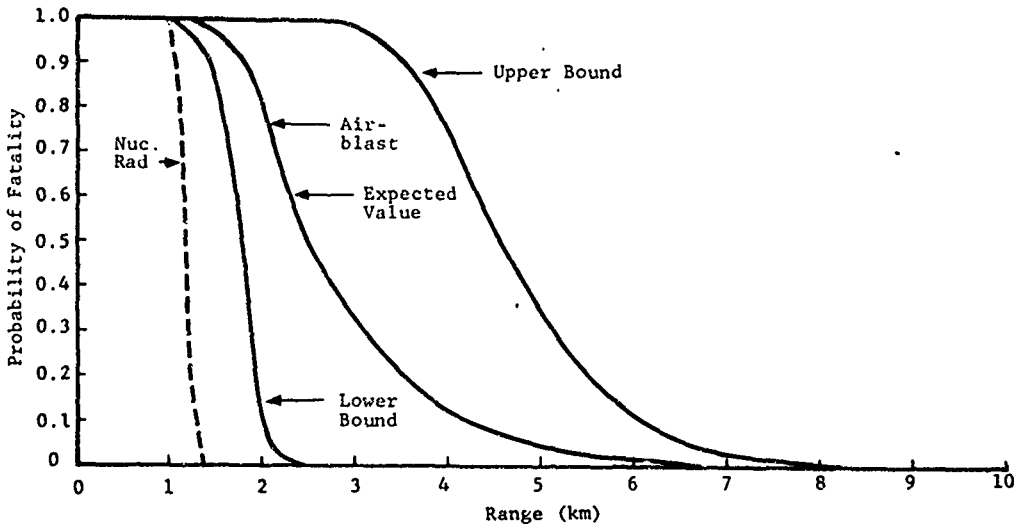

Figure 7.102. Fatality Damage Function, People in Residences, 100 KT, 600 ft/KT$^{1/3}$ Scaled Height of Burst.

7.2.5 Injury Damage Functions, People in Basement

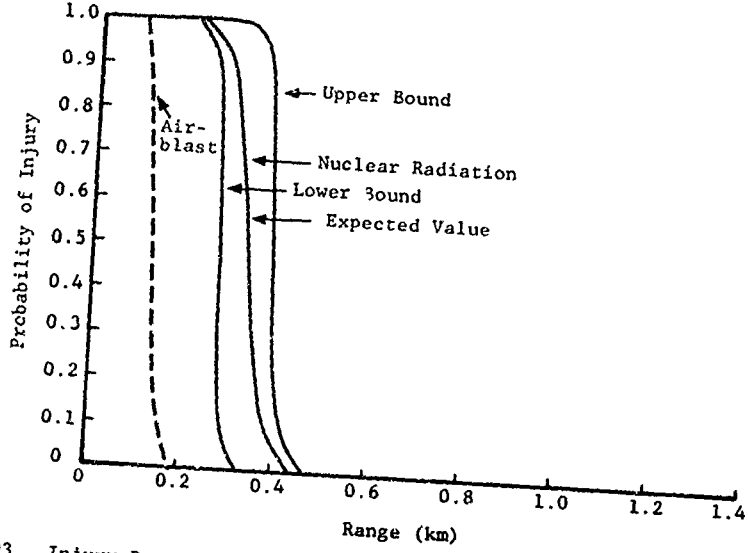

Figure 7.103. Injury Damage Function, People in Basements, 0.1 KT, Surface Burst.

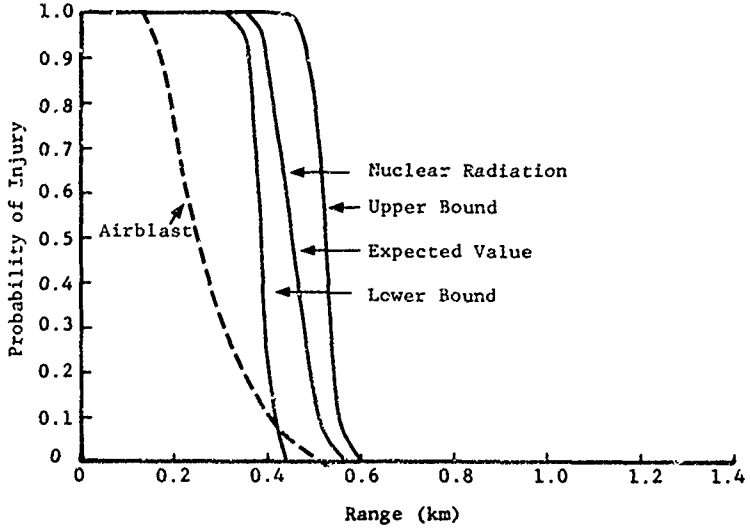

Figure 7.104. Injury Damage Function, People in Basements, 0.3 KT, Surface Burst.

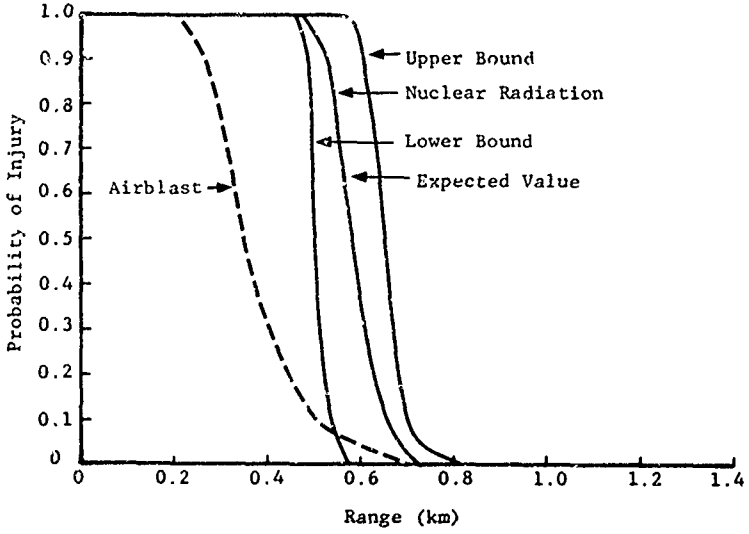

Figure 7.105. Injury Damage Function, People in Basements, 1 KT, Surface Burst.

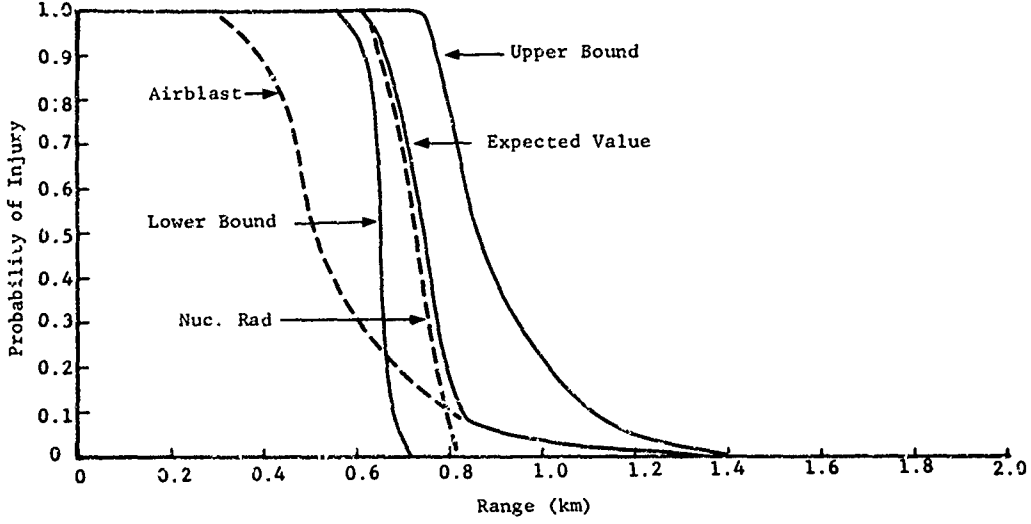

Figure 7.106. Injury Damage Function, People in Basements, 3 KT, Surface Burst.

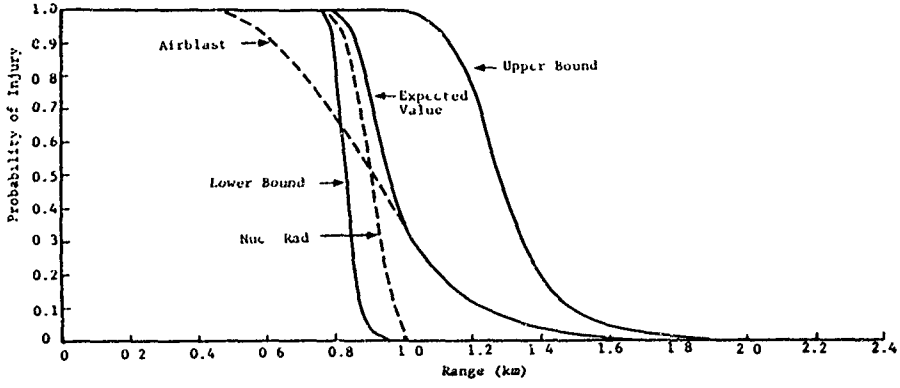

Figure 7.107. Injury Damage Function, People in Basements, 10 KT, Surface Burst.

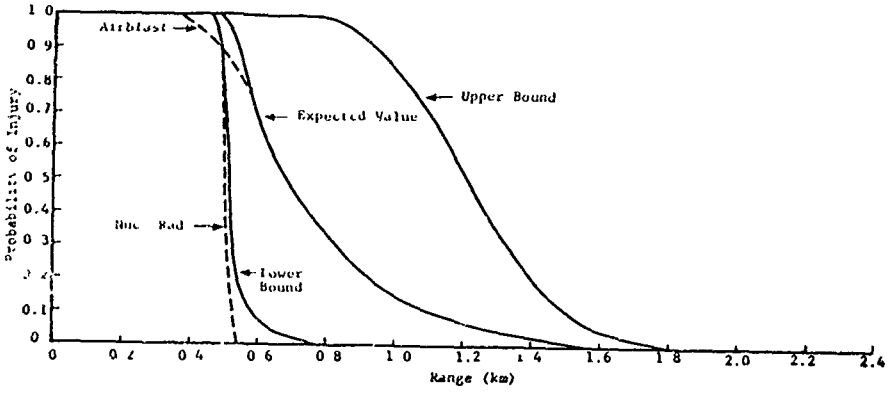

Figure 7.108. Injury Damage Function, People in Basements, 30 KT, Surface Burst.

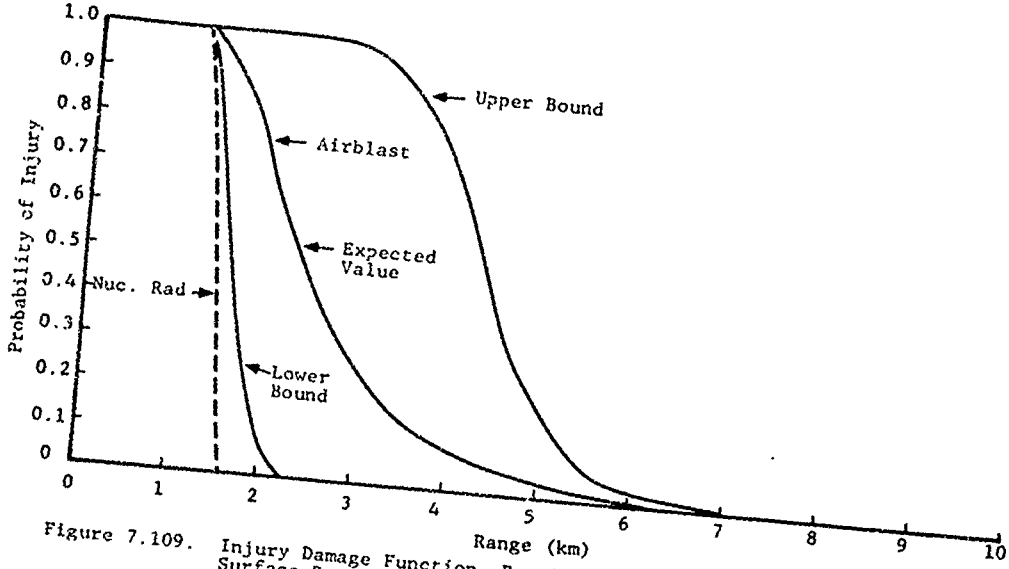

Figure 7.109. Injury Damage Function, People in Basements, 100 KT Surface Burst.

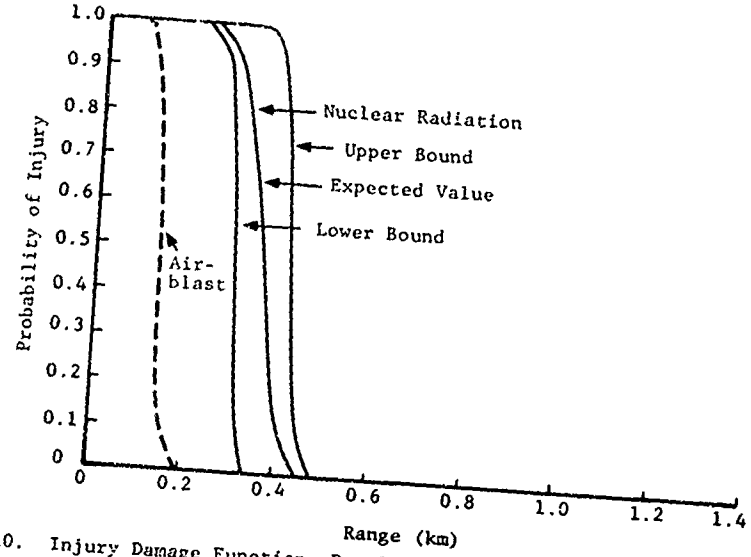

Figure 7.110. Injury Damage Function, People in Basements, 0.1 KT, 200 ft/KT$^{1/3}$ Scaled Height of Burst.

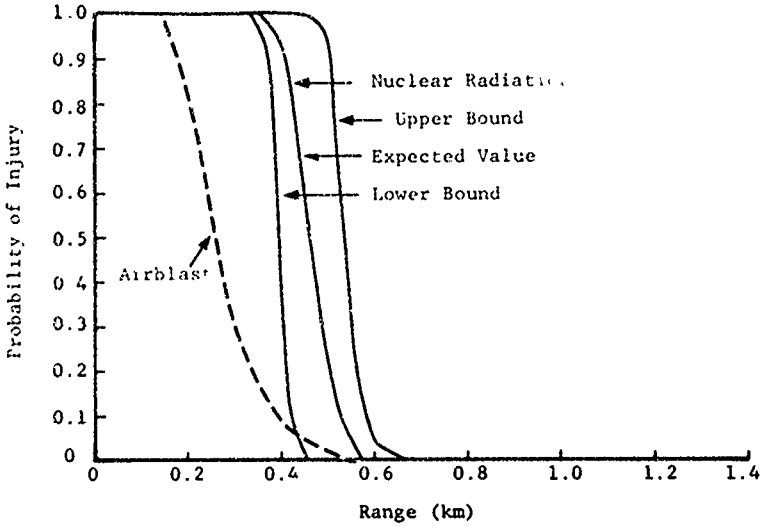

Figure 7.111. Injury Damage Function, People in Basements, 0.3 KT, 200 ft/$KT^{1/3}$ Scaled Height of Burst.

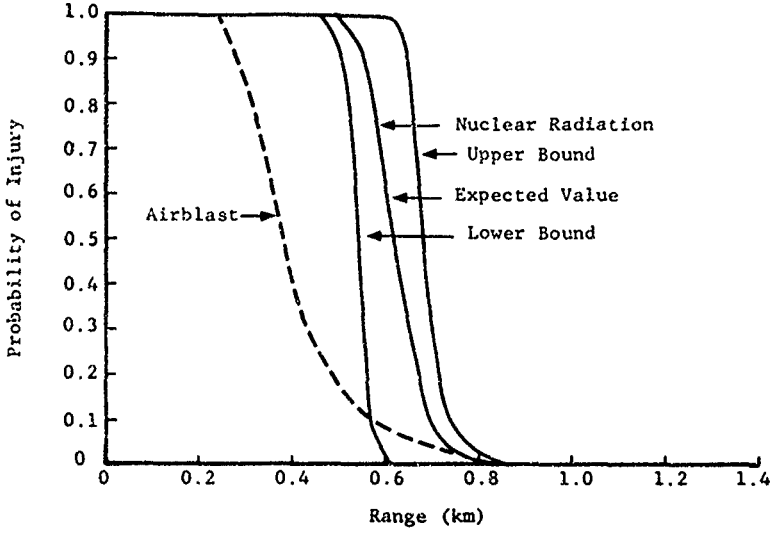

Figure 7.112. Injury Damage Function, People in Basements, 1 KT, 200 ft/KT$^{1/3}$ Scaled Height of Burst.

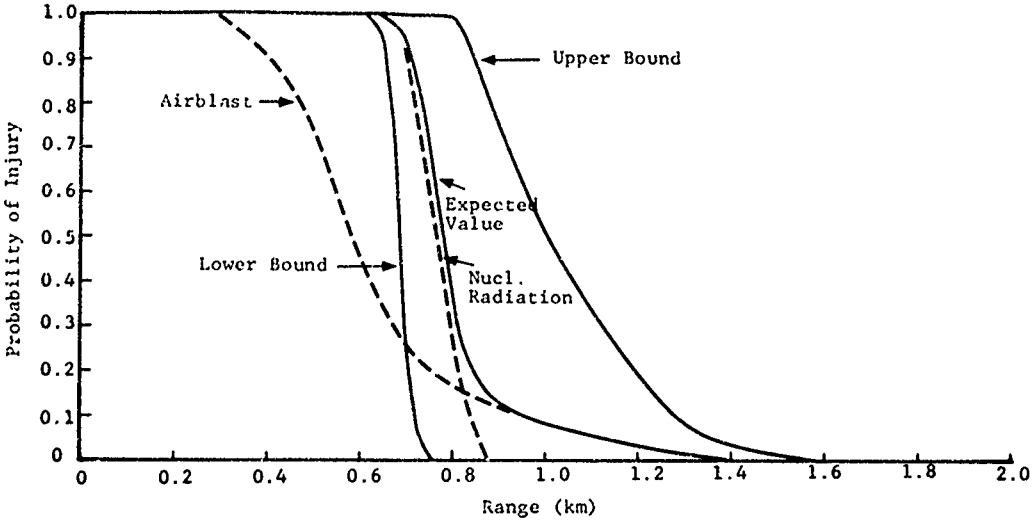

Figure 7.113. Injury Damage Function, People in Basements, 3 KT, 200 ft/KT$^{1/3}$ Scaled Height of Burst.

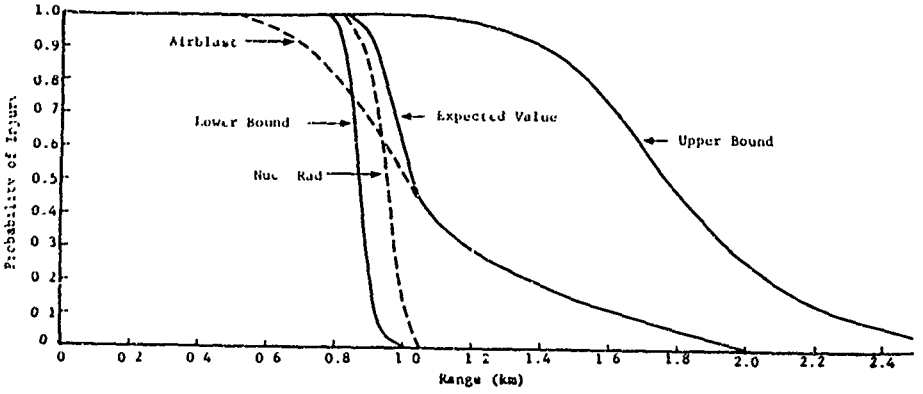

Figure 7.114. Injury Damage Function, People in Basements, 10 KT, 200 ft/KT$^{1/3}$ Scaled Height of Burst.

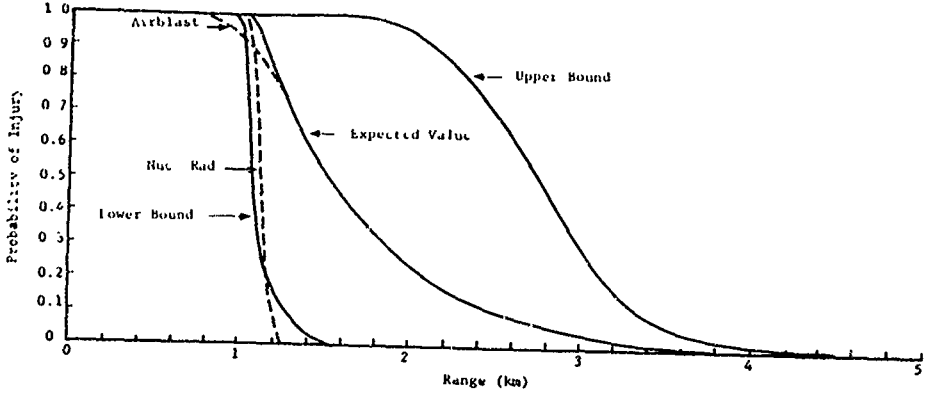

Figure 7.115. Injury Damage Function, People in Basements, 30 KT, 200 ft/KT$^{1/3}$ Scaled Height of Burst.

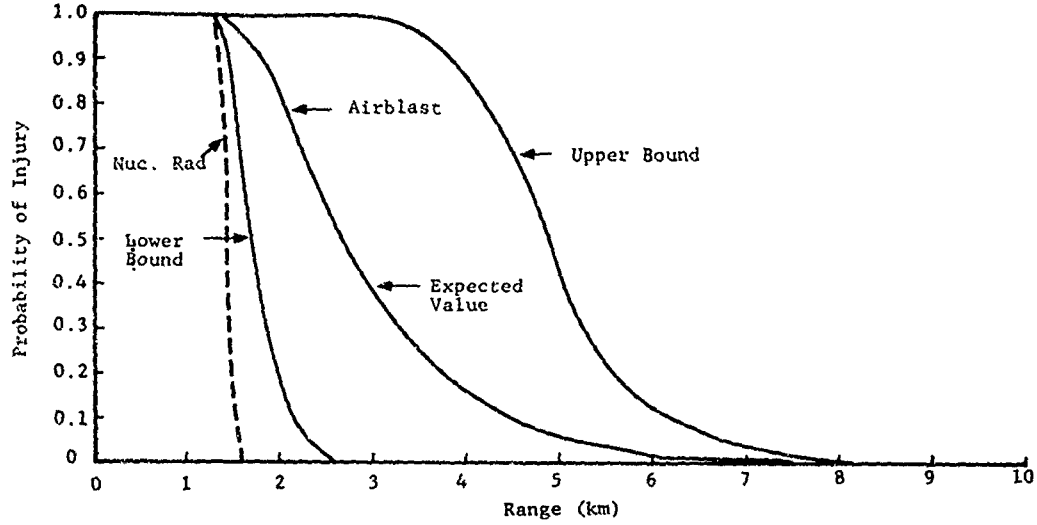

Figure 7.1.16. Injury Damage Function, People in Basements, 100 KT, 200 ft/KT$^{1/3}$ Scaled Height of Burst.

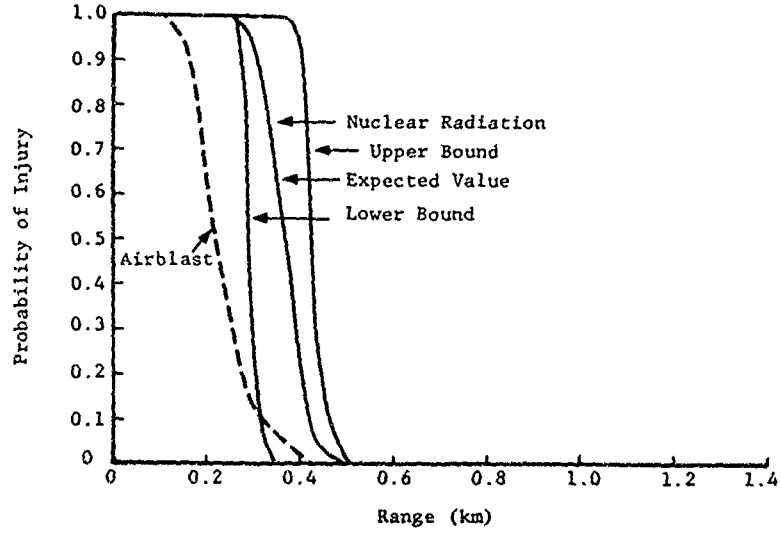

Figure 7.117. Injury Damage Function, People in Basements, 0.1 KT, 600 ft/KT$^{1/3}$ Scaled Height of Burst.

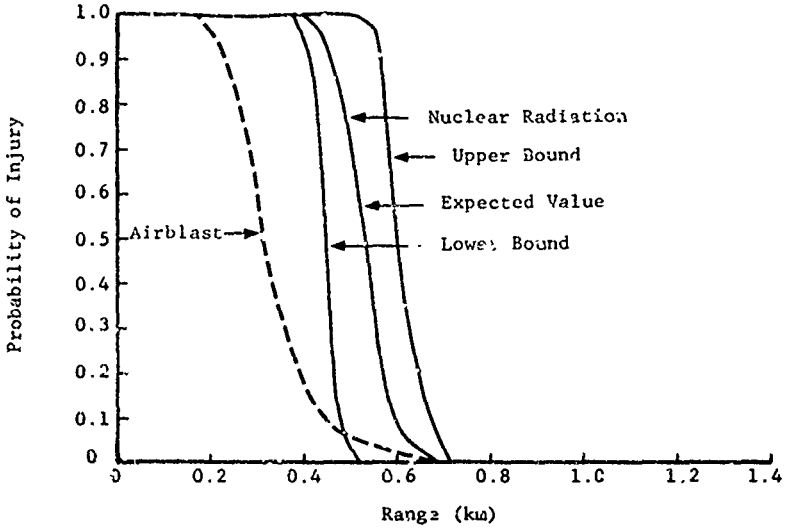

Figure 7.118. Injury Damage Function, People in Basements, 0.3 KT, 600 ft/$KT^{1/3}$ Scaled Height of Burst.

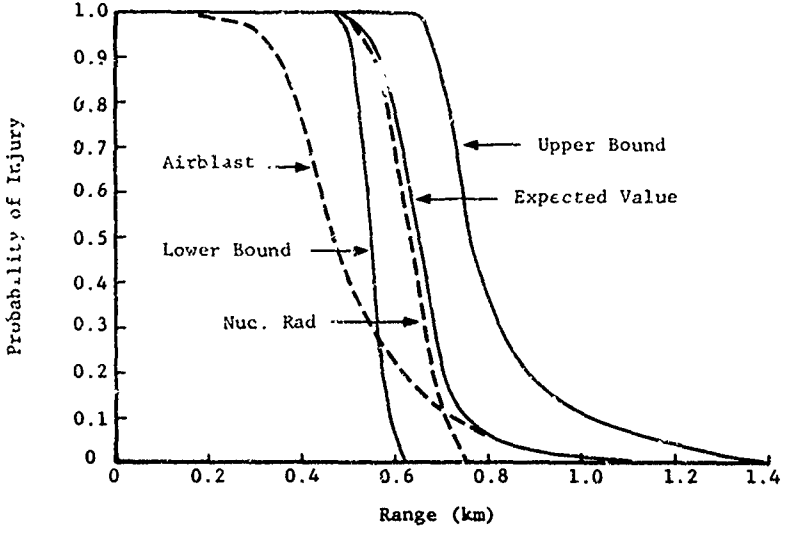

Figure 1.119. Injury Damage Function, People in Basements, 1 KT, 600 ft/KT$^{1/3}$ Scaled Height of Burst.

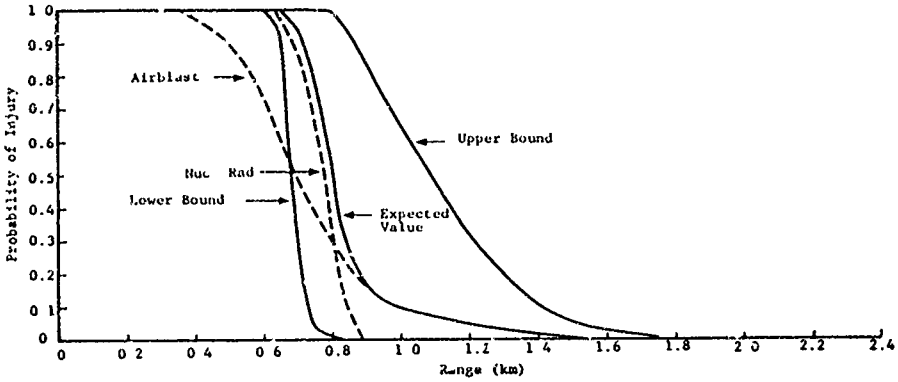

Figure 7.120. Injury Damage Function, People in Basements, 3 KT, 600 ft/KT$^{1/3}$ Scaled Height of Burst.

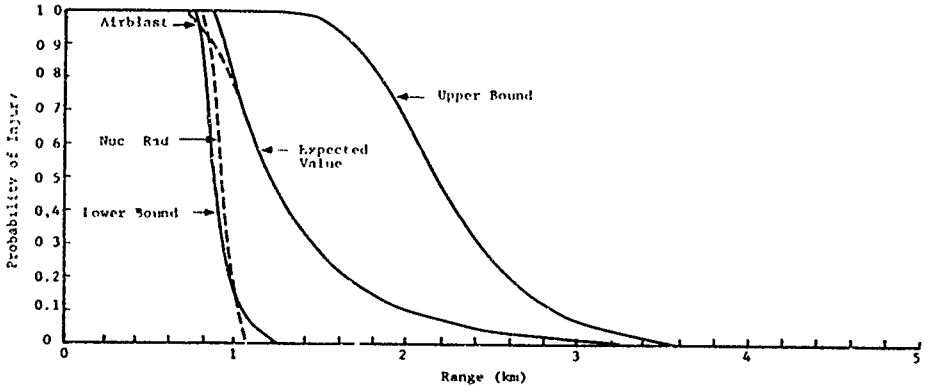

Figure 7.121. Injury Damage Function, People in Basements, 10 KT, 600 ft/kT$^{1/3}$ Scaled Height of Burst.

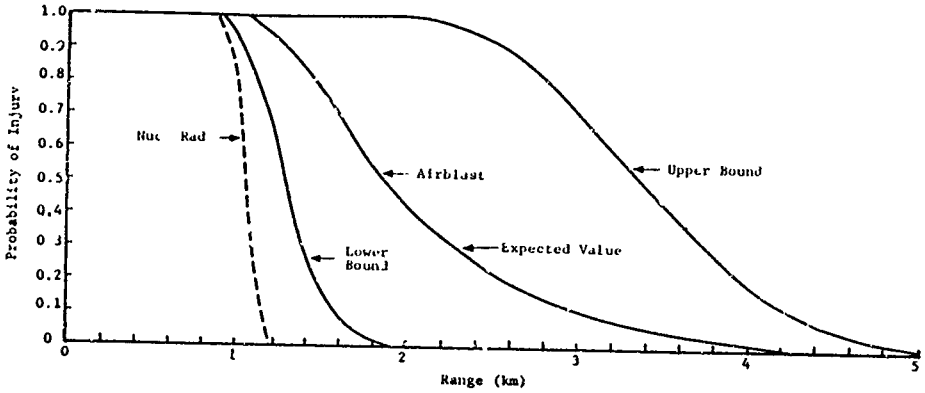

Figure 7.122. Injury Damage Function, People in Basements, 30 KT, 600 ft/KT$^{1/3}$ Scaled Height of Burst.

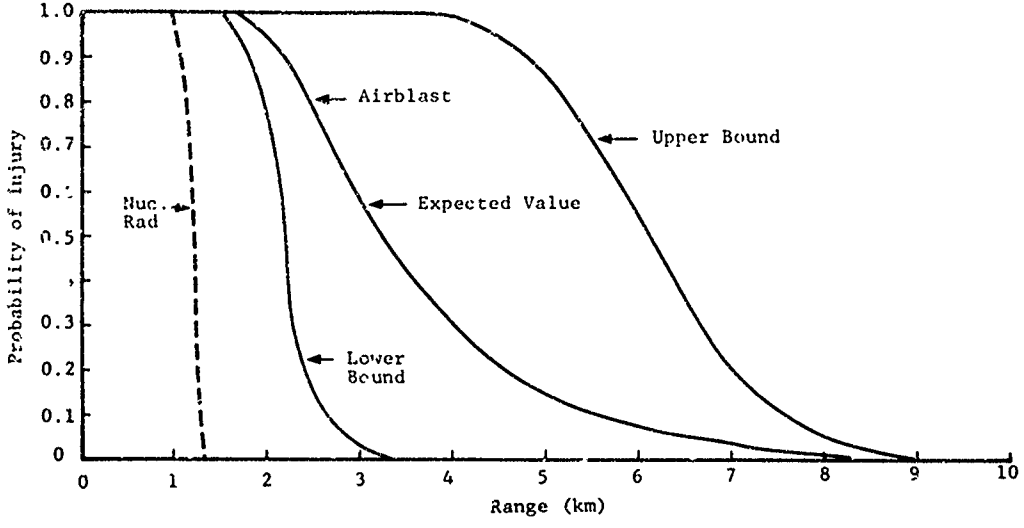

Figure 7.123. Injury Damage Function, People in Basements, 100 KT, 600 ft/$KT^{1/3}$ Scaled Height of Burst.

7.2.6 Fatality Damage Functions, People in Basements

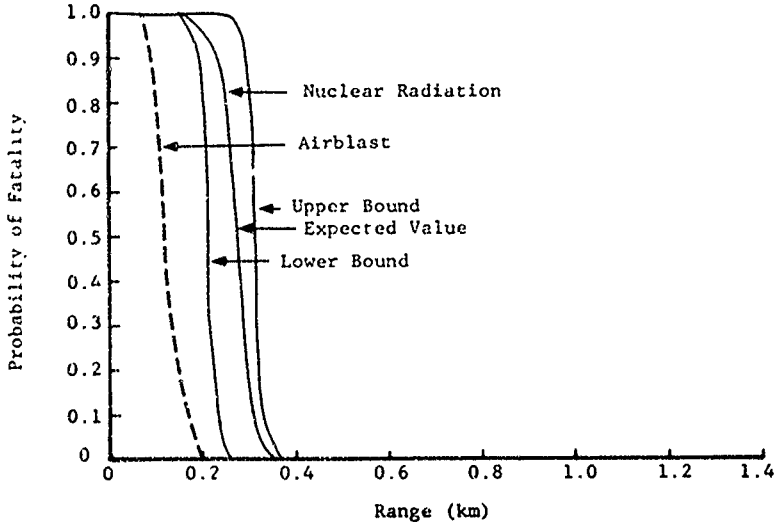

Figure 7.124. Fatality Damage Function, People in Basements, 0.1 KT, Surface Burst.

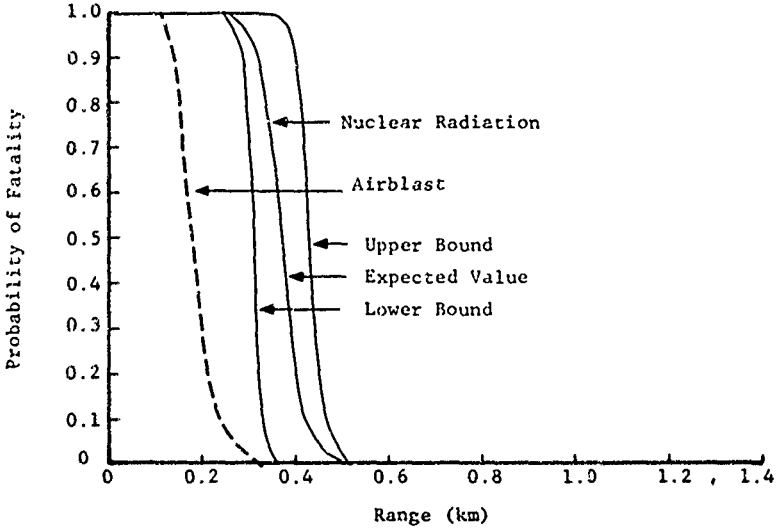

Figure 7.125. Fatality Damage Function, People in Basements, 0.3 KT, Surface Burst.

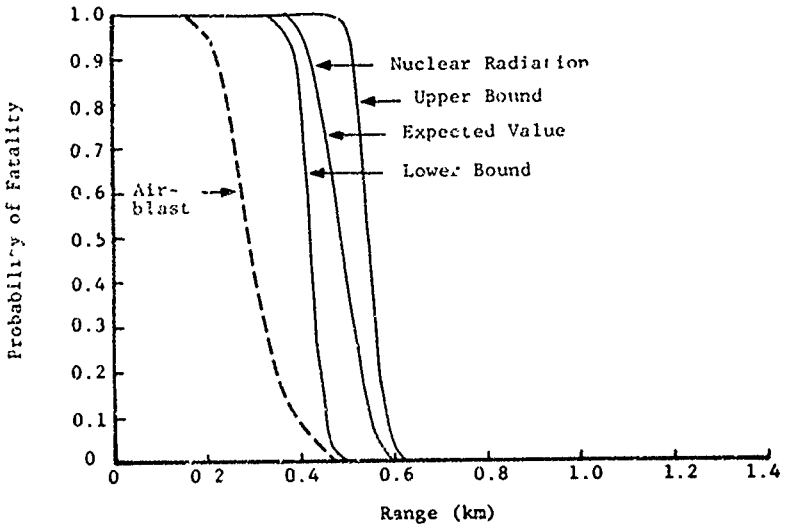

Figure 7.126. Fatality Damage Function, People in Basements, 1 KT, Surface Burst.

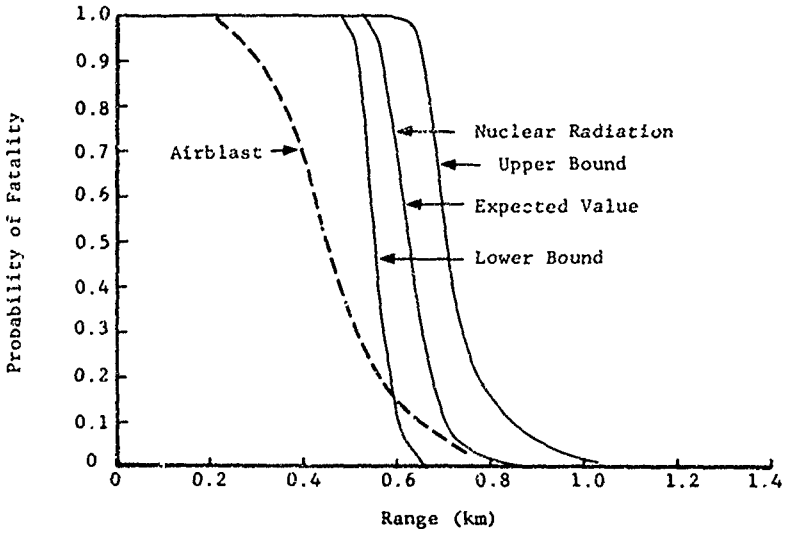

Figure 7.127. Fatality Damage Function, People in Basements, 3 KT, Surface Burst.

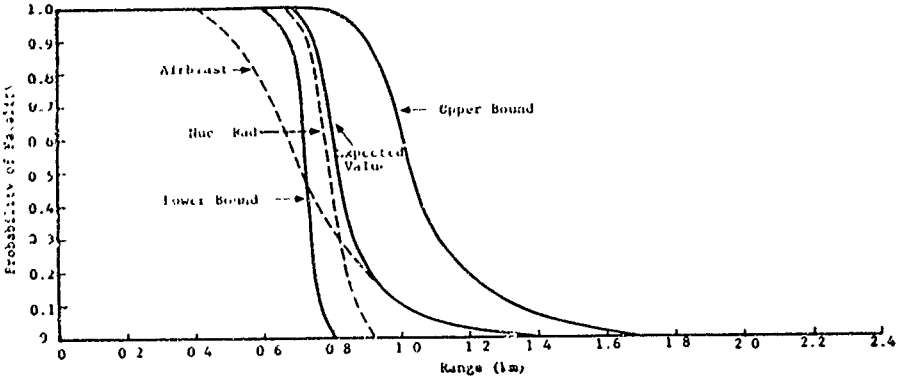

Figure 7.128. Fatality Damage Function, People in Basements, 10 KT, Surface Burst.

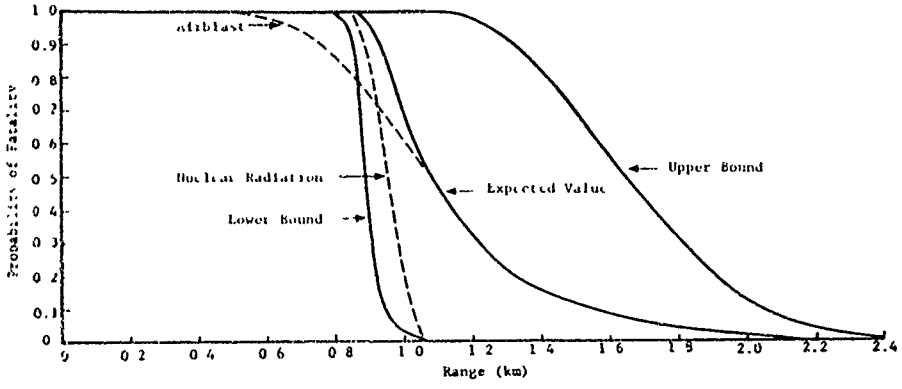

Figure 7.129. Fatality Damage Function, People in Basements, 30 KT, Surface Burst

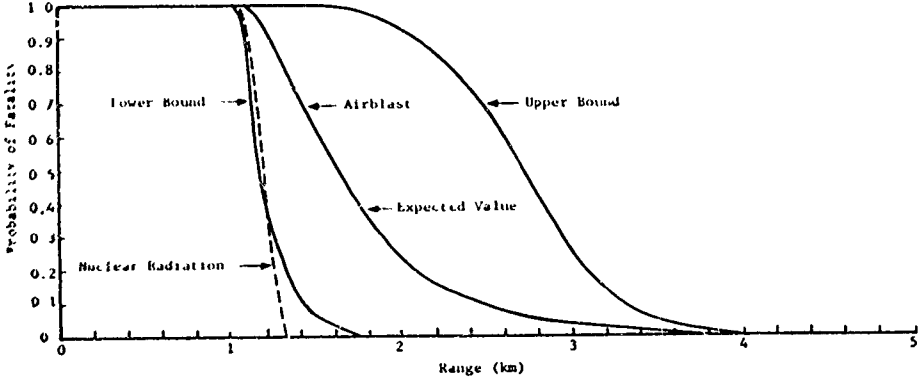

Figure 7 130 Fatality Damage Function, People in Basements, 100 KT, Surface Burst.

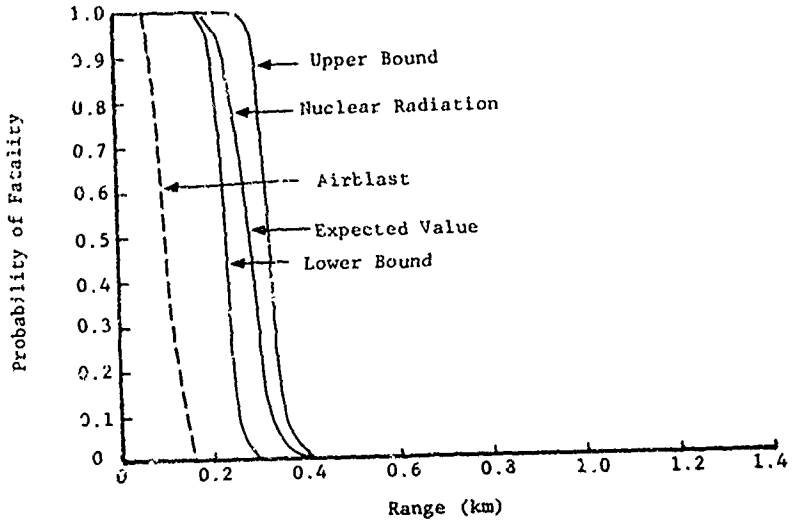

Figure 7.131. Fatality Damage Function, People in Basements, 0.1 KT, 200 ft/KT$^{1/3}$ Scaled Height of Burst.

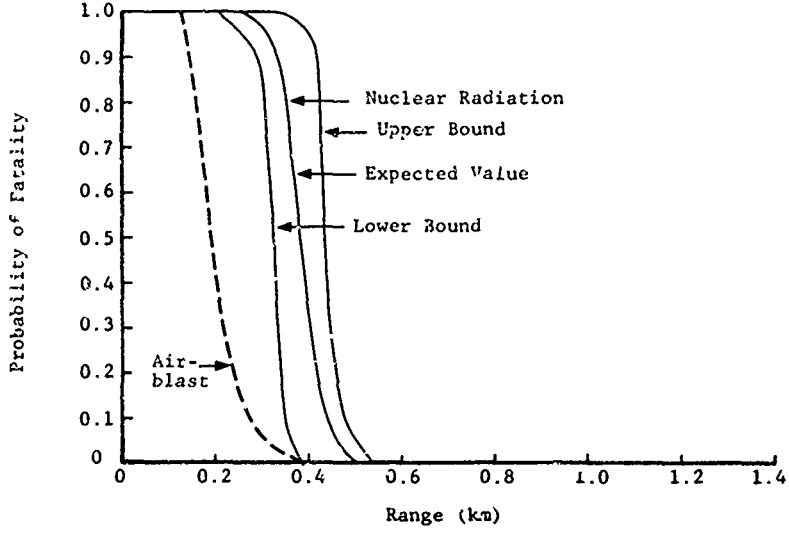

Figure 7.132. Fatality Damage Function, People in Basements, 0.3 KT, 200 ft/KT$^{1/3}$ Scaled Height of Burst.

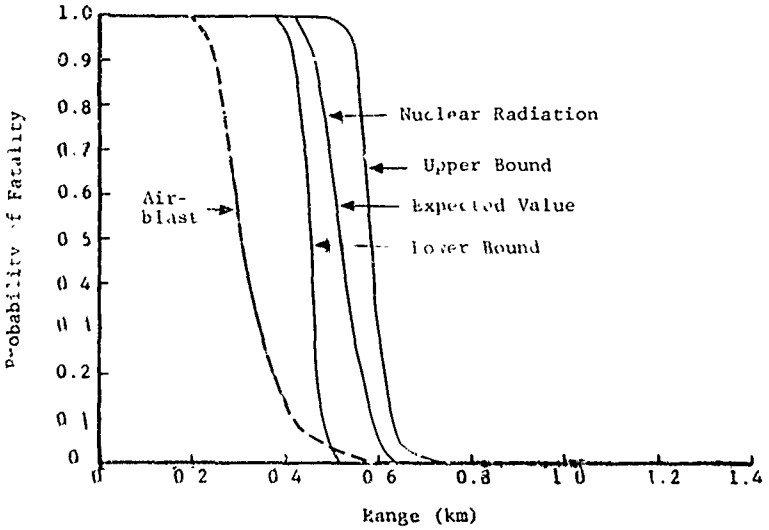

Figure 7-133 Fatality Damage Function, People in Basements, 1 KT
,00 ft/KT$^{1/3}$ Scaled height of Burst

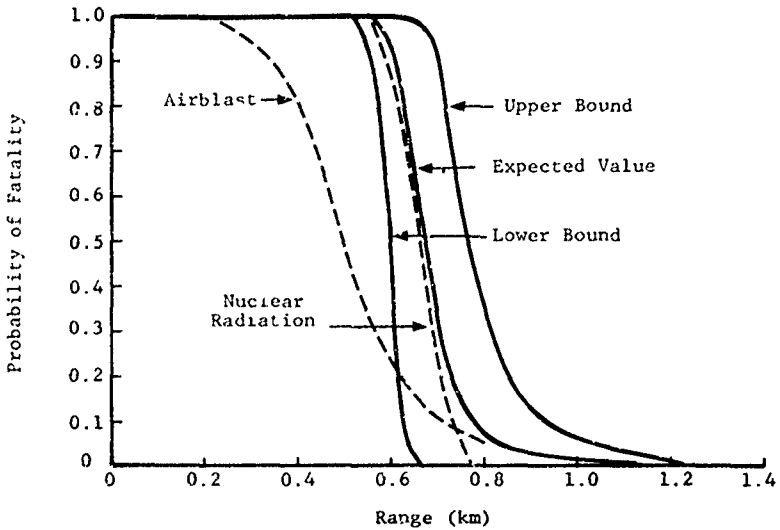

Figure 7 134. Fatality Damage Function, People in Basements, 3 KT 200 ft/KT$^{1/3}$ Scaled Height of Burst.

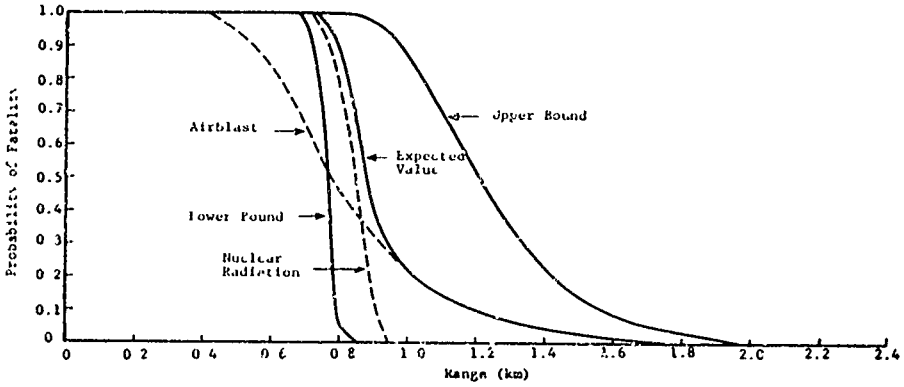

Figure 7.135. Fatality Damage Function, People in Basements, 10 KT, 200 ft/KT$^{1/3}$ Scaled Height of Burst.

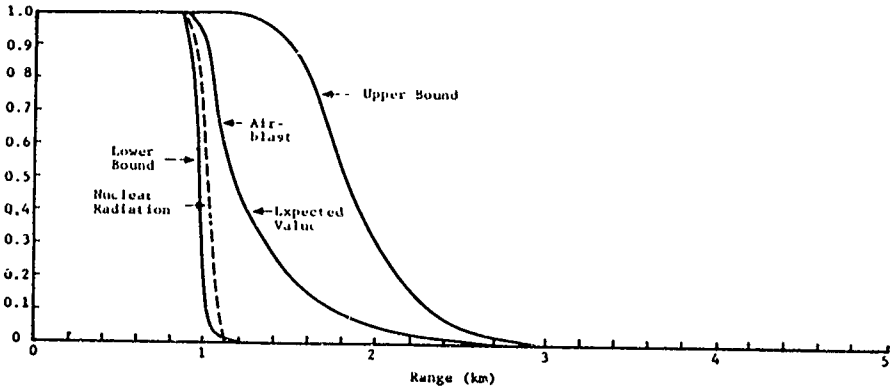

Figure 7.136. Fatality Damage Function, People in Basements, 30 KT, 200 ft/KT$^{1/3}$ Scaled Height of Burst.

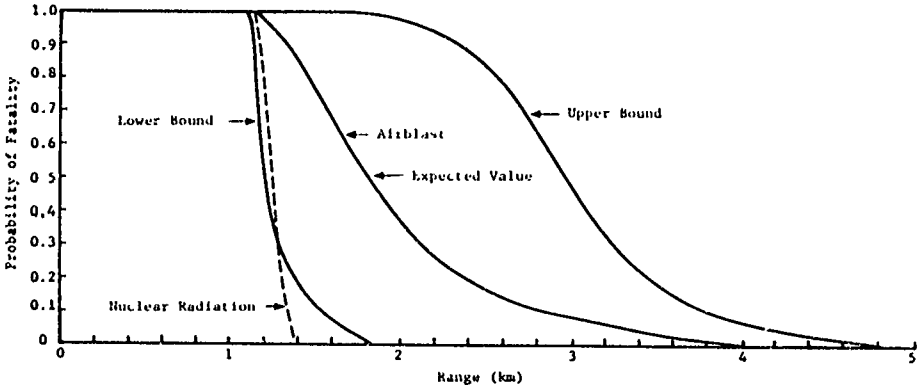

Figure 7.137. Fatality Damage Function, People in Basements, 100 KT, 200 ft/KT$^{1/3}$ Scaled Height of Burst.

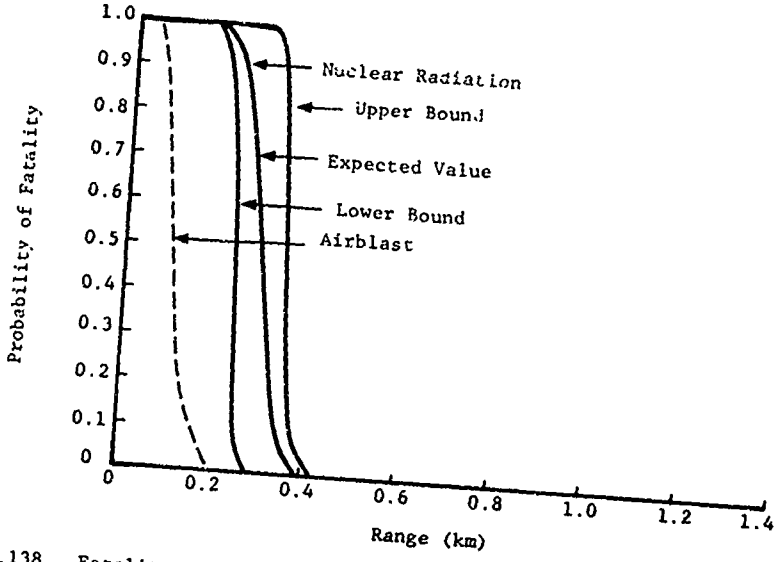

Figure 7.138 Fatality Damage Function, People in Basements, 0.1 KT, 600 ft/$KT^{1/3}$ Scaled Height of Burst.

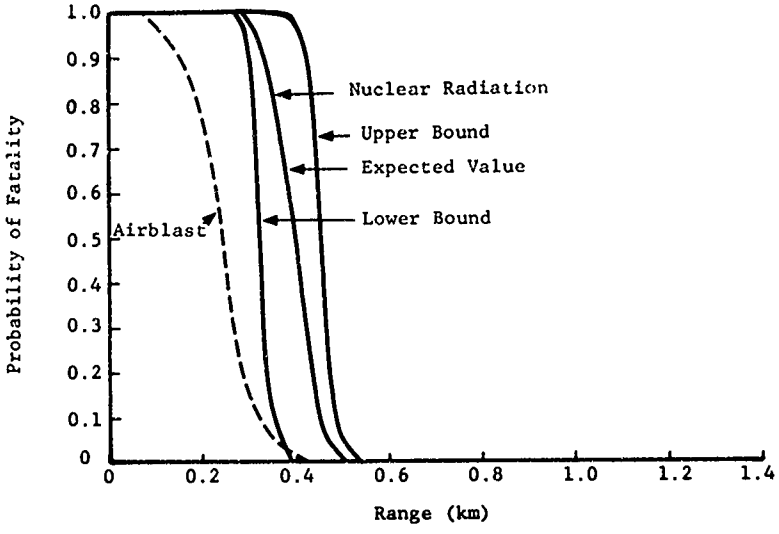

Figure 7.139. Fatality Damage Function, People in Basements, 0.3 KT, 600 ft/$KT^{1/3}$ Scaled Height of Burst.

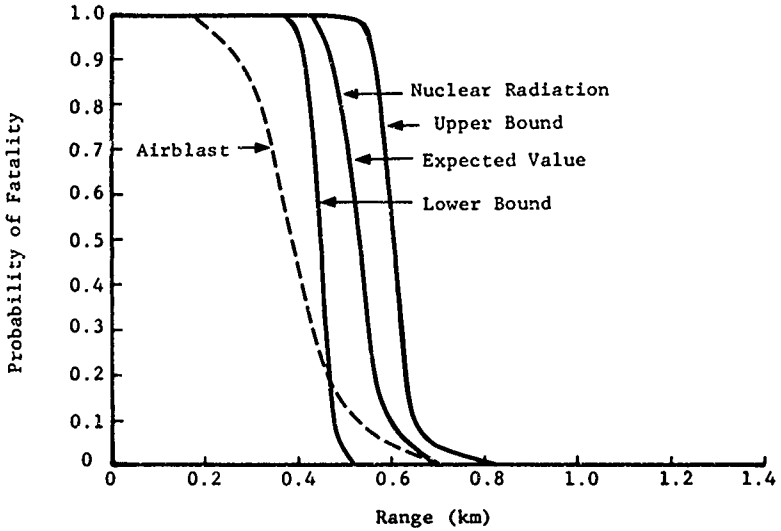

Figure 7.140. Fatality Damage Function, People in Basements, 1 KT, 600 ft/KT$^{1/3}$ Scaled Height of Burst.

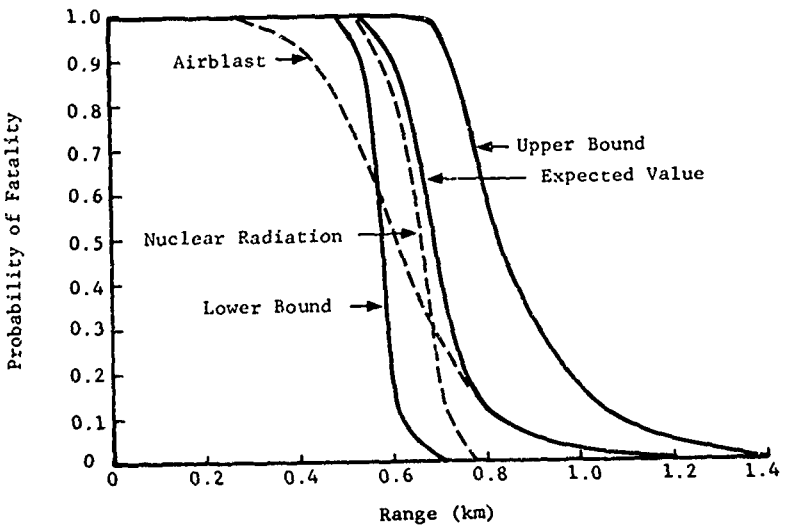

Figure 7.141. Fatality Damage Function, People in Basements, 3 KT, 600 ft/KT$^{1/3}$ Scaled Height of Burst.

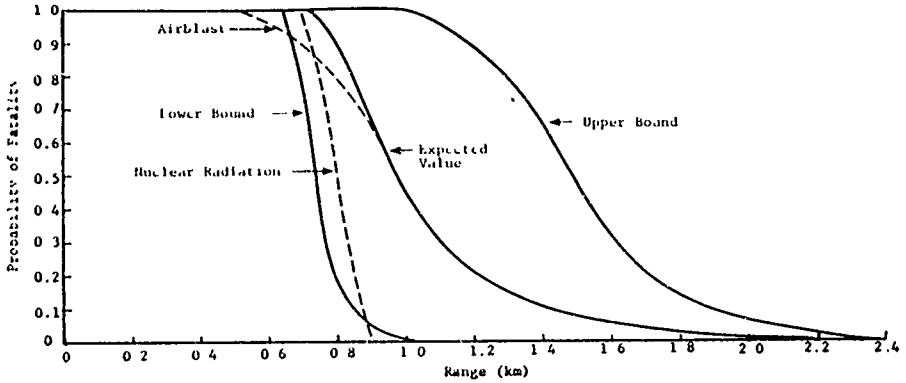

Figure 7.142. Fatality Damage Function, People in Basements, 10 KT, 600 ft/KT$^{1/3}$ Scaled Height of Burst.

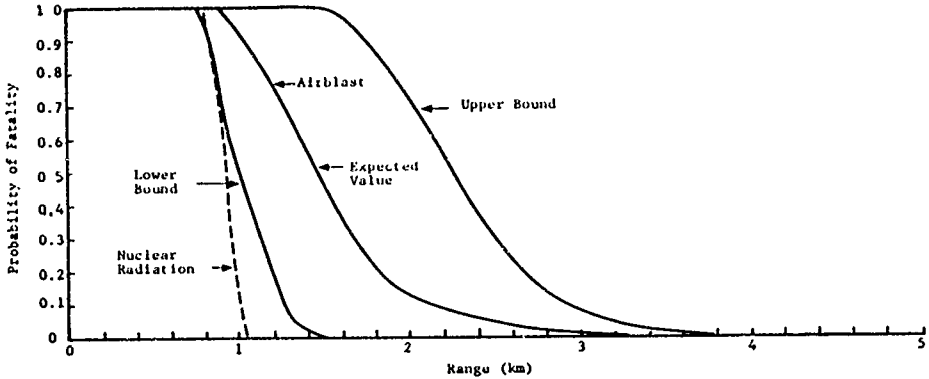

Figure 7.143. Fatality Damage Function, People in Basements, 30 KT, 600 ft/KT$^{1/3}$ Scaled Height of Burst.

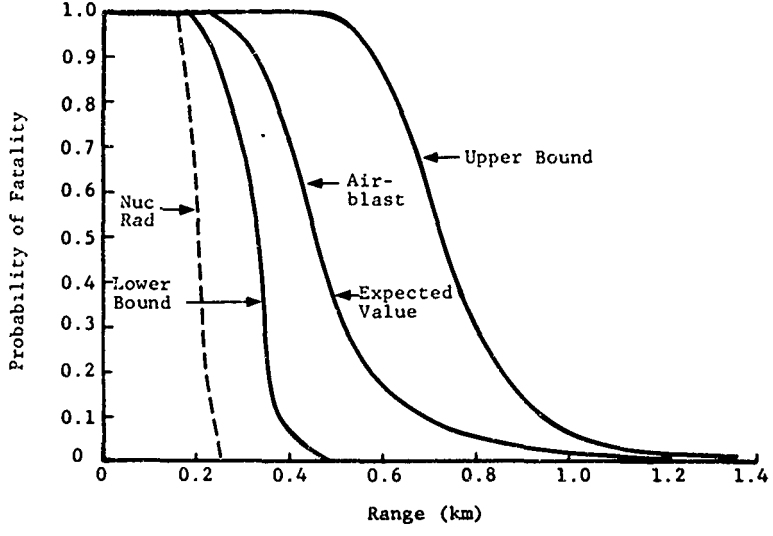

Figure 7.144. Fatality Damage Function, People in Basements, 100 KT, 600 ft/KT$^{1/3}$ Scaled Height of Burst.

DISTRIBUTION LIST

DEPARTMENT OF DEFENSE

AFSOUTH
ATTN U.S Documents Officer

Armed Forces Radiobiology Research Institute
Defense Nuclear Agency
National Naval Medical Center
3 cy ATTN. Director

Armed Forces Staff College
ATTN Reference & Technical Services Branch

Assistant Secretary of Defense
International Security Affairs
ATTN Policy Plans & NSC Affairs
ATTN: European & NATO Affairs

Assistant Secretary of Defense
Program Analysis & Evaluation
ATTN Strategic Programs
ATTN: Regional Programs

Assistant to the Secretary of Defense
Atomic Energy
ATTN. Executive Assistant

Command & Control Technical Center
Department of Defense
ATTN: Strategic Operations Division
ATTN: Military Studies & Analysis Division

U.S. European Command
ATTN J-3
ATTN EC J2-T
ATTN J-5

Commander In Chief, Atlantic
ATTN: J-5
ATTN J-3

Commander In Chief, Pacific
ATTN. J-5
ATTN: J-3

Defense Advanced Rsch Proj. Agency
ATTN TIO

Defense Documentation Center
12 cy ATTN: DD

Defense Intelligence Agency
ATTN DB-4
ATTN DB-1
ATTN DT
ATTN: DV
ATTN RDS-3C
ATTN DE
ATTN: DW-20

Deputy Under Secretary of Defense for Policy
ATTN. D. Murphy

Director Net Assessment
ATTN A Marshall

DEPARTMENT OF DEFENSE (Continued)

Field Command
Defense Nuclear Agency
2 cy ATTN: FCPR

Field Command
Defense Nuclear Agency
Livermore Division
ATTN FCPRL

Interservice Nuclear Weapons School
ATTN TTV

Defense Nuclear Agency
ATTN STNA
ATTN DDST
ATTN: RATN
ATTN OASO
ATTN. STRA
ATTN STSP
ATTN STVL
ATTN STSA
ATTN BA
ATTN STSS
4 cy ATTN VLWS
4 cy ATTN TITL

Joint Chiefs of Staff
ATTN J-5
ATTN SAGA
ATTN J-3
ATTN J-5, Nuclear Division
ATTN J-3, Strategic Operations Division
ATTN. J-5, Strategy Division

Joint Strat. Tgt Planning Staff
ATTN JSTPS/JPS
ATTN JSTPS/JLTW
ATTN JSTPS/JL
ATTN: JSTPS/JP

National Defense University
ATTN: NWCLB-CR

U S. National Military Representative
SHAPE
5 cy ATTN U.S Documents Officer

Los Alamos Branch
Field Command, Defense Nuclear Agency
ATTN W. Willis

Under Secy. of Def. for Rsch. & Engrg.
ATTN Strategic & Space Systems (OS)
ATTN Tactical Warfare Programs, R. Moore

U.S Mission NATO
ATTN CEP Officer

NATO School (SHAPE)
ATTN: LTC Williamson

DEPARTMENT OF THE ARMY

Deputy Chief of Staff for Ops & Plans
Department of the Army
ATTN DAMO-SSN
ATTN DAMO-SSP
ATTN DAMO-ROS

Deputy Chief of Staff for Rsch Dev. & Acq
Department of the Army
ATTN DAMA-CSS-N

Harry Diamond Laboratories
Department of the Army
ATTN DELHD-I-TL
ATTN DELHD-N-P

U S Army Ballistic Research Labs
ATTN Technical Library

U S Army Comb Arms Combat Dev Actv
ATTN ATCA-CFT

U S Army Cond & General Staff College
ATTN ATSW-TA-D

U S Army Concepts Analysis Agency
ATTN MOCA-WGP

U S Army Europe and Seventh Army
ATTN DCSOPS-AEAGC
ATTN DCSOPS-AEAGE

U S Army Forces Command
ATTN AR-OPS

U.S Army Infantry School
ATTN ATSH-CTD

U S Army Materiel Sys Analysis Activity
ATTN DRXSY-S
ATTN DRXSY-DS

U S Army Missile R&D Command
ATTN DRSMI-YDR

U S Army Nuclear & Chemical Agency
ATTN Library

U S Army TRADOC Systems Analysis Activity
ATTN ATAA-TAC

U S Army Training and Doctrine Cond
ATTN ATCD-CF
ATTN ATCD-AJ

U S Army War College
ATTN Library

V Corps
Department of the Army
ATTN G-3

VII Corps
Department of the Army
ATTN G-3

DEPARTMENT OF THE NAVY

Naval Postgraduate School
ATTN Code 0142, Library

Naval Surface Weapons Center
ATTN F31

Naval War College
ATTN Code E-11

Naval Weapons Evaluation Facility
ATTN Technical Director

Office of Naval Research
ATTN Code 713

Office of the Chief of Naval Operations
ATTN OP 604
ATTN OP 981
ATTN OP 96

U S Atlantic Fleet
Department of the Navy
ATTN N-3
ATTN N-2

U S Naval Forces, Europe
ATTN N3262, Nuclear Surety Officer

DEPARTMENT OF THE AIR FORCE

Air Force School of Aerospace Medicine
ATTN Radiobiology Division

Air Force Weapons Laboratory
ATTN NSS
ATTN SUL

Deputy Chief of Staff
Operations Plans and Readiness
Department of the Air Force
ATTN AFXOXFM
ATTN AFXOXRR

Deputy Chief of Staff
Studies and Analysis
Department of the Air Force
ATTN PACG

Foreign Technology Division, AFSC
ATTN TQR
ATTN SDN
ATTN CCN

Strategic Air Command
ATTN NRI-STINFO Library
ATTN XPFS

Tactical Air Command
ATTN DCS/Plans
ATTN XPS

U S Air Forces in Europe
ATTN XPX
ATTN DEP
ATTN INM
ATTN DOT

DEPARTMENT OF ENERGY

Albuquerque Operations Office
ATTN: Lib. Cust., A. Ortiz

Department of Energy
ATTN: Office of Military Application

DEPARTMENT OF ENERGY CONTRACTORS

Lawrence Livermore Laboratory
University of California
ATTN: M. Gustavson
ATTN: D. Blumenthal

Los Alamos Scientific Laboratory
ATTN: Sandoval/Chapin/Best/Dowler

Sandia Laboratories
Livermore Laboratory
ATTN. T. Gold

Sandia Laboratories
ATTN: 3141
ATTN 1313, Systems Studies Division

OTHER GOVERNMENT AGENCY

Central Intelligence Agency
ATTN: OSR/SS/D. D. Linton

DEPARTMENT OF DEFENSE CONTRACTORS

BDM Corp.
ATTN: J. Bode
ATTN: J. Braddock
ATTN: R. Buchanan
ATTN: C. Wasaff

Commander, 66th MI Group
ATTN: RDA for G. Eade
ATTN: RDA for J. Hurley

General Electric Company-TEMPO
Center for Advanced Studies
ATTN: DASIAC

General Research Corp.
ATTN Tactical Warfare Operations

Historical Evaluation & Psch. Org.
ATTN: T. Dupuy

Hudson Institute, Inc.
ATTN: C. Gray

Jaycor
ATTN: R. Sullivan

John Morse
ATTN: John Morse

Kaman Sciences Corp.
ATTN: F. Shelton

Lovelace Biomedical & Environmental
Research Institute, Inc.
ATTN: D. Richmond

Martin Marietta Corp.
ATTN: J. Donathan

DEPARTMENT OF DEFENSE CONTRACTORS (Continued)

Martin Marietta Aerospace
ATTN B. Spivy

Pacific-Sierra Research Corp.
ATTN: G. Lang

R & D Associates
ATTN: C MacDonald
ATTN: W. Graham, Jr.
ATTN L. Hanneman
ATTN. R. Speed

R & D Associates
ATTN J. Thompson
ATTN: H. Cooper

Rand Corp.
ATTN J. Foster
ATTN D. Smallwood

Sam Cohen
ATTN: Sam Cohen

Science Applications, Inc.
ATTN: W. Yengst
ATTN: M. Drake
ATTN: M. Fricke
ATTN: C. Rindfleisch
ATTN D. Groce
ATTN: J. Swenson
ATTN: W. Woolson
ATTN: D. Kaul
ATTN: J. Martin

Science Applications, Inc.
ATTN: W Layson

University of Southern California
School of International Relations
ATTN W. Van Cleave

SRI International
ATTN: J. Nahr

Sy Corporation
ATTN: S. Weiss

System Planning Corp.
ATTN: J. Douglas

Systems, Science & Software, Inc.
ATTN K. Pyatt

Systems, Science & Software, Inc.
Washington Research Center
ATTN: J. Cane

TRW Defense & Space Sys. Group
ATTN. D. Scally
ATTN: P. Dai